

République algérienne démocratique et populaire
Ministère de l'Enseignement Supérieur et de la Recherche
Scientifique
Université Kasdi Merbah-Ouargla



Faculté des Hydrocarbures, des Energies renouvelables et Sciences de la
Terre et de l'univers
Département: Sciences de la Terre et de l'univers

THESE

Présentée en vue de l'obtention du diplôme de Doctorat en Sciences

Spécialité

Géologie pétrolière

Par

DJEBBAS Faycal

Intitulé :

CAPTAGE ET STOCKAGE DE GAZ DE CARBONE DE DIOXYDE
DANS LES GISEMENTS D'HYDROCARBURES

Etude de Simulation de la Combinaison EOR avec stockage de CO₂ (EOR+) sur
le champ SFSW

DEVANT LE JURY

Président:	DOBBI Abdelmadjid	MCA. (Univ. Ouargla)
Directeur de thèse :	ZEDDOURI Aziez,	Pr. (Univ. Ouargla)
Examineurs:	HADJADJ Ahmed	Pr. (Univ. Boumerdes)
	DOKKAR Boubekeur	MCA. (Univ. Ouargla)
	GARECHE Mourad	MCA. (Univ. Boumerdes)

Année universitaire : 2016/2017

People's Democratic Republic of Algeria
Ministry of Higher Education and Scientific Research
University of Kasdi Merbah-Ouargla



**Faculty of Hydrocarbons, Renewable Energies and Earth Sciences and
the Universe**

Department of: Earth Sciences and the Universe

THESIS

Submitted to attain the degree of DOCTOR OF SCIENCES

Speciality

Geology Petroleum

By

DJEBBAS Faycal

Title:

**CAPTURE AND STORAGE OF THE CARBON DIOXIDE GAS IN
HYDROCARBON RESERVOIRS**

Simulation Study of Combining EOR with CO₂ storage (EOR+) in SFSW Field

IN FRONT OF THE JURY

President:	DOBBI Abdelmadjid	MCA. (Univ. of Ouargla)
Thesis Advisor:	ZEDDOURI Aziez	Pr. (Univ. of Ouargla)
Committee members:	HADJADJ Ahmed	Pr. (Univ. of Boumerdes)
	DOKKAR Boubekour	MCA. (Univ. of Ouargla)
	GARECHE Mourad	MCA. (Univ. of Boumerdes)

Academic year: 2016/2017

DISSERTATION. NO.

CAPTURE AND STORAGE OF THE CARBON DIOXIDE GAS IN HYDROCARBON RESERVOIRS

A thesis submitted to attain the degree of
DOCTOR OF SCIENCES

Submitted by
DJEBBAS Faycal

Department of Science of the earth and the universe
University of Kasdi Merbah Ouargla

Doctoral Committee:

President	DOBBI Abdelmadjid	MCA.	Univ_Ouargla
Advisor	ZEDDOURI Aziez	Pr.	Univ_Ouargla
Committee member	HADJAJ Ahmed	Pr.	Univ_Boumerdes
Committee member	GARECHE Mourad	MCA.	Univ_Boumerdes
Committee member	DOKKAR Boubekour	MCA.	Univ_Ouargla

The undersigned have examined the thesis entitled ‘**CAPTURE AND STORAGE OF THE CARBON DIOXIDE GAS IN HYDROCARBON RESERVOIRS**’ presented by **DJEBBAS Faycal**, a candidate for the degree of **Ph.D.** and hereby certify that it is worthy of acceptance.

_____	ZEDDOURI Aziez
Date	Thesis Advisor
_____	DOBBI Abdelmadjid
Date	President of Committee
_____	HADJAJ Ahmed
Date	Committee member
_____	GARECHE Mourad
Date	Committee member
_____	DOKKAR Boubekeur
Date	Committee member

ACKNOWLEDGMENTS

Firstly, I would like to express my sincere gratitude to my advisor Prof. ZEDDOURI Aziez for the continuous support of my Ph.D. study and related researches, for his patience, motivation, and immense knowledge. His guidance helped me in all the time of researches and writing of this thesis. I could not have imagined having a better advisor and mentor for my Ph.D. study.

Besides my advisor, I would like to thank the rest of my thesis committee: President. DOBBI Abdelmadjid, Prof. HADJADJ Ahmed, Dr. GARECHE Mourad and Dr. DOKKAR Boubekour, for their insightful comments and encouragement, but also for the hard question which incited me to widen my research from various perspectives.

I would like to thank too my family: my parents (without forgetting of course my father Boudjema Allah's mercy on him), my wife and my kids, my brothers and sisters for supporting me throughout writing this thesis and my life in general.

TABLE OF CONTENTS

Chapter	Page
ACKNOWLEDGMENTS	i
LIST OF TABLES	ii
LIST OF FIGURES	iii
TABLE OF CONTENTS	vi
CHAPTER 1: INTRODUCTION	1
Preface	1
Problematic	2
Introduction	5
Overview	8
CHAPTER 2: CO ₂ CAPTURE & TRANSPORT TECHNOLOGIES.....	13
CO ₂ CAPTURE	11
CO ₂ Capture Status	12
CO ₂ Capture systems	13
CO ₂ Capture Technologies.....	20
CO ₂ Capture in In-Salah Project in Algeria	25
CO ₂ TRANSPORT	28
CO ₂ Transport Systems.....	29
Ships for CO ₂ transportation	31
CHAPTER 3: CO ₂ Chemical-Physical Properties & Trapping mechanisms.....	33
Physical properties of CO ₂	33
Chemical properties of CO ₂	37

CO ₂ Trapping Mechanisms.....	41
Description of storage mechanisms.....	42
Stratigraphic and structural trapping	42
Residual trapping.....	43
Dissolution trapping.....	46
Mineral trapping	49
CHAPTER 4: CO ₂ Storage Reservoirs Characteristic	53
Geological formation	53
CO ₂ Storage Assessment in geological formations.....	55
CO ₂ Storage Capacity Calculation	56
CO ₂ Storage efficiency	57
Methodologies of estimating CO ₂ storage capacity	60
Volumetric methods	60
Dynamic methods	63
Sealing of The CO ₂ Storage Reservoir	67
Leakage mechanisms	68
Mechanisms of Potential leakage through the caprock.....	68
Migration in Supercritical status.....	69
Cap Rock sealing capacity.....	74
Characterization of gas flow through caprocks.....	76
CHAPTER 5: EFFECT OF THE FRACTURES ON CO ₂ STORAGE.....	81
Natural fractured reservoirs	81
Comparison of geological CO ₂ sequestration performance between homogeneous and fractured reservoir.....	85

Modeling Methodologies	87
Discussing the Results	91
CHAPTER 6: RESERVOIR PROPERTIES DESCRIPTION	94
Petrophysical and Geological significance of FZI	94
Hydraulic Flow Unit Concept	95
Determine the Flow Zone Indicator & Effective Porosity in uncored intervals	96
Artificial Intelligence Methods	96
Adaptive Network Fuzzy Inference System (ANFIS)	96
Data set and methodology	99
Applying ANFIS Results in HFU Technique	101
ANFIS Results	101
Permeability Estimation using HFU Concept	102
Permeability Estimation using Hydraulic Flow Unit Concept	105
Clustering data	105
Log-Log Plot of the RQI versus Φ_{hiz}	105
Generalization of the Technique	107
Results and discussion	108
CHAPTER 7: MODELING OF THE CO ₂ GEOLOGICAL STORAGE IN HYDROCARBON RESERVOIRS	109
Introduction	109
Scientific background	112
Multiphase flow model	112
Reservoir Simulation Software (Nexus/VIP)	113
Modeling and simulation	117

Field presentation (Sif Fatima South-West- SFSW)	117
Geological Modeling of SFSW	118
Static modeling (geology data).....	118
Dynamic modeling (reservoir-fluid data).....	119
Equation of State (EOS) Model.....	119
Relative Permeability and Capillary pressure	120
Validation of the Reservoir Model and Simulation Software.....	122
Effect of the conditions in situ in the Solubility of CO ₂	123
Effect of Pressure CO ₂ Solubility.....	125
Effect of Temperature CO ₂ Solubility.....	129
Effect of the Salinity in the CO ₂ solubility	130
Storage of the CO ₂ in hydrocarbon reservoirs	135
CO ₂ as Enhanced Oil Recovery Mechanism (EOR).....	137
Modeling of the CCS-EOR System	145
CO ₂ Risk Assessment and Monitoring.....	151
Learned lessons from In-Salah Project in Algeria	151
Pilot CO ₂ Geological Storage Project in Hydrocarbon Reservoir.....	155
CO ₂ Flood/Injection Designs	155
Trapping mechanisms and constraints applied in Pilot Project.....	160
Reservoir storage potential evaluation of SFSW field	164
Conclusion and Perspectives.....	171
REFERENCES	173

List of Figures

- 1- Fig.1: Greenhouse effect processes.
- 2- Fig.2: The evolution of the greenhouse gases.
- 3- Fig.3: CO₂ concentration since 1960 to day (ERSL data).
- 4- Fig. 4: Options for Storing CO₂ in deep underground geological formations.
- 5- Fig. 5: CO₂ capture systems.
- 6- Fig. 6: Schema of an oxy-fuel, pulverized coal fired power plant.
- 7- Fig.7: Process flow diagram for CO₂ recovery from flue gas by chemical absorption.
- 8- Fig. 8: CO₂ production forecast from different sources in In Salah project.
- 9- Fig. 9: Schema of CO₂ elimination and regeneration of the Amine.
- 10- Fig. 10: Phase diagram for CO₂.
- 11- Fig. 11: Variation of CO₂ as a function of temperature and pressure.
- 12- Fig. 12: Vapor pressure of CO₂ as a function of temperature.
- 13- Fig. 13: Variation of CO₂ viscosity as a function of temperature and pressure.
- 14- Fig. 14: Pressure-Enthalpy chart for CO₂.
- 15- Fig. 15: Solubility of CO₂ in water (Kohl and Nielsen, 1997).
- 16- Fig. 16: Solubility of CO₂ in brine relative to that in pure water.
- 17- Fig. 17: Dependence of PH on CO₂ concentration in sea water.
- 18- Fig. 18: Schematic representation of the change of trapping mechanisms and increasing CO₂ storage security over time.
- 19- Fig. 19: Examples of (a) structural and (b) stratigraphic physical traps for CO₂.
- 20- Fig. 20: The snap-off process creating residual trapped gas during imbibition when water or brine returns to the CO₂ filled medium.
- 21- Fig. 21: Relative permeability curve for macroscopic behaviour with hysteresis.
- 22- Fig. 22: Large-scale effects of residual trapping after injection stop.
- 23- Fig. 23: Comparison between density-driven convection in the modeled system.
- 24- Fig. 24: Different trapping mechanism of the CO₂.
- 25- Fig. 25: Regional assessment of CO₂ storage capacity as compiled by the Global Energy.
- 26- Fig. 26: Techno-economic resource-reserve pyramid for CO₂ storage capacity.
- 27- Fig. 27: The amount of CO₂ stored as a free gas phase in 1 m³ void space as a function of pressure at different temperatures.
- 28- Fig. 28: The amount of CO₂ stored as dissolution in 1 m³ Weyburn formation brine as a function of pressure at different temperatures.
- 29- Fig. 29: The amount of CO₂ stored as dissolution in 1 m³ Weyburn reservoir oil as a function of pressure at different temperatures.
- 30- Fig. 30: isotherm CO₂ density as function on the pressure and temperature.
- 31- Fig. 31: Solubility as function in the pressure and at T=37 °C.
- 32- Fig. 32: CO₂/brine interfacial tension as a function of pressure for different temperatures at various salinities of each salt in brine.
- 33- Fig. 33: Maximum column H of CO₂ that can be stored in a saline aquifer (in meters) as a function of brine salinity at various temperatures.

- 34- Fig. 34: Measured gas effective permeability vs. time after gas breakthrough for sample A7.
- 35- Fig. 35: Measured gas effective permeability vs. time after gas breakthrough for sample B8.
- 36- Fig. 36: Calculations of CO₂ migration through caprocks by volume flow and molecular diffusion.
- 37- Fig. 37: Different fractures types in fractures reservoirs.
- 38- Fig. 38: Natural fractured reservoir response in well test.
- 39- Fig. 39: Effect of size and shape on imbibition oil recovery.
- 40- Fig. 40: 3-D simulation grid of (a) homogenous reservoir, (b) Fractured reservoir.
- 41- Fig. 41: Capacity storage difference between fractured and homogenous reservoir.
- 42- Fig. 42: Total CO₂ stored in homogenous reservoir.
- 43- Fig.43: Total CO₂ stored in fractured reservoir.
- 44- Fig. 44: Storage capacity behaviour: (a) homogenous reservoir and (b) fractured reservoir.
- 45- Fig. 45: CO₂ Breakthrough time.
- 46- Fig. 46: ANFIS structure.
- 47- Fig.47: ANFIS training process steps.
- 48- Fig. 48-a: Flow zone indicator ANFIS results.
- Fig. 48-b: Effective porosity ANFIS results.
- 49- Fig. 49-a: Regression Function of the effective porosity (train, test and all data).
- Fig. 49-b: MSE and RMSE and error St. Deviation of the effective porosity.
- Fig. 49-c: Regression Function of the FZI (train, test and all data).
- Fig. 49-b: MSE and RMSE and error St. Deviation of the FZI.
- 50- Fig. 50: Predicted FZI and He using ANFIS method for cored well.
- 51- Fig. 51: RQI versus Hz.
- 52- Fig. 52: Predicted Permeability Model.
- 53- Fig. 53: Calculated permeability vs. core permeability.
- 54- Fig. 54: FZI and He using ANFIS method and Predicted Permeability using HFU for uncored well.
- 55- Fig. 55-a: Major components in NEXUS linear solver package SPURSPACK
- Fig. 55-b: Different modules in Nexus Desktop
- 56- Fig. 56-a: The Structure MAP of SFSW
- Fig. 56-b: Relative permeability of water and oil model vs. water saturation.
- Fig. 56-c: Capillary pressure model vs. water saturation.
- 57- Fig. 57: 3-3-D geological model of SFSW.
- 58- Fig. 58: impact of the pressure in the solubility (distilled water).
- 59- Fig. 59: impact of the pressure in the solubility (water salinity 15000 ppm).
- 60- Fig. 60: impact of the pressure in the solubility (water salinity 15000 ppm).
- 61- Fig. 61: Solubility of the CO₂ in fluid in place (inj_pressure = 3000 psia).
- 62- Fig. 62: Solubility of the CO₂ in fluid in place (inj_pressure = 3500 psia).
- 63- Fig. 63: Solubility of the CO₂ in fluid in place (inj_pressure = 4000 psia).
- 64- Fig. 64: Solubility of the CO₂ in fluid in place (inj_pressure = 4500 psia)
- 65- Fig. 65: Cumulative CO₂ Storage in different injection pressure.

- 66- Fig. 66: Effect of the Temperature in the solubility (distilled water).
- 67- Fig. 67: Effect of the Temperature in the solubility (15000ppm NaCl water).
- 68- Fig. 68: Effect of the Temperature in the solubility (25000 ppm NaCl water).
- 69- Fig. 69: Solubility of the CO₂ in fluid in place (Tr. = 170 °F).
- 70- Fig. 70: Solubility of the CO₂ in fluid in place (Tr. = 120 °F).
- 71- Fig. 71: Solubility of the CO₂ in fluid in place (Tr. = 70 °F).
- 72- Fig. 72: Impact of the reservoir temperature in the Solubility of the CO₂.
- 73- Fig. 73: Solubility of the CO₂ in fluid in place (Sal. = 250000 ppm).
- 74- Fig. 74: Solubility of the CO₂ in fluid in place (Sal. = 15000 ppm).
- 75- Fig. 75: Solubility of the CO₂ in fluid in place (Sal. = 15000 ppm).
- 76- Fig. 76: Impact of the brine Salinity in the reservoir storage capacity.
- 77- Fig. 77: Schematic of CO₂-EOR operation
- 78- Fig. 78: Slim-tube oil recoveries at increasing pressures for fixed oil composition and temperatures
- 79- Fig. 79: Weyburn oil production processes.
- 80- Fig. 80: Produced gas and CO₂ injection Performance.
- 81- Fig. 81: The Performance of the CO₂ compared to produced gas.
- 82- Fig. 82: Impact of the CO₂ injection as EOR process in the performance of the field.
- 83- Fig. 83: Cumulative CO₂ stored during EOR process.
- 84- Fig. 84: Krechba field (Ringrose et al. 2009).
- 85- Fig. 85: Location of production and injection wells (at time of the study).
- 86- Fig. 86: 3-D geological model of the Pilot CO₂ storage project.
- 87- Fig. 87: Permeability Distribution across the reservoir.
- 88- Fig. 88: Perforation layers based on FZI values.
- 89- Fig. 89: The Reservoir Pressure Response.
- 90- Fig. 90: Total produced and injected CO₂ rates.
- 91- Fig. 91: CO₂ dissolved process in dynamic phases.
- 92- Fig. 92: CO₂ dissolved process in static phases
- 93- Fig. 93: CO₂ free gas saturation in dynamic phases.
- 94- Fig. 94: CO₂ free gas saturation in static phases.
- 95- Fig. 95: Effect of the CO₂ injection in the aquifer (storage capacity)
- 96- Fig. 96: Effect of the CO₂ injection in the aquifer (reservoir pressure)
- 97- Fig. 97: CO₂ injection rate in the INJ1_CO₂ (in hydrocarbon reservoir)
- 98- Fig. 98: CO₂ injection rate in the INJ2_CO₂ (in hydrocarbon reservoir)
- 99- Fig. 99: CO₂ injection rate in the INJ3_CO₂-AQ (in adjacent aquifer)
- 100 - Fig. 99: CO₂ Store in the pilot project

List of Tables

- 1- Table. 2: Summary of current and planned CCS projects.
- 2- Table. 3: advantages and disadvantages of the different CO₂ capture technologies.
- 3- Table. 4: cost comparison for different CO₂ capture process.
- 4- Table. 5: Comparison of different separation technologies.
- 5- Table. 6: Existing long distance CO₂ pipelines.
- 6- Table. 7: Physical properties of CO₂.
- 7- Table. 8: Thermodynamic data for selected carbon-containing compounds.
- 8- Table. 9: Density and viscosity of CO₂ in different states.
- 9- Table. 10: IFT for different fluids systems.
- 10- Table. 11: Summary of caprock breakthrough pressure results in the literature.
- 11- Table. 12: Homogeneous reservoir data.
- 12- Table. 13: Fractured reservoir data.
- 13- Table. 14: Dynamic data.
- 14- Table. 15: Descriptive static of the input/output data.
- 15- Table. 16-a: The results of FZI and He ANFIS's.
Table. 16-b: Effective Porosity (output) and core data (target)
Table. 16-c: Table 16-a: Flow Zone Indicator results (output) and core data (target)
- 16- Table. 17: Overview of the simulators for geological carbon storage modified.
- 17- Table. 18: Reservoir properties data of the simulation model.
- 18- Table. 19: The initialization reservoir model output.
- 19- Table. 20: CO₂ Solubility in distilled water in different pressure and temperature.
- 20- Table. 21: CO₂ Solubility in 15000 ppm NaCl Water in different pressure & temperature.
- 21- Table. 22: CO₂ Solubility in 25000 ppm NaCl Water in different pressure & temperature.
- 22- Table. 23: Summary of MMV technology applied and lessons learned.

Chapter 1

Introduction General

Preface

This thesis is submitted for the degree of Doctor at the University of Kasdi Merbah- Ouargla, the research described herein was conducted under the supervisor of the Professor Mr. ZEDDOURI Aziez in the department of Geology Petroleum, Faculty of Hydrocarbon, University of Ouargla, between September 2012 and October 2017.

This dissertation is divided into two parts, the first one is the capture and transport of the CO₂ to the storage location and some related chemical and physical properties of the CO₂ in reservoir conditions, different equations to calculate the storage capacity and main mechanisms to trap this CO₂ in the reservoir, as it is not the objective of the thesis, this section was based mainly on previous works done by authors cited in the references section.

The second part of this thesis is the essential part (chapter 5, 6, 7, and the conclusion & Perspective), and is the best of my knowledge original. Neither this, nor any substantially similar dissertation has been or is being submitted for any other degree, diploma or other qualification at any other university

Part of this work has been presented in the following publications:

- Study of the fractures effect on the capacity and security geological storage of the CO₂ in hydrocarbon reservoirs, INTERNATIONAL JOURNAL OF ENERGY and ENVIRONMENT, Volume 9, 2015. 2015.
- Impact of the Fractures on the Capacity and Security CO₂ Geological Storage, Advances in Environmental and Geological Science and Engineering, ISBN: 978-1-61804-314-6. Italy. 2015
- Influence of natural fractures on oil production of unconventional Reservoirs, The International Conference on Technologies and Materials for Renewable Energy, Environment and Sustainability, TMREES14, Energy Procedia 50 (2014) 360 - 367. 2014.
- L'effet de la Tension Interfaciale IFT sur la pression capillaire, la perméabilité relative et la masse volumique au stockage géologique de CO₂ dans les Milieux poreux. Le Séminaire International sur L'Hydrogéologie et l'Environnement 5 - 7 Novembre 2013, Ouargla (Algérie).
- Predicting Accurate Permeability Model from Log Data using Hydraulic Flow Unit Concept and Artificial Intelligence Technique, working is ongoing.

DJEBBAS Faycal

October 2017.

Statement of the Problem

Climate change, also called global warming, refers to the rise in average surface temperatures on Earth. The earth's climate is naturally variable on all time scales. Any factor causes a sustained change to the amount of incoming energy or outgoing energy can lead to climate change [1]. As these factors are external to the climate system, they are referred to as 'climate forcers' and categorized to

Factors related to natural processes: such as

- Changes in volcanic activity.
- Changes in solar radiation.

Factors related to human activity: such as

- Burning of fossil fuels.
- Conversion of land for forestry and agriculture.

The overall effect of human activities was warming effect, driven mainly by emission of CO₂ and enhanced by emission of other greenhouses.

Greenhouse Effect

The Greenhouse Effect is a natural process that warms the Earth, it is quite necessary for our survival. Gases in the atmosphere, like water vapor (clouds), carbon dioxide (CO₂), methane (CH₄), and nitrous oxide (N₂O) act as a natural blanket by preventing the sun's heat energy from radiating back into space. The natural greenhouse effect helps warm the Earth's surface by as much as 33 °C, and without it, the planet would be too cold for humans to survive [2].

The diagram below illustrates the basic processes behind the greenhouse effect.

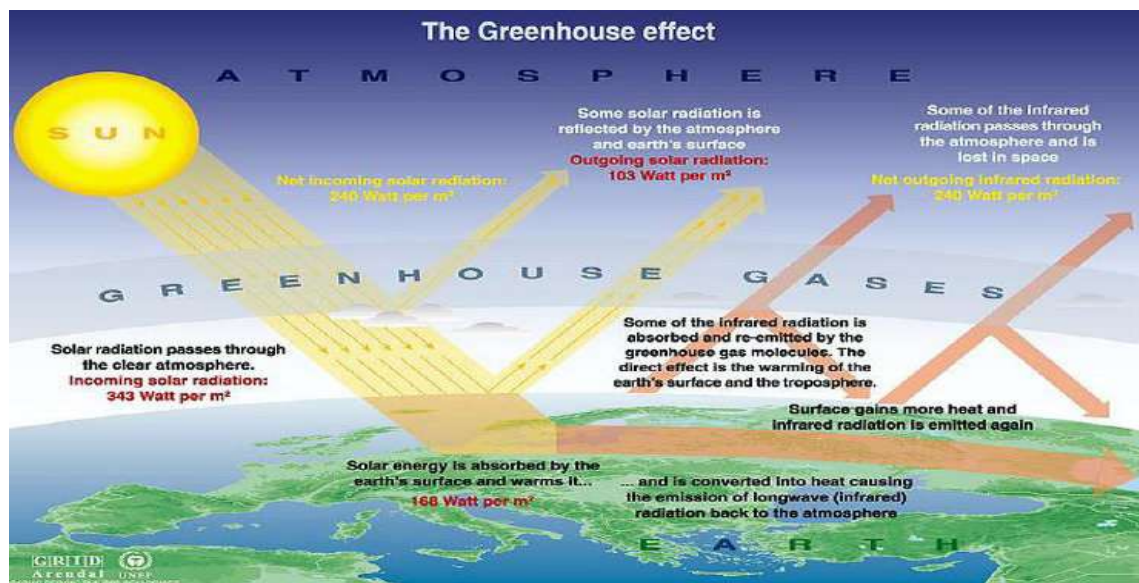


Fig.1: Greenhouse effect processes [1].

Factors affecting the Greenhouse Effect

There are three main factors that directly influence the greenhouse effect:

- The total energy influx from the sun, which depends on the earth's distance from the sun and on solar activity.
- The chemical composition of the atmosphere (what gases are present and in what concentrations).
- Albedo, the ability of the earth's surface to reflect light back into space.

The only factor that has changed significantly in the last 100 years is the chemical composition of the atmosphere—and that is because of human activity.

Human activity has changed the concentration of certain greenhouse gases in the atmosphere since the beginning of the Industrial Revolution (1750), with the most rapid increase occurred over the past fifty years as shown below.

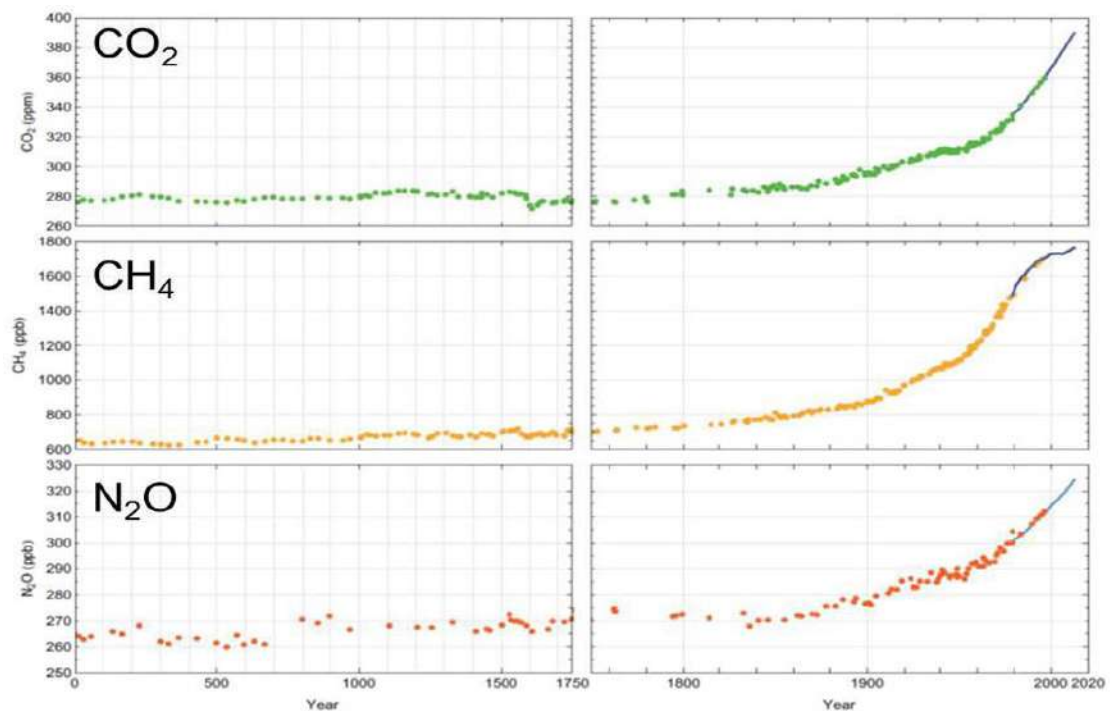


Fig.2: The evolution of the greenhouse gases

According to the earth system research laboratory (Mauna Loa) the concentration of the CO₂ in the atmosphere is increasing dramatically and reached levels of ~ 402 ppm in August 2016 as shown below

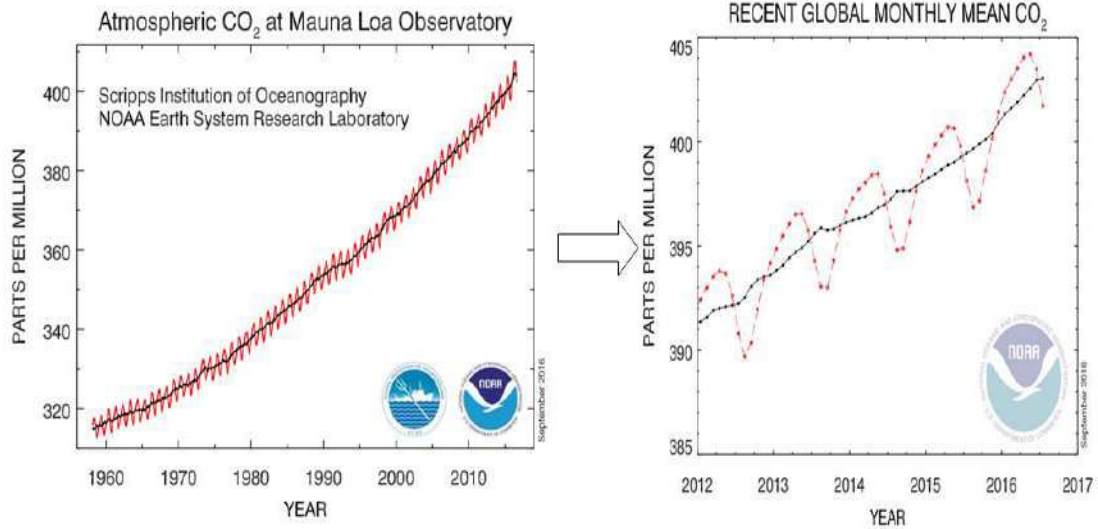


Fig.3: CO₂ concentration since 1960 to day (ERSL data)

According to most scientists, we have to reduce over 50% of greenhouse gases emissions in order to stabilize concentrations in the atmosphere and thus curb climate change.

To achieve this long term goal United Nations UN organizes yearly conference to assess progress in dealing with climate change Kyoto (1997) and Paris (2015) meetings were the most important conferences in the fight against the climate change because of the encouraging decision and actions that have been taken to reduce the greenhouse gases emissions. The COP21 held in Paris (2015) set out a framework for action aimed to strengthen the global response to the threat of climate change by keeping a global temperature rise this century below 2 degrees Celsius above pre-industrial levels and to pursue efforts to limit the temperature increase even further to 1.5 degrees Celsius, to reach this ambitious goal, it should keep the concentration of the principal gas in the greenhouse gases which is CO₂ (dioxide carbon) at 450 ppm.

To achieve this global long-term goal stated in the framework convention on climate change, it is necessary to use all mitigation options, according to the IPCC (Intergovernmental Panel on Climate Change), CCS (Carbon Capture and Storage) has large potential for global emission reductions [2].

Introduction

Climate change, also called global warming, refers to the rise in average surface temperatures on earth due to the dramatic increase of the greenhouse gases concentration in the atmosphere [1-5]. Among the various greenhouse gases, CO₂ is the greatest contributor, accounting for about 64% of the total greenhouse effects. Therefore, reducing the concentration of CO₂ in the atmosphere is a major challenge in any greenhouse gas mitigation strategy. Many approaches are already available for reducing CO₂ emissions to the atmosphere, however, it is unlikely that these methods are sufficient to meet the target of CO₂ mitigation agreed on through the Kyoto Protocol [10-19].

Carbon dioxide capture and storage (CCS) in deep geological formations is one of the most promising emerging technologies for large-scale reduction of CO₂ emissions [1-2].

Depleted or nearly depleted oil and gas reservoirs are ones of the most attractive storage locations for long term sequestration of CO₂ due to a number of technical and economic advantages [20-25]. Studies on CO₂ storage in oil and gas reservoirs have been extensively conducted in different aspects, such as underground migration simulation, geochemical modeling, long-term integrity and risk assessment. CO₂ injection into tertiary oil reservoirs has been widely accepted as an effective technique for enhanced oil recovery (EOR), and has been used by the oil industry for over 50 years.

CO₂-EOR could help achieve a win-win solution for business and for climate change mitigation goals, offering commercial opportunities for oil producers while also ensuring permanent storage of large quantities of CO₂ underground. Transforming practices to support climate change carbon storage objectives in addition to oil extraction, i.e. moving from simple EOR to "EOR+", represents a potentially attractive and cost-effective way to spur greater CCS action [77].

The main aim of this thesis is to investigate the potential of long term CO₂ storage in hydrocarbon reservoirs using computational techniques (reservoir simulation), such as VIP/Nexus landmark software, and apply the study on an oil reservoir located in South East of Algeria (Sif Fatima South West - SFSW) field.

To achieve the main objective of the study, the thesis is divided into two main parts, the aim of the first part is to make a literature review about the CO₂ storage in underground geological formations to learn more about the different technologies used in the CO₂ capture and transport which is the aim of the second chapter, the third chapter describes the physical and chemical properties of the CO₂ in the hydrocarbon reservoirs conditions and the

efficiency of the different trapping mechanisms to prevent CO₂ returns to the atmosphere. How estimating the storage capacity of the underground geological formations from different authors and scientists stand points and the different potential leakages pathways and the impact of the replacement of CO₂ to the original hydrocarbon in place in the reservoir integrity are explained in the fourth chapter.

The second part of this thesis is the essential part. Several works have been carried out and demonstrated in three main chapters in the purpose of investigating all the steps required to assess the capacity, performance and integrity of hydrocarbon reservoirs to store CO₂. The reservoir simulation software (VIP/Nexus), Interactive Petrophysics software (IP) and multi-paradigm numerical computing Matlab code are the main tools that have been used in this works.

Impact of Natural Fractures (chapter 5)

One of the most widespread hydrocarbon formations around the world are naturally fractured reservoirs, why the investigation of presences of natural fractures in reservoir integrity as well as the storage capacity is necessary, yet the effects of fractures are often poorly understood and largely underestimated, naturally fractured reservoirs present a flow paradox, these reservoirs initially may appear highly productivity/injectivity and decline rapidly, the property of high permeability of the fractures could potentially allow CO₂ to migrate quickly through the reservoir weak points, which could damage the prospective storage ability of a specific storage site.

Reservoir Properties Description (chapter 6)

A successful CCS project based mainly on the well-known of the reservoir properties distribution, the proper use of the comprehensive volume data is necessary for well prediction of the reservoir properties. The utilization of Hydraulic Flow Units Approach (HFU) to divide the reservoir into units with similar reservoir flow properties to estimate the permeability with enough accuracy combined with an artificial intelligent technique (ANFIS) to predict the flow zone indicator and effective porosity is the main objective of this chapter.

Modeling CO₂ Geological Storage in Hydrocarbon Reservoirs (chapter 7)

This chapter is the fundamental chapter and it is divided into three sections.

The first section describes the simulation software (Nexus) and its capability to handle the main physical phenomenons such as the solubility of the CO₂ in the

fluid in place (brine) by comparing the simulation results to experimental results.

The second section highlights the importance of “EOR+” which is combination of the carbon dioxide Enhanced Oil Recovery (CO₂-EOR) and permanent CO₂ storage in oil reservoirs and the potential CO₂ storage offered by EOR+.

The third section is a study includes a pilot project as the research based on real field sites is now strongly needed in order to maximize the efficiency of these technologies, to optimize the tools needed for monitoring and verification, and to be able to adapt to the specificity of local geological conditions. The Pilot projects can thus benefit investment decisions for deployment of CO₂ Capture and Storage (CCS) in the foreseeable future. Throughout this work an evaluation of the potential of SFSW to store CO₂ for long term period is carried out by including all previous results and recommendations.

Overview

The suggestion that climate change mitigation could be achieved by storing CO₂ derived from anthropogenic sources (i.e., human-caused release of CO₂) was made relatively recently, Marchetti in the 1970s suggested to store CO₂ in oceans, and Horn & Steinberg in the 1980s were among the first to suggest a process used to separate CO₂ from natural gas. Since the 2005 IPCC Special Report on Carbon Dioxide Capture and Storage (SRCCS), the option of storing CO₂ in ocean water has largely been abandoned because of high costs, low storage permanence, and considerable ecological impacts [1]. The current discussions revolve around the injection of CO₂ into geological reservoirs.

The injection of CO₂ underground was not totally new when it was first suggested for climate change mitigation. In the 1970s and 1980s, as production from oil fields in the United States was declining, oil companies started injecting water, natural gas, and CO₂ to recover more oil and extend the productive lifetime of oil reservoirs. Thousands of kilometres of CO₂ pipelines were constructed to transport the CO₂ from the natural reservoirs of CO₂, the primary CO₂ source, to the depleting oil fields. CO₂-enhanced oil recovery (EOR) was done almost exclusively using CO₂ from natural underground CO₂ reservoirs, so it was not leading to climate change mitigation. However, it did enable learning and practical experience about, for instance, how the subsurface responds to injection of fluids, which cap rock can sustain the CO₂ best, under which pressures injection can best take place, how wells are best placed, and how to organize pipeline transportation of CO₂ in a safe manner. Today, EOR remains a driver for CCS. But in the 1990s and 2000s, climate change mitigation emerged on the policy agenda and temporarily took over as the main driver of CCS. Subsequent IPCC assessment reports (published in 1990, 1996, 2001, and 2007) continued to strengthen the hypothesis that CO₂ and other greenhouse gas (GHG) emissions would lead to harmful and potentially even catastrophic consequences to livelihoods, ecosystems, and the global economy. In 1992, this had already led to the United Nations Framework Convention on Climate Change and in 1997 to the Kyoto Protocol, which included commitments of all developed countries to reduce their GHG emissions (although not all developed countries ratified or complied with the Kyoto provisions). However, despite these international agreements on climate change mitigation, addressing the seemingly unstoppable CO₂ emissions from coal-fired power remained an urgent and challenging problem without a viable solution until CCS emerged as a mitigation option [6-8].

Carbon Capture and Storage (CCS) in underground geologic formations is unique among the options for reducing CO₂ emissions because it offers the promise for continuing to use proven reserves of fossil fuels in a CO₂

constrained future. The basic idea behind CCS is that CO₂ is captured before it is emitted into the atmosphere and then injected deep underground where it would remain for thousands of years or longer. The idea of CCS was first developed in the late 1970's but did not get much attention until the late 1980's when scientists and engineers began to look earnestly for ways to reduce CO₂ emissions to the atmosphere. In that short time it has emerged as one of the most promising options for deep reductions in CO₂ emissions. So much so that, in fact, today 1 million tons of CO₂ is being stored annually at the Sleipner Project beneath the North Sea. Several more commercial projects are in the advanced stage of planning:

- Gorgon Project in Australia.
- Snohvit Project in the continental shelf offshore of Norway.

In addition to these, more are under development, the below table summarize the current and planned CCS projects in the worldwide.

Table. 2: Summary of current and planned CCS projects

Project (Operator)	Application	Mass of CO ₂ Million Tons/yr.	Capture Technology	Storage Formation
Sleipner, North-Sea (Statoil)	Storage of CO ₂ stripped from natural gas	1 since 1996	Amine-Scrubber	Off-shore salt-water sand formation
Weyburn, Canada (Encana)	EOR and CO ₂ storage from coal gasification	1.7 since 2000	Pre-combustion Gasification	On-shore oil reservoir in carbonate rock
In salah, Algeria (BP)	Storage of CO ₂ stripped from natural gas	1 planned for 2004	Amine-Scrubber	On-shore gas reservoir in sandstone.
Gorgon, Australia (Chevron Texaco)	Storage of CO ₂ stripped from natural gas	4 planned for 2006	Amine-Scrubber	Island salt-water sandstone formation
Snohvit, Off-shore Norway (Statoil)	Storage of CO ₂ stripped from natural gas	0.7 planned for 2006	Amine-Scrubber	Off-shore salt-water sandstone formation
San Juan Basin, New Mexico (Burlington)	Enhanced coal-bed methane production		Natural CO ₂ source	On-shore coal bed

Although of these projects current understanding of the most appropriate technologies for CO₂ sequestration in active or depleted oil and gas reservoirs is still limited, particularly outside of the U.S. to realize the large potential that depleted oil and gas reservoirs offer for sequestering CO₂, a number of technical, commercial and administrative obstacles first must be resolved. Overcoming these obstacles could enable CO₂ in depleted oil and gas reservoirs to be applied on a scale large enough to achieve globally meaningful reductions in CO₂ emissions.

Predicting how much CO₂ needs to be captured and stored in order to stabilize atmospheric CO₂ concentrations at safe levels is very difficult. The large number of variables such as future population growth, world-wide prosperity and standard of living, diffusion of new energy technologies, continued use of fossil fuels, natural carbon cycle dynamics and human behaviour all contribute to the uncertainty in predicting CCS requirements. Nevertheless, a number of studies have attempted to address these questions and most agree that trillions of tons of storage could be needed over the next several hundred years.

While the range of estimates is large, there is consensus that the largest potential capacity is in deep salt-water filled sandstones in large sedimentary basins. In fact, it is estimated that salt-water filled formations have the capacity to accommodate hundreds of years at current CO₂ emission rates. However, these capacity estimates have not yet been validated by regional or site-specific field experiments. As pointed out by Burruss (2004), better estimates may be available for oil and gas reservoirs. Burruss estimates that depleted oil and gas reservoirs in the U.S. have 40 to 50 years of storage capacity at today's emission rates.

Chapter 2
CO₂ Capture &
Transport
Technologies

CO₂ Capture & Transport Technologies

1- CO₂ Capture

1-1. Introduction

Capturing CO₂ from industrial gas streams to transport and storage it to appropriate sites is not a new process. In the natural gas industry, separating CO₂ from other gases by absorption processes using chemical solvent have been used since 1930, to produce food chemical grade from gas streams containing 3 to 25 % of CO₂ [8].

In the 1950s and 1960s, gas adsorption processes were developed to separate CO₂ from gas streams associated with hydrogen (H₂) production (refineries), nitrogen (N₂) separation, and dehydration. In the 1970s and 1980s, gas separation membranes were developed for EOR (oil/gas separation) and natural gas processing applications (Kohl and Nielsen, 1997).

The licensing history of the Econamine flue gases (FG) process provides a good example of past applications of CO₂ removal technologies (Chapel et al., 1999). Prior to 1999, 25 facilities were built with CO₂ capture capacities ranging from 635 to 365,000 tonnes per year using this process, three were coal-fired applications capturing 600 to 1,600 tonnes of CO₂ per year [1]. The captured CO₂ from these facilities was used for enhanced oil recovery (EOR), urea production, and in the food and beverage industry.

The capture rates of these facilities reflect the fact that they were built to serve a specific commercial market for CO₂. Other amine-based processes were implemented at similar capture rates during this period. By comparison, a single 550 megawatt (MW) net output coal-fired power plant capturing 90 % of the emitted CO₂ will need to separate approximately 5 million tonnes of CO₂ per year. Scaling up these existing processes represents a significant technical challenge and a potential barrier to widespread commercial deployment in the near term (DOE, 2010a).

A 2009 review of commercially available CO₂ capture technologies identified 17 operating facilities using either chemical or physical capture solvents (Dooley et al., 2009). These included four natural gas processing operations and a syngas production facility in which more than 1 million tonnes of CO₂ are being captured per year. The largest (a natural gas processing operation in Wyoming) captures 3.6 million tonnes per year, similar to the volumes that can be expected from electricity generating plants. However, it is unclear how transferable the experience with natural gas processing is to separation of power plant flue gases, given the significant differences in the chemical make-up of the two gas streams. In addition, integration of these technologies with

the power cycle at generating plants present significant cost and operating issues that will need to be addressed to facilitate widespread, cost-effective deployment of CO₂ capture.

1-2. CO₂ Capture Status

USA is one of the biggest CO emitters, one-quarter of U.S. CO₂ emissions come from the industrial sector, with the highest emissions coming from petroleum refining, chemical production, cement production, pulp and paper, and iron and steel production. Few studies or demonstration projects have enabled the evaluation of the applicability of CO₂ capture technologies to these industrial sources. Some industrial facilities (e.g., lime production, petroleum refineries, natural gas processing, and ammonia plants) produce relatively concentrated CO₂ streams. As previously mentioned, scrubbers have been used at some of these industrial facilities, though at very small scale, to capture CO₂ for specific use, such as EOR. The CO₂ from many of these facilities could likely be captured at lower cost, as the CO₂ is often already separated as part of the industrial process and thus may require little additional processing. However, there are currently few incentives, either regulatory or economic, to capture GHG emissions from these industrial sources. As a consequence, few of the available technologies are being employed on a wide scale.

In general, CO₂ capture technologies applicable to coal-fired power generation can be categorized into three approaches:

Pre-combustion systems are designed to separate CO₂ and H₂ in the high-pressure syngas produced at Integrated Gasification Combined Cycle (IGCC) power plants.

Post-combustion systems are designed to separate CO₂ from the flue gas produced by fossil-fuel combustion in air.

Oxy-combustion uses high-purity oxygen (O₂), rather than air, to combust coal and therefore produces a highly concentrated CO₂ stream.

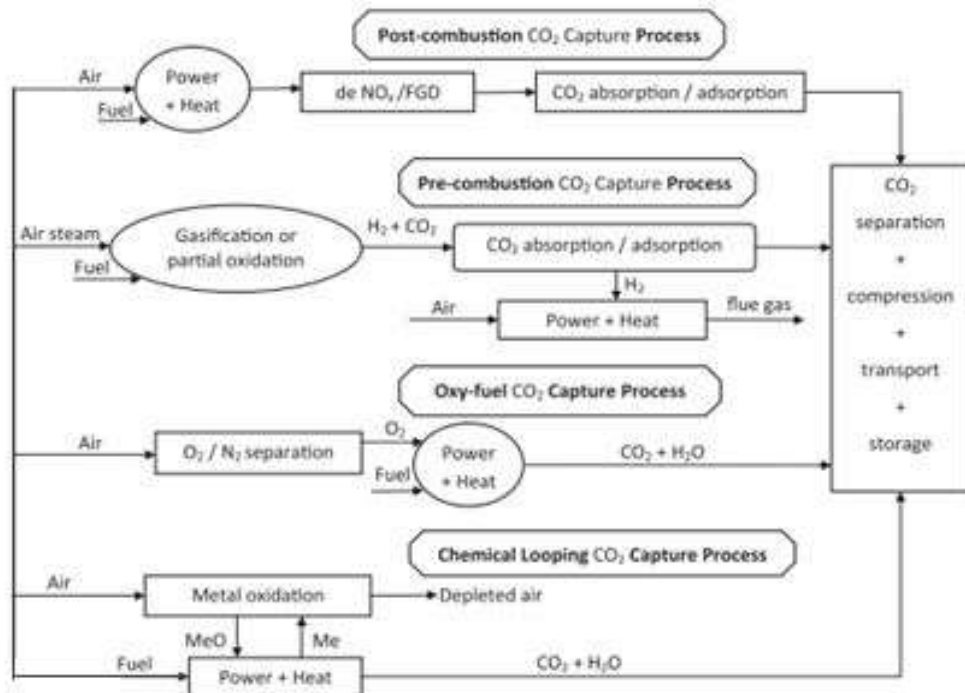


Fig. 5: CO₂ capture systems

Each of the CO₂-capture approaches results in increased capital and operating costs and decreased electricity output (or energy penalty), thereby increasing the cost of electricity (COE). The energy penalty occurs because the CO₂ capture process uses some of the energy produced from the plant.

1-3. CO₂ Capture systems

- Post-combustion capture systems

Post-combustion capture is a downstream process that is analogous to flue gas desulfurization. It involves the removal of CO₂ from the flue gas produced after the combustion of the fuel. Power plants, cement kilns, furnaces in industries and iron and steel production plants are the main stationary source of the anthropogenic CO₂ emissions, for the last centuries in the large scale processes, direct firing of fuel with air in combustion chamber has been the most economic technology to extract and use the fuel's energy but it has high effect in the CO₂ emission in the atmosphere. The post-combustion capture system is important strategy to mitigate CO₂ emission by transporting and storing it in safe underground formation.

Flue gases or stack gases found in combustion systems are usually at atmospheric pressure. Because of the low pressure, the large presence of nitrogen from air and the large scale of the units, huge flows of gases are generated, the largest example of which may be the stack emissions coming

from a natural gas combined cycle power plant having a maximum capacity of around 5 million normal m³/h. CO₂ contents of flue gases vary depending on the type of fuel used (between 3% for a natural gas combined cycle to less than 15% by volume for a coal-fired combustion plant [1]).

In the flue gases produced from the combustion of any type of fuel can be applied, however, the impurities in fuel is important for the design and costing of the entire plant (Rao and Rubin, 2002)

The post-combustion capture systems can be applied to flue gases produced from the combustion of any type of fuel. However, the impurities in the fuel are very important for the design and costing of the complete plant (Rao and Rubin, 2002).

Air pollutant such as SO_x, NO_x, particulates, HCl, HF, mercury, other metals and other trace organic and inorganic contaminants are included in the composition of the flue gases coming from coal combustion which it contains as well CO₂, N₂, O₂ and H₂O. Although capture of CO₂ in these flue gases is in principle more problematic and energy intensive than from other gas streams, commercial experience is available at a sufficiently large scale to provide the basis for cost estimates for post-combustion CO₂ capture systems. Also, a large R&D effort is being undertaken worldwide to develop more efficient and lower cost post-combustion systems, following all possible approaches for the CO₂ separation step (using sorbents, membranes or cryogenics).

- **Oxy-fuel combustion capture systems**

The dilution of the flue gases due to nitrogen is the main disadvantage of post-combustion capture systems, to mitigate this problem it is preferable to use the oxygen instead of the air in the combustion. An excessively high temperatures (as high as 3500°C) will be produced in the burning of fossil fuel in an atmosphere of oxygen.

An improvement in the oxy-fuel combustion process by eliminating nitrogen from the flue gas by combusting a hydrocarbon or carbonaceous fuel in either pure oxygen or a mixture of pure oxygen and a CO₂ - rich recycled flue gas (carbonaceous fuels include biomass).

The temperature limitation in typical gas turbine cycle is about 1300-1400°C and to about 1900°C in an oxy-fuel coal-fired boiler using current technology, which are too low comparing to the combustion of a fuel with pure oxygen (about 3500 °C), the combustion temperature is controlled by the proportion of flue gas and gaseous or liquid-water recycled back to the combustion chamber.

The flue gas contains mainly carbon dioxide and water vapour together and excess oxygen is required to ensure complete combustion of the fuel. After water vapor condensation using cooling, the net flue gas contains 80-98% CO₂ depending on the fuel used and the particular oxy-fuel combustion process. This concentrated CO₂ stream can be compressed, dried and further purified before delivery into a pipeline for storage. The CO₂ capture efficiency is very close to 100% in oxy-fuel combustion capture systems, this concentrated CO₂ stream can be compressed, dried and further purified from impurities SO_x, NO_x, HCl and Hg derived from the fuel used before delivery into a pipeline for storage. The CO₂ is transported by pipeline as a dense supercritical phase. Inert gases must be reduced to a low concentration to avoid two phase flow conditions developing in the pipeline systems. The acid gas components may need to be removed to comply with legislation covering co-disposal of toxic or hazardous waste or to avoid operations or environmental problems with disposal in deep saline reservoirs, hydrocarbon formations or in the ocean. The carbon dioxide must also be dried to prevent water condensation and corrosion in pipelines and allow use of conventional carbon-steel materials.

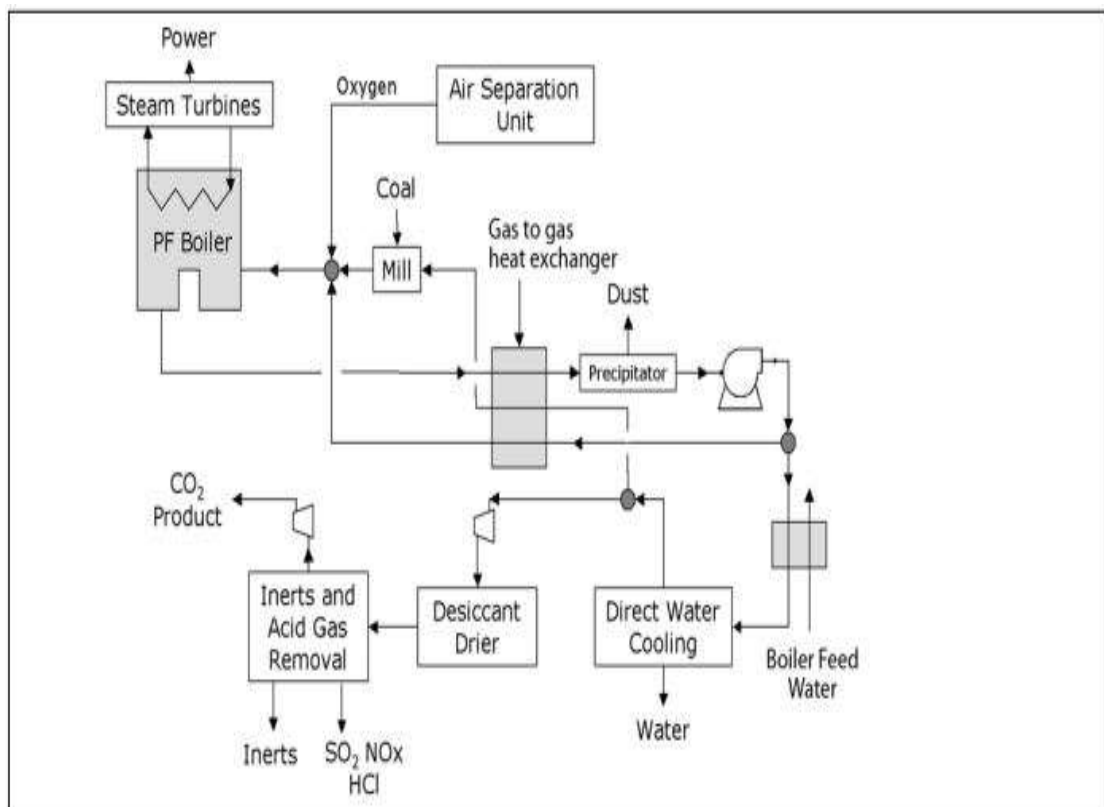
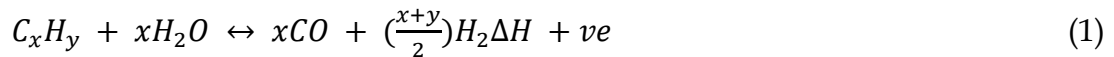


Fig. 6: Schema of an oxy-fuel, pulverized coal fired power plant

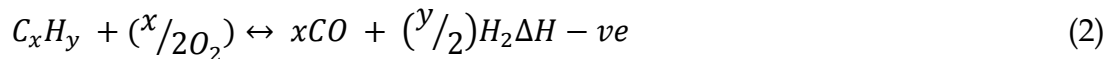
- Pre-combustion capture systems

Pre-combustion technologies either carbon or nitrogen is removed from the process before the combustion, the process is typically comprises several steps, from the primary fuel a mixture of hydrogen and carbon monoxide (syngas) is produced from first stage reaction, the two main routes are to add steam (reaction 1), in which case the process is called (steam reforming), or oxygen (reaction 2) to the primary fuel. In the latter case, the process is often called (partial oxidation) when applied to gaseous and liquid fuels and (gasification) when applied to a solid fuel, but the principles are the same.

Steam reforming

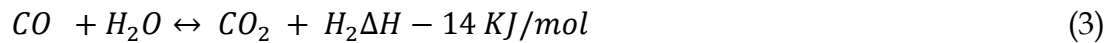


Partial oxidation



This is followed by the (shift) reaction to convert CO to CO₂ by the addition of steam (reaction 3):

Water Gas Shift Reaction



Finally, the CO₂ is removed from the CO₂/H₂ mixture. The concentration of CO₂ in the input to the CO₂/H₂ separation stage can be in the range 15-60% (dry basis) and the total pressure is typically 2-7 MPa. The separated CO₂ is then available for storage. It is possible to envisage two applications of pre-combustion capture.

The first is in producing a fuel (hydrogen) that is essentially carbon-free. Although the product H₂ does not need to be absolutely pure and may contain low levels of methane, CO or CO₂, the lower the level of carbon-containing compounds, the greater the reduction in CO₂ emissions. The H₂ fuel may also contain inert diluents, such as nitrogen (when air is typically used for partial oxidation), depending on the production process and can be fired in a range of heaters, boilers, gas turbines or fuel cells.

Secondly, pre-combustion capture can be used to reduce the carbon content of fuels, with the excess carbon (usually removed as CO₂) being made available for storage. For example, when using a low H: C ratio fuel such as coal it is possible to gasify the coal and to convert the syngas to liquid Fischer-Tropsch fuels and chemicals which have a higher H: C ratio than coal. In this section, we consider both of these applications. This section reports on technologies for

the production of H₂ with CO₂ capture that already exist and those that are currently emerging. It also describes enabling technologies that need to be developed to enhance the pre-combustion capture systems for power, hydrogen or syngas and chemicals production or combination of all three.

- **Chemical looping combustion**

Originally proposed by Richter and Knoche (1983) and with subsequent significant contributions by Ishida and Jin (1994), the main idea of chemical looping combustion is to split combustion of a hydrocarbon or carbonaceous fuel into separate oxidation and reduction reactions by introducing a suitable metal oxide as an oxygen carrier to circulate between two reactors. Separation of oxygen from air is accomplished by fixing the oxygen as a metal oxide. No air separation plant is required. The reaction between fuel and oxygen is accomplished in a second reactor by the release of oxygen from the metal oxide in a reducing atmosphere caused by the presence of a hydrocarbon or carbonaceous fuel. The recycle rate of the solid material between the two reactors and the average solids residence time in each reactor, control the heat balance and the temperature levels in each reactor. The effect of having combustion in two reactors compared to conventional combustion in a single stage is that the CO₂ is not diluted with nitrogen gas, but is almost pure after separation from water, without requiring any extra energy demand and costly external equipment for CO₂ separation.

Possible metal oxides are some oxides of common transition state metals, such as iron, nickel, copper and manganese (Zafar et al., 2005). The metal/metal oxide may be present in various forms, but most studies so far have assumed the use of particles with diameter 100-500 μm. In order to move particles between the two reactors, the particles are fluidized. This method also ensures efficient heat and mass transfer between the gases and the particles. A critical issue is the long-term mechanical and chemical stability of the particles that have to undergo repeated cycles of oxidation and reduction, to minimize the make-up requirement. When a chemical looping cycle is used in a gas turbine cycle, the mechanical strength for crushing and the filtration system is important to avoid damaging carry-over to the turbine.

The temperature in the reactors, according to available information in the literature, may be in the range 800°C- 1200°C. NO_x formation at these typical operating temperatures will always be low. The fuel conversion in the reduction reactor may not be complete, but it is likely (Cho et al., 2002) that the concentrations of methane and CO when burning natural gas are very small. In order to avoid deposit of carbon in the reduction reactor, it is necessary to use some steam together with the fuel.

The chemical looping principle may be applied either in a gas turbine cycle with pressurized oxidation and reduction reactors, or in a steam turbine cycle with atmospheric pressure in the reactors. In the case of a gas turbine cycle, the oxidation reactor replaces the combustion chamber of a conventional gas turbine. The exothermic oxidation reaction provides heat for increasing the air temperature entering the downstream expansion turbine. In addition, the reduction reactor exit stream may also be expanded in a turbine together with steam production for power generation. The cooled low pressure CO₂ stream will then be compressed to pipeline pressure. Another option is to generate steam using heat transfer surfaces in the oxidation reactor. Current circulating fluidized bed combustion technology operating at atmospheric pressure in both the oxidation and reduction stages necessitates the use of a steam turbine cycle for power generation. Using natural gas as fuel in a chemical looping combustion cycle which supplies a gas turbine combined cycle power plant and delivering CO₂ at atmospheric pressure, the potential for natural gas fuel-to-electricity conversion efficiency is estimated to be in the range 45-50% (Brandvoll and Bolland, 2004). Work on chemical looping combustion is currently in the pilot plant and materials research stage.

Table. 3: advantages and disadvantages of the different CO₂ capture technologies [16]

Capture process	Application area	Advantages	Disadvantages
Post-Combustion	Coal-fired and gas-fired plants	Technology more mature than other alternatives can easily retrofit into existing plants.	Low CO ₂ concentration affects the capture efficiency.
Pre-Combustion	Coal-gasification plants	high CO ₂ concentration enhance sorption efficiency, fully developed technology, commercially deployed at the required scale in some industrial sectors, opportunity for retrofit to existing plant.	Temperature associated heat transfer problem and efficiency decay issues associated with the use of hydrogen-rich gas turbine fuel, high parasitic power requirement for sorbent regeneration, inadequate experience due to few gasification plants currently operated in the market, high capital and operating costs for current sorption systems.
Oxyfuel-Combustion	Coal-fired and gas-fired plants	Very high CO ₂ concentration that enhances absorption efficiency, mature air separation technologies available, reduced volume of gas to be treated, hence required smaller boiler and other equipment.	High efficiency drop and energy penalty, cryogenic O ₂ production is costly, corrosion problem may arise.
Chemical looping Combustion	Coal-gasification plants	CO ₂ is the main combustion product, which remains unmixed with n ₂ , thus avoiding energy intensive air separation.	Process is still under development and inadequate large scale operation experience.

Table. 4: cost comparison for different CO₂ capture process

Fuel Type	Parameter	Capture Technology			
		No capture	Post-combustion	Pre-combustion	Oxy-fuel
Coal-fired	Thermal efficiency (%LHV)	44.0	34.8	31.5	35.4
	Capital cost (\$/kW)	1410	1980	1820	2210
	Electricity cost (c/kWh)	5.4	7.5	6.9	7.8
	Cost of CO ₂ avoided (\$/tCO ₂)	-	34	23	36
Gas-fired	Thermal efficiency (%LHV)	55.6	47.4	41.5	44.7
	Capital cost (\$/kW)	500	870	1180	1530
	Electricity cost (c/kWh)	6.2	8.0	9.7	10.0
	Cost of CO ₂ avoided (\$/tCO ₂)	-	58	112	102

1-4. CO₂ Capture Technologies

There are four different CO₂ removal technologies which are widely practiced in industry. These are

- 1) Absorption, both chemical and physical.
- 2) Adsorption.
- 3) Membranes.
- 4) Cryogenic processes.

Absorption processes

Chemical absorption processes at present are the preferred option for post-combustion capture of CO₂. Chemical absorption systems have been in use since the 1930s for the capture of CO₂ from ammonia plants for use in food applications and hence, are a commercially realized technology, though not at the scale required for power plants. CO₂ is separated from the flue gas by passing the flue gas through a continuous scrubbing system. The system consists of an absorber and a desorber [16]. Absorption processes utilize the reversible chemical reaction of CO₂ with an aqueous alkaline solvent, usually an amine. In the desorber, the absorbed CO₂ is stripped from the solution and a pure stream of CO₂ is sent for compression while the regenerated solvent is sent back to the absorber. Heat is required in the reboiler to heat up the solvent

to the required temperature; to provide the heat of desorption and to produce steam in order to establish the required driving force for CO₂ stripping from the solvent [33]. This leads to the main energy penalty on the power plant. In addition, energy is required to compress the CO₂ to the conditions needed for storage and to operate the pumps and blowers in the process.

The key parameters determining the technical and economic operation of a CO₂ absorption system are:

- Flue gas flow rate - The flue gas flow rate will determine the size of the absorber and the absorber represents a sizeable contribution to the overall cost.
- CO₂ content in flue gas - Since flue gas is usually at atmospheric pressure, the partial pressure of CO₂ will be as low as 3-15 kPa. Under these low CO₂ partial pressure conditions, aqueous amines (chemical solvents) are the most suitable absorption solvents (Kohl and Nielsen, 1997).
- CO₂ removal - In practice, typical CO₂ recoveries are between 80% and 95%. The exact recovery choice is an economic trade-off, a higher recovery will lead to a taller absorption column, higher energy penalties and hence increased costs.
- Solvent flow rate - The solvent flow rate will determine the size of most equipment apart from the absorber. For a given solvent, the flow rate will be fixed by the previous parameters and also the chosen CO₂ concentrations within the lean and the rich solutions.
- Energy requirement - The energy consumption of the process is the sum of the thermal energy needed to regenerate the solvents and the electrical energy required to operate liquid pumps and the flue gas blower or fan. Energy is also required to compress the CO₂ recovered to the final pressure required for transport and storage.
- Cooling requirement - Cooling is needed to bring the flue gas and solvent temperatures down to temperature levels required for efficient absorption of CO₂. Also, the product from the stripper will require cooling to recover steam from the stripping process.

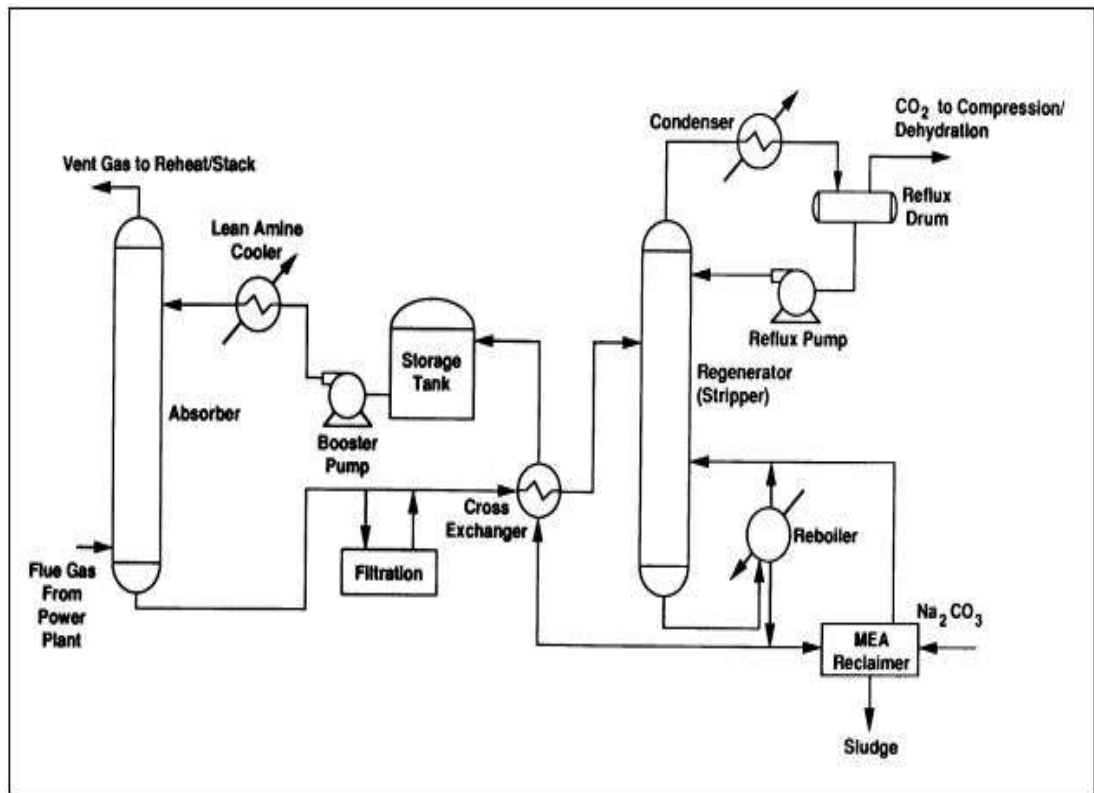


Fig.7: Process flow diagram for CO₂ recovery from flue gas by chemical absorption.

Adsorption Processes

In contrast to absorption processes which use a liquid absorbent, a solids or bent is used to bind the CO₂ on its surfaces. Large specific surface area, high selectivity and high regeneration ability are the main criteria for sorbent selection. Typical sorbents include molecular sieves, activated carbon, zeolites, calcium oxides, hydrotalcites and lithium zirconate. The adsorbed CO₂ can be recovered by swinging the pressure (PSA) or temperature (TSA) of the system containing the CO₂- saturated sorbent [16]. PSA is a commercial available technology for CO₂ recovery from power plants that can have efficiency higher than 85%. In this process, CO₂ is preferentially adsorbed on the surface of a solid adsorbent at high pressure, which will swing to low pressure (usually atmospheric pressure) to desorb the adsorbent and release CO₂ for subsequent transport. In TSA, the adsorbed CO₂ will be released by increasing the system temperature using hot air or steam injection. There-generation time is normally longer than PSA but CO₂ purity higher than 95% and recovery higher than 80% can be achieved. Operating cost of a specific TSA process was estimated to be of the order of 80–150 US\$/tonne CO₂ captured. Finally, the use of residues from industrial and agricultural operations to develop sorbents for CO₂ capture has attracted significant attention to reduce the total costs of capture [13].

Separation with membranes

Separation of the CO₂ using membrane system which is specially manufactured materials that allow the selective permeation of a gas through them, the nature of the material is the main parameter used to select the appropriate membrane, but the flow of gas through the membrane is usually driven by the differential pressure across the membrane, therefore, high-pressure streams are usually preferred for membrane separation. There are many different types of membrane materials (polymeric, metallic, ceramic) that may find application in CO₂ capture systems to preferentially separate H₂ from a fuel gas stream, CO₂ from a range of process streams or O₂ from air with the separated O₂ subsequently aiding the production of a highly concentrated CO₂ stream. Although of many commercial applications currently in industry (large scale, CO₂ separation from natural gas) the membrane separation technology is not yet applicable due to the cost and reliability required for CO₂ capture system. A large worldwide R&D effort is in progress aimed at the manufacture of more suitable membrane materials for CO₂ capture in large-scale applications.

Distillation of a liquefied gas stream and refrigerated separation

Compressing, cooling and expansion steps can make liquid from a gas, by distilling the formed liquid the components of the gas can be separated, in the case of air, this operation is currently carried out commercially on a large scale. Oxygen can be separated from air and be used in a range of CO₂ capture systems (oxy-fuel combustion and pre-combustion capture). As mentioned in the previous paragraphs, the main issue for these systems is the large flow of oxygen required. Refrigerated separation can also be used to separate CO₂ from other gases and to separate impurities from relatively high purity CO₂ streams, for example, from oxy-fuel combustion and for CO₂ removal from natural gas or synthesis gas that has undergone a shift conversion of CO to CO₂.

Hydrate-based separation

Hydrate-based CO₂ separation is a new technology by which the exhaust gas containing CO₂ is exposed to water under high pressure forming hydrates. The CO₂ in the exhaust gas is selectively engaged in the cages of hydrate and is separated from other gases. The mechanism is based on the differences of phase equilibrium of CO₂ with other gases, where CO₂ can form hydrates easier than other gases such as N₂ [31]. This technology has the advantage of small energy penalty (6-8%) and the energy consumption of CO₂ capture via hydrate could be as low as 0.57 kWh/kg-CO₂. Improving the hydrate formation rate and reducing hydrate pressure can improve the CO₂ capture efficiency. Tetrahydrofuran (THF) is a water-miscible solvent, which can form

solid clathrate hydrate structures with water at low temperatures. So the presence of THF facilitates the formation of hydrate and is frequently used as a thermodynamic promoter for hydrate formation [31] found that the presence of small amount of THF substantially reduces the hydrate formation pressure from a flue gas mixture (CO₂/N₂) and offers the possibility to capture CO₂ at medium pressures.

Table. 5: Comparison of different separation technologies [16]

Technology	Advantage	Disadvantage
Absorption	<ul style="list-style-type: none"> - High absorption efficiency (>90%). - Sorbents can be regenerated by heating and/or depressurization. - Most mature process for CO₂ separation. 	<ul style="list-style-type: none"> - Absorption efficiency depends on CO₂ concentration. - Significant amounts of heat for absorbent regeneration are required. - Environmental impact related to sorbent degradation have be unrestored.
Adsorption	<ul style="list-style-type: none"> - Process is reversible and the absorbent can be recycled. - High adsorption efficiency achievable (>85%). 	<ul style="list-style-type: none"> - Require high temperature adsorbent. - High energy required for CO₂ desorption.
Chemical looping combustion	<ul style="list-style-type: none"> - CO₂ is the main combustion product, which remains unmixed with N₂, thus avoiding energy intensive air separation. 	<ul style="list-style-type: none"> - Process is still under development and there is no large scale operation experience.
Membrane separation	<ul style="list-style-type: none"> - Process has been adopted for separation of other gases. - High separation efficiency achievable (>80%). 	<ul style="list-style-type: none"> - Operational problems included low fluxes and fouling.
Hydrate-based separation	<ul style="list-style-type: none"> - Small energy penalty. 	<ul style="list-style-type: none"> - New technology and more research and development is required.
Cryogenic distillation	<ul style="list-style-type: none"> - Mature technology. - Adopted for many years in industry for CO₂ recovery. 	<ul style="list-style-type: none"> - Only viable for very high CO₂ concentration > 90% v/v. - Should be conducted at very low temperature. - Process is very energy intensive.

1-5. CO₂ Capture in In-Salah Project in Algeria

1.5.1- Source of the CO₂ in In-Salah project

In Salah project is the first onshore CO₂ sequestration project in the worldwide, the source of the carbon dioxide CO₂ in In Salah CCS project is the natural gas produced from the different gas reservoirs, Sonatrach and its partners invested around 100 MMUSD to avoid venting the produced CO₂ in the atmosphere, the below plot shows the forecast CO₂ production from different sources [15].

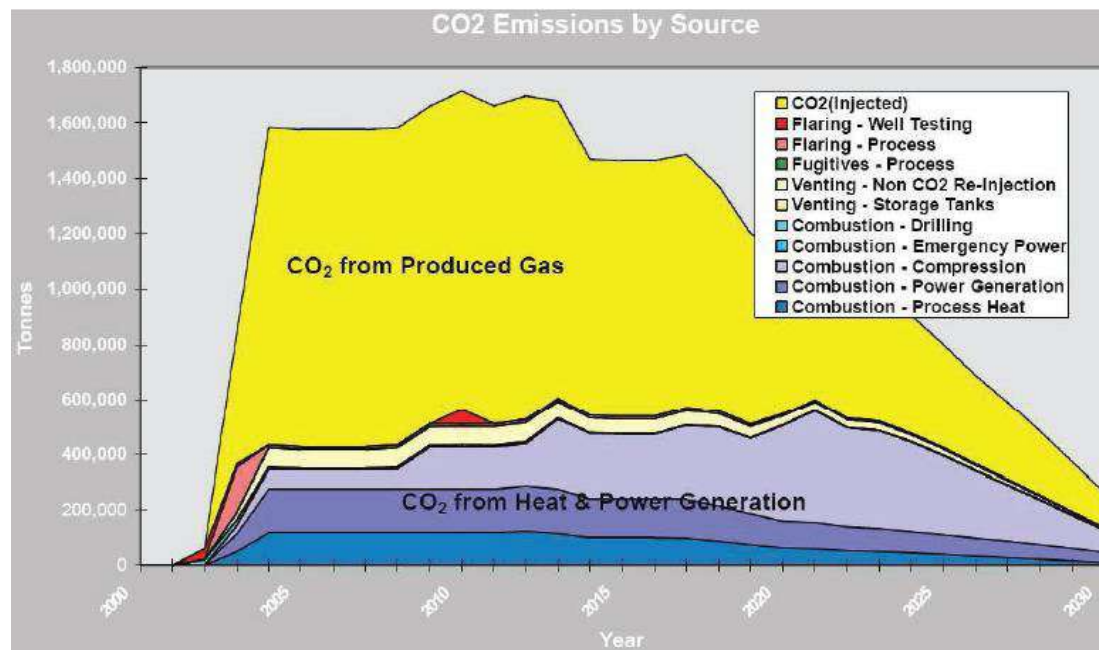


Fig. 8: CO₂ production forecast from different sources in In Salah project [15]

As shown above, the produced gas contains high CO₂ concentration, varying between (1 to 10%), so this CO₂ in the produced gas is captured and removed to meet the marketing standards requirement (0.03%), and instead of venting this considerable amount of CO₂ in the atmosphere, Sonatrach and its partners spent more than 100 MMUSD for dehydrating, compressing, transporting and injecting it into adjacent saline aquifer.

1.5.2- Capture process of the CO₂ in In-Salah project

The development of CCS In-Salah project was guided by the six CVP (Capital Value Process) stages, which are, Appraise, Planning, Monitoring, Execute, Operate and Abandonment, and currently is in operation stage, for the purpose of selecting an appropriate reservoir to be used as secure storage location, technical and risk assessment evaluation of several reservoirs were considered and evaluated. Krechba, Carboniferous reservoir was selected during the definition stage of the CVP process to be used as secure storage location.

The dehydrate gas coming from the other fields in In-Salah is transported via inter fields pipelines and mix with Krechba gas, two inlet separators are

installed to remove liquid, another separation stage is necessary for the resultant gas to ensure the removal of all liquids prior passing through AGRU (Acid Gas Removal Unit), where the CO₂ is removed from the export gas, the removed CO₂ will be compressed and re-injected into Krechba reservoir.

- **Acid Gas Removal Unit (AGRU)**

The capture system used in In Salah CCS project is Post-combustion process, acid gas removal unit is considered as two separation sections, Absorption section of CO₂, Decarbonization in which the CO₂ is eliminated by absorption process using active Amine as absorption agent, the second section is the regeneration of the absorption agent to be reused [15].

- **Decarbonization**

The CO₂ elimination unit is composed of two extraction trains, the treatment of the mixture gas coming from Krechba and the other fields is passing by AGRU installed in Krechba CPF (Centre Production Facilities) to remove the CO₂ and send it through the homogenization cyclone to mix the gases to be ready for exportation.

The feeding gas used in the two CO₂ extraction trains comes with a pressure of 72.3 bars and temperature varying between (25-35) °C, the feed gas preheater is increasing the temperature of the feed gas up to 55°C, exchanging of the heat with amine solution regenerated and cooled with the atmosphere before the entering of the gas into CO₂ absorber column, the increasing of the temperature improve the reaction speed and contact time into the absorber.

The feeding gas preheated is going to the bottom of vertical CO₂ absorber column and it will be in contact with against-flow of poor amine solution flow descending through the column, the rich amine solution going to the top of the column at about 55 °C via liquid distributor, the column has 8 m height allow an intimate contact between the gas flow and absorber agent.

The poor amine solution absorbs CO₂ and H₂S present in the feed gas with required specification. The treated gas leaves the top of the CO₂ absorber column at 71.4 bar pressure and a temperature of 55 °C and pass through the drying equipment for exportation, the mitigated gas leaving the absorber is contains high water percentage according to the operator parameters, its temperature is determined by the poor amine solution in the entered solution, this temperature helps in the water balance around AGRU and drying glycol contactors of the exported gas located in the inlet, through the Feed Gas Preheater located downstream of the air cooler of the regenerated amine solution, it is possible to cool the regenerated solution to a temperature lower than that achievable with the ambient air, and consequently, to control water

loss of AGRU and extra conditions of outside water. In order to reduce the loss of the rich amine solution out of the absorber, a demister is installed at the top of the column.

The AGRU designed for a feed gas global flow rate of 1,338,416 cm³/h and dry gas theoretical concentration of CO₂ and H₂S respectively 6.6 mole% and 15 ppmv.

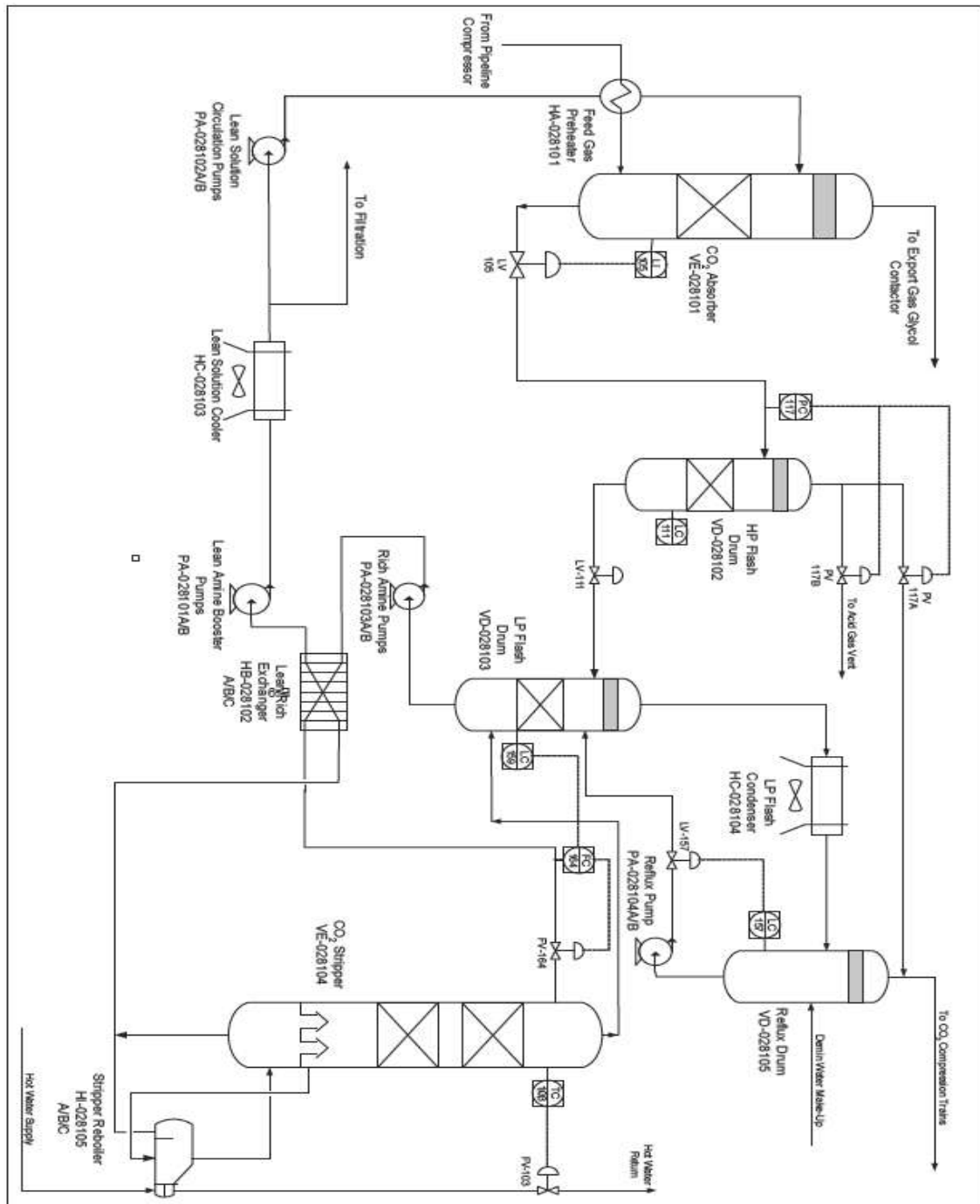


Fig. 9: Schema of CO₂ elimination and regeneration of the Amine.

2- CO₂ TRANSPORT

2-1. INTRODUCTION

Once CO₂ is separated from the rest of the flue gas components it needs to be transported to the storage site or to the facilities for its industrial utilization. CO₂ is transported in three states, gas, liquid and solid. Commercial-scale transport uses tanks, pipelines and ships for gaseous and liquid carbon dioxide, tanks, pipelines and ships for gaseous and liquid carbon dioxide. A study related to CCS in the North Sea highlights that CO₂ transport by ship tanker, using technologies derived from the LPG carriers, is feasible and cost competitive with pipelines with a total cost ranging from 20 to 30USD/tonne when more than 2 MtCO₂/year are transported within the distances involved in North Sea storage [13].

Pipelines are considered to be the most viable method for onshore transport of high volume of CO₂ through long distances as CCS would likely involve when widely deployed, pipelines are also the most efficient way for CO₂ transport when the source of CO₂ is a power plant which life-time is longer than 23 years. For shorter period road and rail tankers are more competitive. The cost of transport varies considerably with regional economic situation. A cost analysis in China shows that for a mass flow of 4000 tCO₂/day the use of ship tankers will cost 7.48 USD/tonne CO₂ compared with 12.64 USD/tonne CO₂ for rail way tankers and 7.05 USD/tonne CO₂ for 300 km pipelines.

Gas transported at close to atmospheric pressure occupies such a large volume that very large facilities are needed. Gas occupies less volume if it is compressed, and compressed gas is transported by pipeline. Volume can be further reduced by liquefaction, solidification or hydration. Liquefaction is an established technology for gas transport by ship as LPG (liquefied petroleum gas) and LNG (liquefied natural gas). This existing technology and experience can be transferred to liquid CO₂ transport. Solidification needs much more energy compared with other options, and is inferior from a cost and energy viewpoint. Each of the commercially viable technologies is currently used to transport carbon dioxide.

For commercial scale CCS projects an extensive network of CO₂ pipelines needs to be developed. An integrate network, where different sources will merge for their final transport to the storage areas, can reduce the total pipelines length by 25%, but it will require that all sources produce CO₂ stream with the same quality (e.g. pressure, T, water content) before being combined together. In order to optimize the mass/volume ratio CO₂ is carried as dense phase either in liquid or supercritical conditions. Supercritical is the preferred state for CO₂ transported by pipelines, which implies that the pipelines operative

temperature and pressure should be maintained within the CO₂ supercritical envelop, i.e. above 32.1 °C and 72.9 atm. The typical range of pressure and temperature for a CO₂ pipeline is between 85 and 150 bar, and between 13 °C and 44 °C to ensure a stable single phase flow through the pipeline. The drop in pressure due to the reduction of the hydraulic head along the pipeline is compensated by adding recompression stations. Larger diameter pipelines allow lower flow rates with smaller pressure drop and therefore a reduced number of recompression stations, on the other hand larger pipelines are more expensive therefore a balancing of costs needs to be considered.

2-2. CO₂ Transport Systems

- Pipeline systems

CO₂ pipeline operators have established minimum specifications for composition of the gas transported. This specification is for gas for an enhanced oil recovery (EOR) project, and parts of it would not necessarily apply to a CO₂ storage project. Low nitrogen content is important for EOR, but would not be so significant for CCS. A CO₂ pipeline through populated areas might have a lower specified maximum H₂S content, Impurities in the CO₂ stream represent a serious issue because their presence can change the boundaries of the pressure and temperature envelope within which a single-phase flow is stable. Moreover, the presence of water concentration above 50 ppm may lead to the formation of carbonic acid inside the pipeline and cause corrosion problems. Hydrates may also form that may affect the operation of valves and compressors. The estimated values of corrosion on the carbon steel commonly used for pipeline's construction can be up to 10mm/year, currently only a few pipelines are used to carry CO₂ and are almost all for EOR projects. The following are the largest pipelines in USA

- Canyon Reef

Is the oldest pipeline in USA, a 352 km pipeline built in 1970 by the SACROC for EOR in Texas (USA), moved 1200 tonnes of anthropogenic produced CO₂ daily (4.4 Mt/yr) from Shell Oil Company gas processing plants in the Texas Val Verde basin

- Bravo Dome Pipeline

Oxy Permian constructed this 508 mm (20 inch) line connecting the Bravo Dome CO₂ field with other major pipelines. It is capable of carrying 7.3 MtCO₂/yr and is operated by Kinder Morgan.

- **Cortez Pipeline**

Built in 1982 to supply CO₂ from the McElmo Dome in S.E. Colorado, the 762 mm (30inch), 803 km pipeline carries approximately 20 Mt CO₂/yr. to the CO₂ hub at Denver City, Texas. The line starts near Cortez, Colorado, and crosses the Rocky Mountains, where it interconnects with other CO₂ lines.

- **Sheep Mountain Pipeline**

BP Oil constructed this 610 mm (24 inch) 772 km line capable of carrying 9.2 MtCO₂/yr. from another naturally occurring source in southeast Colorado. It connects to the Bravo Dome line and into the other major carriers at Denver City and now is operated by Kinder Morgan.

- **Weyburn Pipeline**

This 330 km, (305-356 mm diameter) system carries more than 5000 tonne/day (1.8 Mt/yr) of CO₂ from the Great Plains Synfuels Plant near Beulah, North Dakota to the Weyburn EOR project in Saskatchewan, the composition of the gas carried by the pipeline is typically CO₂ 96%, H₂S 0.9%, CH₄ 0.7%, C₂₊ hydrocarbons 2.3%, CO 0.1%, N₂ less than 300 ppm, O₂ less than 50 ppm and H₂O less than 20 ppm (UK Department of Trade and Industry, 2002). The delivery pressure at Weyburn is 15.2 MPa. There are no intermediate compressor stations. The amount allocated to build the pipeline was 110 US \$ million (0.33 x 10⁶ US\$/km) in 1997.

The following table summarize the existing long-distance pipelines

Table. 6: Existing long distance CO₂ pipelines (Gale and Davison, 2002)

Pipeline	Location	Operator	Capacity (MtCO ₂ /yr.)	Length (km)	Year finished	Origin of CO ₂
Cortez	USA	Kinder Morgan	19.3	808	1984	McElmo Dome
Sheep Mountain	USA	BP Amoco	9.5	660	-	Sheep Mountain
Bravo	USA	BP Amoco	7.3	350	1984	Bravo Dome
Canyon Reef Carries	USA	Kinder Morgan	5.2	225	1972	Gasification plants
Val Verde	USA	Petrosource	2.5	130	1998	Val Verde Gas Plants
Bati Raman	Turkey	Turkish Petroleum	1.1	90	1983	Dodan Field
Weyburn	USA & Canada	North Dakota Gasification Co.	5	328	2000	Gasification Plant
Total			49.9	2591		

2-3. Ships for CO₂ transportation

- Marine transportation system

Carbon dioxide is continuously captured at the plant on land, but the cycle of ship transport is discrete, and so a marine transportation system includes temporary storage on land and a loading facility. The capacity, service speed, number of ships and shipping schedule will be planned, taking into consideration, the capture rate of CO₂, transport distance, and social and technical restrictions. This issue is, of course, not specific to the case of CO₂ transport; CO₂ transportation by ship has a number of similarities to liquefied petroleum gas (LPG) transportation by ship.

What happens at the delivery point depends on the CO₂ storage system. If the delivery point is onshore, the CO₂ is unloaded from the ships into temporary storage tanks. If the delivery point is offshore – as in the ocean storage option – ships might unload to a platform, to a floating storage facility (similar to a floating production and storage facility routinely applied to offshore petroleum production), to a single-buoy mooring or directly to a storage system.

The use of ships for transporting CO₂ across the sea is today in an embryonic stage. Worldwide there are only four small ships used for this purpose. These ships transport liquefied food-grade CO₂ from large point sources of concentrated carbon dioxide such as ammonia plants in northern Europe to coastal distribution terminals in the consuming regions. From these distribution terminals CO₂ is transported to the customers either by tanker trucks or in pressurized cylinders. Design work is ongoing in Norway and Japan for larger CO₂ ships and their associated liquefaction and intermediate storage facilities.

Chapter 3
CO₂ Chemical-
Physical Properties
& Trapping
mechanisms

CO₂ Chemical-Physical Properties & Trapping mechanisms

1- CO₂ Chemical-Physical Properties

1-1. Introduction:

Carbon dioxide is a chemical compound of two elements, carbon and oxygen, in the ratio of one to two, its molecular formula is CO₂. It is present in the atmosphere in small quantities and plays a vital role in the Earth's environment as a necessary ingredient in the life cycle. CO₂ gas has a slightly irritating odour, is colourless and is denser than air. Although it is a normal, if minor, constituent of air, high concentrations of CO₂ can be dangerous.

The successful of the CCS projects requires an accurate representation of the thermodynamic and thermo-physical properties of the fluid in situ (hydrocarbon or brine) and CO₂ mixtures, in the storage reservoir and during the capture and transport stages.

1-2. Physical properties of CO₂

At normal temperature and pressure, carbon dioxide is a gas. The physical state of CO₂ varies with temperature and pressure as shown in below figure, at low temperatures CO₂ is a solid; on warming, if the pressure is below 5.1 bar, the solid will sublime directly into the vapour state. At intermediate temperatures (between -56.5o C, the temperature of the triple point, and 31.1o C, the critical point), CO₂ may be turned from a vapour into a liquid by compressing it to the corresponding liquefaction pressure (and removing the heat produced). At temperatures higher than 31.1o C (if the pressure is greater than 73.9 bar, the pressure at the critical point), CO₂ is said to be in a supercritical state where it behaves as a gas; indeed under high pressure, the density of the gas can be very large, approaching or even exceeding the density of liquid water. This is an important aspect of CO₂'s behaviour and is particularly relevant for its storage.

Heat is released or absorbed in each of the phase changes across the solid-gas, solid-liquid and liquid-gas boundaries. However, the phase changes from the supercritical condition to liquid or from supercritical to gas do not require or release heat. This property is useful for the design of CO₂ compression facilities since, if this can be exploited, it avoids the need to handle the heat associated with the liquid-gas phase change.

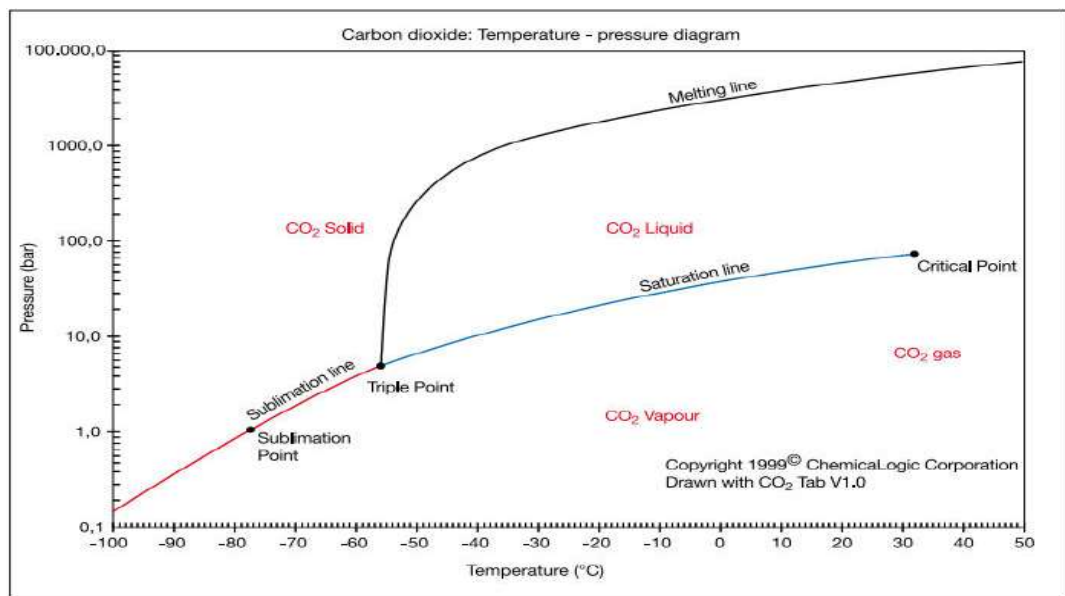


Fig. 10: Phase diagram for CO₂

There is a substantial body of scientific information available on the physical properties of CO₂. Selected physical properties of CO₂ are given in the below Table. The phase diagram for CO₂ is shown in previous Figure. Many authors have investigated the equation of state for CO₂ (e.g., Span and Wagner, 1996). The next figures shown respectively the variation of the density of CO₂ as a function of temperature and pressure, the variation of vapour pressure of CO₂ with temperature, the variation of viscosity with temperature and pressure, further information on viscosity can be found in Fenghour et al. (1998), the pressure-enthalpy chart for CO₂ and the solubility of CO₂ in water.

Table. 7: Physical properties of CO₂

Property	Value
Molecular weight	44.01
Critical temperature	31.1 °C
Critical pressure	73.9 bar
Critical density	467 kg/m ³
Triple point temperature	-56.5 °C
Triple pressure	5.18 bar
Boiling (sublimation) point (1.013 bar)	-78.5 °C
Gas Phase	
Gas density (1.013 bar at boiling point)	2.814 kg/m ³
Gas density (@STP)	1.976 kg/m ³
Specific volume (@STP)	0.506 m ³ /kg
C _p (@STP)	0.0364 kJ/(mol.K)
C _v (@STP)	0.0278 kJ/(mol.K)
C _p /C _v (@STP)	1.308
Viscosity (@STP)	13.72 μN.s/m ² (or μPa.s)
Thermal conductivity (@STP)	14.65 mW (m/K)
Solubility in water (@STP)	1.716 vol/vol
Enthalpy (@STP)	21.34 kJ/mol
Entropy (@STP)	117.2 J mol/K
Entropy of formation	213.8 J mol/K
Liquid Phase	
Vapour pressure (@ 20 °C)	58.5 bar
Liquid density (@ -20 °C and 19.7 bar)	1032 kg/m ³
Viscosity (@STP)	99 μN.s/m (or μPa.s)
Solid Phase	
Density of carbon dioxide snow at freezing point	1562 kg/m ³
Latent heat of vaporisation (1.013 bar at sublimation point)	571.1 kJ/kg

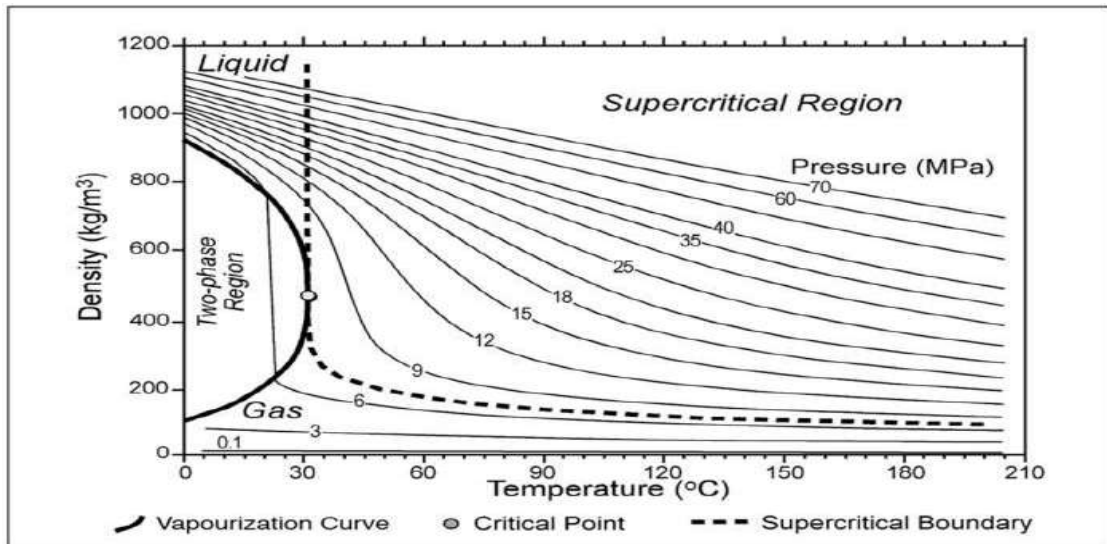


Fig. 11: Variation of CO₂ as a function of temperature and pressure (Bachu, 2003)

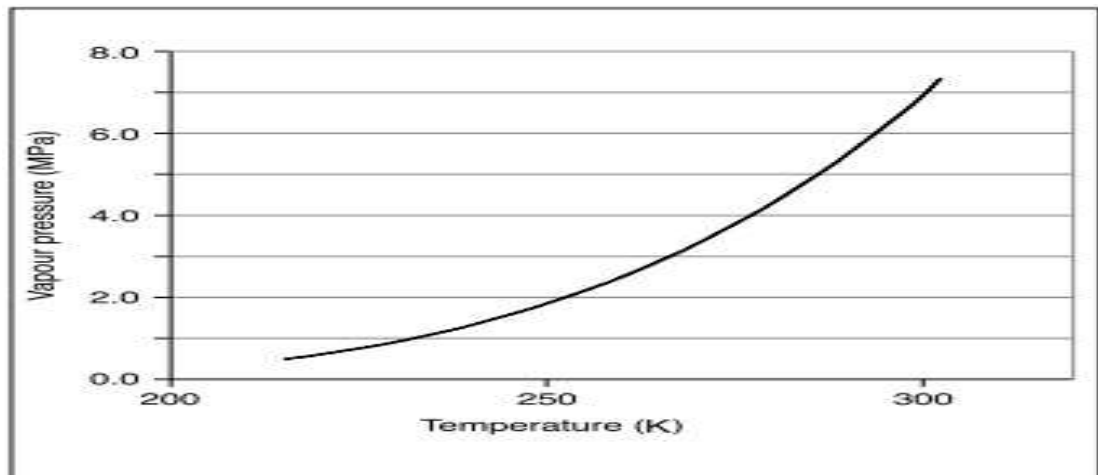


Fig. 12: Vapor pressure of CO₂ as a function of temperature (Span and Wagner, 1996)

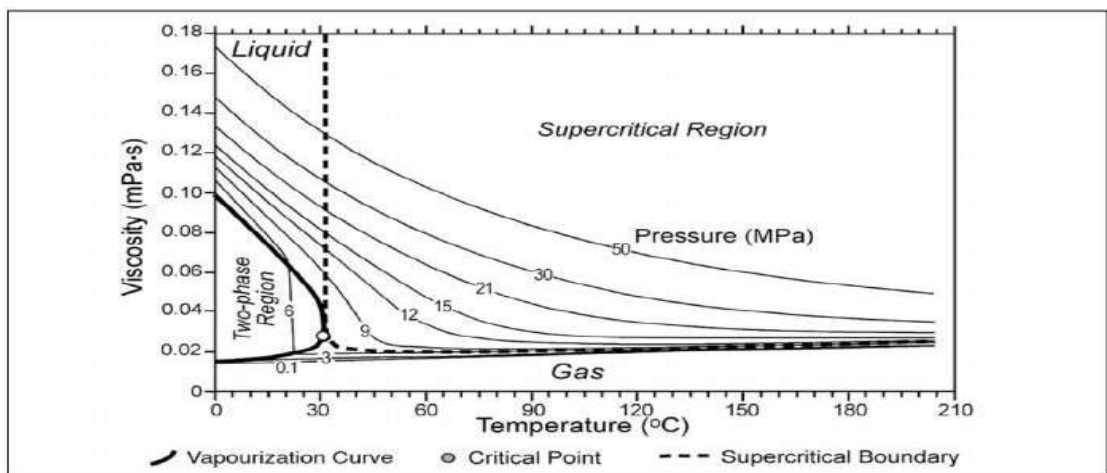


Fig. 13: Variation of CO₂ viscosity as a function of temperature and pressure (Bachu, 2003)

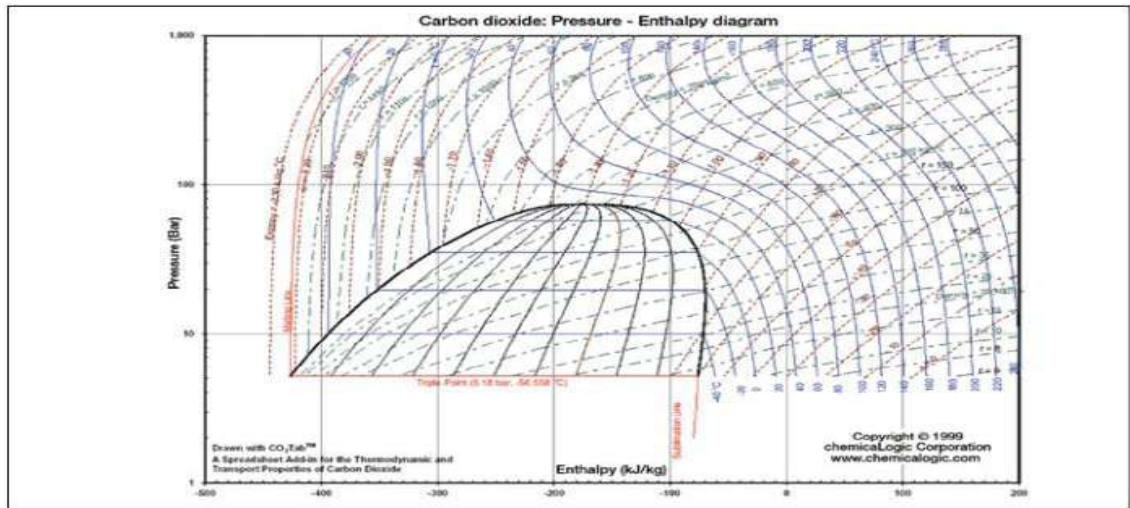


Fig. 14: Pressure-Enthalpy chart for CO₂

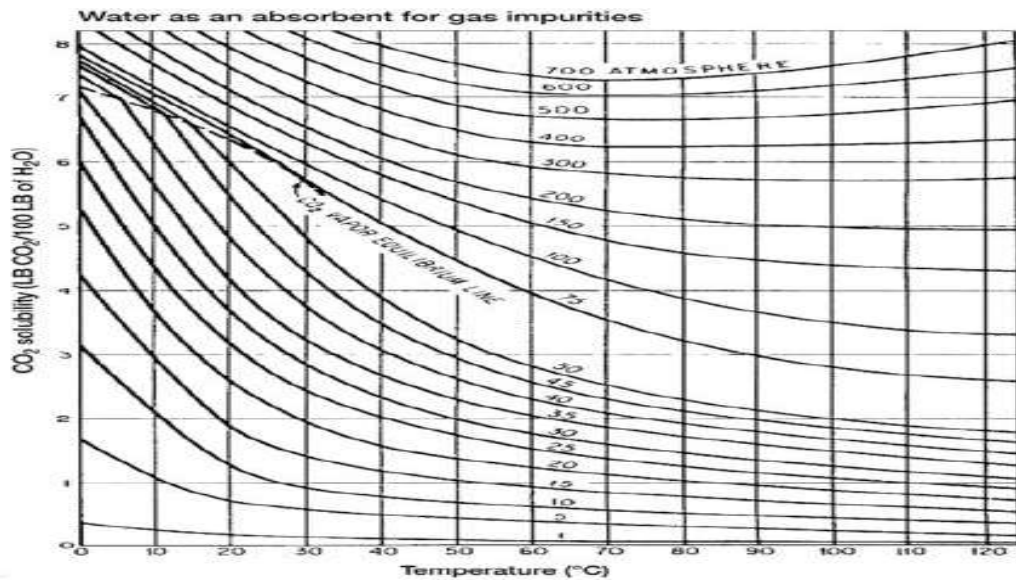


Fig. 15: Solubility of CO₂ in water (Kohl and Nielsen, 1997)

1-3. Chemical properties of CO₂

Some thermodynamic data for CO₂ and a few related compounds are given in Table below,

Table. 8: Thermodynamic data for selected carbon-containing compounds (ref. Cox et al., 1989 and other sources).

Compound	Heat of formation ΔH_f° (kJ/mol)	Gibbs energy of formation ΔG_f° (kJ/mol)	Standard molar entropy S_f° (J/mol.K)
CO (g)	-110.53	-137.2	197.66
CO ₂ (g)	-393.51	-394.4	213.78
CO ₂ (l)		-386	
CO ₂ (aq)	-413.26		119.36
CO ₃ ²⁻ (aq)	-675.23		-50.0
CaO (s)	-634.92		38.1
HCO ₃ ⁻ (aq)	-689.93	-603..3	98.4
H ₂ O (l)	-285.83		69.95
H ₂ O (g)	-241.83		188.84
CaCO ₃ (s)	-1207.6 (calcite)	-1129.1	91.7
CaCO ₃ (s)	-1207.8 (aragonite)	-1128.2	88
MgCO ₃ (s)	-1113.28 (magnesite)	-1029.48	65.09
CH ₄ (g)	-74.4	-50.3	186.3
CH ₃ OH (l)	-239.1	-166.6	126.8
CH ₃ OH (g)	-201.5	-162.6	239.8

In an aqueous solution CO₂ forms carbonic acid, which is too unstable to be easily isolated. The solubility of CO₂ in water (Fig. 15) decreases with increasing temperature and increases with increasing pressure. The solubility of CO₂ in water also decreases with increasing water salinity by as much as one order of magnitude (Fig. 16), the following empirical relation (Enick and Klara, 1990) can be used to estimate CO₂ solubility in brackish water and brine:

$$W_{CO_2,b} = W_{CO_2,w} * (1.0 - 4.893414 \cdot 10^{-2} * S + 0.1302838 \cdot 10^{-2} * S^2 - 0.1871199 \cdot 10^{-4} * S^3) \quad (4)$$

Where W_{CO_2} is CO₂ solubility, S is water salinity (expressed as total dissolved solids in % by weight) and the subscripts w and b stand for pure water and brine, respectively.

A solid hydrate separates from aqueous solutions of CO₂ that are chilled (below about 11°C) at elevated pressures. A hydrate is a crystalline compound consisting of the host (water) plus guest molecules. The host is formed from a tetrahedral hydrogen-bonding network of water molecules; this network is sufficiently open to create pores (or cavities) that are large enough to contain a variety of other small molecules (the guests). Guest molecules can include CH₄ and CO₂. CO₂ hydrates have similar (but not identical) properties to methane

hydrates, which have been extensively studied due to their effects on natural gas production and their potential as future sources of hydrocarbons. CO₂ hydrates have not been studied as extensively.

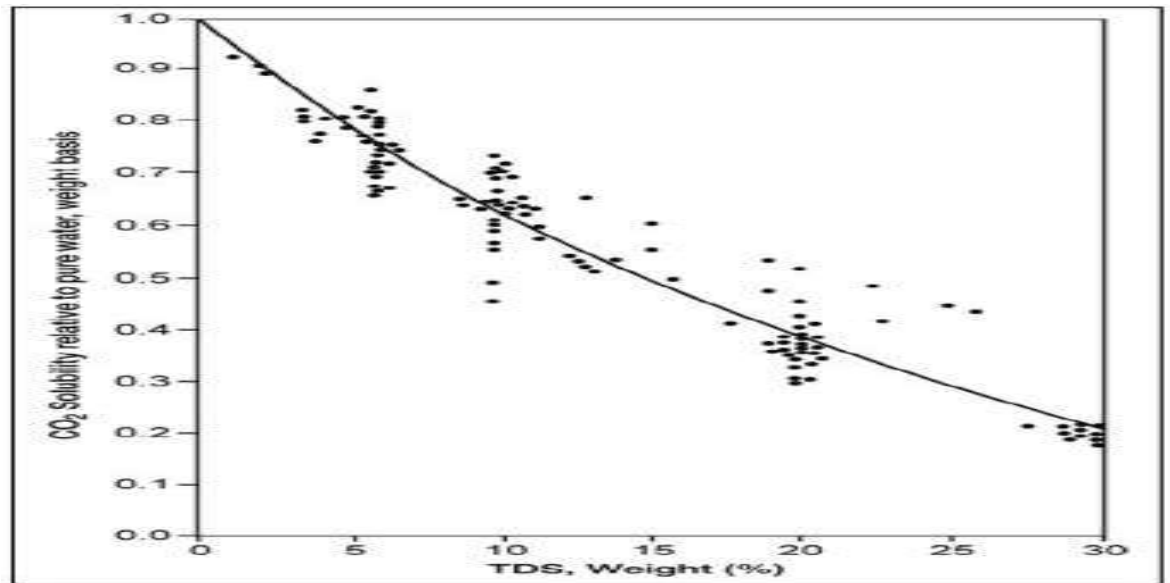
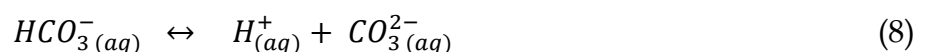
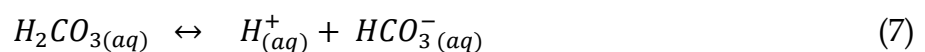
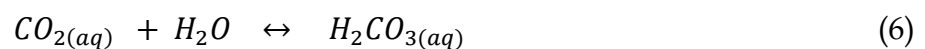


Fig. 16: Solubility of CO₂ in brine relative to that in pure water (comparison between experimental points reported by Enick and Klara 1990 and correlation developed by those authors).

Impact of the CO₂ on pH of water

The dissolution of CO₂ in water (this may be sea water, or the saline water in geological formations) involves a number of chemical reactions between gaseous and dissolved carbon dioxide (CO₂), carbonic acid (H₂CO₃), bicarbonate ions (HCO₃⁻) and carbonate ions (CO₃²⁻) which can be represented as follows:



Addition of CO₂ to water initially leads to an increase in the amount of dissolved CO₂. The dissolved CO₂ reacts with water to form carbonic acid. Carbonic acid dissociates to form bicarbonate ions, which can further dissociate into carbonate ions. The net effect of dissolving anthropogenic CO₂ in water is the removal of carbonate ions and production of bicarbonate ions, with a lowering in pH, (Fig. 8) shows the dependence of pH on the extent to which CO₂ dissolves in sea water at temperatures of 0°C and 25°C based on

theoretical calculations (IEA Greenhouse Gas R&D Programme, 2000) by iterative solution of the relationships (Horne, 1969) for the carbonic acid/bicarbonate/carbonate equilibrium combined with activity coefficients for the bicarbonate and carbonate ions in sea water. The temperature dependence of the ionization of water and the bicarbonate equilibrium were also included in this calculation. This gives values for the pH of typical sea water of 7.8–8.1 at 25°C and 8.1–8.4 at 0°C. These values, which are strongly dependent on carbonate/bicarbonate buffering, are in line with typical data for sea water (Fig.17) shows 2 experimental data points reported by Nishikawa et al., 1992). (Fig.17) also shows that there is a small effect of temperature on the reduction in pH that results from dissolution of CO₂. A minor pressure dependence of water ionization is also reported (Handbook of Chemistry and Physics, 2000). The effect on water ionization of an increase in pressure from atmospheric to 250 bar (equivalent to 2500 m depth) is minor and about the same as would result from increasing temperature by about 2°C. The effect of pressure can therefore be ignored.

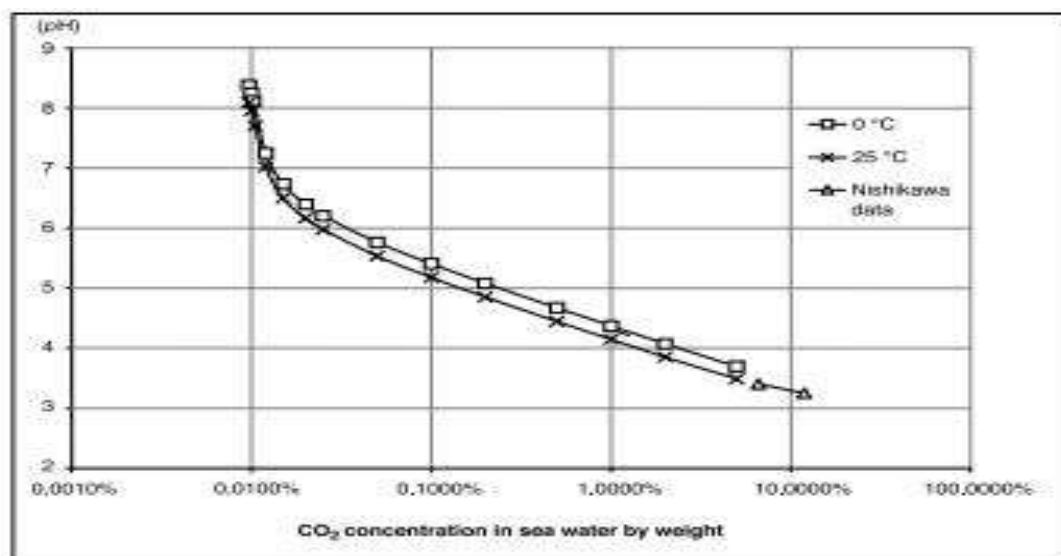


Fig. 17: Dependence of pH on CO₂ concentration in sea water.

2. Trapping Mechanisms

2-1. Introduction

The performance of the CO₂ sequestration projects is based mainly on the trapping efficiency of the stored reservoir (retention of the injected CO₂ inside the target reservoir) [32, 34], the supercritical status of the CO₂ injected below a confining geological formation that prevents its return to the atmosphere, the mechanisms for long-term stabilization and immobilization of CO₂ are:

- 1- Structural and stratigraphic trapping,
- 2- Residual trapping,
- 3- Dissolution in the brine (+dissolution enhancement by induced convection),
- 4- Mineral trapping by geochemical fluid/mineral reactions and precipitation of minerals.

The quantitative contribution of each of these trapping mechanisms will be site-dependent, as the combination of the injection strategy, geological architecture and the migration pattern at later stages of stabilization will determine their efficiency in immobilizing parts of the CO₂ plume.

So far only the very conceptual plot from the IPCC report is widely used to illustrate the long-term safety development for geological storage (Fig. 18) [1].

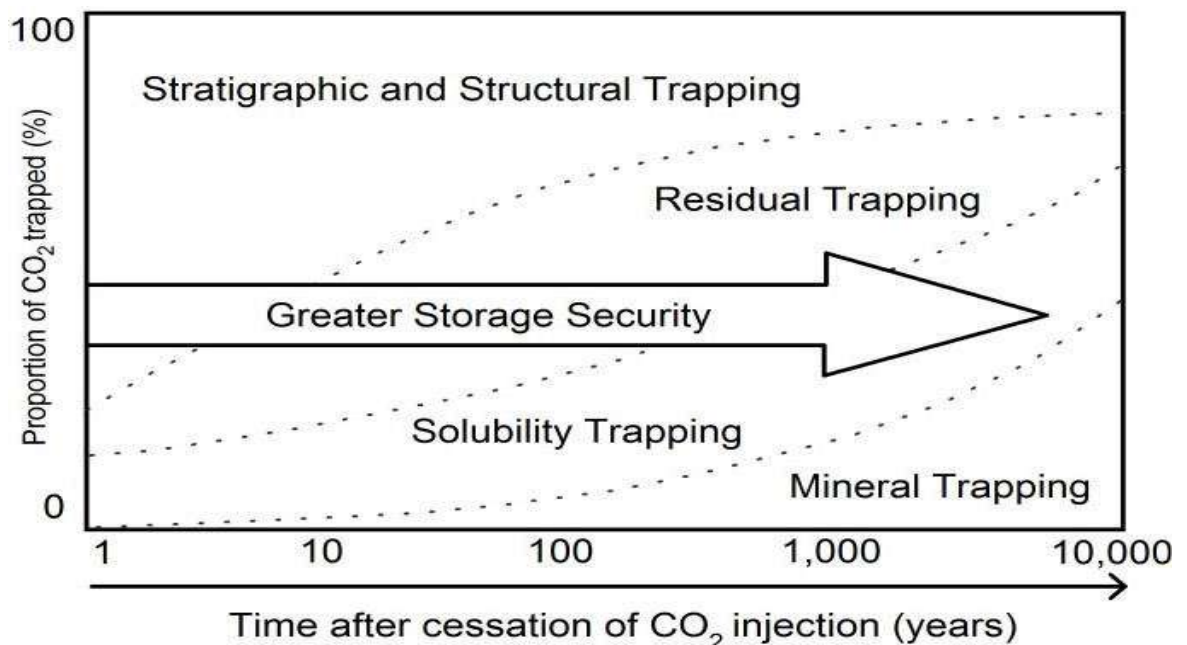


Fig. 18: Schematic representation of the change of trapping mechanisms and increasing CO₂ storage security over time (modified after Class *et al.*, 2009; IPCC, 2005).

Once CO₂ is injected into target reservoir the trapping mechanisms evolve over time (Fig. 18) with containment of CO₂ dominated by structural, stratigraphic and/or hydrodynamic traps over the 30-35 year injection stage of the project. A number of geochemical reactions also occur and become increasingly important after CO₂ injection has finished. CO₂ may be partially contained via residual trapping as the plume moves away from the wellbore and also mixes with and dissolves in the formation water at the leading and trailing edges of the plume (solubility trapping).

Dissociation of the CO₂ dissolved in the formation water creates acidity that reacts with minerals in the formation and may dissolve fast reacting carbonate minerals (if present) in the acidified zone surrounding the injection well leading to an increase in dissolved bicarbonate (so-called ionic trapping). In the longer term dissolution of silicates such as plagioclase and chlorite causes pH to increase and carbonates may precipitate in the previously acidified zone as CO₂ partial pressure declines (mineral trapping).

2-2. Description of storage mechanisms

2-2-1. Stratigraphic and structural trapping

Initially, physical trapping of CO₂ below low-permeability seals (caprocks), such as very low-permeability shale or salt beds, is the principal means to store CO₂ in geological formations. Sedimentary basins have such closed, physically bound traps or structures, which are occupied mainly by saline water, oil and gas. Structural traps include those formed by folded or fractured rocks. Faults can act as permeability barriers in some circumstances and as preferential pathways for fluid flow in other circumstances. Stratigraphic traps are formed by lateral changes in rock type caused by variation in the setting where the rocks were deposited. Both of these types of traps are suitable for CO₂ storage. A special case for structural trapping can occur in saline formations that do not have a closed trap but consists of a slightly tilted aquifer where fluids migrate very slowly over long distances. When CO₂ is injected into a formation, it displaces saline formation water and then migrates buoyantly upwards, because it is less dense than the water. When it reaches the top of the storage formation, it continues to migrate as a separate phase until it is dissolved (potentially helped by gravity instability and mixing), trapped as residual CO₂ saturation or gets arrested in local structural or stratigraphic traps below the sealing formation [1].

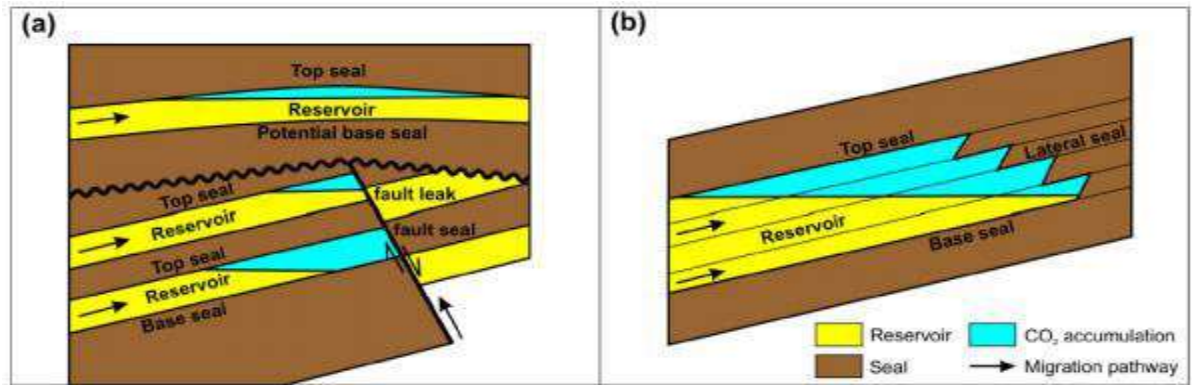


Fig. 19: Examples of (a) structural and (b) stratigraphic physical traps for CO₂ (From CO₂CRC, 2008).

2-2-2. Residual trapping

Consider a medium that is initially filled with water or brine. The solid grains are usually made of minerals that are naturally wetting to water and, therefore the medium is preferentially water wet. During CO₂ injection into the aquifer or oil/gas reservoir, the non-wetting CO₂ phase invades the pore space. This is a drainage process in which the only mechanism for displacement of water by CO₂ is piston-type displacement, the CO₂ invades the porous medium in the form of a continuous, connected cluster. Water, however, remains present not only in small pores that have not been filled with CO₂ but also in the corners and crevices of the pores that have been invaded. Consider now the displacement of the CO₂ by water.

During this process, there are several physical mechanisms by which the water can displace the CO₂ [41]. In addition to piston-type displacement, cooperative pore-body filling and snap-off may occur (Fig. 20). For water wet rocks, snap-off is the dominant mechanism (Al-Futaisi and Patzek, 2003; Valvatne and Blunt, 2004). The important point is that snap-off and cooperative filling may lead to disconnection and bypassing of the CO₂ (Juanes et al. 2006).

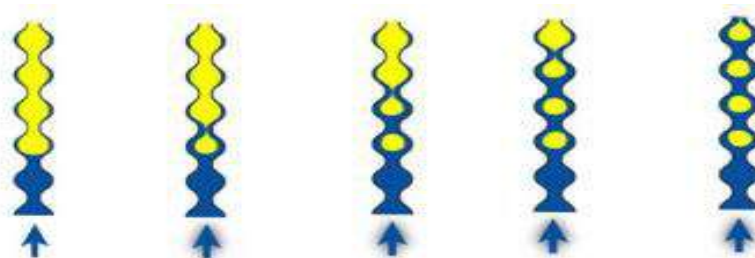


Fig. 20: The snap-off process creating residual trapped gas during imbibition when water or brine returns to the CO₂ filled medium (Tchelepi 2009).

The macroscopic consequences of these pore scale processes are trapping and relative permeability hysteresis. In accordance with the pore-scale explanation

given above, experimental data strongly suggest that the non-wetting phase experiences much more pronounced hysteresis than the wetting phase (Juanes et al. 2006). Residual Trapping of the non-wetting phase (CO_2) is caused by wettability and capillary effects in porous media. (Fig. 20) shows the relative permeability curves for CO_2 injection. During injection, when the CO_2 phase (dense phase) saturation increases, the relative permeability curve for CO_2 follows the drainage relative permeability curve (k_{rg}^d) (black curve). If at a saturation (S_{gi}^*), the saturation decreases, the relative permeability curve for CO_2 would follow the imbibition curve (k_{rg}^i) (red curve). If the saturation continues to decrease until k_{rg} is zero, the residual trapped non-wetting-phase saturation (S_{gt}^*) is reached. In below figure, $S_{g,\max}$ is the maximum saturation and $S_{gt,\max}$ is the maximum trapped saturation.

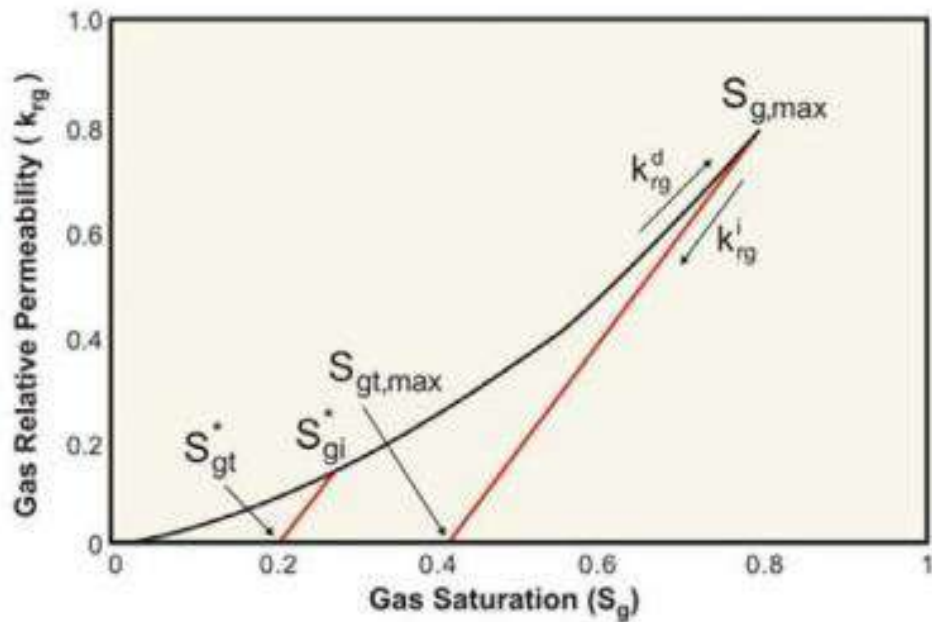


Figure 21: Relative permeability curve for macroscopic behaviour with hysteresis (Nghiem et al. 2009).

In many sedimentary rocks, supercritical CO_2 is typically the non-wetting phase relative to the ambient brine. At the front of the CO_2 plume, the CO_2 saturation increases, and the brine is drained from the pore space. The capillary entry pressure prevents the drainage of the brine from the smallest pores, resulting in an incomplete displacement. We refer to the brine left behind the advancing CO_2 front as the residual brine S_{br} . Bachu & Bennion (2007) [24] showed with laboratory experiments that S_{br} can range from 0.2 to 0.68 at storage conditions in saline aquifers. The high end of these values is surprising and may in part be due to heterogeneity and gravity segregation in the experiments. They also show that the presence of residual water reduces the apparent permeability of the CO_2 to approximately 1/5 of the single-phase

permeability. We refer to this value as the relative permeability of CO₂, denoted k_{rc} . If the CO₂ plume is migrating laterally as a gravity current, the CO₂ saturation decreases at the trailing edge of the plume (Fig. 21), and the ambient brine imbibes into the pore space previously occupied by CO₂. Preferential imbibition of the brine into the smaller pores and interfacial instabilities leave CO₂ behind as disconnected bubbles and ganglia of CO₂ which are effectively immobile. We refer to this immobile CO₂ saturation as the residual CO₂ saturation, S_{cr} and to the process as residual trapping. Bachu & Bennion (2007) report values of S_{cr} from 0.1 to 0.35 for saline aquifers in the Alberta basin, indicating that they will trap CO₂ efficiently. Most work on residual trapping during CO₂ storage has focused on the effect of hysteresis on the magnitude of S_{cr} , and the design of injection strategies that maximize residual trapping during, or shortly after, the injection period (Mo et al. 2005; Juanes et al. 2006; Ide, Jessen & Orr 2007, Hesse et al. 2008).

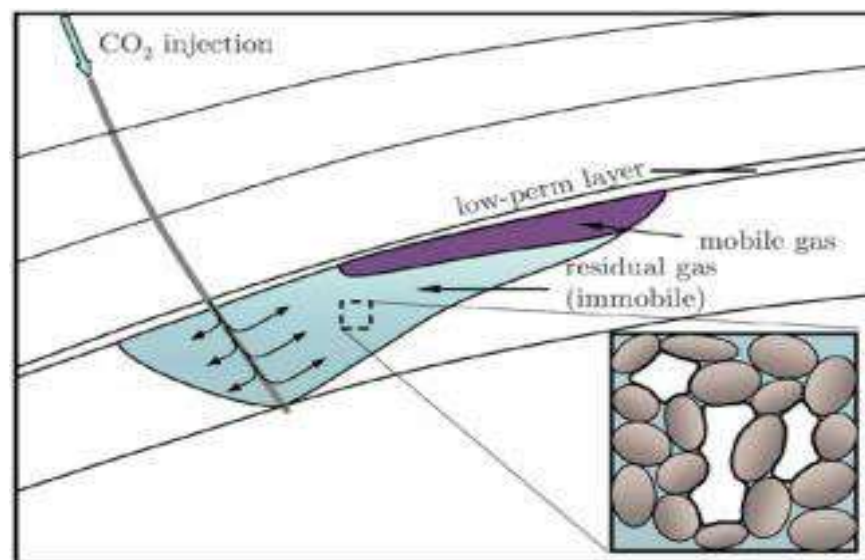


Fig. 22: Large-scale effects of residual trapping after injection stop (Juanes et al. 2006)

Results suggest that lateral migration of the injected CO₂ along the seal will trap the CO₂ relatively quickly as residual saturation. Residual trapping is quite effective in sloping aquifers with small mobility ratios and high residual CO₂ saturations [41].

Injection of water slugs alternating CO₂ injection (in the spirit of classical WAG for enhanced oil recovery (Spiteri and Juanes, 2006) increases the effectiveness of the storage project. The injected water forces breakup of large connected CO₂ plumes, enhancing trapping and immobilization of the CO₂. On the other hand, a WAG strategy leads to higher bottom hole pressures at injection wells, which may be limited by seal integrity, regulatory or economic constraints. The identification of WAG as a potentially effective strategy for CO₂ storage lends

itself to an optimization problem to maximize the amount of trapped CO₂ by varying the well rates and well completions, subject to BHP constraints. The hysteresis effect is also in action when injection is stopped intermittently for well maintenance or other activities.

2-2-3. Dissolution trapping

Once CO₂ dissolves in formation water, a process commonly called solubility trapping occurs. The primary benefit of solubility trapping is that when CO₂ is dissolved, it no longer exists as a separate phase, thereby eliminating the buoyant forces that drive it upwards. The CO₂ solubility in formation water decreases as temperature and salinity increase. Dissolution is rapid when formation water and CO₂ share the same pore space, but dissolution outside the immediate contact zone is slow since it depends on diffusion as the transport mechanism. Over longer time-spans, the increased density of the brine with dissolved CO₂ can create gravitational instability and may cause convection that mixes the different brines and further enhances dissolution.

As underlined by various authors (Bachu et al. 2007) [25], CO₂ dissolution is a significant trapping mechanism and saturating formation water with CO₂ would create huge CO₂ storage capacities (Bachu & Adams, 2003). Nevertheless, it is also indicated that dissolving CO₂ is a long-term process, coupling molecular diffusion and in some cases aided by gravitational instabilities in the formation water.

- On the Utsira case, dissolution processes is expected to develop from 300 to 5000 years after the injection period (Chadwick et al. 2008),
- A 1000 year period is modeled to dissolve the CO₂ by Van der Meer & Wees (2006),
- A parametric study is presented by Ennis-King & Paterson (2003) illustrating the impact of the permeability anisotropy on the time required to dissolve the CO₂, with 25% of the CO₂ being dissolved after 300 to 20000 years depending k_v , because of the difference between the density of the brine with and without dissolved CO₂ the mixing time t_{mix} required for the entire supercritical phase to dissolve depends mainly on vertical permeability of the stored reservoir :

$$t_{mix} \approx \frac{\alpha \cdot L \cdot \mu}{k_v \cdot \Delta \rho \cdot g} \quad (9)$$

α is the density ratio of gas to brine, L is the reservoir thickness, μ is the viscosity, k_v is the vertical permeability, $\Delta \rho$ is the density difference between brine with and without dissolved CO₂, and g is the acceleration of gravity.

Using typical parameters ($\phi = 0.2$, $\mu = 5 \times 10^{-4} \text{ Pa.s}$, $k_v = 10^{-15} - 10^{-14} \text{ m}^2$, $\Delta\rho = 10 \frac{\text{kg}}{\text{m}^3}$, $L = 10 \text{ m}$, and $\alpha = 10$) for a likely storage site, value of t_{mix} range from 1600 to 16000 years, estimate of mixing time for the CO₂ gas bubble at Sleipner from 3D model is about 7000 years for an average $k_v = 200 \text{ mD}$ (Lindeberg and Bergmo, 2002), Ennis-King & Paterson (2003) consider this result as an underestimate due to the dilution of fingers as they propagate.

As such, CO₂ is expected to significantly dissolve a long time after the end of the injection period. For an industrial storage project, the question is then how much CO₂ can reasonably dissolve during the injection period, which could reduce the pressure pulse due to the CO₂ injection? Simple assumptions are made to evaluate the fraction of CO₂ that can dissolve during the injection period. Indeed, CO₂ injection results in drainage processes only, no imbibition is to take place before injection stops; CO₂ dissolves into formation water in direct contact with the CO₂ dense phase, and molecular diffusion (transportation of dissolved CO₂) can be neglected due to the short time-span in question; the formation water in direct contact with CO₂ in dense phase is the residual water in CO₂ flooded areas. With typical numbers of 20% residual water saturation, a CO₂ content of the CO₂ saturated aqueous phase of 50 kg/m³ and a CO₂ density of 500 kg/m³, one gets:

- Dissolved CO₂ mass per unit of pore volume of: $20\% \times 50 = 10 \text{ kg/m}^3$.
- Dense phase CO₂ mass per unit of pore volume of: $80\% \times 500 = 400 \text{ kg/m}^3$.

Hence, less than 3% of the CO₂ is to dissolve in the formation water. As a consequence of these, a very limited fraction of CO₂ is expected to dissolve in the formation water during the injection period and this dissolution is expected to have a minor impact when it comes to pressure build up due to CO₂ injection (Thibeau et al. 2011).

- Diffusion transport

Diffusion will transport CO₂ away from the interface between aqueous and gas phases, thus providing a mechanism for dissolving additional CO₂, although as a very slow process. The rate of transport has been illustrated with a calculation by (Pruess and Nordbotten 2011). The diffusivity of CO₂ is approximately $D = 2 \times 10^{-9} \text{ m}^2/\text{s}$ (Tewes and Boury 2005; Farajzadeh 2009); which leads to an effective diffusivity of $D_{eff} = 1 \times 10^{-9} \text{ m}^2/\text{s}$. After 300 years (= $9.5 \times 10^9 \text{ s}$) it would penetrate a distance of only 3.1m into the aqueous phase, which is equal to a movement of approximately 1 cm/year. The process has therefore absolutely no distribution effect during the injection period. In the

longer time-scale after injection has stopped, the main interest in the diffusion transport mechanism should be linked to the caprock.

- **Convection transport**

A recent review of the processes involved in density-driven brine convection has been presented by (Kneafsey and Pruess 2011), and is quoted in the following. At some distance from the injection well where the CO₂ has spread out under the cap rock, there will likely be a nearly horizontal interface between a free CO₂ phase above and the aqueous phase below. Geometric details of the interface will be affected by the properties of the porous media; for simplicity, we will consider the interface to be flat. At the interface, CO₂ will dissolve into the aqueous phase. If the aqueous phase was immobile, the rate of CO₂ dissolution would be limited by the rate at which CO₂ can be removed from the interface by molecular diffusion. This is a slow process, and the rate of CO₂ dissolution will decrease with time. CO₂ dissolution causes the density of the aqueous phase to increase on the order of 0.1 to 1%, depending on CO₂ pressure, temperature, and salinity (Garcia 2001). This density increase induces a gravitational instability because denser CO₂-rich aqueous fluid overlies less-dense fluid. The instability can trigger convection of fluid at a variety of scales, which could greatly increase the rate at which dissolved CO₂ is removed from the interface with the overlying free CO₂, thereby accelerating CO₂ dissolution. CO₂ dissolution-induced convection has been studied by many investigators because of its relevance for security and permanence of CO₂ storage. The earliest published study on CO₂ dissolution-induced density increase and its importance for CO₂ storage was by (Weir et al. (1995, 1996)). (Lindeberg and Wessel-Berg 1997) evaluated the conditions under which vertical convective flow will occur in a medium subjected to both a thermal gradient and the presence of a CO₂ dissolution-induced dense layer. (Lindeberg and Bergmo 2003) examined multi-scale numerical simulation problems related to the Sleipner Vest CO₂ storage project in the Norwegian Sector of the North Sea. Studies have also been performed investigating stability analysis for the onset time for convection, the preferred wavelength for the growth of convective fingers, and growth rates (e.g., Ennis-King and Paterson 2003a,b; Ennis-King et al. 2005; Hesse et al. 2006; Riaz et al. 2006; Xu et al. 2006). This summary by (Kneafsey and Pruess 2010) is associated with analysis and comparison of laboratory flow experiments and modeling of these systems with a numerical model and they found good agreement (Fig. 23).

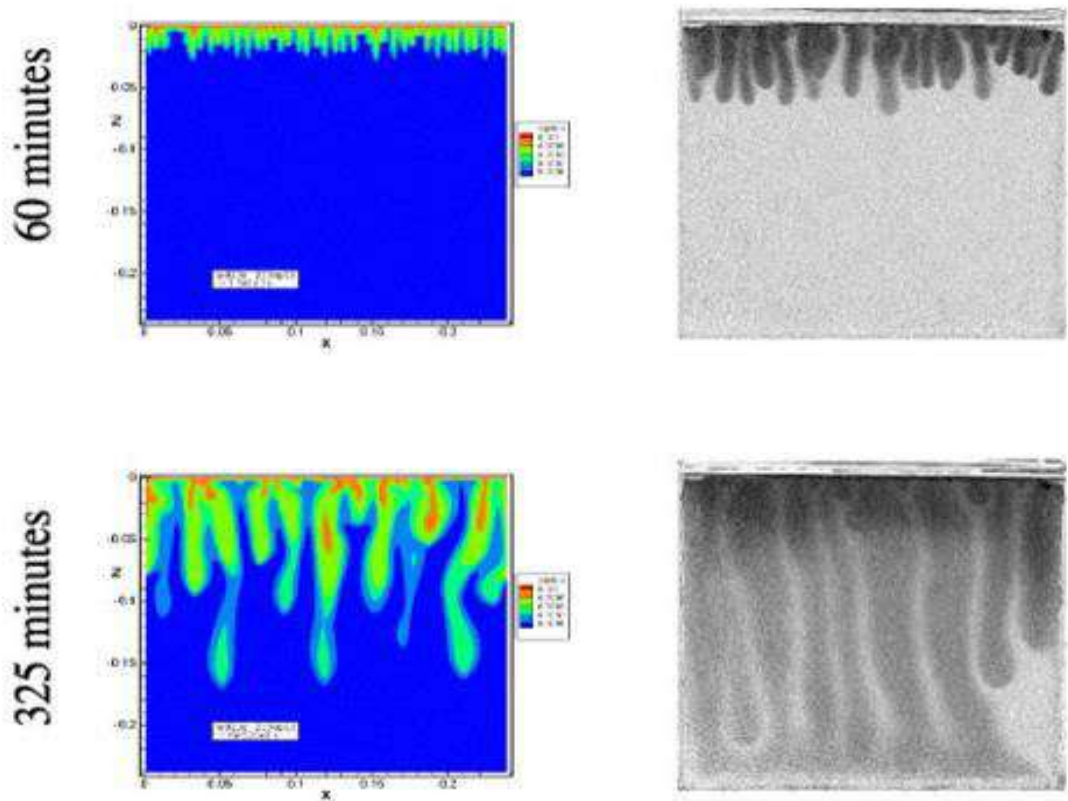


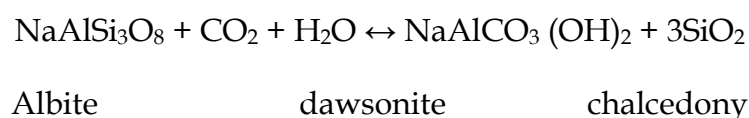
Fig. 23: Comparison between density-driven convection in the modeled system (left) and experimental system (right) (From Kneafsey and Pruess 2010).

2-2-4. Mineral trapping

One of the criteria that have to be fulfilled when assessing the impact of CO₂ storage is the evolution of the storage site towards a situation of long-term stability. Mineral trapping is a time dependent process whose contribution to CO₂ immobilization increases slowly with time, representing CO₂ incorporated into minerals due to chemical precipitation (Gaus et al., 2008). While during injection phase mineral trapping is almost negligible (Bachu et al., 2007), it constitutes a safe mechanism with a large storage potential when considering residence times in the order of geologic times (Audigane et al., 2007). It has to be stressed out that the presence of a water phase is essential to chemical reactions; dry gas and rock interactions are orders of magnitude slower and less relevant than those occurring in aqueous solutions, and are usually neglected. Depleted gas reservoirs with low residual water saturation are therefore less prone to chemical alteration due to CO₂ injection. Once the CO₂ is in the subsurface, geochemical interactions within the fluid as well as between the fluid and the rock matrix will take place. First CO₂ dissolves in the formation fluid, acidifying it (see dissolution trapping). This will lead to fast dissociation of carbonic acid to form the bicarbonate ion. Primary host rock minerals will start to dissolve due to low pH, releasing divalent cations which react with the dissolved bicarbonate species forming Ca, Mg and Fe (II)

carbonates. If carbonate and sulfate minerals are being solved from the matrix to buffer the pH, the reaction kinetic will be fast. This will especially be the case during injection phase in the near well environment. In the time after injection, however, slow reactions, which play the major role in terms of mineral trapping, will continue to take place. Aluminosilicate minerals such as clay minerals, micas, chlorites and feldspars that can function as cation donors dissolve very slow at reservoir temperatures. Since precipitation of carbonate minerals requires Ca and Mg sources, siliciclastic formations are considered more suitable for CO₂ storage than carbonate formations which are fast pH buffer (Zhang et al., 2009). In addition to fast and slow dissolution/precipitation kinetic reactions, other aqueous reactions like redox processes, sorption and ion exchange could play a role.

Factors that affect rate and capacity of mineral trapping are the chemical composition of formation waters and of the rock matrix (primary minerals), initial CO₂ fugacity, temperature and pressure as well as dissolution and precipitation kinetic rates (Zerai et al., 2006). Kinetic rate law depends among other parameters on reactive surface area which is very difficult to estimate. Pressure, temperature and also the salinity of the fluid have an impact on CO₂ properties, such as density, viscosity and solubility. Therefore arises the question: How should long-term mineral trapping capacity be assessed? Considering the complexity and interdependency of chemical and physical processes as well as the time factor, numerical modeling turns out to be the best tool to use, backed up where possible by laboratory experiments (Soong et al., 2004; Labus & Bujok, 2011). Site specific long-term geochemical or reactive transport modeling results show that for CO₂ disposal in deep saline siliciclastic aquifers, mineral trapping will occur primarily in the form of dawsonite (NaAlCO₃ (OH)₂) and the calcite-group carbonates, most significantly siderite(FeCO₃), ankerite (Ca (Fe, Mg, Mn)(CO₃)₂), magnesite (MgCO₃), calcite (CaCO₃) and their solid solutions (Gaus et al., 2005; Xu et al., 2010; Johnson et al., 2004; Zerai et al., 2006; Zhang et al., 2009). In favorable cases mineral trapping capacity would be comparable to that of solubility trapping reaching up to 7-10 kg per m³ medium (Xu et al., 2004; Xu et al., 2010; Zhang et al., 2009). An often-cited reaction is the alteration of albite resulting in permanent trapping of CO₂ as dawsonite (Audigane et al., 2007; Gaus, 2010; Labus & Bujok, 2011; Gaus et al., 2005; Zerai et al., 2006):



The detailed level of knowledge and data needed for the modeling is joined by uncertainties, especially with regard to kinetic of long-term reactions. Estimation of reactive surface area may be based on geometric surface area (Gaus et al., 2005; Xu et al., 2010; Cantucci et al., 2009), therefore different approaches are available. Once this is done and since mineral surface is not smooth, a surface roughness factor could be defined, increasing geometric-based surface value. If it is taken into account that only selective sites of the mineral surface are involved in the reaction, geometric-based surface value could be decreased up to three orders of magnitude. Not all authors consider all of these effects, but they all seem to agree on the fact that reactive surface area for precipitating minerals is very difficult to estimate, thus same values of dissolution are mostly used for precipitation. Gaus et al. (2005) solves the problem by assuming that 50% of total reactive surface area corresponds to the surface area for precipitating minerals. Since the quantification process is questionable and its impact on results could be of several orders of magnitude (Zerai et al., 2006), uncertainty in reactive surface area is often assessed through sensitivity analysis (Gaus et al., 2005; Zhang et al., 2009). Difficulties concerning consistency in thermodynamic databases (differences in equilibrium constants used in the internal database of numerical codes) and activity models at high salinity of the formation fluid also affect the reliability of modeling results (Gundogan et al., 2010).

Besides increasing the accuracy of input data and working on availability of unknown parameters, derivation of consolidated findings from CO₂-analogues constitutes a further challenge. Natural CO₂-rich reservoirs (analogues) are widespread: Montmiral (Southeast Basin, France), Messokampos (Florina Basin, Greece), Triassic Lam Formation (Shabwa Basin, Yemen), Honggang Anticline (Songliao Basin, China) are some of them. It is expected that they could reveal which CO₂ trapping minerals actually may form. There are doubts about dawsonite being able to trap CO₂ permanently. It has been suggested that it becomes unstable as reservoir pressure decreases after injection (Hellevang et al., 2005). Also the difficulty to verify dawsonite formation through laboratory experiments supports the skepticism. On the other hand it has been found in many CO₂ analogues (Worden, 2006; Liu et al., 2011), providing evidence of its existence in connection with high CO₂ pressure. This highlights the fact that mineral trapping relies on time-scale. Since analogues act as long-term laboratories it is crucial to incorporate them into the analysis. Information about geochemical interaction and their impact on reservoir lithologies, the existence of a flow regime and the thermodynamic equilibrium conditions vs. time could also be deduced from the studies of natural analogues (Gaus et al., 2005 (2)).

The following figure illustrate the different elements in the trapping of CO₂. All elements except one are formed by the dynamic development of the natural storage site, and the only part we calculate outside the natural processes is the “Residual CO₂ at time steps” which is calculated as the residual at a given time-step resulting from optimal production of maximum amount of CO₂ from the storage site. The exact amount can be calculated from a reservoir model by the Land’s equation depending on the maximum saturation reached.

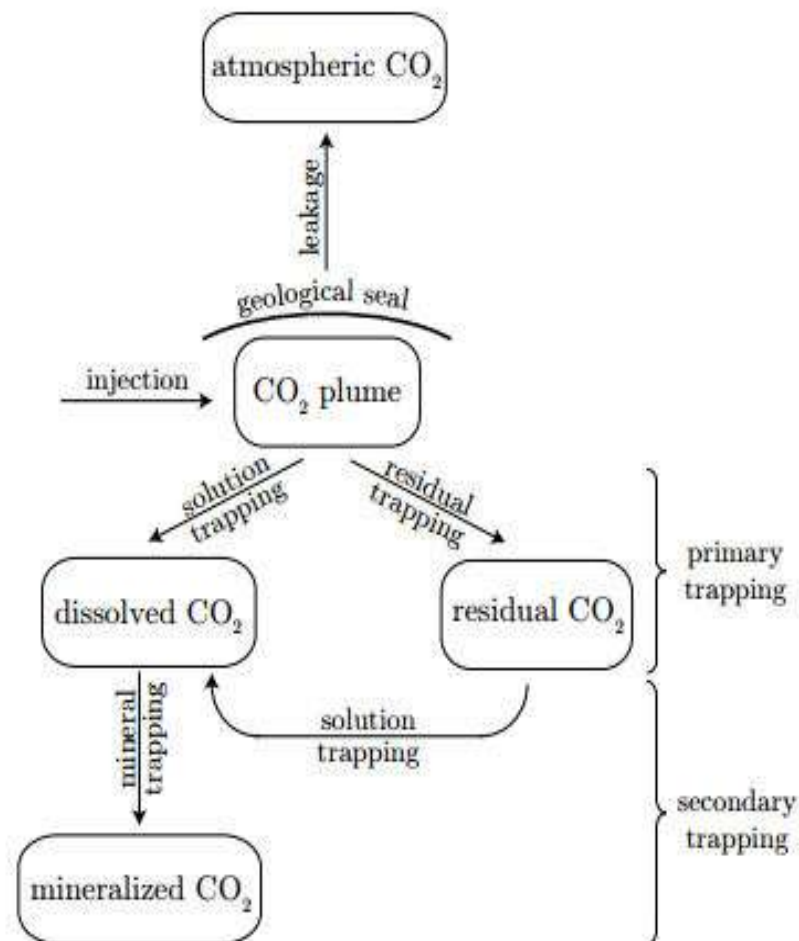


Fig. 24: Different trapping mechanism of the CO₂

Chapter 4

Characteristic of CO₂ Storage Reservoirs

Reservoir Capacity storage and Sealing properties

1- CO₂ Storage Reservoirs Characteristics

1-1. Geological Formation

CO₂ storage reservoirs are sedimentary basins created by the gradual deposition and compaction of sediments that have eroded from mountains. Deposits, as thick as tens of thousands of feet, have accumulated in sedimentary basins around the world. Typically, sedimentary basins consist of alternating layers of coarse (sandstone) and fine-textured sediments (clay, shale or evaporites) [18]. The sandstone layers, which provide the storage reservoir, have high permeability, allowing the CO₂ to be injected. The shale or evaporites layers have very low permeability and act as seals to prevent CO₂ from rapidly returning to the surface. Interestingly, naturally occurring CO₂ reservoirs exist in North America, Australia, China and Europe, proving that CO₂ can be stored underground for hundreds of thousands, even millions of years. In addition, many oil and gas reservoirs also contain large quantities of CO₂ confirming that oil and gas reservoirs can also store CO₂ over geologic time scales. The technology to inject CO₂ underground is mature and practiced routinely in CO₂ enhanced oil recovery projects. Little to no new injection technology will be required to enable CCS. To ensure storage and capture integrity, locations for underground geologic storage of CO₂ would need to be selected to ensure that CO₂ would remain safely underground for thousands of years or longer. Regions with seismic or volcanic activity that could compromise the security of the storage site should not be selected. The best storage reservoirs are at depths of greater than 3000 feet below the ground surface, have several hundred feet of porous and permeable sands, and are overlain by at least one, and preferably more, thick and continuous seals. Under these conditions, CO₂ would be stored very securely and efficiently, with the density and physical properties of a liquid [19].

Government regulations will need to be established and enforced to ensure that satisfactory sites such as these are selected for CO₂ storage. Several authors describe how depleted oil and gas reservoirs are especially promising early opportunities for long-term storage because they have seals with 3-dimensional closure that have stood the test of time and a comparatively small effort will be needed to evaluate their storage potential. They are also attractive because CO₂ storage can be combined with CO₂ enhanced oil and gas recovery – a mature practice that is applicable to an estimated 80% of oil reservoirs [28]. During the early stages of a storage project, the remaining oil can be extracted from the reservoir. Eventually, oil production will stop and the reservoir can be filled to capacity for long-term storage of carbon dioxide. The availability of an abundant low-cost supply of CO₂ could be a boon to the domestic oil industry.

A similar idea can be applied to enhance the recovery of natural gas from deep coal beds.

Sandstone formations filled with salt water, are estimated to have much greater storage capacity than oil and gas reservoirs. However, as pointed out by Burruss (2004), a significant effort will be required to characterize the storage reservoirs in salt-water filled formations and more importantly, to characterize the low permeability rocks that form the seal. The technology to characterize salt-water filled formations and their seals has already been developed for an analogous purpose, storage of natural gas to accommodate fluctuations in daily and seasonal demand. In the United States, natural gas is stored deep underground at over 400 sites, including over 50 aquifer storage sites, which are essentially identical to the salt-water filled formations that are contemplated for CO₂ storage. Natural gas storage technology is very similar to CO₂ storage and its successful application lends credence to the idea that CO₂ can be safely and effectively stored in salt-water filled formations.

Estimates of global storage capacity indicate that the storage capacity for CO₂ in geological formations is much higher than the global annual CO₂ emissions, which were 26 GtCO₂ annually in 2004, the below figure show CO₂ storage capacity in the worldwide based in the expectation to be economically and technically viable.

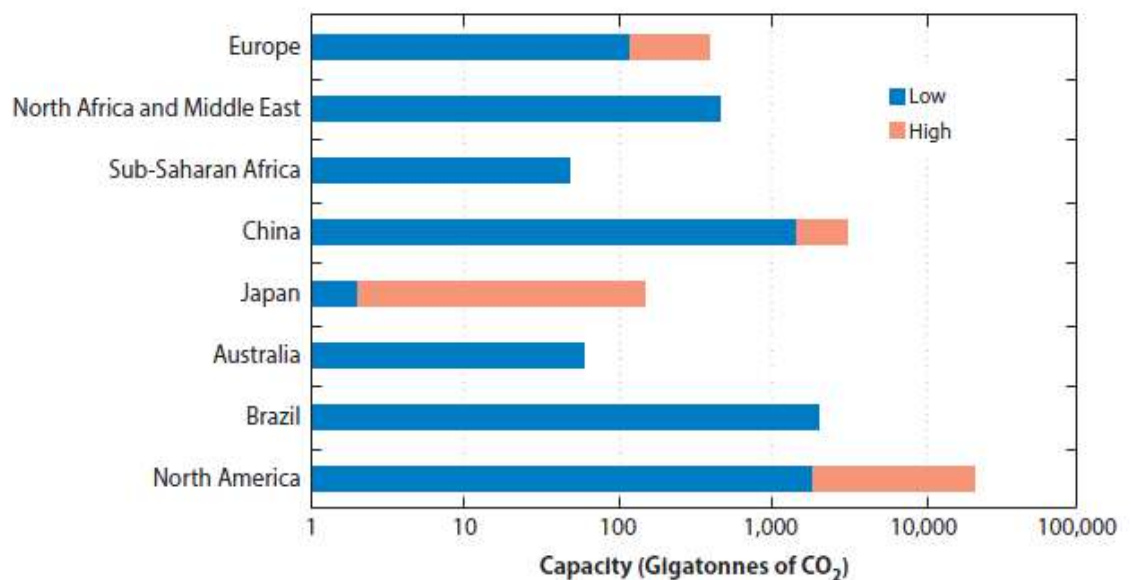


Fig. 25: Regional assessment of CO₂ storage capacity as compiled by the Global Energy.

1-2. CO₂ Storage Assessment in geological formations

A uniform definition of the assessment units is necessary to construct a consistent methodology to assess resources. A storage assessment unit must consist of a porous storage formation and an overlying sealing formation (also called cap-rock or confining layer) to retain the CO₂. These are the primary important characteristics need to be defined for the CO₂ storage sites. Although CO₂ storage in known oil and gas reservoirs and saline formations are geologically and hydrologically linked because they occur in the same formation.

The use the geologic, geochemical, petrophysical and hydrologic parameters of the known traps is necessary to evaluate saline formations using measured properties of the formation.

These properties can be extrapolated into the areas of the saline formation that contain no known traps. Because the known traps have retained buoyant fluids for hundreds of thousands to hundreds of millions of years, they have seals that are known to be effective. Conversely, if the seal over a known trap has leaked hydrocarbons, there may be geochemical evidence such as mixing of oil and gas types in overlying reservoirs or residual oil staining in the known traps. The largest oil and gas fields have produced fluids that occupied over 1 billion cubic meters of pore volume in the subsurface, allowing characterization of the flow characteristics of a storage formation in areas capable of sustaining injection of CO₂ from the emissions of the largest industrial sources for many decades [29]. The only true distinction between storage in known traps and saline formations is the potential for hydrodynamic and capillary trapping in saline formations that are laterally unconfined and open to hydrologic recharge and discharge. In this case CO₂ trapping and storage is a function of the relative rates of flow of formation water and buoyant displacement of the CO₂ plume.

Hydrodynamic trapping and the kinetics of CO₂ dissolution and reaction with host rock imply a length of time for all trapping processes to become effective.

Resource assessments commonly define a fixed timeframe for the assessed quantities. (Reserve growth) implies that our knowledge of the resource evolves over time as do the technologies, economic factors, and policy drivers that impact utilization of the resource. Furthermore, consideration of a time frame for assessments allows evaluation of the total volume of storage necessary for initial full-scale deployment of geologic sequestration. For example, any sequestration project that captures 1 million tons (MT) CO₂/yr. that is forecast to operate for 20 years will require at least 20 MT of CO₂ storage. Likewise, sequestration projects operating at the scale of a large,

1000MW_e, coal-fired power plant over a 50-year lifetime of the power plant will require 400 MT of CO₂ storage. Decadal timeframes of the injection phase of storage projects are short relative to the geologic, hydrologic and geochemical processes that affect the long-term storage of CO₂. Therefore the primary processes that define contingences for classifying the resource of storage volume in an assessment of storage capacity are those related to displacement of formation fluids.

The parameters needed to evaluate the potential storage capacity for CO₂ in known oil and gas traps are no different from those needed to evaluate storage in saline formations because commonly they are complementary parts of the same assessment unit. If the storage volume of at least one known trap in the assessment unit exceeds a minimum size for a full-scale CCS project operating over a number of years (for example, 1 MT/y for 20 years) then the assessment unit is clearly identified as a target for more complete characterization of storage capacity. The empirically observed flow properties of the known traps derived from the oil, gas and water production histories can be used to evaluate injectivity at the scale of a fully deployed sequestration project within a saline formation. The storage volumes in the known traps of a saline formation are the minimum of the contingent storage resource within the saline formation. As geologic, hydrologic, geochemical and geophysical knowledge of storage processes in known traps advances, additional volumes of the total resource of the saline formation can be identified as contingent resources, causing the storage resource to grow over time. This is a bottom-up method of assessment of storage capacity that starts with the part of the saline formation that is best characterized, the known traps. This method is distinct from other methods that estimate the total volume of potential storage in a saline formation whereby further characterization will only decrease the volume of potential storage [29].

1-3. CO₂ Storage Capacity Calculation

Estimation of the geological reservoir capacity to store CO₂ is not a straightforward or simple process. Some authors have tried to make simplistic estimates at the regional or global level, but have largely been unsuccessful. At the worldwide level, estimates of the CO₂ storage potential are often quoted as (very large) with ranges for the estimates in the order of 100 to 10,000 s Gt CO₂. Although in principle storage capacity estimation relies on a simple series of algorithms that depend on the storage mechanism under consideration to calculate the available capacity in a certain volume of sedimentary rock at a given depth, temperature and pressure, applying them to a specific region or site is complex. It is particularly difficult due to the various trap types and trapping mechanisms that can occur, the different time frames over which

trapping becomes effective, and the different physical states in which the CO₂ might occur. All these parameters affect the effectiveness of geological storage of CO₂, often in different directions. The highly variable nature of geological settings, rock characteristics, and reservoir performance combine to make some estimates unreliable when they are made with methodologies that generalise the inputs for evaluating potential storage capacity [20].

There are many levels of uncertainty within assessments of storage capacity. The different levels of assessment require extensive datasets from multiple disciplines that must be integrated to develop meaningful assessments. The most accurate way to estimate storage capacity at the local scale is through construction of a geological model and use of that information in reservoir simulations. Such analyses are resource, time and data intensive. Given the significant variability that exists in many estimates and in their underlying criteria, it is necessary to document the limitations of many of the assumptions used, and to make suggestions and give examples of how better and more reliable estimates can be determined.

Any geologic CO₂ storage resource assessment estimate is based on the mass of CO₂ that can be stored within the pore space of subsurface rocks. However, the differences between classes of resource estimate, and indeed, the disparity among estimates of any single class, are the result of constraints placed on what constitutes (available) pore space. Assessments of subsurface CO₂ storage potential are constrained by:

- Geology and the understanding of the subsurface (e.g. geologic data and models).
- Engineering considerations (i.e. technologies available to exploit the available pore space and ability to implement them).
- Economics (e.g. storage resources that are infinitely expensive to access are not useful).
- Socio-political factors (e.g. acceptance of use of the subsurface for CO₂ storage, or regulatory limitations on the use of certain technologies).

1-4. CO₂ Storage efficiency

A key component necessary to estimate CO₂ storage is typically referred to as storage efficiency. The storage efficiency represents the fraction of accessible pore volume that will be occupied by free phase CO₂. The time at which storage efficiency is evaluated affects its value. For example, Gorecki et al. (2009) performed a comprehensive study on storage efficiency as a function of lithology, describing a model that estimated the efficiency based on the time at which CO₂ injection stopped, but the CO₂ plume was still mobile. Szulczewski et al. (2012) issued a method to estimate efficiency numerically in two scenarios

- (1) Migration-limited efficiency factor, which expresses the amount of CO₂ that can be injected such that it all becomes sequestered by residual trapping and solubility trapping mechanism before reaching the boundary of the aquifer.
- (2) Pressure-limited efficiency factor, which expresses the amount of CO₂ that can be injected over a given time period without fracturing the seal. The type of trapping influences the magnitude of storage efficiency, with buoyant trapping being the most efficient.

There is considerable uncertainty over what storage efficiency factor should be used in assessment methodologies. Current analytical techniques for estimating the storage efficiency (Juanes, MacMinn and Szulczewski, 2010; Okwen, Stewart and Cunningham, 2010) allow for the storage efficiency of an entire geological unit to be estimated given temperature and pressure gradients, depth ranges, estimates of the irreducible water saturation at the leading edge of a mobile CO₂ plume, the residual gas saturation at the trailing edge of the plume, and the relative permeability between the CO₂ and the ground water. These estimates come primarily from experimental data (e.g., Bennion and Bachu, 2005, 2008; Burton, Kumar and Bryant, 2008; Okabe and Tsuchiya, 2008; Okabe et al., 2010; Akbarabadi and Piri, 2013).

The controls on storage efficiency are

- The volume of rock contacted by the CO₂ plume, also known as the sweep efficiency.
- How easily CO₂ will move relative to the fluid present within the pore space, also known as relative permeability.
- The amount of liquid (water in case of saline aquifer) that will be displaced by the leading edge of the CO₂ plume, also known as drainage.
- How much liquid (water in case of saline aquifer) re-enters the pore space at the trailing edge of the CO₂ plume, also known as imbibition.
- A ratio of the viscosity of the CO₂ to the viscosity of the liquid in place, which estimates how much liquid, can be displaced by the lower viscosity CO₂.
- A ratio of the density of the CO₂ to the density of the liquid, to determine the control of gravity forces, or buoyancy, on how the CO₂ plume moves, and the shape of that plume from the injection well through the storage formation.
- whether any pressure management methods will be allowed during CO₂ injection – the lack of pressure management might significantly reduce the storage efficiency values (Zhou et al., 2008)

1.4.1- Resource pyramid

The concept of resource pyramids was advanced by McCabe (McCabe, 1988) as a method to describe the accumulation around the world of hydrocarbons in different categories. This concept is proposed here to represent the similar issue of capacity for CO₂ storage in geological formations. Because of the multi-faceted aspects of this issue, the techno-economic resource-reserve pyramid for CO₂ storage capacity (CSLF, 2005; Bachu et al., 2007) [21] is shown in below figure

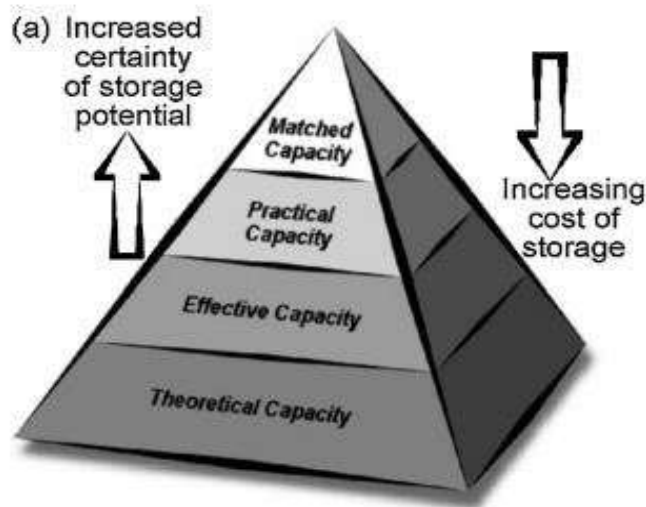


Fig. 26: Techno-economic resource-reserve pyramid for CO₂ storage capacity (CSLF, 2007).

There are four types in the pyramid – theoretical, effective, practical and matched storage capacities, and each of them is a subset of the previous one except theoretical capacity. The theoretical storage capacity (Bachu et al., 2007) represents the physical limit that the geologic system can accept, and it occupies the entire resource pyramid. The effective storage capacity (Bachu et al., 2007) can be acquired by applying a range of technical (geological and engineering) cut-off limits in a storage capacity assessment.

The volumetric balance theory is commonly adopted to calculate storage capacity (Bachu and Shaw, 2003, 2005; Bachu et al., 2007). However, the effect of CO₂ dissolved in the remaining oil and water of the storage capacity, which is considerable and essential in the storage capacity calculation (Enick and Klara, 1990; Kovscek, 2002), was not been taken into consideration in their studies.

1-5. Methodologies of Estimating CO₂ storage capacity

Methods available for estimating subsurface volumes are widely and routinely applied in oil and gas, ground water, underground natural gas storage, and underground injection Control (UIC) disposal-related estimations. In general, these methods can be divided into two categories: static and dynamic. The static models are volumetric and compressibility; the dynamic models are decline curve analyses, material balance, and reservoir simulation.

1.5.1- Volumetric Methods

- Estimation of CO₂ storage capacity in oil and gas reservoirs

Carbon Sequestration Leadership Forum (CSLF) provided equations for oil and gas fields assume that reserves can be replaced by CO₂:

For gas fields:

$$M_{CO_2tg} = OGIP_s \times R_f \times \rho_{CO_2} \times (1 - F_{IG}) \times \left(\frac{(P_s \times Z_r \times T_y)}{(P_r \times Z_s \times T_s)} \right) \quad (10)$$

For oil fields:

$$M_{CO_2to} = \rho_{CO_2} \times \left(\frac{(R_f \times OOIP)}{(B_o - V_{tw} - V_{pw})} \right) \quad (11)$$

An alternative version for oil and gas fields is based on the geometric size of the reservoir:

$$M_{CO_2th} = \rho_{CO_2r} \times (R_f \times A \times h \times \varphi \times (1 - S_w) - V_{iw} + V_{pw}) \quad (12)$$

The effective version of this calculation assumes that most the recoverable reserves of the oil can be largely replaced with CO₂ [21]. This is generally valid for pressure-depleted reservoirs that are not subject to water drive from surrounding aquifers, or where water-flooding has not been applied. Where water has invaded the reservoir, it is assumed that CO₂ can displace some but not all of this fluid, and so the estimated storage capacity is reduced. Storage capacity is also affected by the difference in density between oil and CO₂ (leads to gravity segregation), CO₂ mobility with respect to water and reservoir heterogeneity.

The United States Department of Energy applied another method to calculate CO₂ theoretical storage capacity, based on CO₂ enhanced oil recovery theory and volumetric balance theory. The general form of the volumetric equation to calculate CO₂ theoretical storage capacity in oil reservoirs is shown below equation (Goodman et al., 2011) [21].

$$M_{CO_2to} = \rho_{CO_2s} \times (A \times h \times \varphi \times (1 - S_{wi}) \times B_o \times E_{oil}) \quad (13)$$

Others (Shaw and Bachu, 2006; Shen and Liao, 2009; Brennan et al., 2010) presented a number of various methods according to different reservoir development characteristics, but all of them were based on the volumetric balance theory.

The effective storage capacity is calculated as

$$M_{CO_2eh} = M_{CO_2t} \times (C_m \times C_b \times C_h \times C_w \times C_a) \quad (14)$$

The formula used for the COACH and NZEC projects, including a discount to allow for irreversible water invasion is based on the above calculations. The storage coefficient was based on the reports of Vangkilde–Pederson for the value of the storage coefficient where insufficient data are available (based on simulation models):

$$M_{CO_2eh} = URR_s \times B_o \times \rho_{CO_2} \times S_{coeff} \quad (15)$$

The practical storage capacity requires the effective storage capacity value and takes into account economic factors. For example, many reservoirs have a small storage capacity, rendering them uneconomic. Building the infrastructure is costly, so larger storage sites are preferred. Matched capacity is identified when sources and matched to storage sites (sinks).

The CSLF methodologies do not calculate CO₂ storage during CO₂-EOR. However, (Bachu et al, 2007) note that the storage capacity obtained during the simulations is considered an effective estimate. Initial screening of reservoir sites for EOR is usually based on reservoir depth, temperature and pressure, minimum miscibility pressure (MMP) and oil gravity and that this selection is narrowed to CSLF (practical capacity) based on the recoverable reserves.

- Estimation of CO₂ storage capacity in aquifers

Aquifer storage is based on displacement of native pore fluid. For significant storage to be possible, it is necessary for a significant proportion of the native pore fluid to be displaced from the aquifer over the injection period. This may occur either by production of formation water (additional wells required) and/or by migration of groundwater into adjacent formations and/or to the ground surface or seabed. Overall storage capacity is the amount of CO₂ that will be eventually trapped by filling structural and stratigraphic traps plus CO₂ trapped on the migration pathway or dissolved into the pore fluids. Mineral precipitation is considered a slow process and so not considered over injection timescales. The calculation of storage capacity for aquifers mainly depends on the estimated volume for the aquifer which lies within closed traps. The theoretical CSLF calculation assumes all the pore space can be filled.

$$M_{CO2ta} = A \times h \times \varphi \times \rho_{CO2} \times (1 - S_{wirr}) \quad (16)$$

The effective capacity considers the volume of closed traps, trap heterogeneity, irreducible water saturation and buoyancy coefficient. For NZEC, these capacity limiting factors were amalgamated into a single storage coefficient. The CSLF based methodology (Bachu et al., 2007) for storage capacity in aquifers is calculated using the following formula:

$$M_{CO2ta} = A \times h \times \varphi \times \rho_{CO2} \times (1 - S_{wirr}) \times C_c \quad (17)$$

This formula was simply written as:

$$M_{CO2ta} = A \times h \times \varphi \times \rho_{CO2} \times S_{coeff} \quad (18)$$

- Compressibility

The compressibility approach is generally applied to fluids with nearly constant total compressibility (Ct) over some increase or decrease in pressure (p) from an initial pressure (Po). As such, single-phase oil reservoirs and confined saline-water filled formations are typical applications. The principle behind using this relationship to estimate CO₂ storage is that for an incremental increase in pore pressure (due to CO₂ injection), the water volume will decrease and the effective pore volume will increase. The sum of these volume changes is the additional volume that CO₂ can occupy.

The injection of CO₂ into a saline formation suggests two phases, CO₂ and brine water, but for estimating CO₂ storage using the compressibility formula, only the change to the water phase is relevant. The equation below shows the compression of the original water volume (Vow) due to an increase in pressure (P) above the initial pressure (Po). The change in volume (ΔVw) is the volume that CO₂ can occupy as a consequence of increasing the pressure from Po to P via the injection process.

$$M_{CO2} = \Delta V_w = V_{ow} \cdot C_t \cdot (P - P_0) \quad (19)$$

The pressure (P) in this equation is the average pressure in the area of the injection well, a static, shut-in pressure, not an injection pressure. The analyses of a pressure falloff test (injection followed by a shut-in period) yields an average pressure. The original water volume Vow is determined by the volumetric equation using A, h, and Φ. The Ct is the sum of the pore compressibility of the formation (Cp) and the in-situ water saturating the formation (Cw).

$$C_t = C_p + C_w \quad (20)$$

For an estimate of the CO₂ storage capacity of a site, p could be defined as the maximum capillary pressure of the sealing rock or a maximum pressure that may cause a boundary (e.g., a fault) to leak. This pressure is not the injection pressure of a well that may initiate or propagate a fracture due to relatively high pressure injection, but is the average water pressure of the entire Vow. Because the pore pressure could be controlled by the production of water, the economics and regulations of a specific site would determine if water production was an option.

Consequently, a pressure constraint would not be used to calculate the storage resource, but a site specific storage capacity.

1.5.2- Dynamic Methods

- Decline Curve Analyses

The decline curve is one of the simplest and most frequently used equations in the petroleum industry to forecast oil rates and ultimate production. An analogy for CO₂ injection is developed. The basis for estimating subsurface storage volumes using active injection assumes a type of injection rate - time relationship. Primarily because of its simplicity, the most common relationship used in the oil industry is exponential decline. Injection rate (q_{CO_2}) is expected to be an exponential function of time based on an initial injection rate (q_{CO_2i}) and a decline coefficient (D) that reflects various flow characteristics of the formation. The general form of this equation follows:

$$q_{CO_2} = q_{CO_2i} \cdot e^{-Dt} \quad (21)$$

The exponential decline equation is used to determine the decline coefficient (D), given an injection rate history. The slope of a semi-log plot of $\log(q)$ vs. time yields the decline coefficient (D).

If an abandonment or minimum economic injection rate (q_{CO_2A}) is determined, the cumulative injection volume of CO₂ between rates of q_{CO_2i} and q_{CO_2A} is calculated and related to the ultimate storage volume. The projected CO₂ capacity (G_{CO_2}) is based on the following equation:

$$G_{CO_2} (capacity) = \frac{q_{CO_2i} - q_{CO_2A}}{D} \quad (22)$$

Use of the storage efficiency factor (E) could be used to estimate the storage resource available within the injection area of this well that might be available using the following relationship.

$$G_{CO_2} (resource) = G_{CO_2} (capacity) / E \quad (23)$$

- **Material Balance**

The complete material balance equation includes the cumulative CO₂ injection and the corresponding pore pressure (P) at various times. Fluid properties that reflect CO₂ compressibility (z) or the gas formation volume factor (Bg) are required. The formula for CO₂ sequestration in saline formations can be derived very similarly to the p/z plot used in natural gas reservoir and underground gas storage reservoirs, which is shown below:

$$P/z = \left(1 - G_p/G\right) \cdot \left(P_i/Z_i\right) \quad (24)$$

The estimate of gas in place (G) is estimated from this plot using the cumulative gas produced (Gp). The subscript "i" is the initial conditions prior to production. (An aquifer influx or efflux term can be included based on specific applications; in this case, aquifer properties such as water and formation compressibility are required.)

By analogy, the material balance equation can be developed for sequestration.

$$P/z = \left(1 - G_{inj-CO_2}/G_{CO_2}\right) \cdot \left(P_a/Z_a\right) \quad (25)$$

This formula can be written so that a straight line appears on a cumulative CO₂ injection (G_{inj-co2}) versus p/z where z_i is the z-factor of CO₂ evaluated at pressure p. However, unlike when gas is produced from a gas reservoir and pressure decreases, during sequestration gas pressure will increase with time and the aquifer efflux (W_e) must be included because of the brine water that is leaving the injection zone around the well. Unfortunately, introducing the W_e to this formula yields a nonlinear relationship. The general form using the Bg form can be written below:

$$G_{CO_2} \cdot (B_g - B_{ga}) + W_e = G_{inj-CO_2} \cdot B_g \quad (26)$$

The term $G_{inj-CO_2} \cdot B_g$ is the cumulative subsurface volume of CO₂ injected. The term $G_{CO_2} (B_g - B_{ga})$ (capacity) is the volume that the ultimate CO₂ storage volume would occupy at the current pressure, P. The W_e term is the aquifer effect.

1.5.3- Maximization of the storage capacity

Although depleted oil and gas reservoirs are the most attractive geological media for CO₂ storage, their total capacity is limited. Therefore, it is crucial to utilize fully the capacity of a given reservoir and there by maximize the value of the depleted oil and gas reservoirs in reducing CO₂ emissions. For CO₂ storage in a depleted oil reservoir, the capacity primarily includes the storage as a free supercritical CO₂ gas phase and its dissolution in the formation water and residual oil. The trapping through mineralogical reaction is not considered in the storage injection stage, although it may play an important role in the long-term sequestration. Since the capacity, both as a free gas phase and dissolution in reservoir liquids (oil, water), increases with increasing pressure, the most straightforward option to maximize the storage capacity of a given reservoir is to increase the storage pressure. However, the increase in storage capacity becomes limited after the pressure reaches a certain level, for three types of storage capacity as a function of pressure in a 1 m³ void space of a hypothetical reservoir. Both the brine and oil used in the calculations were collected from the Weyburn reservoir [56].

Although all of these three types of storage capacity increase with increasing pressure, the slope of capacity vs. pressure becomes gradually smaller after the pressure exceeds a certain value. For the reservoir temperature in the Weyburn field, 59 °C, the amount of CO₂ stored as each of these three types of storage almost levels off after 20 MPa. The increase of pressure from 20 to 30 MPa gives an increase in storage capacity of less than 10% as shown in the following figures. This may be of little worth in practical applications, since the resulting risks of the containment are considerably amplified with such a dramatic increase in pressure.

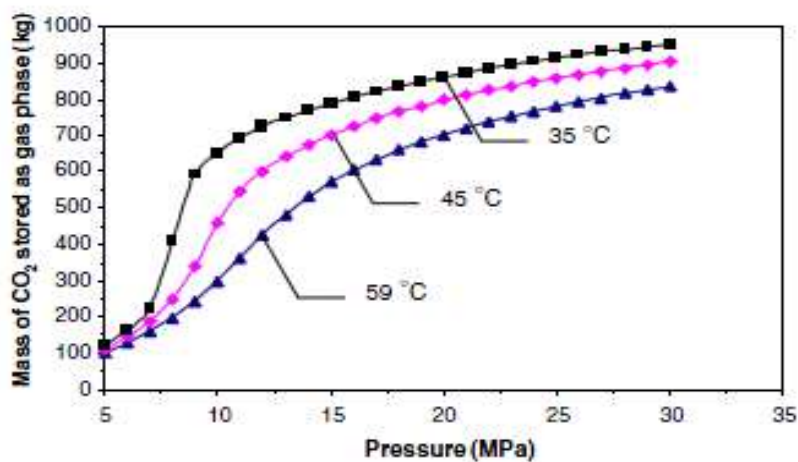


Fig. 27: The amount of CO₂ stored as a free gas phase in 1 m³ void space as a function of pressure at different temperatures [56].

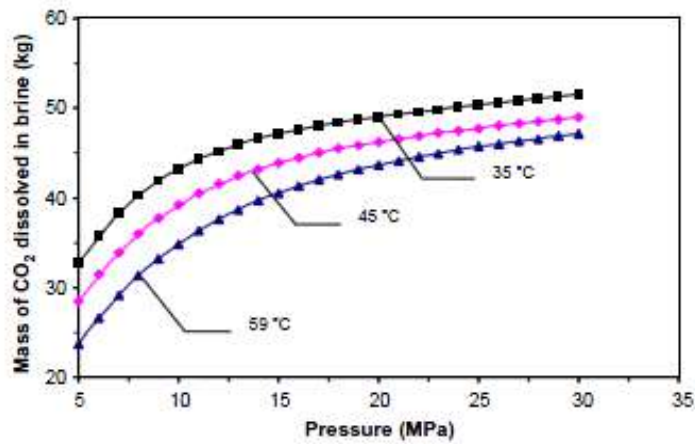


Fig. 28: The amount of CO₂ stored as dissolution in 1 m³ Weyburn formation brine as a function of pressure at different temperatures [56].

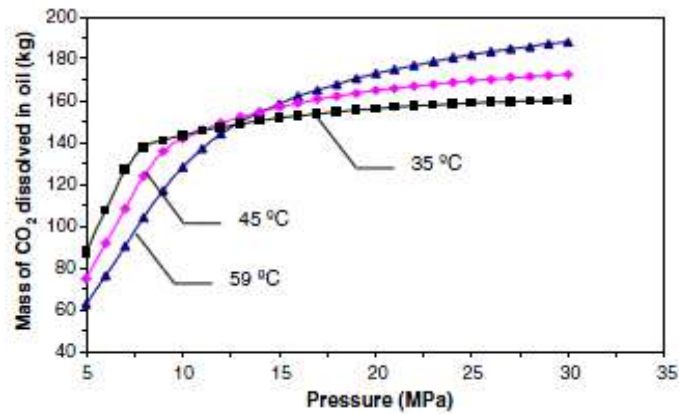


Fig. 29: The amount of CO₂ stored as dissolution in 1 m³ Weyburn reservoir oil as a function of pressure at different temperatures [56].

The storage capacity calculations based on 1 m³ void reservoir space also show that for a given reservoir volume, the storage capacity as a free gas phase is much larger than that as dissolution in the water and oil. In depleted oil reservoirs that have undergone secondary and enhanced oil recovery processes, most of the pore space is filled with water injected to displace oil, maintain reservoir pressure, or improve the sweep efficiency (in the water alternating gas process) during the secondary and tertiary recovery processes.

2. Sealing of the CO₂ storage reservoirs

2-1. Introduction

Comparing to deep saline aquifers that probably have largest potential in volume for CO₂ storage, the depleted or nearly depleted oil and gas reservoirs are the most appealing geological storage locations for CO₂ sequestration for the following reasons:

- The sealing capacity of the caprock, which had successfully sealed the original hydrocarbon in the reservoirs for a geological time, is sufficient to prevent the injected CO₂ from escaping into the upper formations.
- Oil and gas reservoirs have been extensively investigated during the oil exploitation stage.
- The underground and surface infrastructure (wells, equipment and pipelines) is already available.

Studies on CO₂ storage in depleted oil and gas reservoirs have been extensively conducted in different aspects, such as underground migration simulation, geochemical modelling, long-term integrity and risk assessment [31, 37].

Many criteria should be investigated prior the implementation of any CO₂ sequestration project, the original reservoir pressure is the primary criterion, and the sequestration is considered to be safe as long as the pressure of the injected CO₂ is lower than the original reservoir pressure. This criterion is based on the assumption that the sealing capacity of the caprock that retained the oil and gas in the first place should be adequate to prevent the injected CO₂ from escaping through the caprock. However, when the hydrocarbon (oil/gas) is replaced by the injected CO₂, the interfacial tension (IFT) of CO₂/brine system decreases comparing to that of the original hydrocarbon/brine system which can lower the capillary sealing pressure of the cap rock [38].

Caprocks are essentially defined as low (μ Darcy, 10-18 mD) or very low (nDarcy, 10-21 mD) permeability formations, and sometimes, but not necessarily, with low porosity (<15%). Caprocks are generally viewed as hermetic layers above the storage into which no CO₂ should migrate.

Different mechanisms for CO₂ migration are possible, from small to large scales:

- Molecular diffusion of dissolved CO₂ in the pore water from the reservoir zone into the caprock formation.
- CO₂ dyshasic flow after capillary breakthrough.
- CO₂ flow through existing open fractures.

The following mechanisms can accelerate or slow down the migration:

- Chemical alteration of the mineralogical assemblage of the caprock formation under the influence of acid water.
- Re-opening of pre-existing fractures or micro-cracks induced by overpressure of the reservoir below.
- A combination of the above (chemical alteration of the mineral filling the fractures).

2-2. Leakage mechanisms

Leakage of CO₂ stored in geological formations is a major concern, and the research in this field is growing rapidly. Given a laterally continuous seal and a structural trap, Metz et al. (2006) identify the following leakage pathways:

- Through the pore system in low-permeability caprocks, such as shale, if the capillary entry pressure at which CO₂ may enter the caprock is exceeded.
- Through openings in the caprock, such as lateral discontinuities or fractures and faults.
- Through anthropogenic pathways, such as poorly completed and/or abandoned pre-existing wells.

Gasda et al. (2004) have identified abandoned wells as one of the most probable leakage pathways for CO₂ storage projects, due to their high density in many sedimentary basins, i.e., 350000 wells in the Alberta basin. Nordbotten et al. (2004) have used semi-analytic solutions to show that leakage through multiple passive wells is not a simple sum of single well leakage rates, due to leakage induced draw-down around passive wells. They have also identified that multiple aquifers mitigate leakage into shallow zones, because of loss of CO₂ into the intervening aquifers. Numerical comparisons under less restrictive assumptions have shown that the inclusion of additional processes leads to reductions in leakage rates (Ebigbo et al., 2006).

2-3. Mechanisms of Potential leakage through the caprock

Structural trapping therefore occurs when the caprock prevents migration of the carbon dioxide injected into the reservoir. Poor containment can lead to leakage of carbon dioxide, either in supercritical form or when dissolved in the water. The mechanisms governing these two forms of transport are obviously different. In supercritical form, the bubble pressure of the CO₂ must be sufficient to overcome the capillary forces. This is the capillary breakthrough. In dissolved form, CO₂ can be transported by molecular diffusion, but also by permeation in response to a pressure gradient (Bentham and Kirby, 2005).

The characterization of caprocks for CO₂ sequestration is therefore a very important step in the evaluation of a storage location. Convenient storage site

must exhibit low transport properties and good integrity, i.e. absence of fracture and other preferential pathway (Moreno et al., 2005).

Investigations of gas leakage through caprocks have been reported in the literature. Two mechanisms were found responsible for gas migration into the adjacent formations [38]. One is compressible flow of the free gas phase, called volume flow or slow Darcy flow, and the other is molecular diffusion. Between them, the volume flow would be more efficient once it occurs and, thus, more dangerous in CO₂ storage. The prerequisite for the occurrence of volume flow is for the pressure difference across the caprock to exceed the breakthrough pressure of the caprock. Although the volume flow could be prevented through selecting a proper storage injection pressure, further quantitative estimations of the migration rate caused by volume flow are important in understanding the basic scenarios and the related risks when the caprock is broken through.

2-4. Migration in Supercritical status

2.4.1- CO₂ Supercritical properties

The density of the CO₂ is considered as the key thermodynamic parameter in CO₂ geological sequestration, in the deep geological formations the supercritical conditions (T_c, P_c) are the most probable conditions. A supercritical fluid combines the properties of gases and liquids. Thus, if its density approaches to that of a liquid, its viscosity tends towards to that of a gas (this characteristic is very important in case of using CO₂ injection as enhanced oil recovery (EOR)). One of the results of these remarkable properties is the compressibility of these fluids, which may be very large and tends even to infinity at the critical point (Caude et Thiebaut, 1998). The density increases considerably with the pressure and the viscosity remains low. In fact, the viscosity decreases as the temperature increases but for high temperatures values the viscosity increases (Lumia, 2002).

The following table summarize the different values of the density and viscosity of CO₂ in gas, liquid and supercritical stat in different pressure and temperature values.

Table. 09: Density and viscosity of CO₂ in different stats (National Institute of Standards and Technology, 2002) [39].

Stat of fluid	Density (kg.m ⁻³)	Viscosity (10 ⁻⁵ Pa.s)
Gases (1bar, 15-30 °C)	1.8472 to 1.7543	1.44451.5174
Supercritical	- 379.49	- 2.7176
- (P _c =73.8 bar,T _c =31 °C)	- 480.53	- 3.7190
- (200 bar, 100°C)		
Liquid (100 bar, 0- 10°C)	974.05 to 920.46	11.5 to 9.870

The dependence of the CO₂ density on the pressure and temperature is shown below

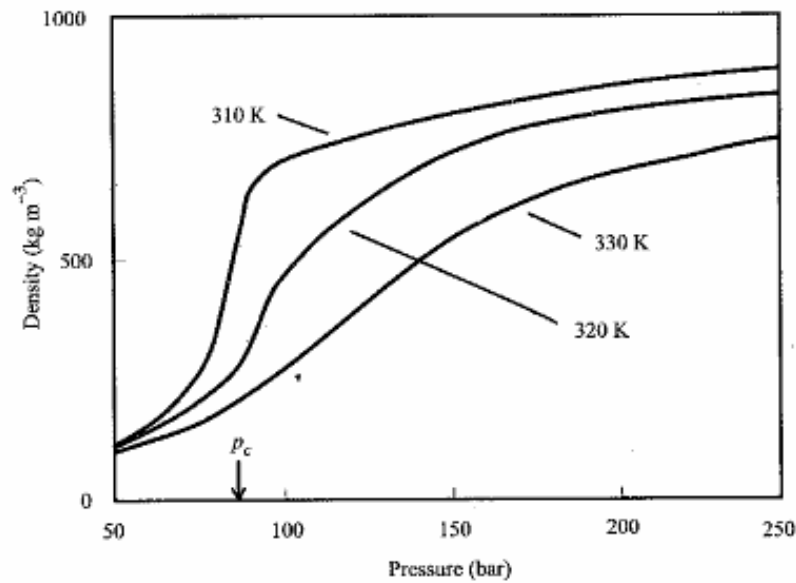


Fig. 30: isotherm CO₂ density as function on the pressure and temperature (Clifford, 1998).

2.4.2- Solubility of the CO₂

The solubility of the CO₂ into the water is defined as the amount of CO₂ that can dissolve into the water depends on several factors, most notably pressure, temperature, and salinity of the brine (e.g. Spycher et al. 2003; Lagneau et al. 2005; Koschel et al. 2006; Oldenburg 2007). At the reservoir conditions, CO₂ solubility increases with increasing pressure (i.e. depth) but decreases with increasing temperature and salinity. The experiments in the literature (Bench-scale experiments) demonstrate that CO₂ dissolution is rapid at high pressure when the water and CO₂ share the same pore space (Czernichowski-Lauriol et al. 1996). However, in a real injection system, CO₂ dissolution may be rate-limited by the magnitude of the contact area between the CO₂ and the fluid phase. As almost of reservoirs the temperature is constant the solubility is highly affected by the reservoir pressure as shown in the below figure.

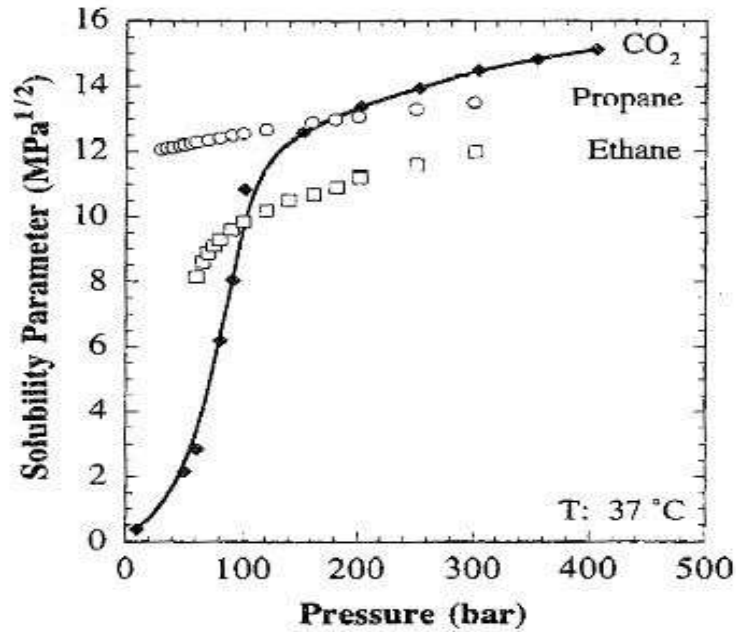


Fig. 31: Solubility as function in the pressure and at T=37 °C (Harrison, 1996).

2.4.3- Interfacial Tension CO₂/Brine $\sigma_{CO_2/brine}$

The most important interfacial property is the interfacial tension (IFT) between CO₂ and brine that saturates the caprock and pre-exist in the aquifers/reservoirs. IFT affects the multiphase flow properties of the porous formation, such as the relative permeabilities, and CO₂ capillary breakthrough pressure which is defined as the critical pressure above which CO₂ may leak through the caprock.

Under real storage conditions, the brine of reservoirs is a mixture of different salts containing the anion Cl^- whereas the cation is either monovalent or divalent (NaCl, KCl, CaCl₂, MgCl₂etc.) [60]. It is very important to know the dependence of IFT on salinity when the brine is composed of various salts, and the dependency of the IFT on the pressure and temperature.

- Effects of pressure and temperature on CO₂/brine IFT

The experimental results stated in the literature reveal that under constant temperature, IFT is a decreasing function of pressure, since CO₂ solubility in brine increases as pressure increases (Fig. 32). At lower pressures the decrease of IFT is steeper, while at higher pressures the rate of IFT decrease weakens and gradually vanishes. Finally, at elevated pressures and over all temperatures, IFT tends asymptotically to a constant value and a pseudo-plateau is approximated (Fig. 32).

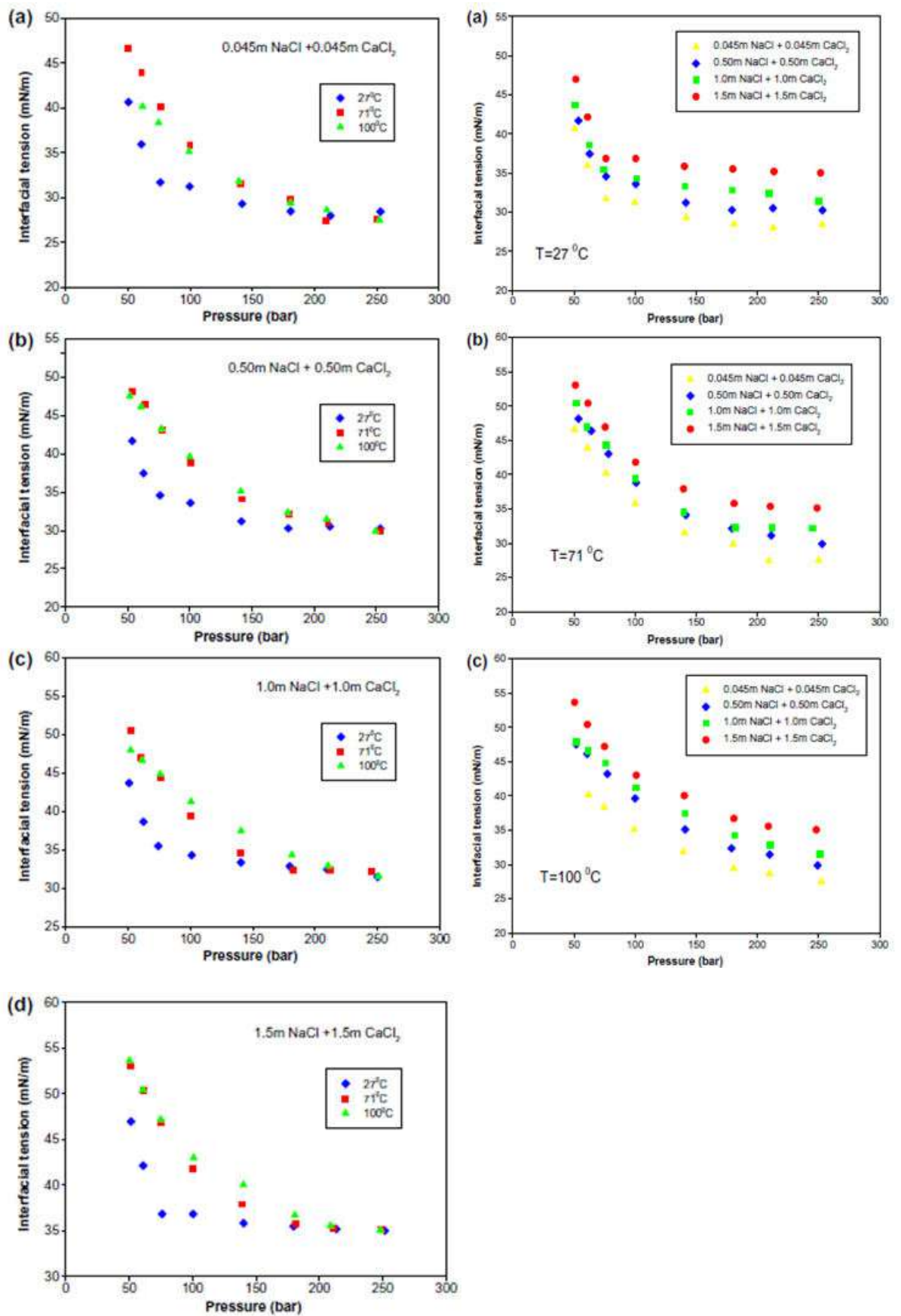


Fig. 32: CO₂/brine interfacial tension as a function of pressure for different temperatures at various salinities of each salt in brine (a) 0.045m, (b) 0.50m, (c)1.0m and (d) 1.5m [40].

The dependence of CO₂/brine IFT on temperature is similar to that reported in the literature for CO₂/NaCl solution and CO₂/CaCl₂ solution systems. From the below Figure, it becomes clear that for pressures $P < P_{\text{plateau}}$, CO₂/brine IFT increases with the temperature increasing from $T = 27 \text{ }^{\circ}\text{C}$ to $T = 71 \text{ }^{\circ}\text{C}$, but remains unaltered in the temperature range $T = 71 \text{ }^{\circ}\text{C}$ - to $T = 100 \text{ }^{\circ}\text{C}$, particularly with reference to low salinities (Fig. 32a and b). For higher salinities (Fig. 32c and d), a small increase of IFT is observed as temperature increases from $T = 71 \text{ }^{\circ}\text{C}$ - to $T = 100 \text{ }^{\circ}\text{C}$. After IFT plateau has been reached, the interfacial tension becomes almost unaltered regardless of the temperature. From the abovementioned observations, it becomes clear that the dependence of CO₂/brine IFT on temperature is complicated and no linear correlation between IFT variation and temperature can be drawn [40].

- Effect of salt concentration on CO₂/brine system IFT

Saline aquifers, as it determines the entry capillary pressure of the caprock and, subsequently, the maximum CO₂ pressure that the reservoir seal can sustain and thus the reservoir storage capacity. CO₂/brine IFT depends on the pressure, temperature, salinity, as well as the valence of the cations present in the brine. Generally in aquifers, the brine is composed of various salts, such as NaCl, KCl, CaCl₂, and MgCl₂...etc. The concentration of salts containing monovalent cations is about 70% of the total mass concentration of the brine, while the corresponding one of divalent cations is about 30%. Based on IFT measurements conducted in [60] between CO₂ and brine containing NaCl and CaCl₂, we realized that the total IFT increase is the sum of the individual IFT increments caused by each salt.

CO₂/brine IFT increases with brine salinity, but so does the density difference between brine and CO₂. In order to find out the net effect of brine salinity on the maximum column height, H , of CO₂ that can be trapped in a given formation which is defined as:

$$H = \frac{2\sigma_{CO_2/b} \cdot \cos\theta}{(\rho_b - \rho_{CO_2}) \cdot g \cdot r_p} \quad (27)$$

In order to find out the net effect of brine salinity on the maximum column H of CO₂ that can be stored in a saline aquifer, (C.A. Aggelopoulos et al., 2011) carried out some calculations using IFT and density data for all temperatures considered in this study. At elevated pressures and $T = 27 \text{ }^{\circ}\text{C}$, H decreases substantially as brine salinity increases. It was found that H is about 50% lower at brine salinity (1.5m NaCl + 1.5m CaCl₂) than that estimated at brine salinity (0.045m NaCl + 0.045m CaCl₂). As temperature increases, H tends to be independent of brine salinity (H decreases about 15% at $T = 71 \text{ }^{\circ}\text{C}$ and 10% at $T = 100 \text{ }^{\circ}\text{C}$) as shown below

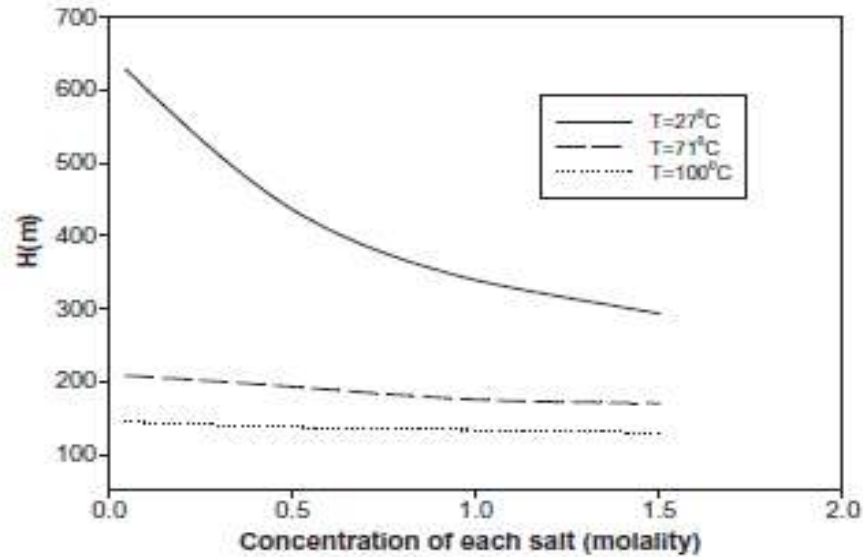


Fig. 33: Maximum column H of CO₂ that can be stored in a saline aquifer (in meters) as a function of brine salinity at various temperatures. For this application, the radius R of the caprock is assumed to be constant, at a value of 10⁻⁷ m [40].

2-5. Cap Rock sealing capacity

The sealing capacity of a caprock is indicated by the magnitude of the breakthrough pressure (or sealing pressure), defined as the differential pressure across the caprock that just exceeds the capillary pressure of a series of interconnected pore throats with an arbitrarily large size, thus causing the non-wetting phase to flow through these pore throats. In essence, the capillary pressure within the arbitrarily large pore throats determines the breakthrough pressure. Thus, the capillary pressure correlation can be used to analyse the breakthrough pressure. The capillary pressure P_c in a pore throat is expressed by:

$$P_c = \frac{2\sigma}{r_p} \cos\theta \quad (28)$$

This equation shows that for a given caprock, the capillary pressure of the largest interconnected channels or, eventually, the breakthrough pressure depends on the IFT and the contact angle, the contact angle would be close for CO₂ to CH₄ or N₂. As a result, the breakthrough pressure is primarily determined by the IFT of the gas/water system for a given caprock. The ability of oil and gas to be retained in the reservoir over a geological time span is mainly attributed to the high sealing pressure of the caprock due to the high IFT and extremely small size of the caprock pore throats, especially for those abnormally high pressure oil and gas reservoirs (with reservoir pressure in excess of the hydrostatic pressure).

Once an oil reservoir has undergone a CO₂ injection process, a supercritical CO₂ phase will replace the original hydrocarbon and stay at the top of the reservoir formation in contact with the caprocks. The breakthrough pressure changes owing to the change of IFT at the interface of the non-wetting/wetting phase. The below table summarizes the literature results of IFTs between different non-wetting/wetting phases at conditions close to those of typical oil and gas reservoirs. It is seen from Table below that the IFT of the CO₂/water system is much lower than that of oil/water systems and even lower than that of methane (or nitrogen)/water systems. Accordingly, the breakthrough pressure of the same caprock is to be reduced proportionally when CO₂ is injected to replace the original hydrocarbons in the top of the reservoir (most oil reservoirs have natural gas caps in the top).

Table. 10: IFT for different fluids systems.

Systems	Conditions	IFT (mN/m)
CH ₄ /water	10-30 MPa, 40-80 °C	48.6-61.7
N ₂ /water	10-30 MPa, 40-80 °C	53.7-67.2
Medium oil/watr	>6.9MPa, 54,4-81.1 °C	30-35
N-alkane C ₆ -C ₁₆)/water	10-30 MPa, 25-50 °C	49-54
CO ₂ /water	10-30 MPa, 40-80 °C	16-30

The resulting lower breakthrough pressure for CO₂ due to the reduced IFT of the CO₂/water system indicates that the trapping capability of the caprock that retained the oil and gas in the first place may not be sufficient to seal the injected CO₂ within the reservoir. Injection of CO₂ to restore the reservoir pressure to its original reservoir pressure can be risky, especially for those closed reservoirs. These reservoirs are considered as ideal geological containers for CO₂ storage after the hydrocarbon has been extracted. It is crucial to obtain the caprock breakthrough pressure for closed reservoirs prior to the CO₂ storage injection because the caprock breakthrough pressure for CO₂ might be smaller than the original reservoir pressure. In such a case, the caprock will be broken through before the original reservoir pressure is reached. On the other hand, the breakthrough pressure, if greater than the original reservoir pressure, is also useful for determining how much overpressure can be applied for storing CO₂. For reservoirs in contact with bottom or edge waters, the reservoir pressure might be released to a different extent as the invaded water is pushed back by the CO₂ injection. However, since the pressure built up in the vicinity

of the injection wells during the injection process is usually much higher than the average reservoir pressure, the caprock breakthrough pressure is still necessary to avoid leakage through the caprock in this high pressure zone. The caprock breakthrough pressure for CO₂ is an important constraint in designing and implementing CO₂ storage injection. The following table summarize the caprock breakthrough pressure mentioned in the literature.

Table. 11: Summary of caprock breakthrough pressure results in the literature.

Caprock lithology	Non-wetting/wetting system	Breakthrough pressure (MPa)
Sandstone, limestone and dolomite.	N ₂ /water	0.14-4.83
Sandstones, shales and chinks. Limestone, siltstone, clay-stone Pelitic rocks (clays, clay-stones, shales, mud-rocks, and siltstones). Evaporite	N ₂ /water	0.12-2.2 (with one sample exceeding 3.6 MPa, but not determined) ^a
	N ₂ /water	
	N ₂ /water	0.2-19.8 ^a
	N ₂ /water	0.06-6.7
	N ₂ /water	9.2-21.4

a: Data converted from the measured Hg/air system breakthrough pressures using IFTs and contact angles of two different systems (Hg/air and CH₄/water).

2-6. Characterization of gas flow through caprocks

When the differential pressure across the caprock exceeds the breakthrough pressure because CO₂ injection has raised the reservoir pressure, a continuous gas volume flow will finally occur, (Zhaowen Li et al., 2005) investigated the volume flow of gas through caprocks using caprock samples collected from the Weyburn oil fields. Then both the gas absolute permeability and the effective permeability when water exists were determined, and calculations were made with the measured permeability values.

The migration of CO₂ through caprocks by volume flow is a two-phase (gas/water) flow in tight porous media coupled with capillary effects, which can be predicted once the two-phase relative permeability curve is measured. However, due to the extremely low permeability of the caprock samples, determination of the relative gas/water permeability curves appears to be difficult. Since only the gas migration through the caprock is of concern in CO₂ storage, a shortcut is to measure directly the effective gas permeability after a

water saturated rock sample is broken through and then apply the measured gas effective permeability to predict the gas migration through the caprock.

Before a gas effective permeability measurement, the water-saturated caprock sample was first broken through by CO₂ with a stepwise increase of gas pressure until a continuous liquid flow, followed by a gas bubble flow, was observed at the outlet of the core sample. Then, the flow rate was measured as a function of time until a steady gas flow was reached. The effective permeability was calculated from the measured flow rate.

Physically, this experiment simulated well the process of CO₂ breaking through the caprock and then migrating into the upper layers. Two samples from the Weyburn Midale Evaporite caprock were selected for the flow measurements, A7 and B8 with a porosity of 1.5% and 0.7%, respectively. The gas broke through the samples at about 2.9 MPa (A7) and 1.1 MPa (B8). The measured effective permeability was plotted against time in (Fig. 34 and 35), respectively.

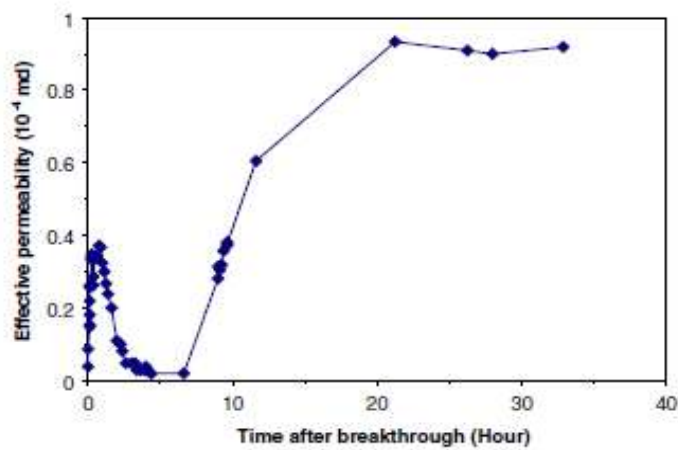


Fig. 34: Measured gas effective permeability vs. time after gas breakthrough for sample A7.[38]

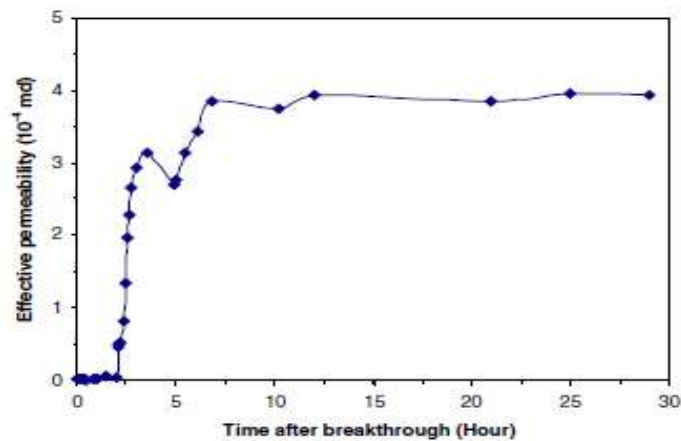


Fig. 35: Measured gas effective permeability vs. time after gas breakthrough for sample B8. [38]

The above figures show that the gas flow can be divided into two regions after the gas broke through. The early region is characterized by an extremely low and fluctuating gas flow, probably because the gas phase in some channels is not continuous in this period and, thus, the resistance to gas flow is relatively high. As well, the water phase (wetting phase) may be re-distributed due to the inhibition effect, thus blocking the gas from flowing through the caprock. So, in this early region, both the water and the gas phase are mobile. After a significant amount of time, all the mobile water in the channels where the gas flow prevails is carried out by the gas so that the gas forms a continuous phase and the water phase becomes immobile or irreducible. The gas effective permeability reaches its maximum value and remains stable.

It is seen that the measured effective permeabilities are significantly reduced compared with the absolute gas permeability. The ultimate effective gas permeability is about 1×10^{-4} md for sample A7 and 4×10^{-4} md for sample B8, only about 10% of the corresponding absolute gas permeability. This might be attributed to the extremely narrow pore throats in the tight caprocks, i.e. a large amount of the pore throats that allow single gas flow are completely blocked by the water slugs when water exists, the immobile water film occupies a significant portion of the channels broken through by the gas, and the gas only flows as fine filaments in these channels. Based on the observed reduction of the gas effective permeability compared with the measured absolute gas permeability, the effective permeability for Weyburn caprocks is estimated to be in the range of 3×10^{-5} to 6×10^{-4} md. This range is just covered by the results measured by (Hildenbrand et al., 2002) for Boom Clay caprocks, which have effective permeabilities ranging from 2.4×10^{-21} to 1×10^{-18} m².

2.6.1- Estimation of volume flow and comparison with molecular diffusion

Once the gas effective permeability is determined, the migration of the injected CO₂ after the caprock is broken through can be estimated. Calculations of the amount of CO₂ migration through the caprock as a function of time at different effective permeabilities 10^{-3} , 10^{-4} and 10^{-5} md is studied by (Zhaowen Li et al., 2005) and given in (Fig. 36).

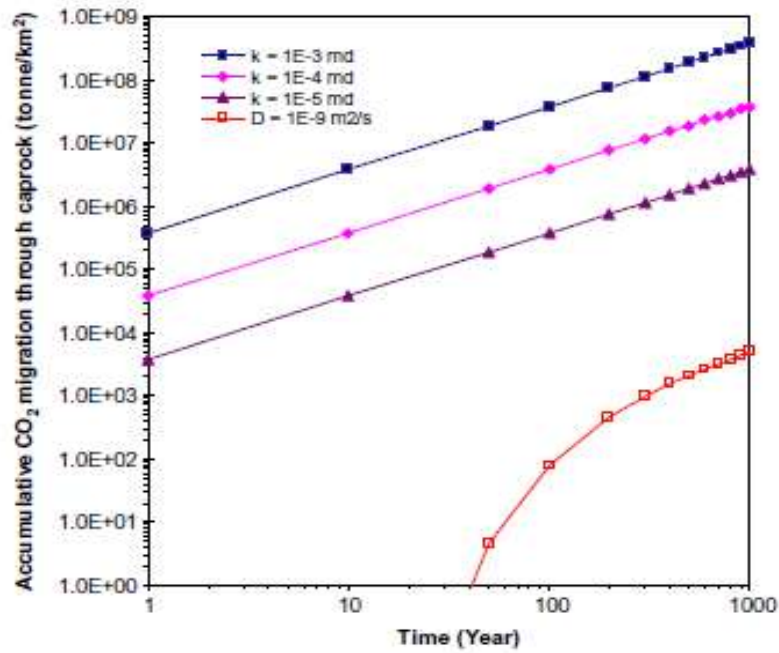


Fig. 36: Calculations of CO₂ migration through caprocks by volume flow and molecular diffusion [38].

The effective permeabilities used in the calculation are based on the measurements but are extended to a wider range. In the calculation, the reservoir pressure is assumed at 25 MPa and the pressure above the caprock is 15 MPa, yielding an average pressure within the caprock of 20 MPa. The thickness of the caprock is 10 m. The area in calculation is 1 km². The viscosity of the CO₂ is about 0.06 MPa.s, at 59 °C, 20 MPa [38]. The values of the above parameters are set to construct a scenario in the Weyburn CO₂ storage project. Here, it is also assumed that both the reservoir and overburden pressures do not change during the injection and leakage processes. The gas migration is only through the caprock, i.e. the leakage through the wellbore is not considered. It is seen from (Fig. 36) that the mass of CO₂ migrated into the upper layers increases linearly with time at each effective permeability. The consequence of this leakage rate in CO₂ storage injection can be well recognized when it is compared with the actual injection scenario in Weyburn. Based on the available results from the Weyburn project, the ultimate CO₂ storage potential in the Weyburn Unit, with an area of 180 km², is around 54.8 million tonnes over 50 years through CO₂-EOR and post-EOR CO₂ injection processes. The averaged storage efficiency is about 6.09 × 10⁴ tonne/km²/year. If volume flow occurs, the leakage rate is around 3.69 × 10³ tonne/km²/year even when the gas effective permeability of 10⁻⁵ md is used. This will cause a migration of 6% of the CO₂ that could be stored in the reservoir to the upper formations, which may eventually reach the surface. Fortunately, the high sealing quality of the caprocks in Weyburn, as indicated by the high

breakthrough pressure, is capable of preventing the injected CO₂ from leaking through a volume flow. However, it is of the first priority to re-evaluate the breakthrough pressure of the caprocks for different reservoirs once they are selected as the injection sites. The sealing pressure of the caprock should be considered as an important constraint in CO₂ storage injection.

In addition to the volume flow, the molecular diffusion of CO₂ into the adjacent formations would be much larger than that of light hydrocarbons as reported in the literature, due to the higher solubility of CO₂ in water than that of hydrocarbons. Using the model of diffusion through a plane sheet, the diffusion leakage of CO₂ through Weyburn caprock (under similar conditions as those for Darcy flow) was also calculated and is plotted in (Fig. 36). The caprock porosity used in the calculation is 2%. The solubility of CO₂ in brine is about 4.4 kg/m³ (0.001 mol/cc). The effective diffusion coefficient used is 10⁻⁹ m²/s; the leakage caused by molecular diffusion is negligible compared with the volume flow once the caprock is broken through. However, since molecular diffusion is a ubiquitous process over geological time, it may have significant impacts on the rock properties due to the mineralogical reactions caused by CO₂ in long-term containment.

Chapter 5

Effect of the fracture in CO₂ geological storage

Effect of the Fractures on CO₂ Storage Capacity and Reservoir Sealing

1- Introduction

One of the most widespread hydrocarbon formations around the world are naturally fractured reservoirs. Nearly all hydrocarbon reservoirs are affected in some way by natural fractures which represent the most largest reservoirs in term of reserve in place (theoretical storage capacity for CO₂ sequestration), yet the effects of fractures are often poorly understood and largely underestimated, naturally fractured reservoirs present a flow paradox, these reservoirs initially may appear highly productivity (in case of hydrocarbon production) / injectivity (in case of CO₂ storage) and decline rapidly [42, 43, 44].

A successful CCS project should guarantee safe and reliable long-term storage of injected CO₂. Among various risks and concerns, CO₂ leakage through naturally fracture/fault system could raise the risk of acidification of drinking water resources [49]. Densely fractured natural reservoirs are rarely considered as suitable candidates for CO₂ sequestration projects due to issues related to safe and secure long-term storage. Nevertheless, assessment of CO₂ storage processes including fluid migration in a storage medium with fractures is critical, as fractures occur in nearly all geological settings and play a major role in hydrocarbon migration as well as entrapment.

Two-phase flow in fractured rocks is much more complex due to dynamic interactions among the capillary, buoyancy, and viscous forces. Furthermore, the geometry of the fracture-matrix systems can result in complex flow patterns. The exchange mechanism between fractures and matrix is mainly driven by diffusion phenomenon that can affect highly in the storage capacity in case of CO₂ sequestration project.

In this section of the thesis, a comparison study between fractured and homogeneous reservoirs is conducted to verify the effect of fractures presence on sealing and storage capacity.

2- Natural fractured reservoirs

Fractured reservoirs are becoming a major issue throughout the entire world for both old and new fields. Many newly discovered oil and gas fields happen to be fractured and their development constitutes a real challenge. Naturally Fractured Reservoirs often abbreviated as NFRs - have been the subject of extensive studies during the past decades.

Natural fractures exist practically in all reservoirs, dividing the reservoir rock in pieces, called matrix blocks. In this case one must distinguish between matrix and fracture porosity and permeabilities.

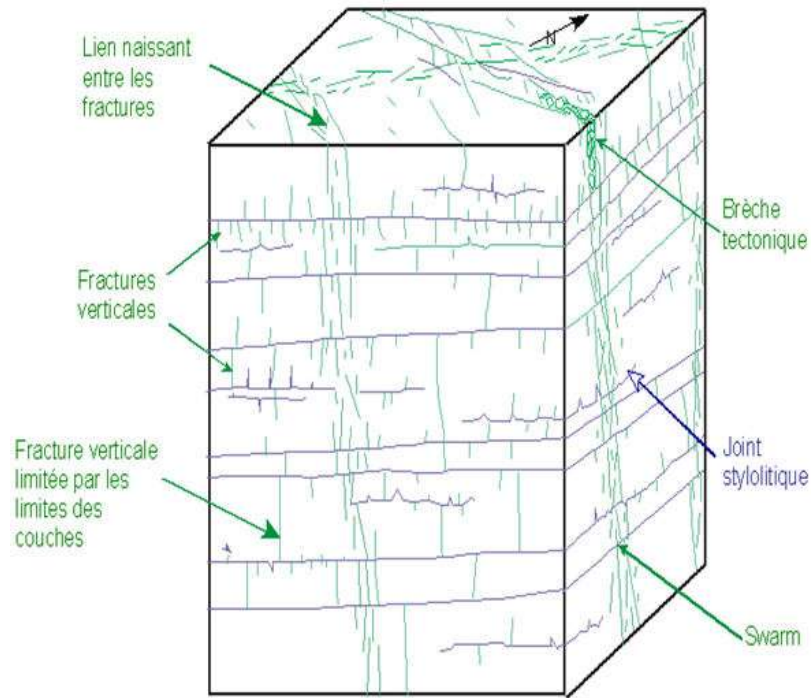


Fig. 37: Different fractures types in fractures reservoirs. [48]

- Dual Porosity

Porosity can be classified as primary or secondary. Primary porosity forms during deposition of sediments and includes inter-particle and intra-particle porosities. Secondary porosity forms after deposition and develops during diagenesis by dissolution, dolomitization and through production of fractures in the rock. The fracture porosity is always a secondary one and generally refers to porosity that occurs along breaks in sediment or rock body where there has been little mutual displacement along the fracture.

The fractures porosity is close to 1, but its relative volume is very small (less than 1%), which means that the storage of the hydrocarbon leads in the matrix blocs. The storativity of the reservoir (matrix and fractures) is defined by:

$$\omega = \frac{\phi_f C_f}{\phi_f C_f + \phi_m C_m} \quad (27)$$

Where ϕ_f, ϕ_m are the fracture and matrix porosity respectively, and C_f, C_m are the capacity (compressibility), generally the fracture porosity is neglected comparing to the matrix porosity.

- Dual Permeability

The permeability of a porous rock is a measure of the ability to transmit fluids. A reservoir can have primary and secondary permeability. The primary permeability is referred to as matrix permeability, the secondary permeability

can be either called fracture permeability or solution vugs permeability. Matrix-fracture permeabilities are other important parameters that have to be known for an estimate of the influence of the fractures on the overall reservoir performance. Open fractures in Naturally Fractured Reservoirs generally have a higher permeability than the matrix, building the flow channels of the system.

It is evident from the definition of the permeability that the fracture permeability is higher than the matrix permeability, several tools can be used to indicate the presence of fractures in case of fractured reservoir, and the response of the well during a well test is very useful tool as shown below.

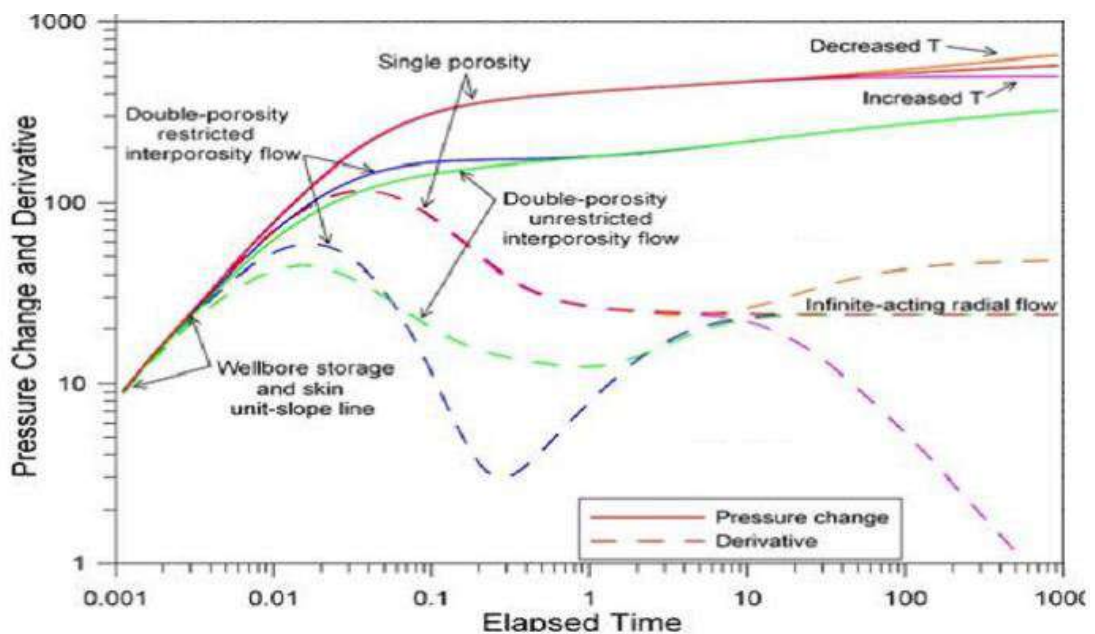


Fig. 38: Natural fractured reservoir response in well test

Generally, the permeability and the porosity are key parameters in reservoir performance assessment that express the ability of the fluid to flow through the reservoir and the storage capacity, in the fractured reservoirs the fluid flows throughout the fractures and stored in the matrix.

- **Fracture-Matrix Exchange**

The exchange mechanism between the matrix blocs and the fracture is driven microscopically by the diffusion phenomenon and macroscopically by matrix bloc geometry and matrix/fracture permeability rapport.

- **Diffusion**

Hydrocarbon may be recovered by diffusion during gravity drainage in fractured reservoirs. Methods for estimating the amount and rate of this

recovery in such reservoir processes are in early stages of development and poorly tested, the most extensive diffusion period is occurred before the production stage of the reservoir, once the fractures fluid is produced the production regime and the diffusion mechanism exchange between matrix bloc and fractures is not similar, the high production regime is very rapid and the diffusion mechanism could not feed the fractures by fluid from the matrix with same intensity, hence, the effects of diffusion on overall recovery is probably very small and can for most systems be neglected for practical purposes.

- **Matrix Block Shape and Size**

The matrix bloc shape and size affects strongly the matrix-fracture fluid exchange process, experiments have been conducted and stated in the literature show the impact of the different shape and size in the fractures-matrix fluid exchange.

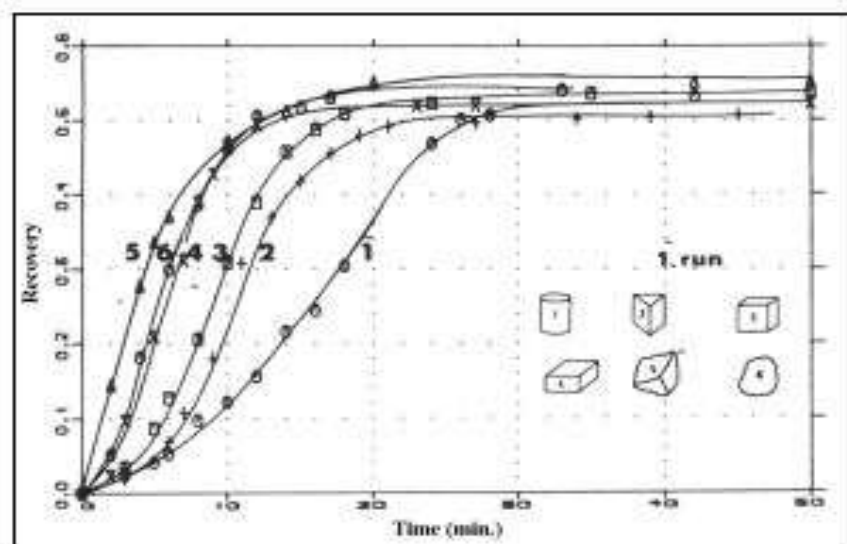


Fig. 39: Effect of size and shape on imbibition oil recovery [48].

This characteristic is defined in the following parameter (λ):

$$\lambda = \alpha \cdot r_w^2 \cdot \frac{K_m}{K_f} \tag{28}$$

3- Comparison of geological CO₂ sequestration performance between homogeneous and fractured reservoir

3.1- CO₂ Storage Capacity

The estimation of the CO₂ storage capacity plays an essential role in the evaluation, analysis, prediction of future performance, and making decisions regarding development of CO₂ storage project, this key parameter is very complicate and depends on the nature of the storage location, in deep saline aquifers is very complex because of the trapping mechanisms that act at different rates are involved, and at time, all mechanisms may be operating simultaneously. Estimation of the CO₂ storage capacity in depleted (or nearly depleted) oil and gas reservoirs is not straightforward process and is based on recoverable reserves, reservoir properties and in situ CO₂ characteristics, Bachu and Shaw (2003, 2005) and Bachu et al. (2007) used the original gas in place (IGIP) at standard conditions and the gas recovery factor to calculate the theoretical mass storage capacity for CO₂ at in situ conditions for gas reservoirs. As mentioned in the previous sections the principle methods for predicting CO₂ storage capacity are the volumetric (static) method and the material balance (dynamic) method, the volumetric method is based on geological data to define the reservoir areal extent, core and log data to define the reservoir rock properties and distribution of fluids inside the reservoir. The volumetric method provides a sketchy estimate, however, the material balance method is based on pressure-production data for estimating the initial gas in-place and the simplest method is to plot P/Z vs. G_p and extrapolate to zero-pressure. The both methods are mentioned (see section 7), in this section a dynamic method based on material balance equations is applied to compare the storage capacity of homogeneous and fractured oil/gas reservoirs.

3.2- Material balance method - Homogenous Reservoirs

As stated above the starting point to calculate the CO₂ storage capacity is the Material Balance method with different assumptions, Chi-Chung Tseng et al. [32] assume that the pore volume of the reservoir is unchanged during gas production and CO₂ injection, this assumption is valid only for low pressure completely seal off "volumetric" gas reservoir.

$$G_i B_{gi} = (G_i - G_p + G_{CO_2}) B_g + W_e \quad (29)$$

However, in oil reservoir case or if the reservoir initially has abnormally high formation compressibility, as observed in some high pressure gas reservoirs, the rate of pressure drop may increase with gas production. This is due to the fact that the compaction of the reservoir rock will provide pressure support at the high pressure level. In the present study we apply the Material Balance method to estimate the volume capacity storage of the oil-gas reservoir

destined for CO₂ Enhanced oil recovery (EOR) and storage project, of course, the starting of any CO₂ storage project should not be before 40-50 % of hydrocarbon recovery (may be less for oil reservoir), at this stage of development the total hydrocarbon pore volume should be known and highly accurate, but it will be not the total mass storage capacity due to the irreversibility phenomenon of the petrophysical parameters (porosity, compressibility,...). The material balance equation of the homogenous reservoirs with taking into consideration all sources of expansion (formation expansion, connate water expansion) and water influx from associated aquifer can be expressed as:

4. Gas Reservoir

$$G_i(B_g - B_{gi}) + G_{CO_2}B_{g/CO_2} + W_e + \Delta V_w + \Delta V_p = G_p B_{g/CO_2} + W_p B_w \quad (30)$$

5. Oil Reservoir

$$N_i(B_o - B_{oi}) + G_{CO_2}B_{o/CO_2} + W_e + \Delta V_w + \Delta V_p = N_p B_{o/CO_2} + W_p B_w \quad (31)$$

3.3- Material balance method - Fractured Reservoirs

The internal architecture of fractured reservoirs is more complex than that of homogenous reservoirs. This stems precisely from the presence of an additional network of fractures in the porous medium, which results from tectonic forces which have “broken” the rock. The presence of the fractures in the oil-gas reservoirs can be advantage for hydrocarbon recovery but disadvantage for CO₂ geological storage project. The material balance equation for the fractured reservoirs with taking into consideration the dual feature (dual porosity-permeability) of the formation and all sources of expansion (formation expansion, connate water expansion) and water influx from associated aquifer can be expressed as:

- Oil Reservoir

$$F = N_1 + N_2 \frac{E_{02}}{E_{01}} + G_{CO_2}B_{o/CO_2} + W_e - W_p B_w \quad (32)$$

Where E₀₁ represents the net expansions of the original oil phase in matrix system and E₀₂ is the net expansion of the original oil-phase in the fracture network and expressed as:

$$F = N_p [B_o + (R_p - R_s)B_g] \quad (33)$$

$$E_{01} = N_1 \left[B_o - B_{oi} + (R_{si} - R_s)B_g + \left(\frac{C_w S_{wi} + C_m}{1 - S_{wi}} \right) \Delta P B_{oi} \right] \quad (34)$$

$$E_{02} = N_2 \left[B_o - B_{oi} + (R_{si} - R_s) B_g + \left(\frac{C_w S_{wi} + C_f}{1 - S_{wi}} \right) \Delta P B_{oi} \right] \quad (35)$$

Where N_1 is OOIP in the rock matrix and N_2 is OOIP in the fractures C_m and C_f represent the compressibility of the rock matrix and the average compressibility of the fractures. From the previous equations we derive that the theoretical storage capacity of the homogenous and fractured reservoirs are not same.

- Gas Reservoir

All the formulation applied for oil reservoirs are valid for gas reservoir with appropriate changes of G instead of N and FVF factor.

4- Modeling Methodologies

4.1- Model geometry

Mathematically the oil in place in the fractured and homogenous reservoirs is not the same as shown previously. In this study, simple reservoir model is built to evaluate the storage capacity and flow behaviour of the CO₂ stored in the homogenous and fractured reservoir. The both models have same dimension with the presence of the fractures properties in the fractured reservoir model as shown below tables.

- Static Data

Table. 12: Homogeneous reservoir data

Parameter	Unit	value
$\Delta X \Delta Y \Delta Z$	ft	2000×1000×250
Pi	psia	4910
Tres	°F	208
Pb	psia	3536
POR	%	29
Kx,Ky,Kz	md	10,10,0.1
Co	1/psi	0.0000197

Table.13: Fractured reservoir data

Parameter	Unit	value
$\Delta X \Delta Y \Delta Z$	ft	2000×1000×250
Pi	psia	4910
Tres	°F	208
Pb	psia	3536
PORM	%	29
PORF	%	0.01
Kxm,Kym,Kzm	md	10,10,0.1
Kxf=Kyf=Kzf	md	10.10.90.20.20

- **Dynamic Data**

A compositional model used in this study with two wells (oil producer well and gas injector well), the initial reservoir pressure was considered as the pressure constraint storage (to be safe and below the reservoir hydraulic pressure), the dynamic model data is shown in the below table

Table. 14: Dynamic data

Parameters	Unit	Value
Pinj	psia	6000
BHP	psia	5000
Pb	psia	4500
QCO ₂ Max	MSCF	2000
Qo Max	STB	2000

The geometry of the reservoir is shown in below figures

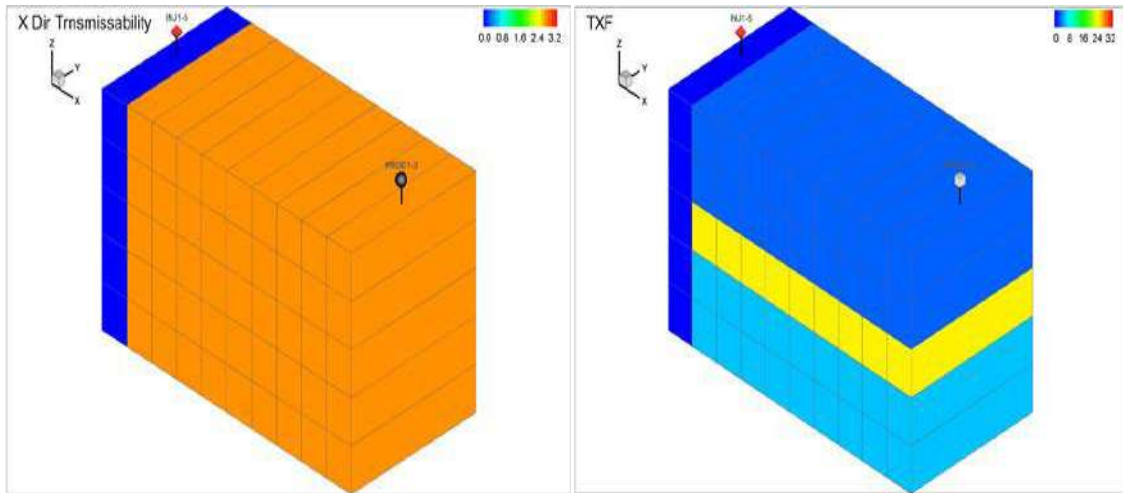


Fig. 40: 3-D simulation grid of (a) homogenous reservoir, (b) Fractured reservoir

To get consistency in our study the fractured model has same properties as the homogenous model with adding fracture properties as shown in the above tables. Initially the reservoir is filled of oil and the injection of the CO₂ is starts with the start-up of production and considered as EOR mode.

The theoretical storage capacity (expressed initially by the produced volume at standard conditions, Bchu and Shaw (2003, 2005) and Bachu et al. (2007)) is higher in the homogenous reservoir than the fractured reservoir.

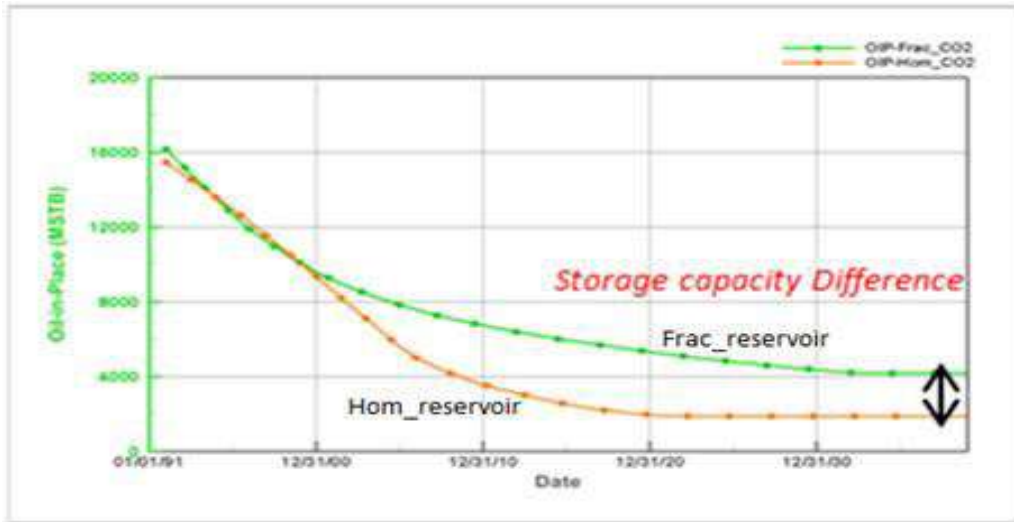


Fig. 41: Capacity storage difference between fractured and homogenous reservoir

- **Homogenous reservoir**

To confirm the real storage capacity of the homogenous reservoir the below curve shows the difference between the injected CGI (Cumulative gas (CO₂) injected) and produced CGP (cumulative gas produced).

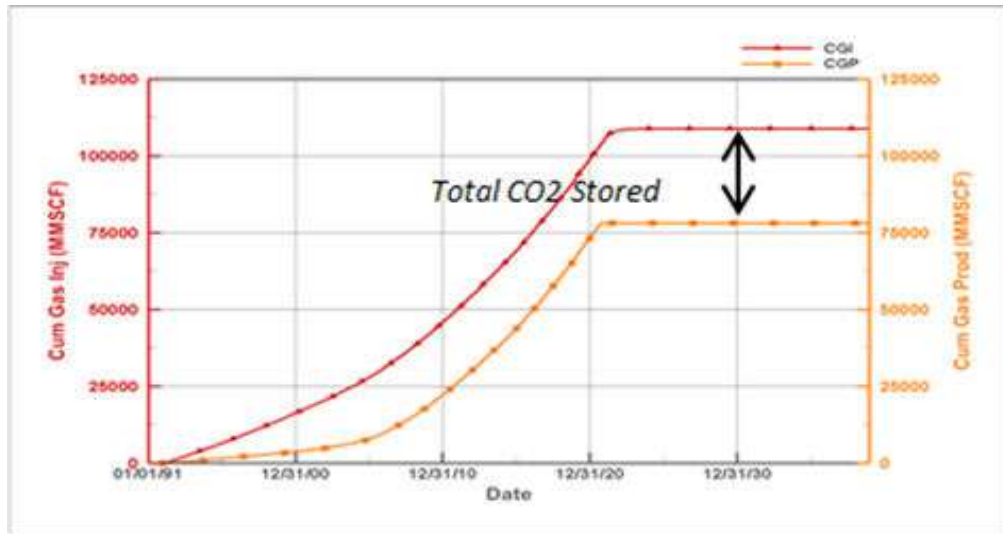


Fig. 42: Total CO₂ stored in homogenous reservoir

The total CO₂ stored in the homogenous reservoir is expressed as:

$$TOTAL_{CO_2\text{stored}} = TOTAL_{CO_2\text{injected}} - TOTAL_{CO_2\text{produced}} \quad (36)$$

According to the simulation results we have:

$$TOTAL_{CO_2\text{stored}} = (108.7 - 78)10^9 = 30.710^9 \text{ SCUF} = 30.710^9 \times 0.510^{-3} = 15.35\text{MMRB}$$

As stated above, the BHP limit is above the bubble pressure to be sure that all produced gas is coming from the injected gas CO₂ (no dissolution gas is produced), and the initial oil FVF is $B_{oi} = 2.066$ rb/stb.

The cumulative oil produced from the homogenous reservoir is:

$$COP_{RB} = COP_{STB} B_{oi} \quad (37)$$

$$COP_{RB} = (15.4 - 1.9) \times 2.066 = 27.89 \text{MMRB}$$

In order to determine the compressibility of the CO₂ used in our study we need to calculate the Oil-CO₂ compressibility multiplier factor $MC_{\text{Oil-CO}_2}$

$$MCF_{\text{Oil-CO}_2} = \frac{\text{TotalCO}_2\text{stored}_{RB}}{COP_{RB}} = \frac{15.35}{27.89} = 0.5$$

The compressibility of the oil of our study is 19.7×10^{-6} , which it means that the CO₂ injected (in supercritical status), is more compressible two times than the oil in place.

$$C_{CO_2} = 19.710^{-6} \times 2 = 39.410^{-6} \text{ (1/ psi)}$$

- Fractured reservoir

As explained previously, the reservoir properties of the fractured and homogeneous reservoir are same with exception of fractures properties (dual porosity-permeability) add to the fractured reservoir model, it mean the bulk volume of both model are same.

The results show that the storage capacity of the fractured reservoir is less than the homogenous reservoir.

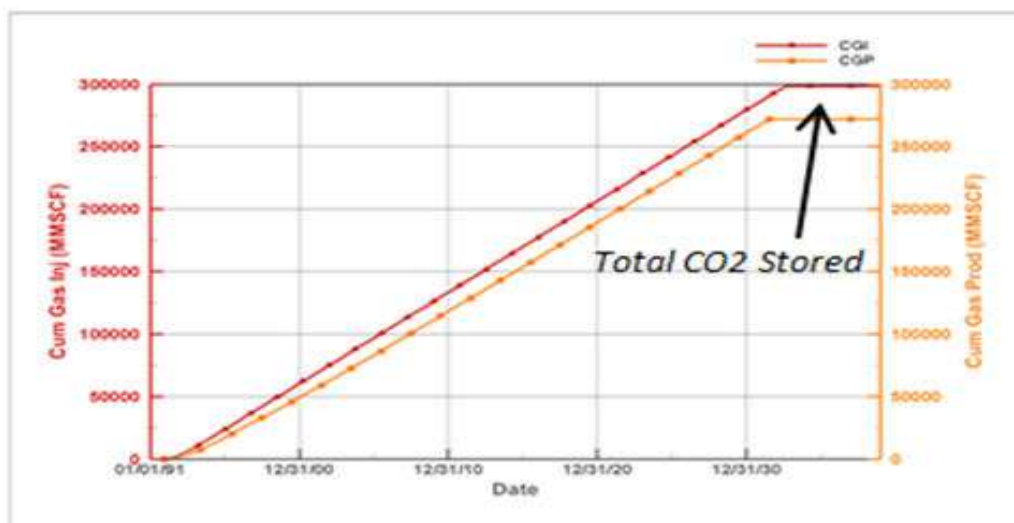


Fig. 43: Total CO₂ stored in fractured reservoir

Using same calculation methodology used with the homogenous reservoir, the total CO₂ stored in the fractured reservoir is

$$\begin{aligned} TOTAL_{CO_2\text{stored}} &= (298.2 - 271.8)10^9 = 26.410^9 \text{ SCUF} \\ &= 26.410^9 \times 0.510^{-3} = 13.2 \text{ MMRB} \end{aligned}$$

5- Discussing the Results

According to these results, the real storage capacity of a fractured reservoir is less than that of homogeneous reservoir, the fractures features affected negatively on the storage capacity, due to quick breakthrough of the gas in fractured reservoir (the gas flows through preferential paths (fractures)), and the considerable amount of oil that should be replaced by the CO₂ by dissolution and capillary forces stays in the matrix blocs, the pressure that it helps to increase the storage capacity prevents oil from flowing out of matrix blocs.

The exchange mechanism between matrix-fractures is neglected at that stage of production the main factor could help oil to flow out of matrix is the matrix blocs shape and size, which mean more the fracture network is important more the storage capacity is less.

This stage of EOR is considered as pre-CCS project, several authors mentioned that the recovery of 1 STB of oil required 5-10 MSCF of CO₂ and the half of this quantity of CO₂ will be left into the reservoir.

The real storage project will be started once the reservoir is depleted or economically is not any more gainful, the behaviour of the storage capacity in homogeneous and fractured reservoir is totally different, and the injection pressure will be the key parameter, this pressure should be less than the minimum pressure value that can allow the CO₂ escaping through the weak point in our system (cap rock or down hole of the abandoned wells) and the presence of the fractures in the system will accelerate the arrival of the CO₂ to this weak points.

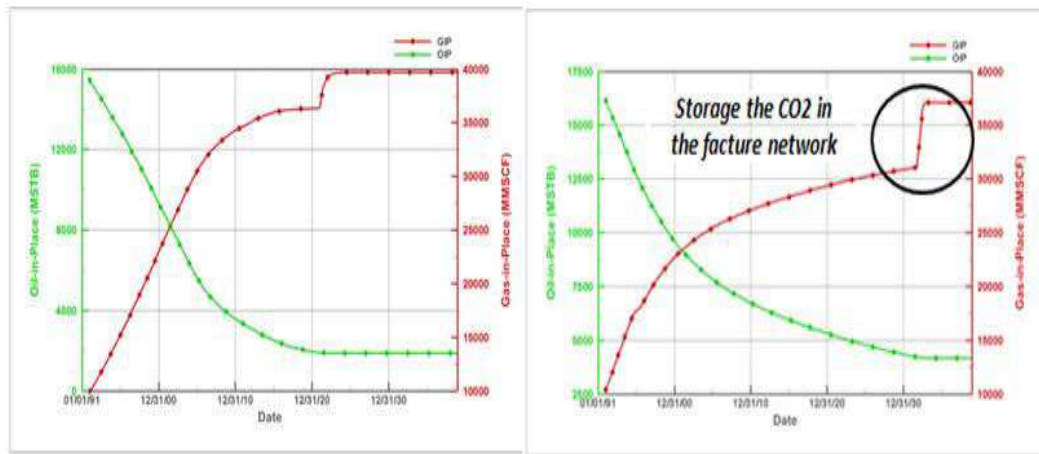


Fig. 44: Storage capacity behaviour: (a) homogenous reservoir and (b) fractured reservoir

As shown in the previous plots, the stored CO₂ in homogeneous reservoir during the EOR process is higher than that of fractured reservoir, this result confirms that injection of CO₂ for EOR process can be considered as pre-CCS project. When the oil producer well is shut in, the amount of the CO₂ stored in the reservoir is driven by the injection pressure, as the simulation model is controlled by the reservoir pressure limit, which means keep injecting gas till getting maximum pressure this value should be provided by the user and considered as the maximum allowable pressure to keep CCS project safe.

According to the simulation results during the EOR process the homogenous reservoir stored around 12.8 MMRB of CO₂ and the fractured reservoir stored around 9.2 MMRB of CO₂ (the ratio of the homogenous reservoir capacity storage to the fractured reservoir is around 1.4).

Once the oil producer well is shut in, the mount of CO₂ stored in homogeneous reservoir is around 2.15 MMRB and around 4 MMRB stored in the fractured reservoir and the high amount of CO₂ is stored in the fractures network.

Another factor considered as very important parameter for the security of a CCS project is the breakthrough time of the CO₂, in this study, CO₂ breakthrough was very high in the fractured reservoir than the homogeneous as shown below.

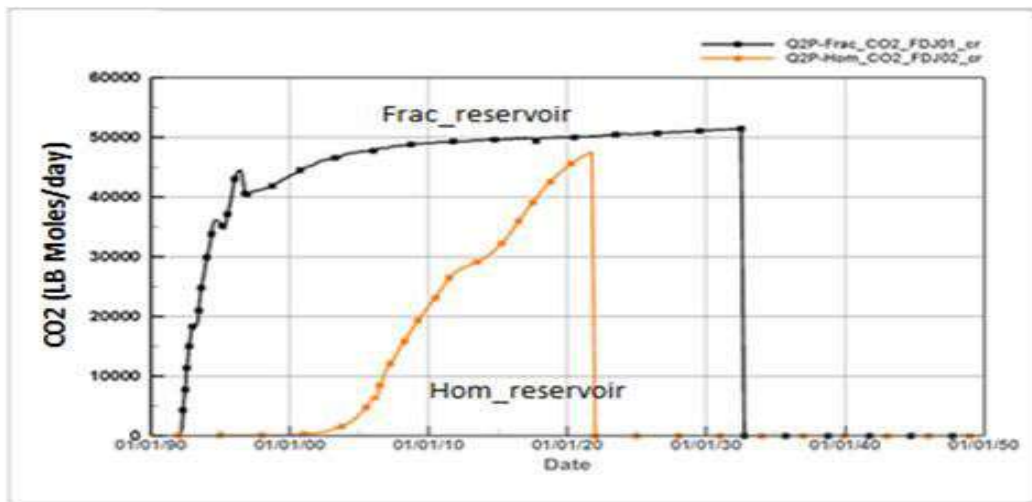


Fig. 45: CO₂ Breakthrough time

The fractures have always been regarded as potential escape routes for CO₂, which could damage the prospective storage ability of a specific storage site [32]. Fractures have low storage and high permeability values compared to the matrix. These high permeabilities of the fractures could potentially allow CO₂ to migrate quickly through the cap rock or down hole of abandoned wells to the surface. Local pressure increase caused by CO₂ injection can also lead to hydro fracturing in the vicinity of injection wells.

Chapter 6

Reservoir properties

Description

Reservoir Properties Description

1- Introduction

An accurate description of reservoir properties is necessary for reservoir simulation and performance prediction, modelling a hydrocarbon reservoir to investigate its capability to store CO₂ to mitigate the climate change is the main aim of this thesis.

Correct estimation of the permeability is important for better reservoir simulation prediction performance, the proper use of the comprehensive volume of data available obtained during the exploitation of the reservoir is necessary to predict accurate reservoir properties such as permeability, porosity and flow zone indicator.

The hydraulic flow unit approach is being one of the most popular techniques used in the estimation of the permeability (Amaefule et al., 1993) [50], which is a function of the flow zone indicator and effective porosity. The concept of this technique is to divide the reservoir into units (classes) based on fluid-flow characteristics each unit has unique flow zone indicator value.

Coring the entire net pay interval or all the field wells is very expensive operation, in this section of the thesis a combined method between the hydraulic flow unit and Adaptive Network Fuzzy Inference System (ANFIS) is applied to estimate a permeability model with enough confident in term of accuracy and low cost.

2- Petrophysical and geological significance of FZI

Statistical techniques based on permeability variations only serve to classify the reservoir into layers do not provide a good reservoir classification due to the absence of information regarding the geological attributes that control reservoir zonation. Conversely, the flow zone indicator incorporates the geological attributes of texture and mineralogy by discriminating distinct pore geological facies and the petrophysical attributes of flow potential of the fluid into the reservoir, and can be considered as key parameter in the hydraulic flow units concept [50].

Despite the importance of the flow zone indicator in the hydraulic flow unit concept, there is no explicit method (formulation) to determine this parameter directly, and it is defined as a function of the tortuosity (τ), surface area per unit grain volume (S_{gv}) and the shape factor (F_s).

3- Hydraulic Flow Unit Concept

Hydraulic flow unit concept is widely defined in the literature, these definitions are varying depending of the aspect in which each author is defining this concept, but all the definitions are based on the depositional and diagenetic process, (Bear, J., 1972) defined the HFU as the representative volume of total reservoir rock within which geological properties that control fluid flow are internally consistent and predictably different from properties of the other rocks volume, this section presents the fundamental equations of HFU concept.

Kozeny and Carman equation applied in porous media is given by Eq. (38):

$$K = \frac{\phi_e^3}{(1-\phi_e)^2} \left[\frac{1}{F_s \tau^2 S_{gv}^2} \right] \quad (38)$$

K is in μm^2 , F_s is the shape factor, ϕ_e is the effective porosity and S_{gv}^2 is surface area per unit grain volume.

The Eq. (38), can be written in field unit (K in mD) as follows:

$$0.0314 \times \sqrt{\frac{k}{\phi_e}} = \left[\frac{\phi_e}{(1-\phi_e)} \right] \left[\frac{1}{\sqrt{F_s \tau S_{gv}}} \right] \quad (39)$$

The above equation can be written as follow:

$$\text{RQI} (\mu\text{m}) = 0.0314 \times \sqrt{\frac{k}{\phi_e}} \quad (40)$$

RQI is the rock quality index.

$$\phi_z = \left[\frac{\phi_e}{(1-\phi_e)} \right] \quad (45)$$

ϕ_z is the normalized porosity (pore volume to grain volume)

$$\text{FZI}(\mu\text{m}) = \left[\frac{1}{\sqrt{F_s \tau S_{gv}}} \right] \quad (46)$$

FZI(μm) is the Flow Zone Indicator.

The FZI indicator is defined as function in the normalized porosity and rock quality index as follows:

$$\text{FZI}(\mu\text{m}) = \frac{\text{RQI} (\mu\text{m})}{\phi_z} \quad (47)$$

$$\text{LOG}(\text{RQI}) = \text{LOG}(\text{FZI}) + \text{LOG}(\phi_z) \quad (48)$$

Plotting RQI versus ϕ_z ; all samples with similar FZI will lie on straight line with unit slope, the value of the FZI can be determined from the intercept of the unit slope straight line at $\phi_z = 1$.

The permeability at each point will be calculating using the mean (average) flow zone indicator value and effective porosity using the following equation

$$K(\text{mD}) = 1014 \times (\text{FZI}_{\text{mean}})^2 \times \frac{\phi_e^3}{(1-\phi_e)^2} \quad (49)$$

3.1- Determination of the Flow Zone Indicator and Effective Porosity in uncored intervals

The determination of the flow zone indicator and effective porosity in uncored intervals and wells is required for the HFU technique to calculate the permeability (equation 49). In the recent years the use of artificial intelligence methods to solve nonlinear problems is widely used in all domains and showed a powerful capabilities of calculation and provide very encouraging results.

Adaptive Network Fuzzy inference system (ANFIS) is considered one of the main techniques used in artificial intelligence methods has been used in this work to predict the flow zone indicator and effective porosity required in the HFU technique.

- Artificial Intelligence Methods

The statistical science knows in the last recent years real revolution in the artificial intelligence techniques which are used widely in the petroleum industry to help find solution to the complex problems encountered in some fields such as reservoir properties estimation, one of these techniques that has been used in this study is the Adaptive Network Fuzzy inference system (ANFIS) method [51, 59].

- Adaptive Network Fuzzy Inference System (ANFIS)

Adaptive Network Fuzzy inference system (ANFIS) was presented by Jang in 1993, and is widely explained in the literature, which considered as simple data learning technique using fuzzy logic to transform an input to output through highly interconnected neural network processing elements and information connections, which are weighted to map the numerical inputs into outputs [54, 57].

ANFIS network structure is composed of five layers; each layer contains several node sits structure as shown in (Fig. 46)

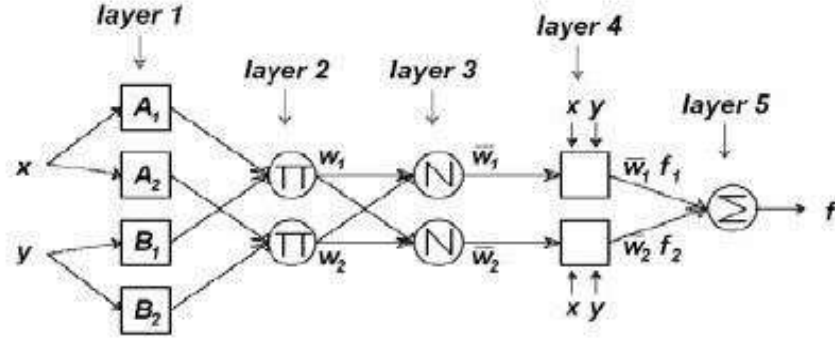


Fig. 46: ANFIS structure

Layer1: executes a fuzzification process which denotes membership functions (MFs) to each input. In this paper we choose Gaussian functions as type of membership functions:

$$O_i^1 = \mu_{A_i} = \exp\left(\frac{-(x-c)^2}{\sigma^2}\right)$$

Layer2: executes the fuzzy AND of antecedents part of the fuzzy rules

$$O_i^2 = w_i = \mu_{A_i}(x_1) \times \mu_{B_i}(x_2), \quad i = 1, 2, 3, 4$$

Layer3: normalizes the MFs

$$O_i^3 = \bar{w}_i = \frac{w_i}{\sum_{j=1}^4 w_j}, \quad i = 1, 2, 3, 4$$

Layer4: executes the conclusion part of fuzzy rules

$$O_i^3 = \bar{w}_i y_i = \bar{w}_i (\alpha_1^i x_i + \alpha_2^i x_i + \alpha_3^i), \quad i = 1, 2, 3, 4$$

Layer5: computes the output of fuzzy system by summing up the outputs of the fourth layer which is the defuzzification process.

$$O_i^5 = \text{overall output} = \sum_{i=1}^4 \bar{w}_i y_i = \frac{\sum_{i=1}^4 w_i y_i}{\sum_{i=1}^4 w_i}$$

The ANFIS system training process is summarized in the below organigram:

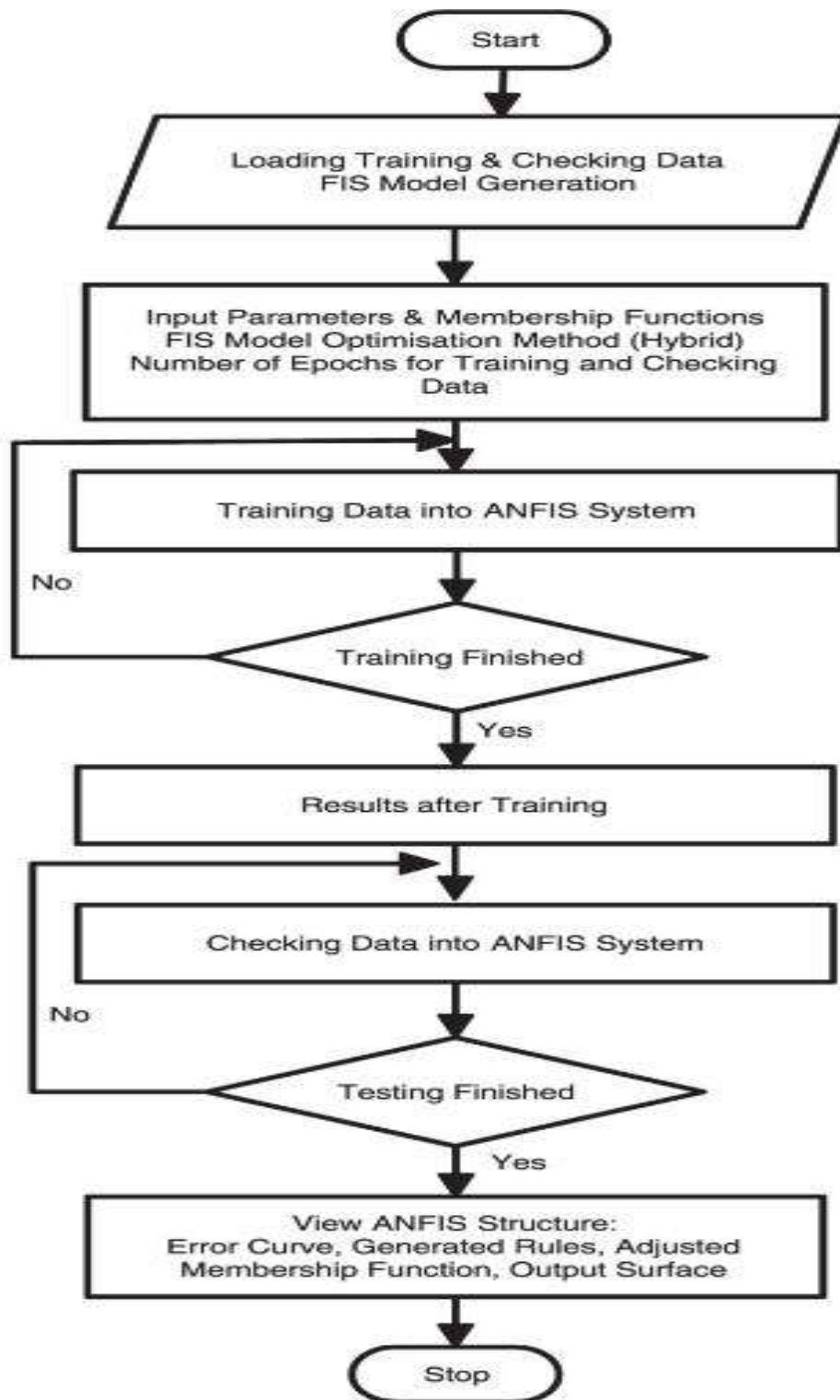


Fig.47: ANFIS training process organigram

3.2- Data Sets and Methodology

Data provided for this study includes conventional core and wireline logs data of six wells from SFSW field. Available wireline logs are gamma ray (GR), sonic (DT), density (RHO), deep resistivity (DR), and neutron porosity (NPHI) and water saturation (SW). These logs data are calibrated at exact core depth. Cores data had similar dimensions in all cored wells, data from wells, and were used for the construction of intelligent models (data points), the data of each cored well is divided to testing, training and generalizing data to check the reliability of the model before generalizing the method for the no cored wells, the wells are not cored used the model of the more close cored well as they have similar properties.

The below are the main steps of this method

- Regrouping the wells (uncored wells with closest cored well).
- Organizing the log and core data to inputs and targets data.
- Normalizing the input data using Max-Min rule.
- Running Matlab ANFIS program.
- De-normalization the output data.

Descriptive statics of the Inputs and Output data are shown in the below table

Table. 15: Descriptive static of the input/output data

Descriptive statistics				
	Mean	Min	Max	Std.Dev.
GR	81.83344	36.4613	166.75	32.65977
DT	74.91348	65.2904	100.8806	5.488045
RHO	2.497526	2.3089	2.72	0.094358
DR	3.030603	0.8151	9.9185	1.567715
NPHI	0.181927	0.1118	0.3648	0.047318
PHIE	6.21827	5.178	20	7.337798
FZI	0.984705	0.2336	11.9065	1.800531

Following an iterative calculation an optimum FIS model has been selected of each reservoir property (the flow zone indicator and effective porosity (FZI, ϕ_e)).

Input-Output of ANFIS model for Flow Zone Indicator (FZI) are show below

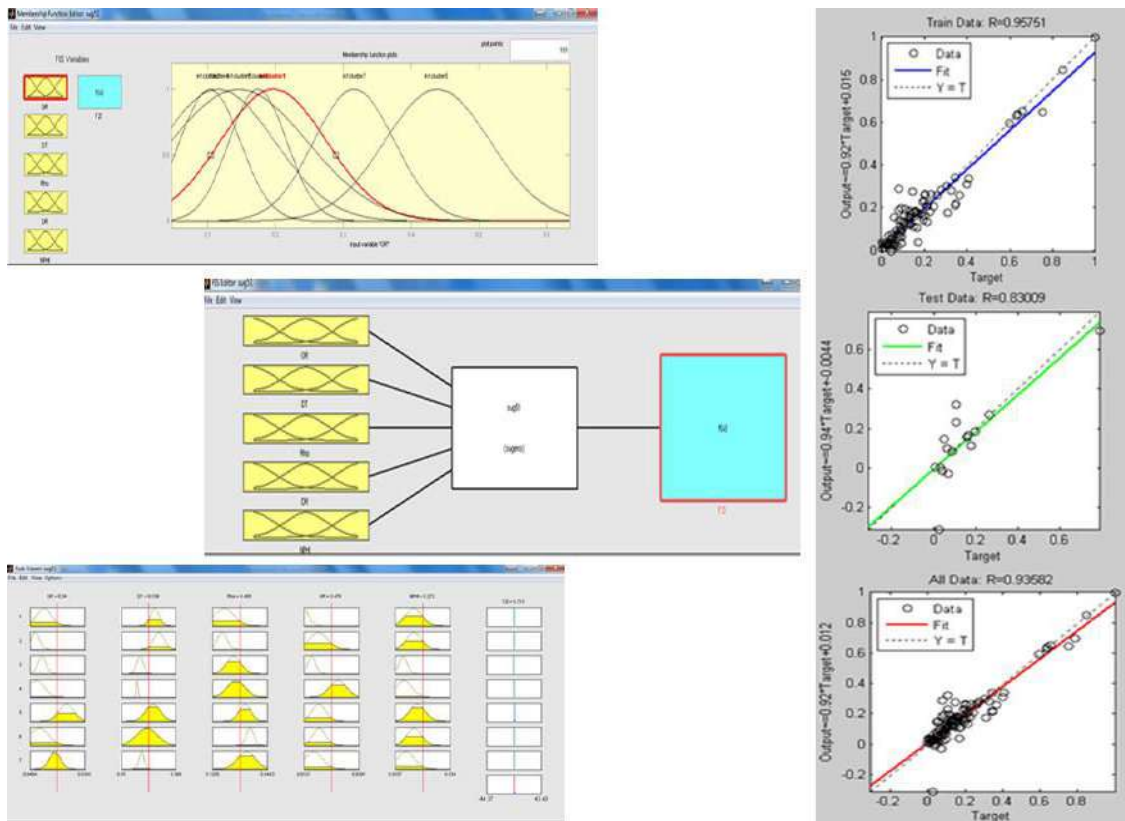


Fig. 48-a: Flow zone indicator ANFIS results

Input-Output of ANFIS model for effective porosity (ϕ_e) are show below

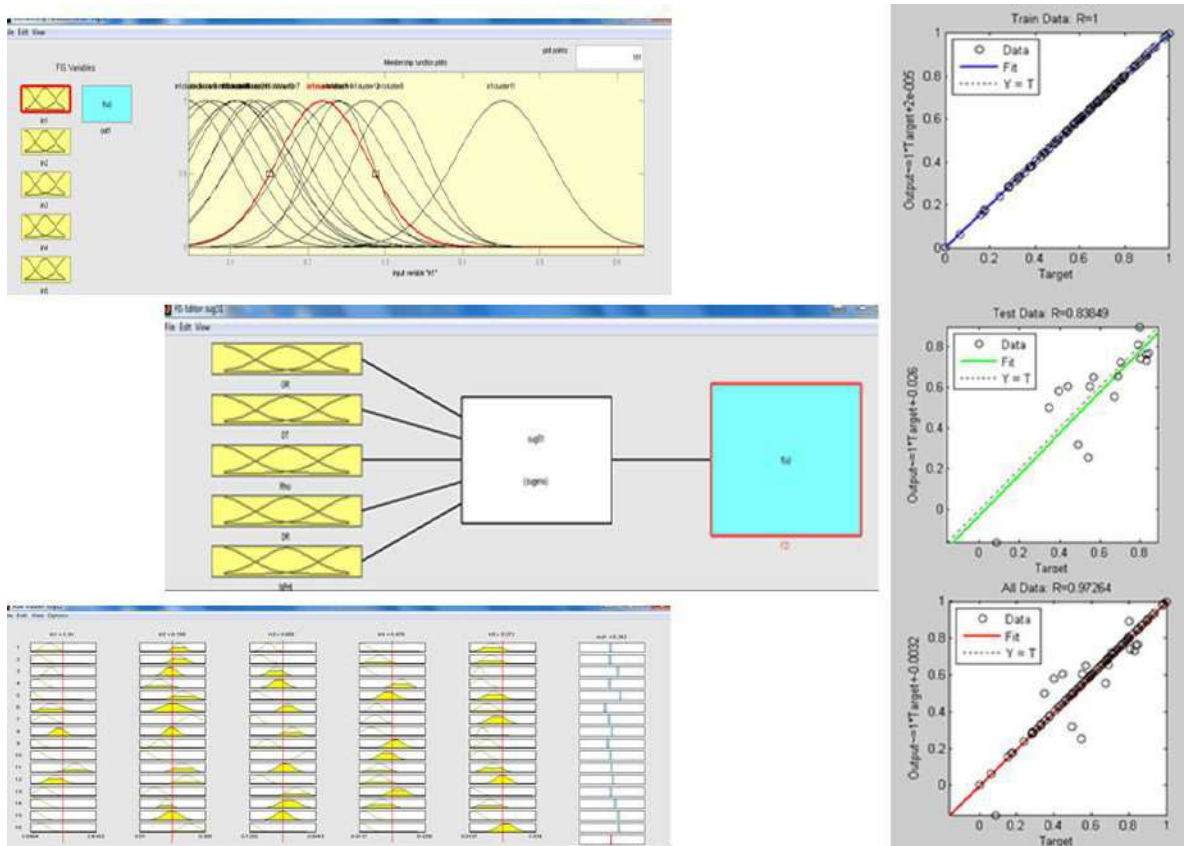


Fig. 48-b: Effective porosity ANFIS results

4- Applying ANFIS Results in Hydraulic Flow Units Technique

4.1- ANFIS Results

The accuracy of the ANFIS technique results shown in the value of correlation coefficient (R^2), in this study, ANFIS technique provides very encouraging results for the flow zone indicator and effective porosity in cored wells as shown below:

Table 16-a: the results of FZI and ϕ_e ANFIS's

	R2 for train data	R2 for test data	R2 for all data
Flow zone indicator	0.95	0.830	0.93
Effective porosity	1	0.85	0.97

4.2- Trend Analysis

As mentioned above ANFIS model provided very encouraging results.

4.2.1 Effective Porosity

The values of the regression, mean square error (MSE) and the Root-mean-square (RMSE) indicate the accuracy of the statistical method applied in our study as shown below.

- Regression Function

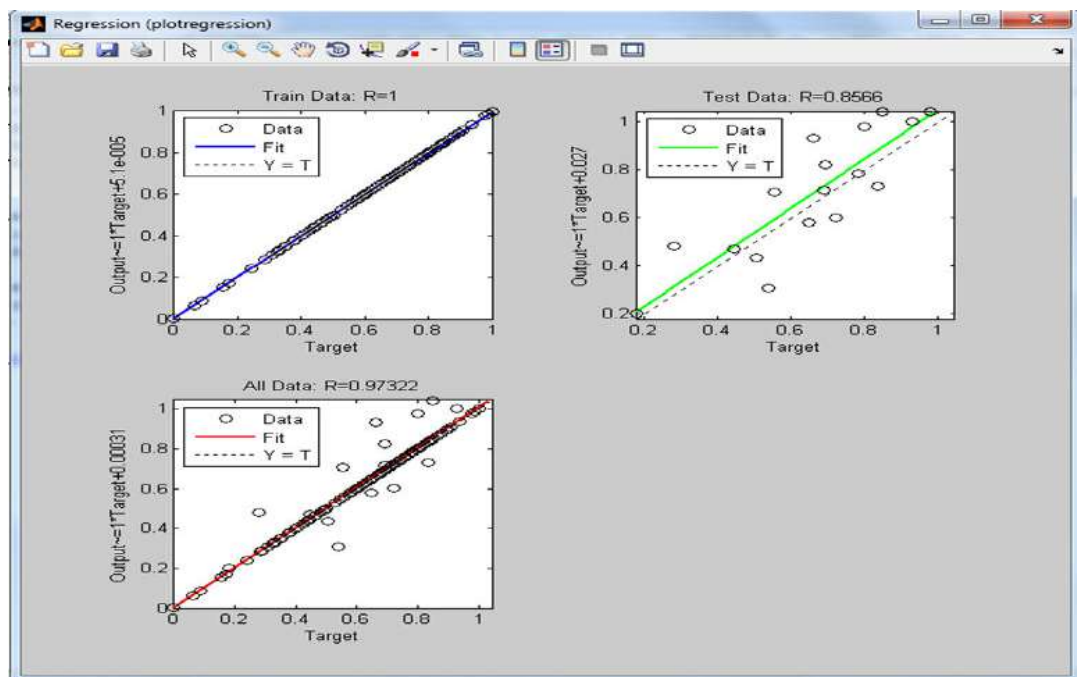


Fig. 49-a: Regression Function of the effective porosity (train, test and all data)

- The MSE and RMSE

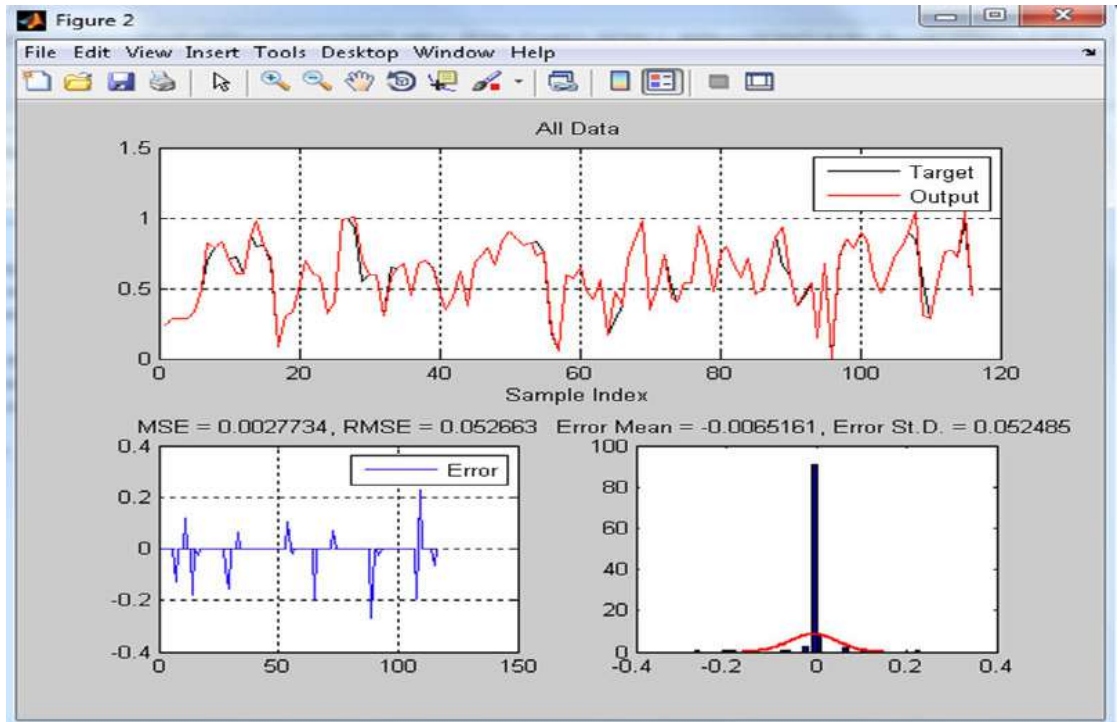


Fig. 49-b: MSE and RMSE and error St. Deviation of the effective porosity.

4.2.2 Flow Zone Indicator (FZI)

The values of the regression, mean square error (MSE) and the Root-mean-square (RMSE) indicate the accuracy of the statistical method applied in our study as shown below.

- Regression Function

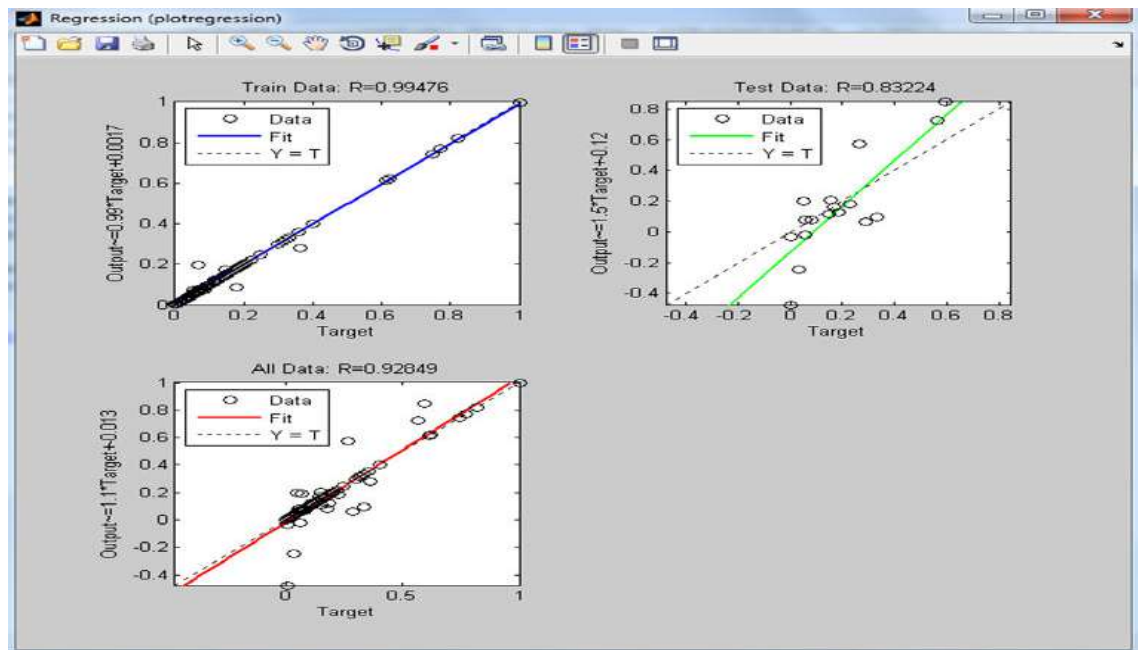


Fig. 49-c: Regression Function of the FZI (train, test and all data)

- The MSE and RMSE

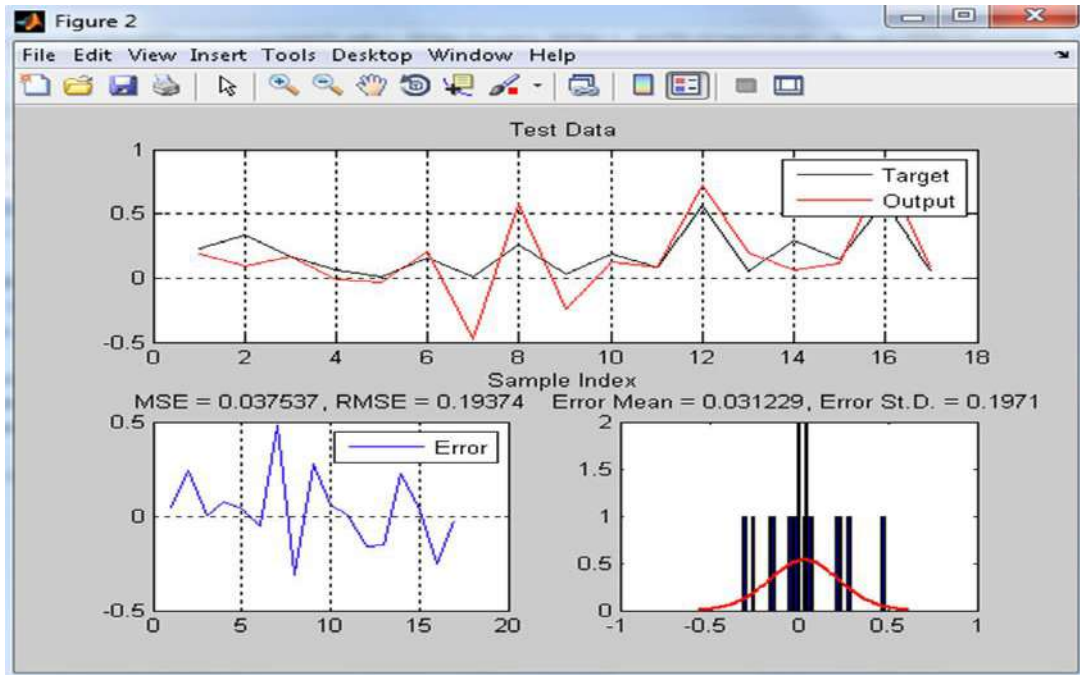


Fig. 49-d: MSE and RMSE and error St. Deviation of the FZI.

The below tables show the results of model (output) versus the core (target) data.

Table 16-b: Effective Porosity (output) and core data (target)

DEPTH M	Phie_Anfis %	Phie_Core %
3110.027	8.75202029	8.752
3110.332	9.422946644	9.423
3110.484	9.377068232	9.377
3110.789	9.418100592	9.418
3111.094	10.11686082	10.117
3111.246	9.882377726	12.513
3111.856	15.42011393	15.42
3112.008	16.79278003	16.793
3112.313	16.46292083	17.561
3112.618	15.87650874	15.648
3112.77	15.88304931	15.883
3112.922	14.15099469	14.151
3113.227	18.2110072	18.211
3113.532	17.01023288	17.01
3113.837	16.16590385	17.15
3113.989	15.41498624	15.415
3114.294	2.79291211	6.451
3114.599	9.734097907	9.734
3114.904	10.0618312	10.062
3115.208	12.99503105	12.995
3115.666	15.52674418	15.527
3115.818	14.19033897	14.19
3115.97	13.68332962	13.685
3116.275	9.966414131	9.966
3116.58	13.78652721	11.085
3116.732	19.82398761	19.824
3116.885	19.99987492	20
3117.19	18.92814856	18.928
3117.494	14.14347099	13.367
3117.799	14.01794638	14.018
3117.952	13.94955629	13.95
3118.256	9.731373846	9.73

3118.561	14.77237045	14.772
3118.714	14.71226527	14.712
3119.018	15.2427755	15.243
3119.171	11.78509575	11.785
3119.476	15.19487217	15.195
3119.78	14.89398922	15.44
3119.933	14.74648306	14.747
3120.238	12.01302464	12.013
3120.542	12.55699268	10.327
3120.695	11.65398177	11.654
3121	14.36788489	14.368
3121.304	10.83608543	10.836
3121.609	15.31567873	15.316
3121.762	16.10834446	16.108
3122.066	16.84090447	16.841
3122.371	15.09387056	15.094
3122.676	17.63175036	17.631
3122.981	18.62294692	18.624
3123.286	17.7436558	17.744
3123.438	18.40727109	17.093
3123.743	17.3990128	17.399
3124.048	16.04135559	17.54
3124.2	16.36893636	16.369
3124.505	7.820982039	7.821
3124.81	6.112006008	6.112
3124.962	14.06298621	14.063
3125.267	14.79352657	13.662
3125.572	14.8628507	14.863
3125.724	12.59206115	12.592
3130.296	10.78106956	10.781
3130.601	15.72331449	15.723
3130.753	17.75520164	17.755
3131.058	19.65271956	19.653
3131.21	10.39400462	10.394
3131.515	12.48594495	12.486
3131.82	16.14891164	16.149
3132.125	12.64283058	12.643
3132.277	11.20916674	11.209
3132.582	13.21719116	13.217
3132.734	13.24900409	13.249
3133.039	19.08497957	19.085
3133.344	16.93878346	16.941
3133.496	12.30444782	12.302

3133.801	16.17593158	16.176
3134.106	17.13615872	16.958
3134.258	13.39078394	15.172
3134.563	13.7186857	13.718
3134.716	15.71892398	15.72
3135.02	11.98944993	11.989
3135.325	12.41781271	12.418
3135.782	14.56020028	14.56
3135.935	17.99891537	17.999
3136.24	14.97497018	14.975
3136.544	13.94833087	13.948
3136.849	10.75232547	10.752
3137.002	11.75553043	11.756
3137.306	8.924559179	13.234
3137.611	7.458010597	7.458
3137.764	15.22098331	15.221
3138.068	5.178001495	5.178
3138.221	15.9620188	15.962
3138.526	16.5440637	17.712
3138.83	16.78416229	16.784
3138.983	18.42953544	18.43
3139.288	17.79414866	17.794
3139.592	13.81822001	13.819
3139.745	12.09548183	12.095
3140.05	14.0277615	14.028
3140.202	16.20293657	16.204
3140.507	17.06006848	17.06
3140.812	18.45930182	18.46
3140.964	17.7577503	17.758
3141.421	13.1340948	13.134
3141.574	9.422670261	9.422
3141.726	13.27374215	13.273
3142.031	16.44844237	16.449
3142.336	16.62580633	16.625
3142.488	15.83103489	15.83
3142.793	19.68006594	19.68
3143.25	14.13318233	11.739

Table 16-c: Flow Zone Indicator results (output) and core data (target)

DEPTH M	FZI_Anfis Dec	CC_FZI Dec							
3110.027	2.205007	2.2049	3121.304	0.349056	0.314	3137.306	1.320933	1.3211	
3110.332	4.903326	4.9025	3121.609	0.283511	0.277	3137.611	1.815833	1.8159	
3110.484	4.315465	1.1726	3121.762	0.908822	0.9547	3137.764	2.382226	2.3822	
3110.789	2.571858	2.5775	3122.066	0.886365	0.8845	3138.068	3.910581	0.4377	
3111.094	0.339112	1.7343	3122.371	1.029027	1.9644	3138.221	2.669193	2.6669	
3111.246	1.146526	1.141	3122.676	2.296423	1.3996	3138.526	2.485178	2.4725	
3111.856	2.202171	2.2018	3122.981	3.831066	3.8358	3138.83	2.633137	2.5977	
3112.008	0.901639	2.095	3123.286	2.141343	2.136	3138.983	2.900528	2.9286	
3112.313	3.540758	1.5101	3123.438	2.522791	2.5284	3139.288	2.713617	2.7074	
3112.618	3.311382	3.3111	3123.743	2.136974	2.135	3139.592	1.471707	1.4665	
3112.77	1.308519	1.3056	3124.048	2.531907	2.5337	3139.745	7.188439	7.1907	
3112.922	1.465711	1.4668	3124.25	9.004495	9.0058	3140.05	0.623138	0.6251	
3113.227	4.034542	4.0344	3124.505	2.789735	2.7884	3140.202	3.430771	1.3263	
3113.532	4.269458	4.2688	3124.81	0.585346	0.5853	3140.507	1.95003	1.9526	
3113.837	2.835218	3.4742	3124.962	18.5715	9.4222	3140.812	2.073395	2.0758	
3113.989	11.90433	11.9065	3125.267	4.250558	4.2561	3140.964	1.767576	1.7724	
3114.294	1.297373	0.8018	3125.572	1.214938	1.264	3141.421	0.483994	0.4829	
3114.599	0.542844	0.5442	3125.724	1.297308	1.2468	3141.574	0.352469	0.3262	
3114.904	0.558001	0.5526	3130.296	7.90712	7.9121	3141.726	1.967436	1.1093	
3115.208	0.726567	0.7307	3130.601	1.478162	1.4648	3142.031	1.465945	1.4598	
3115.666	-1.4802	0.7899	3130.753	2.580732	2.5901	3142.336	1.64662	1.6585	
3115.818	0.834068	0.8344	3131.058	4.217138	4.2303	3142.488	1.130164	1.1291	
3115.97	0.536171	0.53	3131.21	7.770467	1.1904	3142.793	5.00027	5.0007	
3116.275	0.312273	0.3113	3131.515	1.245827	1.2488	3143.25	1.363114	1.3643	
3116.58	2.173112	2.1768	3131.82	2.704547	2.7034				
3116.732	1.785122	1.7878	3132.125	1.754525	1.7547				
3116.885	1.784826	1.7847	3132.277	1.23221	1.232				
3117.19	1.692787	1.6923	3132.582	2.061871	2.0643				
3117.494	0.605255	0.6046	3132.734	1.907442	1.908				
3117.799	0.783653	0.7716	3133.039	4.500706	4.5017				
3117.952	7.618668	7.6191	3133.344	3.262499	3.2582				
3118.256	0.266	0.2641	3133.496	10.13038	10.1329				
3118.561	0.412008	0.6091	3133.801	3.050819	3.0517				
3118.714	0.886438	0.6762	3134.106	3.783485	3.7833				
3119.018	0.747038	0.7389	3134.258	2.4543	2.4518				
3119.171	0.908174	1.1124	3134.563	2.854717	2.8566				
3119.476	0.412744	0.2336	3134.716	2.027858	2.0256				
3119.78	0.853334	0.7974	3135.02	4.46135	1.7436				
3119.933	0.913029	0.9239	3135.325	1.696232	1.6956				
3120.238	1.013872	1.0428	3135.782	1.66807	0.9825				
3120.542	0.459619	0.4647	3135.935	2.278036	2.2792				
3120.695	0.631658	0.6237	3136.24	1.20683	1.2075				
3121	0.707523	0.6947	3136.544	1.309323	1.3071				
			3136.849	1.092114	1.0928				
			3137.002	0.964181	0.9624				

The flow zone indicator and effective porosity for the entire reservoir height (cored and uncored) intervals is given in the below curves.



Fig. 50: Predicted FZI and ϕ_e using ANFIS method for cored well

4.3- Permeability Estimation using Hydraulic Flow Unit Concept

After the determination of the flow zone indicator and the effective porosity across the entire reservoir height (cored and uncored) intervals using ANFIS technique, the permeability can be determined using hydraulic flow unit concept following the below steps.

4.2.1- Clustering data

In the literature many of statistical techniques exist to determine the number of clusters (hydraulic flow units) based in the FZI such as: K-means, cluster analysis, probability plots, multivariable regression ...etc.

In the present study, K-means technique is applied and it provides 10 HFU as shown in the figure below.

4.2.2- Log-Log Plot of the RQI versus ϕz

An average flow zone indicator for each distinct HFU can be determined from the below plots by the intercept of the unit slope straight line with $\phi z=1$ of each HFU, which is required for the estimation of the permeability (Eq. 49)

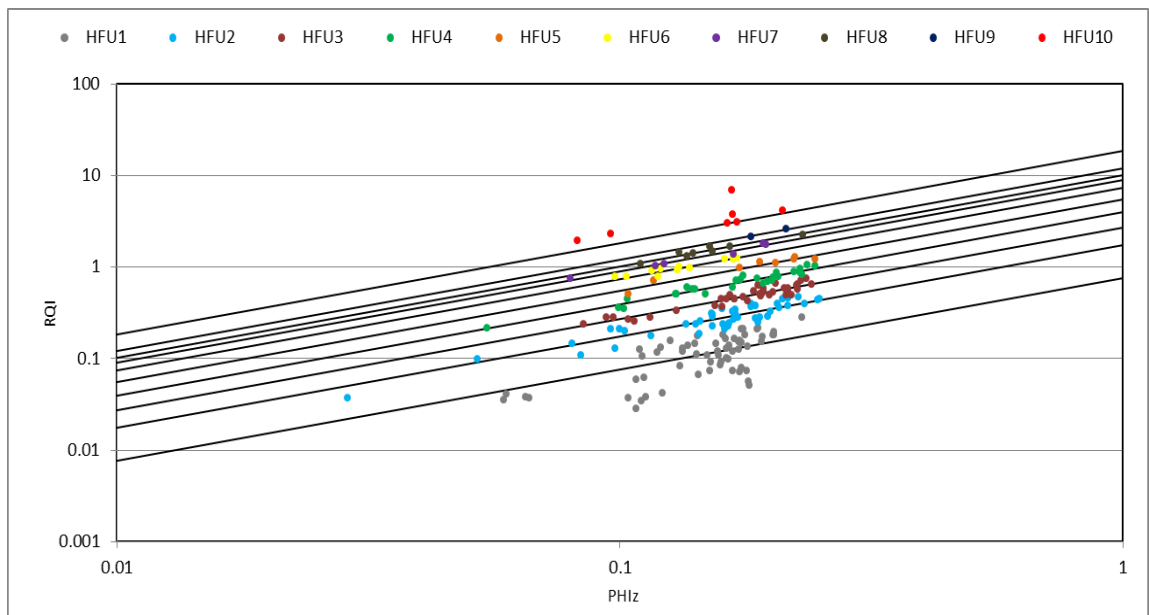


Fig. 51: RQI versus ϕz

As explained above, the predicted permeability using HFU concept can be determined using (Eq. 49), by the use of the average FZI and effective porosity determined previously.

According to the correlation coefficient ($R^2=0.96$) obtained from the ratio between the calculated permeability using HFU technique and core permeability, we note that HFU is good technique to predict an accurate permeability.

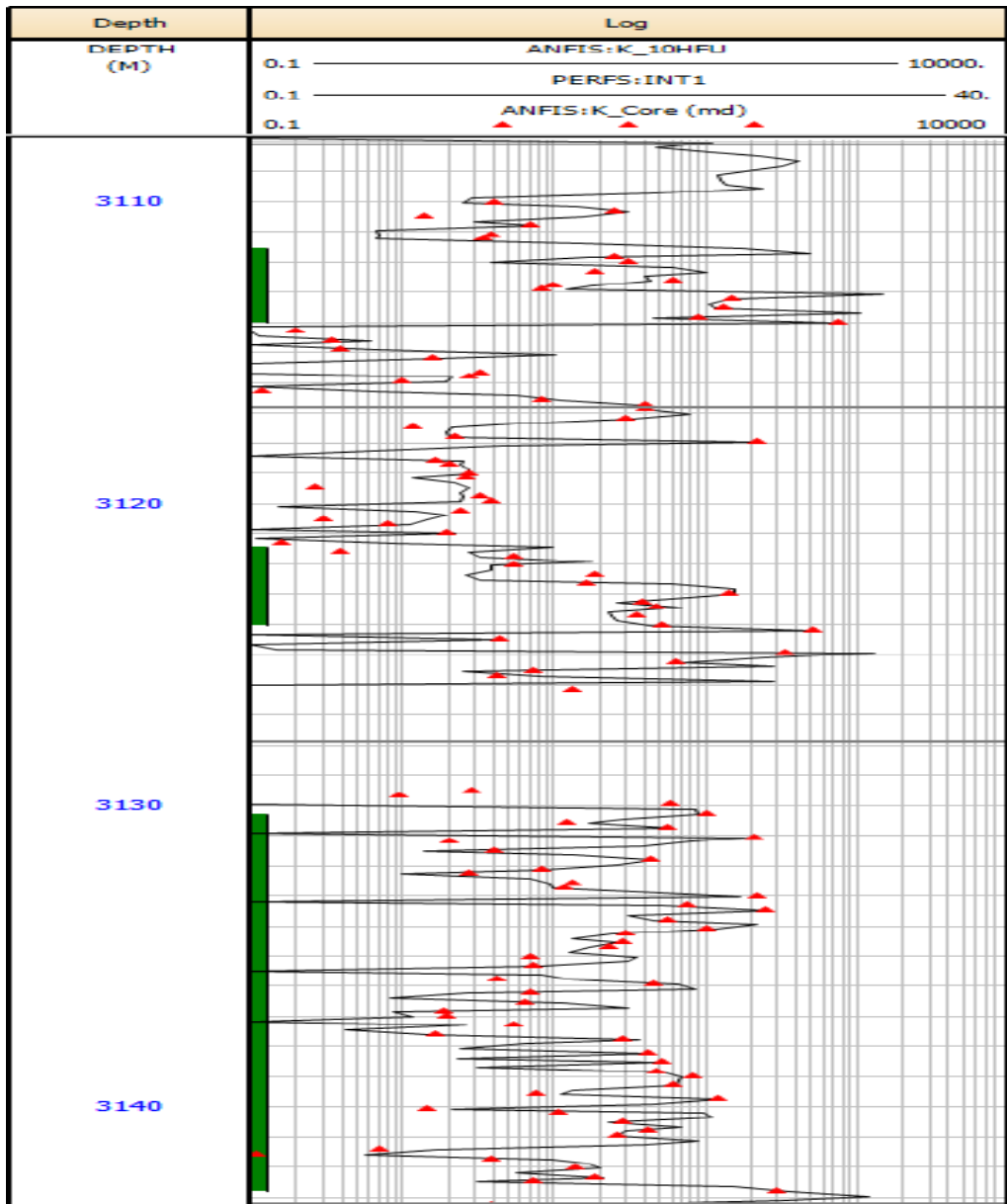


Fig. 52: Predicted Permeability Model

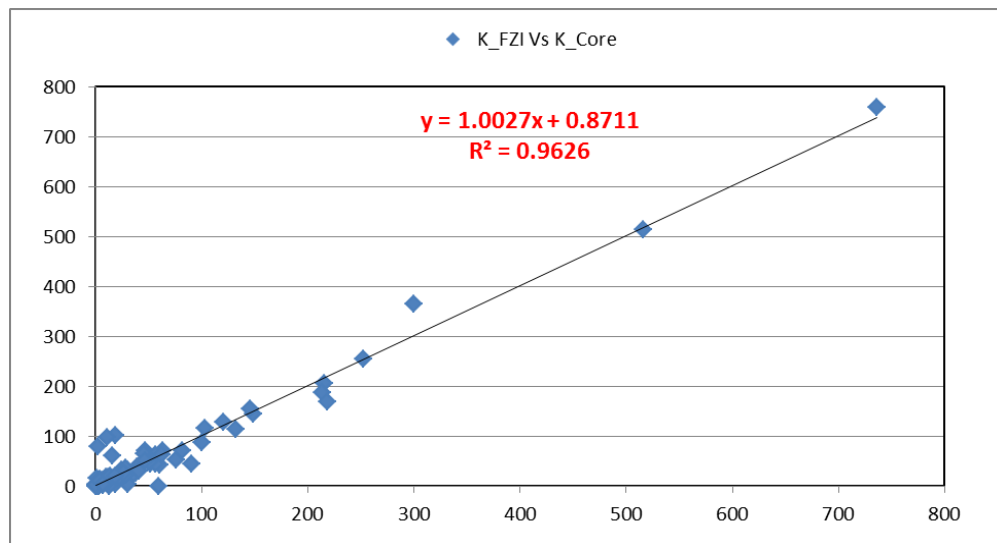


Fig. 53: Calculated permeability vs. core permeability

5- Generalization of the Technique

The encouraging results obtained previously, allow generalizing ANFIS model in the uncored well to calculate the flow zone indicator and effective porosity.

The flow zone indicator and effective porosity calculated by ANFIS technique and the predicted permeability using HFU technique are shown in the figure below

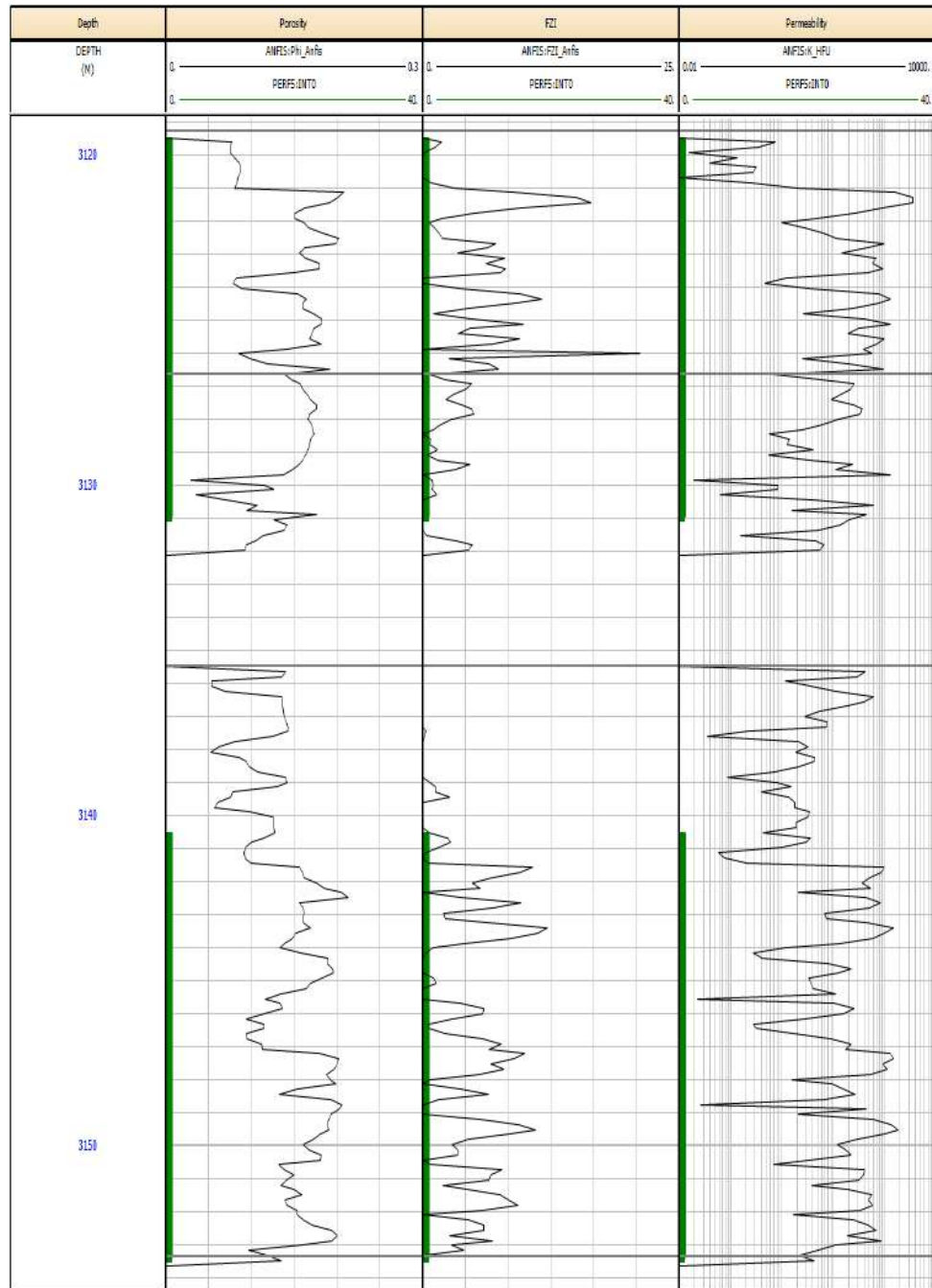


Fig. 54: FZI and ϕ_e using ANFIS method and Predicted Permeability using HFU for uncored well

6- Results and discussion of the method

A successful CCS project based mainly on the well-known of the reservoir properties distribution, the proper use of the comprehensive volume data obtained previously is necessary for well prediction of the reservoir properties.

Permeability (a measure of fluid conductivity in porous media) is a critical parameter in models for reservoir characterization, reserve estimation, production forecast, storage capacity and CO₂ migration behavior across the reservoir. Estimation of permeability in a heterogeneous reservoir is a very complex task, a poorly estimated permeability will make the model inaccurate and unreliable, thus, affecting the degree of success of many oil and gas operations based on such models.

An improvement in the prediction of permeability distribution from standard well logs and core data through the utilization of Hydraulic Flow Units Approach (HFU) and an intelligent network (ANFIS) presented in this work. Flow zone indicator (FZI), a unique parameter for each hydraulic unit, was used to characterize each rock type. The number of hydraulic flow units and mean values of FZI for each HFU were calculated based on statistical K-means technique. Using this approach, the optimal number of HFUs was found to be equal to 10 units.

Values of FZI and effective porosity for un-cored intervals and wells calculated using Adaptive Network Fuzzy inference system (ANFIS) and well log data. The set of logs GR, DT, RHO, DR, and NPHI were used as inputs for the ANFIS and the core effective porosity and FZI was the output (targets). The calculated FZI and effective porosity values obtained from ANFIS were fairly consistent with that of core data. Also, the average relative error between ANFIS's calculated FZI and effective porosity and the measured core data were very encouraging. The presented methodology was successfully applied to a large data set of core data and well logging measurements.

Chapter 7

Modeling of the CO₂ Geological Storage in Hydrocarbon Reservoirs

Modeling of the CO₂ Geological Storage in Hydrocarbon Reservoirs

1- Introduction

The simulation of CO₂ storage in hydrocarbon reservoirs is challenge, because the dominant physical processes change as the plume evolves, the domain may be very large, several key physical processes as well as geological heterogeneity require high spatial resolution, and the uncertainty in the geological parameters is large.

To store carbon geologically, CO₂ will be injected as a supercritical liquid into high-permeable strata that is limited upward by low-permeable strata (caprock) that inhibits flow. The injected CO₂ has lower density than the formation fluids and will form a plume that migrates upward by buoyancy forces. Aquifers are typically connected to the surface through permeable strata, and the injected CO₂ may therefore in principle travel in the up-dip direction and eventually leak back to the atmosphere through sedimentary outcrops. In practice, this process will take thousands of years because of the long distances involved. Moreover, as the plume migrates upward, some of the CO₂ will be contained in structural and stratigraphic traps (structural trapping), be trapped as small droplets between rock grains (residual trapping) or dissolve into the formation water (dissolution trapping), or react with rock minerals and become permanently trapped.

The operator will obviously also want to ensure operational safety and minimizing financial costs. Similar assessments will be desired by companies, investors, and/or government that take an environmental, societal, or financial risk through the operation. The only viable way to make such assessments upfront is through model studies (Simulation studies) that aim to investigate the likely outcomes of a storage operation. The main controls in a model study are the storage reservoir geology and the physics of the flow processes.

The uncertainty in the description of the geological storage site requires many simulations to assess the uncertainty in model predictions (Kovscek & Wang, 2005). Similarly, the updating of the geological model through monitoring data requires a large number of simulations (Doughty et al., 2007). Current reservoir simulation technology may not be able to provide adequate numerical resolution to capture physical processes and at the same time allow for the reasonable exploration of the uncertainty through the investigation of many equally probable geostatistical realizations of the storage site.

Several Simulation softwares provided simple CO₂ storage models as shown in the below table

Table. 17: Overview of the simulators for geological carbon storage modified from (Jiang, 2011).

Simulator	Main application	Numerical features (methods for discretisation / integration)
VIP/Nexus (Landmark product)	Three-phase and 3D fluid flow in porous media with cubic EOS, pressure dependent permeability values, etc.	The method used for time-stepping is IMPES or IMPLICIT, solving no structural grids, coupling implicitly reservoir to surface network
ATHENA/ACCRETE	Thermal multiphase 3D - reactive-transport numerical code	Finite volume method, reaction and flow iteratively coupled
CHILLER (companion to SOLVEQ)	Multi-component multi-phase equilibrium geochemical calculation software based on minimum free-energy	Newton-Raphson method for solving a system of mass balance and mass action equations
CODE-BRIGHT	Solution of the flow, heat and geo-mechanical model equations	Finite element method for spatial discretisation; implicit finite-difference for temporal discretisation
DUMUX	Multi-scale multi-physics toolbox for the simulation of flow and transport processes in porous media	Vertex-centered finite volume method for spatial discretisation; implicit temporal discretisation
ELSA	Semi-analytical tool to estimate fluid distributions and leakage rates involving vertically integrated sharp-interface equations and local 3D well models	Spatial discretisation is essentially grid free; several schemes for temporal discretisation including implicit pressure explicit saturation, etc.
FEFLOW	Solving the ground water flow equation with mass and heat transfer, including multi-component chemical kinetics	Finite element method for spatial discretisation; implicit/explicit/Crank-Nicolson temporal discretisation
FEHM	Fully coupled heat, mass and stress balance equations for 3D, non-isothermal, multi-phase fluid flow in porous media	Control volume finite element method for spatial discretisation; implicit temporal discretisation
GEM	EOS compositional reservoir simulator	IFDM for spatial discretisation; implicit temporal discretisation
Geochemist's workbench	Interactive aqueous geochemistry tools	Equilibrium modeling, reaction path modelling calculations, etc.
IPARS-CO ₂	Parallel multi-block, multi-physics approach for multi-phase flow in porous media	Mixed finite element method for space discretisation; implicit pressure, explicit concentration sequential algorithm for temporal discretisation
MIN3P	Multi-component reactive transport modeling in variably saturated porous media	Finite volume method for spatial discretisation; implicit temporal discretisation
MODFLOW	Solving the groundwater flow equation to simulate the flow through aquifers	Finite difference method for spatial discretisation; implicit or Crank-Nicolson for temporal discretisation
MT3DMS	Modular 3D transport model simulating convection, dispersion, and chemical reactions of dissolved constituents	Finite difference/particle-tracking based Eulerian-Lagrangian/finite-volume method for spatial discretisation; implicit/explicit temporal discretisation

MUFTE	Isothermal and non-isothermal multi-phase flow problems including compositional effects	Vertex-centred finite volume method for spatial discretisation; implicit temporal discretisation
PFLOTRAN	Parallel 3D reservoir simulator for subsurface multi-phase, multi-component reactive flow and transport based on continuum scale mass and energy conservation	Finite element method for spatial discretisation; implicit/semi-implicit time integration
PHAST	Simulating groundwater flow, solute transport, and multi-component geochemical reactions	Finite difference method for spatial discretisation; implicit or Crank-Nicholson for temporal discretisation
PHREEQC	Simulating groundwater flow, solute transport, and multi-component geochemical reactions	Finite difference method for spatial discretisation; implicit or Crank-Nicholson for temporal discretisation
PHREEQC	Low-temperature aqueous geochemical simulator	Based on an ion-association aqueous model; chemical equilibrium, kinetic, transport, and inverse-modeling calculations
RETRASOCODE Bright	Reactive transport of dissolved and gaseous species in non-isothermal saturated or unsaturated problems, geomechanics	Direct substitution approach for solving the reactive transport equations
ROCKFLOW	Multi-phase flow and solute transport processes in porous and fractured media	Finite element method for spatial discretisation; implicit temporal discretisation
RTAFF2	2D/3D non-isothermal multi-phase and multi component flow	Finite element method for spatial discretisation; implicit temporal discretisation
SUTRA	Fluid movement and transport of either energy or dissolved substances in a subsurface environment	Hybrid finite element and integrated finite difference method for spatial discretisation; implicit temporal discretisation
TOUGHREACT + TOUGH2	Chemically reactive multi-component, multiphase, non-isothermal flows in porous and fractured media	IFDM for spatial discretisation; implicit temporal discretisation

All simulation models are dependent on the types of numerical methods used to translate the governing equations into a finite form, appropriate for computational manipulation and analysis. All of these methods have been used in the available simulators for carbon storage, which are wide ranging in terms of the physical models considered and numerical methods used. Table 2 shows the main features of some available packages/simulators for geological carbon storage, and the complexity of the simulators depends heavily on the number of fluid phases and the number of components considered, as well as the discretization methods used [79].

2- Scientific background

2.1. Multiphase flow model

The governing equations in the numerical models used for simulations of geological CO₂ injection and storage are similar to those used to describe oil, water and gas flow through porous reservoirs. Darcy's law, together with equations of conservation of mass and energy are used in the simulations and have recently been reviewed by Jiang (2011). Darcy's equation is described as:

$$q = -\frac{K}{\mu}(\nabla p - \rho g) \quad (50)$$

Where: q is a vector quantity in a three-dimensional (3D) coordinate system representing discharge per unit area, expressed in units of velocity. In Eq. (1), the permeability tensor K represents the ability of the medium to transmit fluids through the pore spaces, μ is the viscosity of the fluid, ∇p is the pressure gradient, ρ is density, and g is gravitational acceleration.

Velocity through the porosity of the medium calculated from equation 1:

$$v = \frac{q\alpha}{\phi} = -\frac{K}{\phi}(\nabla p - \rho g) \quad (51)$$

For the positive z -direction as vertically up (opposite to gravity), the multi-phase extension of Darcy's law, for an individual fluid phase, can be given as:

$$v_\alpha = \frac{q_\alpha}{\phi} = \frac{Kk_\alpha}{\mu_\alpha\phi}(\nabla p_\alpha - \rho_\alpha g \nabla z) \quad (52)$$

Where: k is the relative permeability of the phase. For carbon storage, the flow needs to be modeled as a multi-phase (CO₂, brine, porous solid matrix, etc.) and multi-component (CO₂ and water, etc.) system. The number of phases and components considered can be different depending on the application. In Eq.(4), the conservation of mass is expressed by the balance of four terms representing all the possible mechanisms of mass transfer, which include: 1) the temporal rate of change of mass at a fixed point (or the local derivative or storage term), 2) convective mass transport, 3) diffusive mass transport, and 4) source/sink term for mass. The tortuosity refers to the ratio of the diffusivity in the free space to that in the porous medium and is generally larger than unity. The source/sink term S_i in the mass conservation equation represents geochemical reactions.

$$\frac{\partial}{\partial t}[\phi \sum_\alpha (\rho_\alpha S_\alpha X_i^\alpha)] + \sum_\alpha \nabla(\rho_\alpha X_i^\alpha q_\alpha) - \sum_\alpha \nabla(\phi S_\alpha \tau_\alpha D_\alpha \rho_\alpha \nabla X_i^\alpha) = S_i \quad (53)$$

Where: s is saturation of the phase, X_i is the mole fraction of component i , and D is diffusivity. Capillary force (P_c) is a pressure difference between the non-

wetting phase (P_n) and the wetting phase (P_w) in the porous medium. Capillary forces (P_c) are important both in correlated structural/stratigraphic and residual trapping. In the cap-rock (or the seal) the capillary force threshold is high enough to keep the non-wetting (for example gas phase or CO_2 fluid) from entering through the small pore throat in the cap-rock.

$$P_c = P_n - P_w \quad (54)$$

Capillary forces will also keep small bubbles of CO_2 phase immobile in small pore-spaces of the reservoir during migration of CO_2 . This phenomenon is defined as residual trapping (Figure 5).

2.2. Reservoir Simulation Software (Nexus/VIP)

In the past decade, the need for complex reservoir studies has escalated due to increased energy demands and the depletion of easy-to-produce oil. Planning the optimal development of a reservoir is more critical than ever to reduce field costs and maximize production, and it requires accurate models for both the history matching and prediction phases of reservoir simulation workflows. Reservoir engineers now must assess the deliverability of hydrocarbons from one or more reservoirs to the point of sale. This requires engineers to model not only the flow within the reservoir to the wells, but also the flow through the surface. The effect of pressure feedback on the reservoir caused by the surface facilities can only be captured accurately by modeling the reservoir, wells and surface facilities as a single integrated system. Poor development plans and sub-optimal production are the results of ignoring pressure feedback during simulation prediction runs.

Nexus next-generation reservoir simulation software provides users the integrated modeling tool needed to solve today's challenging problems. Reservoirs, wells, and surface facilities can be included in Nexus models at the level of detail required to understand the behavior of the asset. The flow models are coupled across the surface and subsurface with an implicit pressure solution, ensuring a robust and accurate accounting of physical effects within a single application. Competing solutions use multiple applications that are loosely coupled; this limits their performance and stability.

Recent improvements in algorithms and physical modeling techniques included in Nexus software provide significant performance improvements over prior generation reservoir simulators. With its combination of speed, accuracy, and usability, Nexus software gives reservoir engineers a single tool that can solve their most challenging field management problems—while remaining easy to use for everyday work like reserves estimation.

2.2.1. Solver:

At each Newton iteration, it is necessary to solve a matrix equation. Depending on the number of cells used to represent the reservoir, the reservoir part of this equation must be solved iteratively. For the simulation to be successful, this iteration must converge in a reasonable number of iterations.

In general, the overall convergence rate will be limited by convergence of a particular part of the overall process. Potentially limiting the convergence rate are the following

- Convergence problems related to the coupling between the facility network and the reservoir.
- In implicit computations, convergence of the CPR (Constrained Pressure Residual) computation.
- Convergence of the reservoir pressure solution.
- In multiple subgrid runs, which typically use multiple processors, convergence problems related to coupling between neighbouring subgrids.

The following chart shows major components in NEXUS linear solver package SPURSPACK:

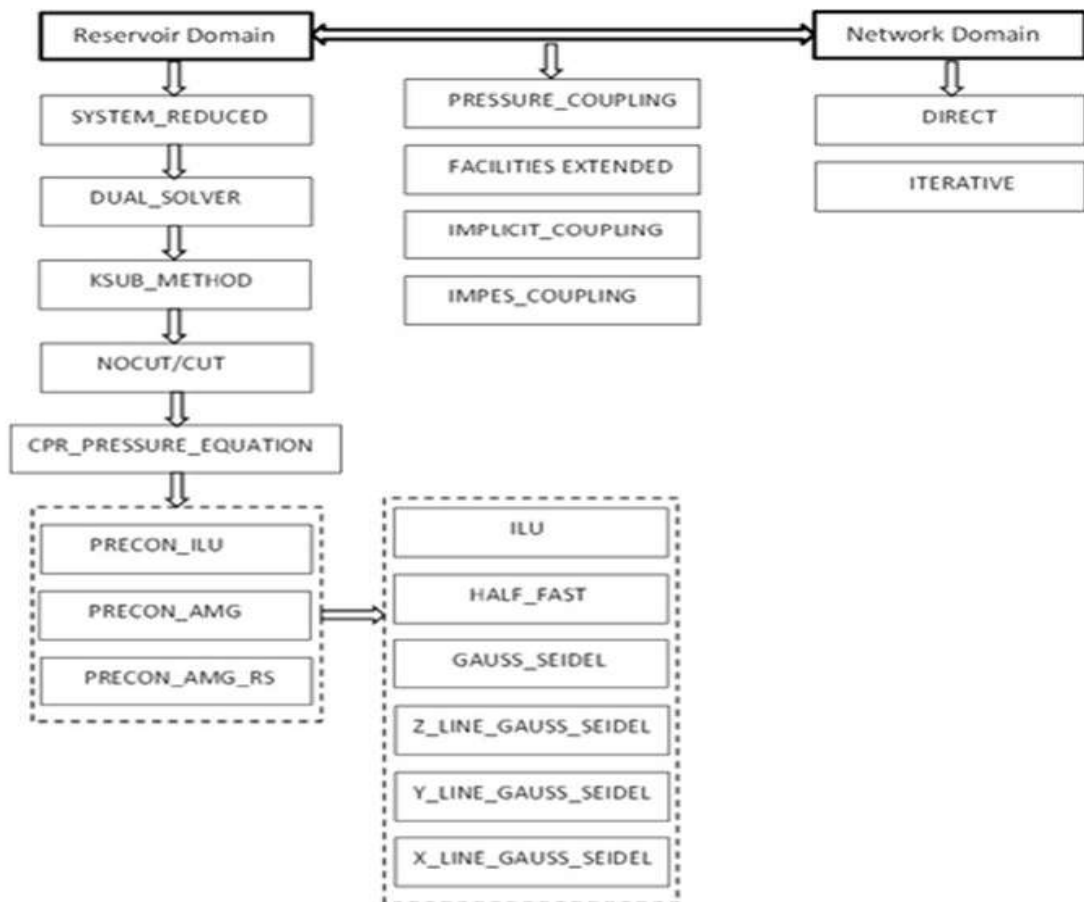


Fig. 55-a: Major components in NEXUS linear solver package SPURSPACK

Landmark's Nexus. Suite reservoir simulation equips reservoir engineers with the integrated modeling capabilities needed to assess, validate, plan and execute asset development optimization from start to finish. With faster run-times and multi-reservoir modeling capabilities, Nexus tools increase both model accuracy and asset team productivity, yielding integrated solutions that help increase confidence in key decisions and lifecycle management strategies for optimum asset development.

2.2.2. Nexus Suite

- **PowerGrid:** increase reservoir simulation efficiency by reducing the number of gridblocks while retaining important geologic features. Integrates many features with Landmark's DecisionSpace Earth Modeling, enabling collaboration of geomodelers and reservoir engineers.
- **SimDataStudio:** build full Nexus simulation decks or import existing files for editing, and generate the complete set of input files needed for Nexus reservoir simulation.
- **Nexus:** run simulations of fluid flow for one or multiple assets, and model the reservoir, wells, and surface and subsurface facilities as a single system for the most comprehensive representation of asset behavior.
- **SurfNet:** visualize, validate, and analyze your Nexus surface network for complete tracking of fluid flow paths within the entire network.
- **StreamCalc:** compute streamlines based on a full-physics Nexus simulation run with a methodology that retains the accuracy of the predicted flow.
- **Nexus View:** visualize reservoir simulation results in 3D.
- **SimResults:** plot well field rates in 2D.

The figure below gives an organization of the modules and its applications of the Nexus desktop.

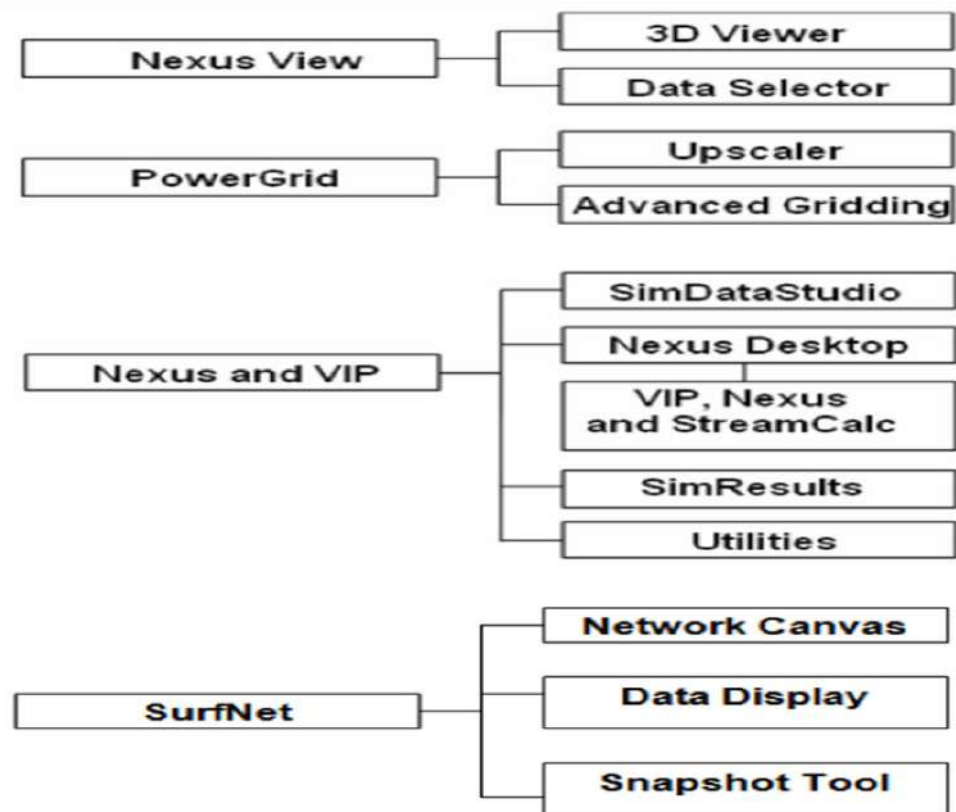


Fig. 55-b: Different modules in Nexus Desktop

The key benefits of the Nexus software are that it enables streamlined static to dynamic modeling, fully coupled/fully implicit solution for single or multiple reservoirs, and rapid, robust production and reserves forecasts.

2.2.3. Nexus Functionality

- Fully coupled network, facility, and subsurface modeling
- Ability to model complex reservoirs supported with multiple fluid models
- Datasets may be run individually and as a combination of individual reservoirs, coupled by a surface network.
- Both serial and optimized parallel capability
- Minimal tuning is required to achieve optimal performance. In many cases, no tuning is required.
- Integration with other products such as PowerGrid software
- Integration with existing VIP® programs such as SimDataStudio software
- Ability to convert existing VIP projects to Nexus projects
- Significant speed improvements over older commercial simulators

3. Modeling and simulation

Numerical analyses can be used to assess the fate of injected CO₂ both on short- and long timescales and can be used complementary to experimental work. The results of simulations are limited by the accuracy of input such as reservoir properties (permeability, porosity, FZI,...) and constraints limits (reservoir pressure, surface equipment capacities).

The numerical simulations are thus not only complementary, but also strongly reliant to experimental work. This chapter gives an idea about the validation of the simulation software (Nexus) and reservoir model inputs in term of capabilities to model the major physical phenomenons such as the solubility of the CO₂ in the fluid in place (brine) by comparing the consistency of the results between the simulation results and experimental work results done by M. Adel Salem (2013).

3.1. Field presentation (Sif Fatima South-West- SFSW)

The SFSW field is a mature oil field discovered in January 2003 situated in the South east of Algeria. The reservoir is moderately heterogeneous TAGI sandstones with an average porosity of 14.5 % and an average permeability of 175 mDarcy. The reservoir has two TAGI zones (horizon) U sand and M sand with similar reservoir properties and different fluid in place PVT as each zone has own aquifer , only U zone is targeted for CO₂ injection. The reservoir oil was initially under-saturated, with a bubble point pressure 1100 pisa below the initial reservoir pressure. The oil production has started by reservoir depressurization (natural depletion). To quantify the potential of this reservoir to store CO₂, an enhanced oil recovery mechanism is applied by continuous injection of CO₂ for about 10 years after the production start.

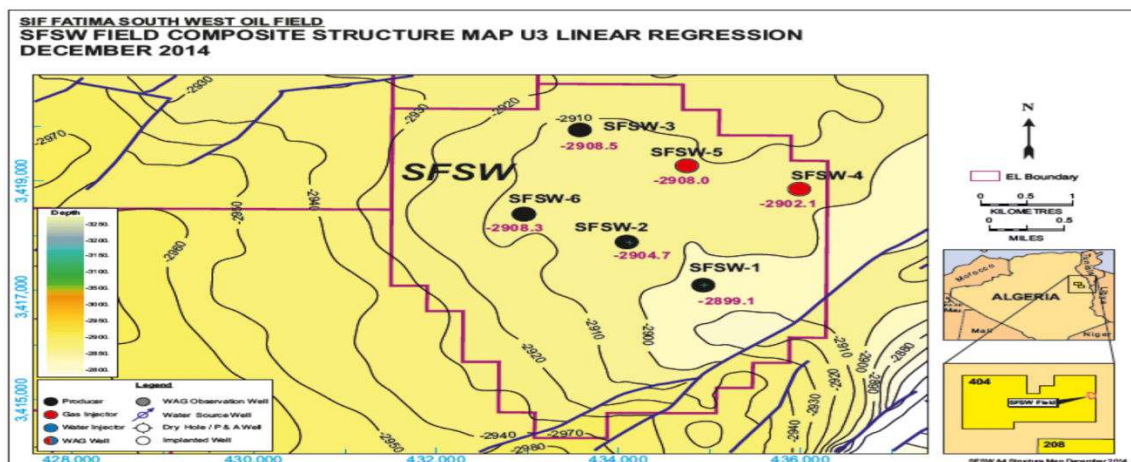


Fig. 56-a: The Structure MAP of SFSW

3.2. Geological Modeling of SFSW

3.2.1. Static modeling (geology data)

The structural 3D model was developed with Petrel software, a common 3D modeling and simulation tool in the oil and gas industry produced by Schlumberger. The development of the 3D structural model consisted of several steps including creation of geological horizons, layers and grid discretization, a grid dividing a 3D model into small boxes called grid cells.

The field-scale reservoir model (8190 cells: 35x39x6 grid) was constructed. The remaining challenge for the model was to capture the formation heterogeneity to optimize the injection, the FZI is useful value to quantify the flow character of the different reservoir layers in this study the FZI was used as perforation indicator to maximize the storage capacity and minimize the leakage risk by targeting the optimum layers of the reservoir.

The geological model generated by Petrel software using stochastic modeling method, stochastic simulation model is based on a series of realizations representing a range of possibilities. The range of these possibilities depending on the variogram, variance of the input data etc. These realizations will have similar outputs (with the same input data) but with varying details. Stochastic modeling algorithms are more complex than deterministic [71]

The reservoir properties were distributed randomly in petrel software with the guidance of the geologist by including the history match data got from the exploitation phase, this workflow helps for best forecast, all the grid data (grid coordination, net to gross, permeability, porosity water saturation,...) were included as include files.

The below table summarize the main static data

Table.18: Reservoir properties data of the simulation model

Properties	Value
Dimensions	35X39X06 grid
Reservoir Temperature	197.1 Degrees Fahrenheit
Initial reservoir pressure @ Depth 9563.6 feet	4882 psia
Initial WOC	9563.6 feet
Initial bubble point pressure	3781 psia
Boundary condition	Aquifer
Water density (g/cc)	1.034
FVF (water)	1.0
Water viscosity	1.E-6
Rock compressibility	5.E-6

3.2.2. Dynamic modeling (reservoir-fluid data)

- Equation of State (EOS) Model

Nexus uses a generalized form of a cubic EOS as follows:

$$p = \frac{RT}{v-b} - \frac{a}{(v+C_1b)(v+C_2b)} \quad (55)$$

Where p is the absolute pressure, T is the absolute temperature, and v is the molar volume. C_1 and C_2 are constants that depend on the equation of state, while a and b are parameters that are compositionally dependent.

a for a single component i is defined as

$$a_i = \Omega_{ai} \alpha_i \frac{R^2 T_{ci}^2}{P_{ci}} \quad (56)$$

b for a single component i is defined as

$$b_i = \Omega_{bi} \frac{R T_{ci}}{P_{ci}} \quad (57)$$

Where Ω_{ai} and Ω_{bi} are equation of state constants that have different defaults for different equations of state, T_{ci} is the critical temperature of component i , P_{ci} is the critical pressure of component i , and R is the universal gas constant.

For the Redlich-Kwong equation of state (RK-EOS), and the Soave-Redlich-Kwong² equation of state (SRK-EOS), the default value of Ω_{ai} is 0.4274802 and the default value of Ω_{bi} is 0.08664035. The value of constant C_1 is 1 and value of constant C_2 is 0.

For the RK-EOS

$$\alpha_i = \sqrt{\frac{T_{ci}}{T}} \quad (58)$$

For the SRK-EOS

$$\alpha_i = [1 + m_i(1 - \sqrt{T_{ri}})]^2 \quad (59)$$

Where

$$m_i = \omega_i(-0.176\omega_i + 1.574) + 0.48 \quad (60)$$

And ω_i is the acentric factor.

For the Peng-Robinson³ equation of state (PR-EOS), the default value of Ω_{ai} is 0.457235529 and the default value of Ω_{bi} is 0.077796074. The value of constant C_1 is $(1 + \sqrt{2})$ and value of constant C_2 is $(1 - \sqrt{2})$.

To calculate ω_i , (equation 60) is applied to PR-ESO, bur the definition of m differs.

$$m_i = \omega_i(-0.26992\omega_i + 1.54226) + 0.37464 \text{ For all } \omega_i \quad (61)$$

For PR-EOS⁴ m_i has different expression related the value of ω_i , if it is greater or lower of 0.49.

The EOS model used to model the PVT of our reservoir (SFSW) is Peng Robinson Equation (PR-EOS), the software used to model the EOS is PVTIsim software by decomposing the hydrocarbon reservoir fluid (oil) to 18 components C_{11+} plus CO_2 and N_2 non hydrocarbon components total of 20 components, Constant Composition Expansion (CCE) and Differential Liberation Expansion (DLE) experimental results have been used to tune the EOS model.

- **Relative Permeability and Capillary pressure**

The relative permeability and capillary pressure models of the reservoir-fluid used in this study are show in the below plots:

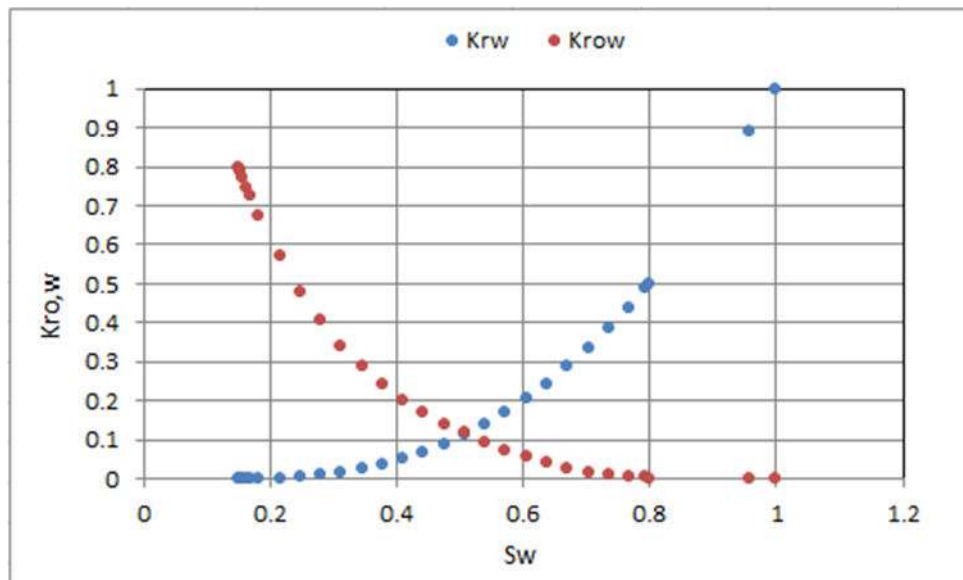


Fig. 56-b: Relative permeability of water and oil model vs. water saturation

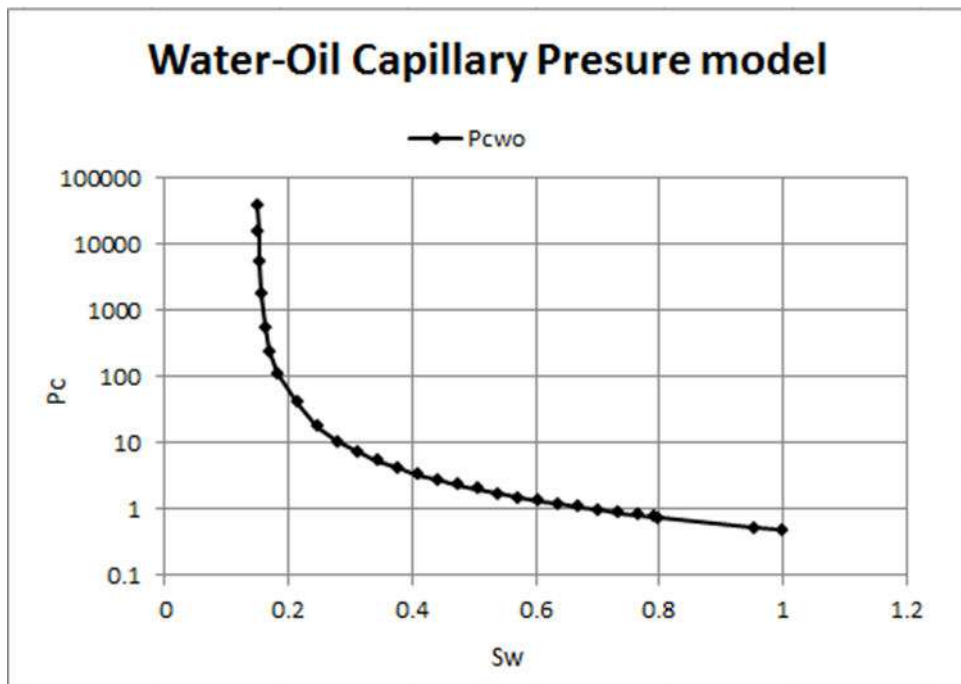


Fig. 56-c: Capillary pressure model vs. water saturation

The 3-D view of the reservoir model and wells configuration are shown in the below MAP

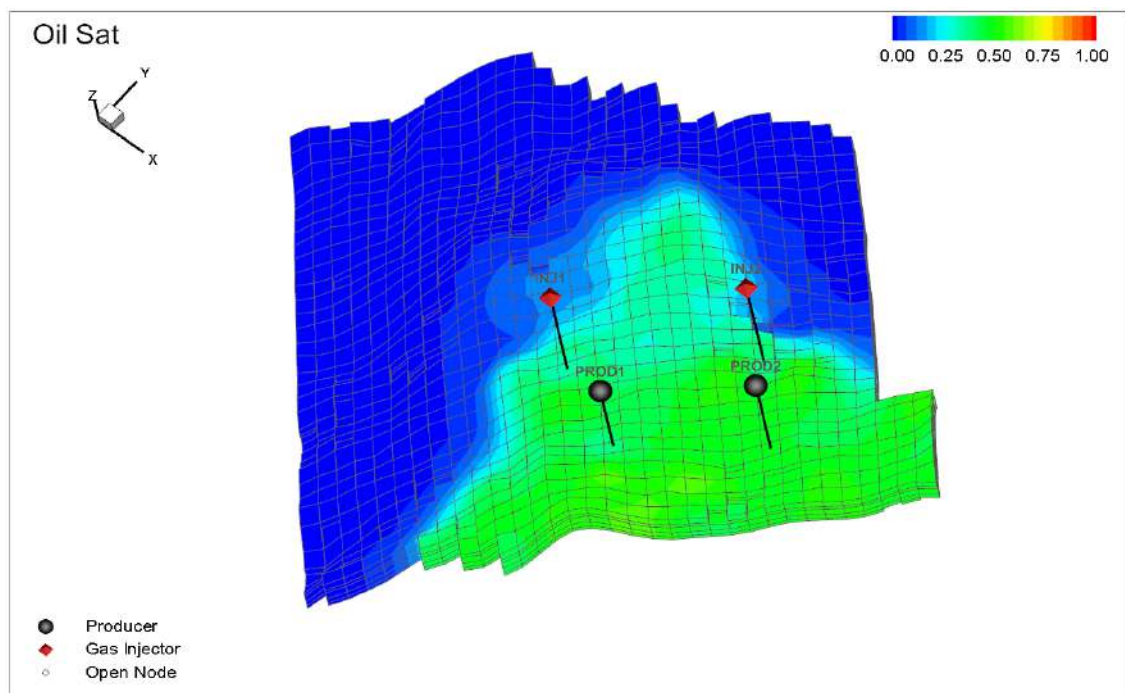


Fig. 57: 3-D geological model of SFSW

The initialization output are summarized below

Table. 19: The initialization reservoir model output.

Structural Model CO2 FLOODING, 20-COMPONENT MODIFIED PENG-ROBINSON EOS CO2 SOLUBILITY IN WATER OPTION, 1 EQUILIBRIUM REGION (U3)						
	REGION	REGION	REGION	REGION	REGION	TOTAL
REGION NUMBER	1	2	3	4	5	
REGION NAME						
AVERAGE PRESSURE, PSIA						
WEIGHTED BY HC PV AT DATUM	0.0	4827.7	0.0	0.0	0.0	4827.7
WEIGHTED BY TOTAL PV AT DATUM	0.0	4818.8	0.0	0.0	0.0	4818.8
WEIGHTED BY HC PV	0.0	4870.6	0.0	0.0	0.0	4870.6
WEIGHTED BY TOTAL PV	0.0	4891.6	0.0	0.0	0.0	4891.6
FLUIDS IN PLACE						
SURFACE VOLUMES						
TOTAL OIL (MSTB)	0.	23251.	0.	0.	0.	23251.
CONDENSATE IN F.G. (MSTB)	0.	0.	0.	0.	0.	0.
TOTAL GAS (MMSCF)	0.	13003.	0.	0.	0.	13003.
FREE GAS (MMSCF)	0.	0.	0.	0.	0.	0.
WATER (MSTB)	0.	139025.	0.	0.	0.	139025.
RESERVOIR VOLUMES						
TOTAL PORE VOLUME (MRB)	0.	167768.	0.	0.	0.	167768.
HC PORE VOLUME (MRB)	0.	28603.	0.	0.	0.	28603.
RESERVOIR OIL (MRB)	0.	28603.	0.	0.	0.	28603.
RESERVOIR GAS (MMRCF)	0.	0.	0.	0.	0.	0.
RESERVOIR WATER (MRB)	0.	139165.	0.	0.	0.	139165.
MOBILE RES OIL (MRB)	0.	15325.	0.	0.	0.	15325.
MOBILE RES GAS (MMRCF)	0.	0.	0.	0.	0.	0.
MOBILE RES WATER (MRB)	0.	71132.	0.	0.	0.	71132.
AVG OIL SATURATION (FPV)	0.000000	0.170490	0.000000	0.000000	0.000000	0.170490
AVG GAS SATURATION (FPV)	0.	0.	0.	0.	0.	0.
AVG WTR SATURATION (FPV)	0.000000	0.829510	0.000000	0.000000	0.000000	0.829510
AVERAGE COMPOSITION						
CO2	0.0000	0.0064	0.0000	0.0000	0.0000	0.0064
N2	0.0000	0.0024	0.0000	0.0000	0.0000	0.0024
C1	0.0000	0.3440	0.0000	0.0000	0.0000	0.3440
C2	0.0000	0.0813	0.0000	0.0000	0.0000	0.0813
C3	0.0000	0.0530	0.0000	0.0000	0.0000	0.0530
IC4	0.0000	0.0070	0.0000	0.0000	0.0000	0.0070
C4	0.0000	0.0368	0.0000	0.0000	0.0000	0.0368
IC5	0.0000	0.0116	0.0000	0.0000	0.0000	0.0116
C5	0.0000	0.0227	0.0000	0.0000	0.0000	0.0227
C6	0.0000	0.0224	0.0000	0.0000	0.0000	0.0224
C7	0.0000	0.0435	0.0000	0.0000	0.0000	0.0435
C8	0.0000	0.0473	0.0000	0.0000	0.0000	0.0473
C9	0.0000	0.0354	0.0000	0.0000	0.0000	0.0354
C10	0.0000	0.0304	0.0000	0.0000	0.0000	0.0304
C11	0.0000	0.0250	0.0000	0.0000	0.0000	0.0250
HVY1	0.0000	0.1367	0.0000	0.0000	0.0000	0.1367
HVY2	0.0000	0.0533	0.0000	0.0000	0.0000	0.0533
HVY3	0.0000	0.0407	0.0000	0.0000	0.0000	0.0407
HVY4	0.0000	0.0000	0.0000	0.0000	0.0000	0.0000
HVY5	0.0000	0.0000	0.0000	0.0000	0.0000	0.0000
TOTAL LB-MOLES	0.	70781496.	0.	0.	0.	70781496.

4. Validation of the Reservoir Model and Simulation Software

The validation of numerical codes and models is a necessary preliminary step before their application to safety and risk assessment analysis. In this context, numerical simulations of CO₂ flow behavior across the reservoir have been checked versus an experimental work. The experimental data were taken from the work done by M. Adel Salem et al. (2013) which were designed to investigate the solubility of the CO₂ in the fluid in place (brine) as function of the conditions in situ (pressure, temperature and salinity).

This study presents a comparison between the simulation results and the experimental measurements in order to assess the accuracy of the software with different modeling approaches.

4.1. Effect of the conditions in situ in the Solubility of CO₂

As the concentration of aqueous CO₂ in solution is important for estimating of the amount of carbon dioxide that can be stored, knowledge of the solubility of CO₂ in pure water and salt solutions is necessary, over the past decades there have been many experimental studies on the CO₂-H₂O and CO₂-H₂O-salt systems, over a wide pressure-temperature range. At the same time theoretical efforts have been made to model the solubility of carbon dioxide in aqueous solutions (Nighswander et al., 1989; Carroll et al., 1991; King et al., 1992; Duan& Sun, 2003; Duan et al., 2005; Portier& Rochelle, 2005). The most complete model developed until now is that of Duan and Sun (2003; 2005), which models the solubility of CO₂ in pure water and aqueous solutions from 0 to 260°C and from 0 to 2000 bar total pressure, up to ionic strengths of 4.5 mol/kg water. The model is extended to not only predict the solubility of CO₂ in pure water and NaCl solution but also in more complex systems, which may include Ca²⁺, K⁺, Mg²⁺, and SO₄²⁻ ions.

The pressure, temperature and Salinity are the primary parameter affecting CO₂ solubility, in the following section, an experimental work have been done by Adel M. Salem et al. (2013) predicting the behaviour of the CO₂ solubility in different pressure-temperature and salinity as shown in the below tables, in this study and for the purpose of checking the ability of the software used in this project and the consistency of the its results versus an experimental work.

The below tables summarize the behaviour of the CO₂ solubility when the salinity, pressure and temperature are changing.

Table.20: CO₂ Solubility in distilled water in different pressure and temperature

Pressure (Psia)	CO ₂ Solubility (RSW in SCF/STB) @ different temperature for Distilled Water		
P/T	70 °F	120 °F	170 °F
0	0	0	0
300	75.8	48.6	29.5
600	126.4	83.4	61.8
900	158.6	123.8	92.6
1200	168.5	137.8	110.3
1500	179.8	147.9	123.7
2000	195.2	163.2	144.2
4000	210.3	186.1	179.3
6000	227.4	196.4	193.1

Table.21: CO₂ Solubility in 15000 ppm NaCl Water in different pressure & temperature

Pressure (Psia)	CO ₂ Solubility (RSW in SCF/STB) @ different temperature for 15000 ppm NaCl water		
P/T	70 °F	120 °F	170 °F
0	0	0	0
300	48.6	34.7	23.5
600	91.4	64.7	47.8
900	128.6	73.8	74.6
1200	132.5	101.8	77.3
1500	138.5	113.6	102.3
2000	153.6	122.5	106.4
4000	162.9	138.4	137.7
6000	177.6	141.6	140.8

Table.22: CO₂ Solubility in 25000 ppm NaCl Water in different pressure & temperature

Pressure (Psia)	CO ₂ Solubility (RSW in SCF/STB) @ different temperature for 25000 ppm NaCl water		
P/T	70 °F	120 °F	170 °F
0	0	0	0
300	25.8	21.8	20.1
600	86.4	56.2	53.3
900	102.6	75.6	70.3
1200	121.5	86.5	73.4
1500	136.2	108.9	84.6
2000	141.6	120.2	100.2
4000	156.3	128.1	125.8
6000	160.2	139.4	138.8

4.1.1. Effect of Pressure CO₂ Solubility

The below plots indicates that for the same brine salinity and the same reservoir temperature, the increase of pressure increases the carbon dioxide solubility.

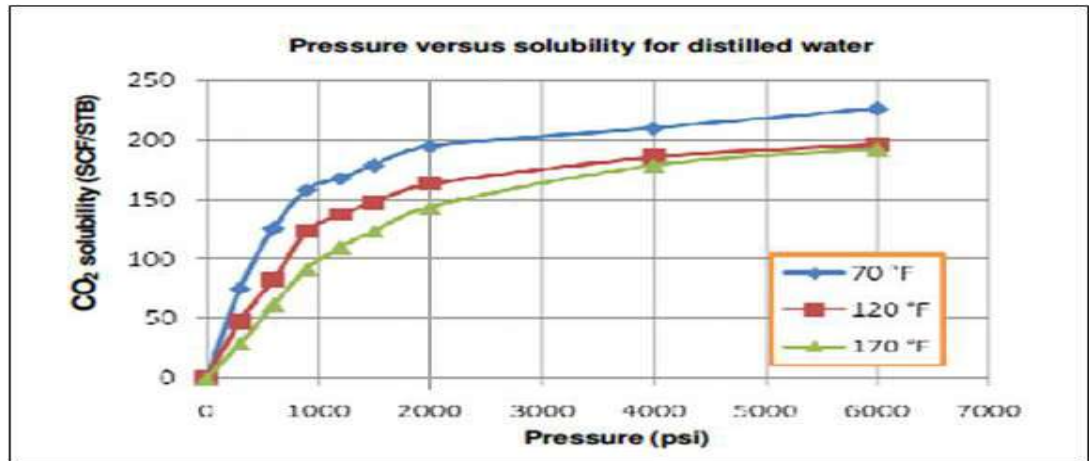


Fig. 58: impact of the pressure in the solubility (distilled water) [79]

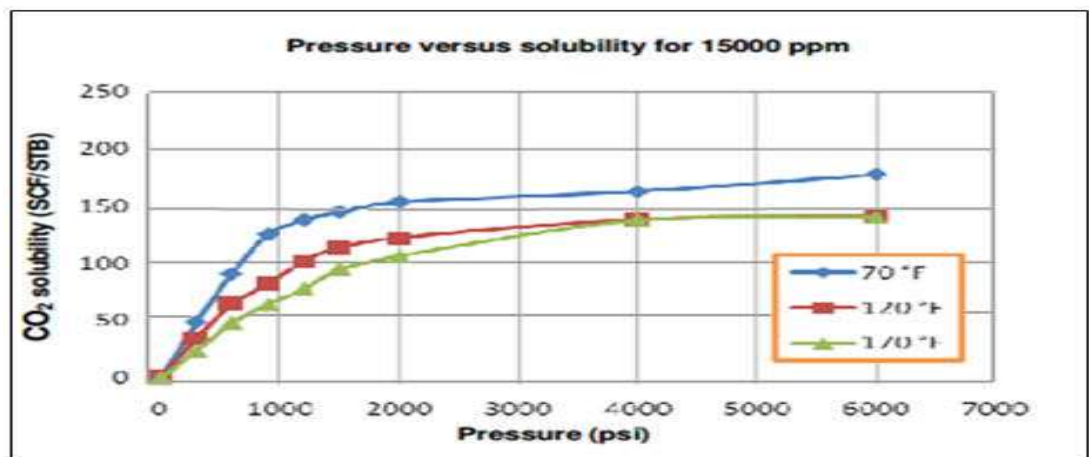


Fig. 59: impact of the pressure in the solubility (water salinity 15000 ppm) [79]

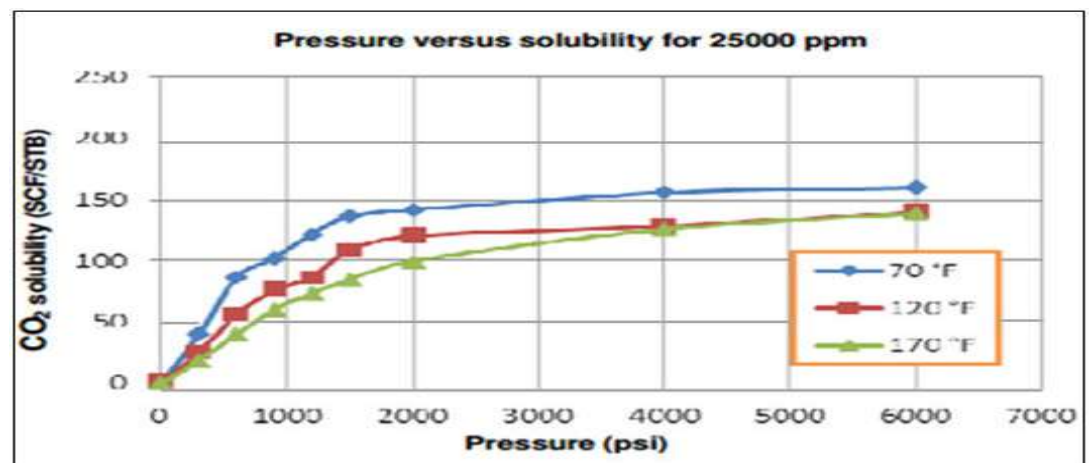


Fig. 60: impact of the pressure in the solubility (water salinity 15000 ppm) [79]

A sensitivities cases by changing the injection pressure within range of (3000-4500 psia) and fixing the water salinity and reservoir temperature have been ran and provide the below results

- Case 1: the Injection pressure is 3000 psia

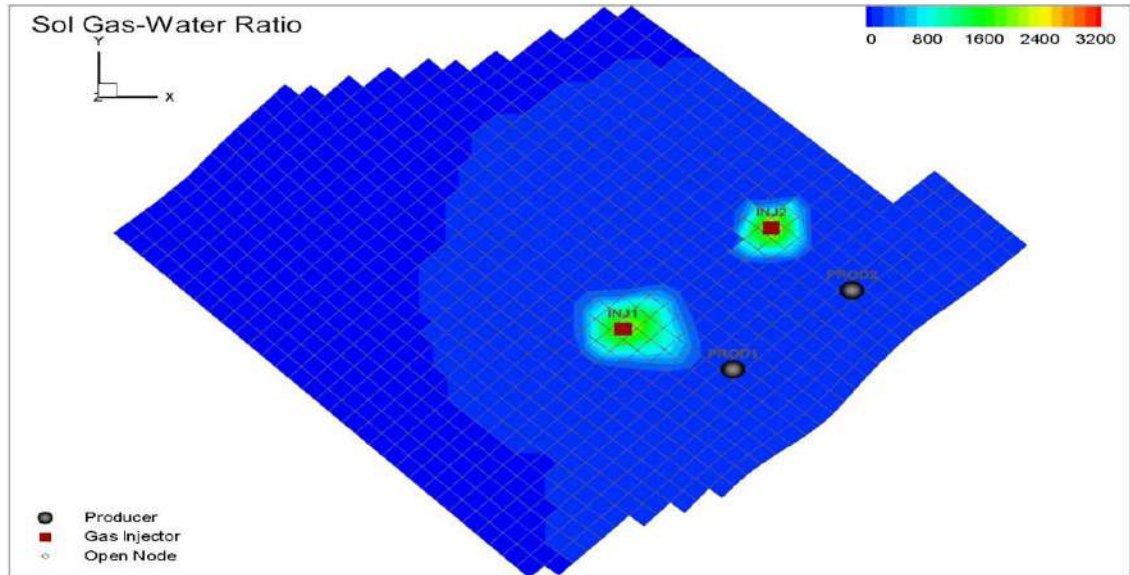


Fig. 61: Solubility of the CO₂ in fluid in place (inj_pressure = 3000 psia)

- Case 2: the Injection pressure is 3500 psia

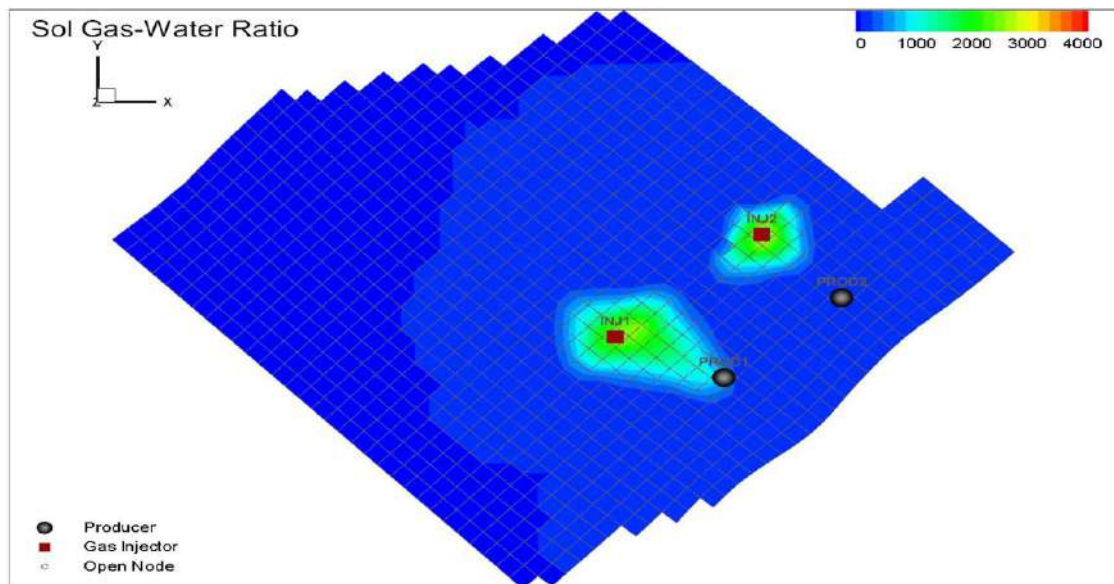


Fig. 62: Solubility of the CO₂ in fluid in place (inj_pressure = 3500 psia)

- Case 3: the Injection pressure is 4000 psia

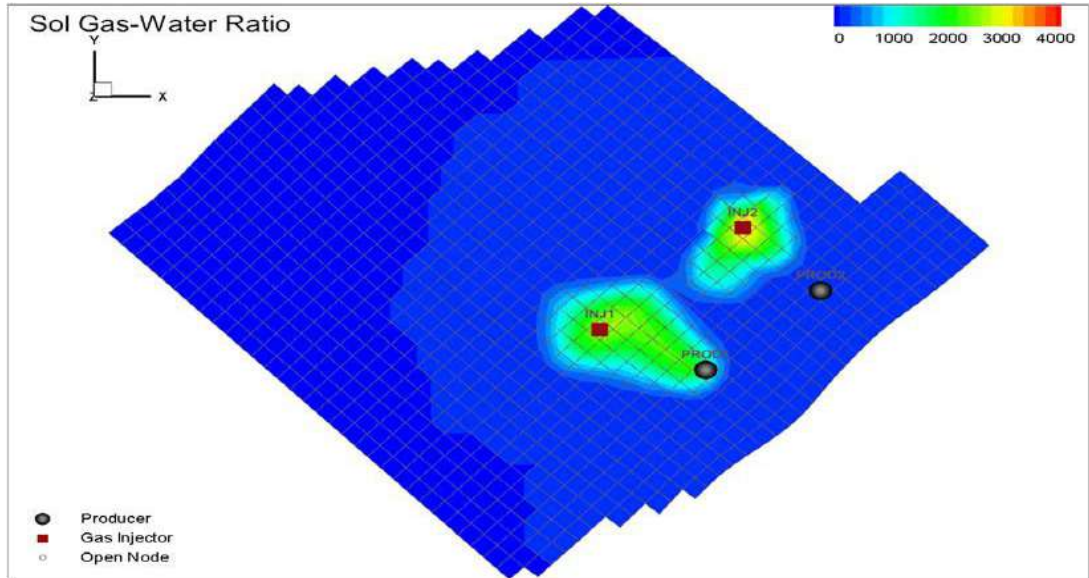


Fig. 63: Solubility of the CO₂ in fluid in place (inj_pressure = 4000 psia)

- Case 4: the Injection pressure is 4500 psia

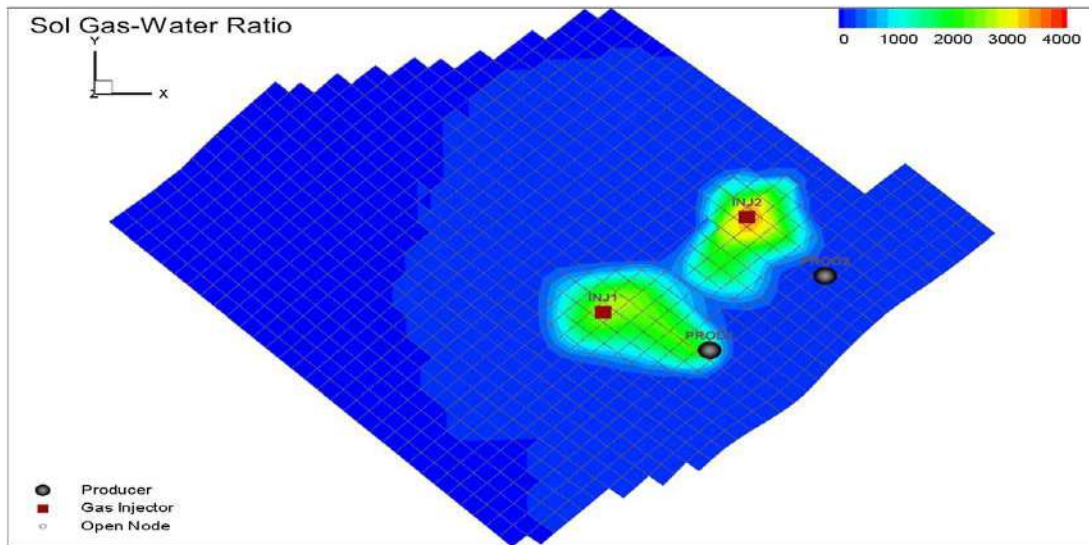


Fig. 64: Solubility of the CO₂ in fluid in place (inj_pressure = 4500 psia)

The pressure build-up caused by the injection pressure of the CO₂ into the reservoir is important to the safety of geologic carbon sequestration. An excessive pressurization may

- Fracture the caprock because of mechanical damage.
- Drive brine upward through localized pathways into shallower groundwater resources in case of injection in the aquifer.
- Cause induced seismicity.

Efforts to reduce these environmental risks by limiting injection pressure will impact the effective storage capacity of sedimentary basin formations. The pressure response to CO₂ storage will depend on the boundary conditions of the storage reservoir.

Recent modeling studies on open systems have indicated that the storage capacity for CO₂ may be limited by pressure effects in response to the injection and storage of additional fluid volumes, because the pressure build-up in a storage formation cannot exceed a maximum tolerable pressure gradient that would assure geomechanical integrity of the caprock [78]. Brine migration through localized pathways (e.g., leaky faults and wells) driven by elevated pressure may degrade shallower groundwater resources, further limiting effective storage capacity. On the other hand, pressure bleed-off caused by diffuse brine migration into and through semi-pervious sealing units and/or by lateral brine displacement in the storage formation may enhance the effective storage capacity of an open or a semi-closed system. Reservoir pressurization is effectively reduced by such brine migration, while environmental impact on overlying groundwater resources is typically not of concern due to the very small flow velocity and displacement length.

The reservoir pressure which is varying as function of the injection pressure should not exceeded minimum allowable pressure that was defined in (chapter 4) as the minimum required pressure to overcome the entry capillary pressure.

This value can help to calculate the effective storage capacity. The variation of the storage capacity as function of the injection pressure is shown below

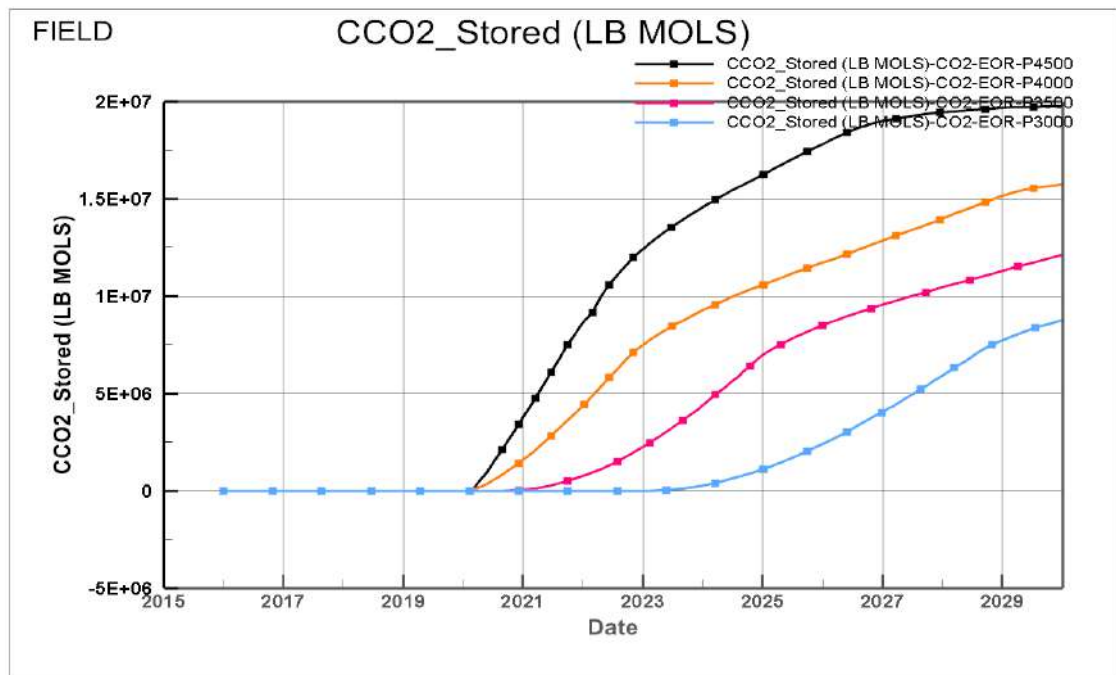


Fig. 65: Cumulative CO₂ Storage in different injection pressure

4.1.2. Effect of Temperature CO₂ Solubility

The below plots indicates that for the same brine salinity and the same reservoir pressure, the increase of temperature decreases the carbon dioxide solubility.

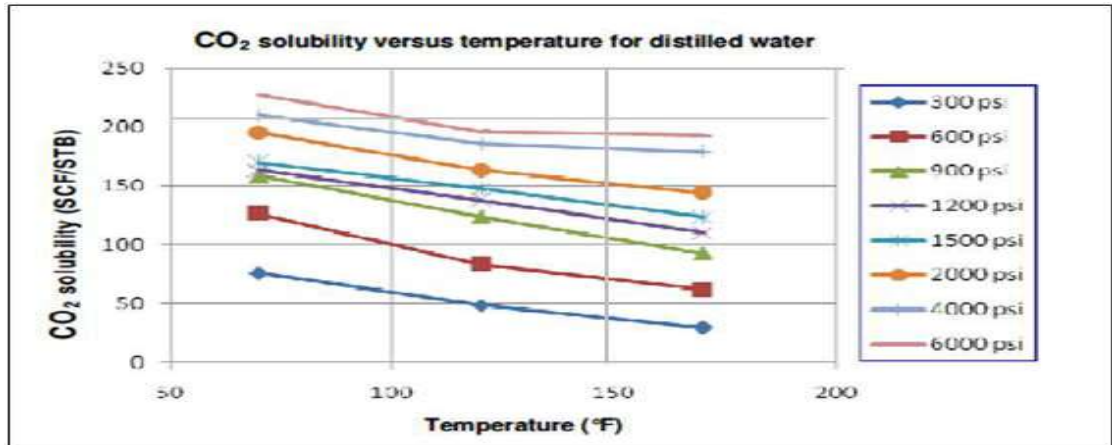


Fig. 66: Effect of the Temperature in the solubility (distilled water) [79]

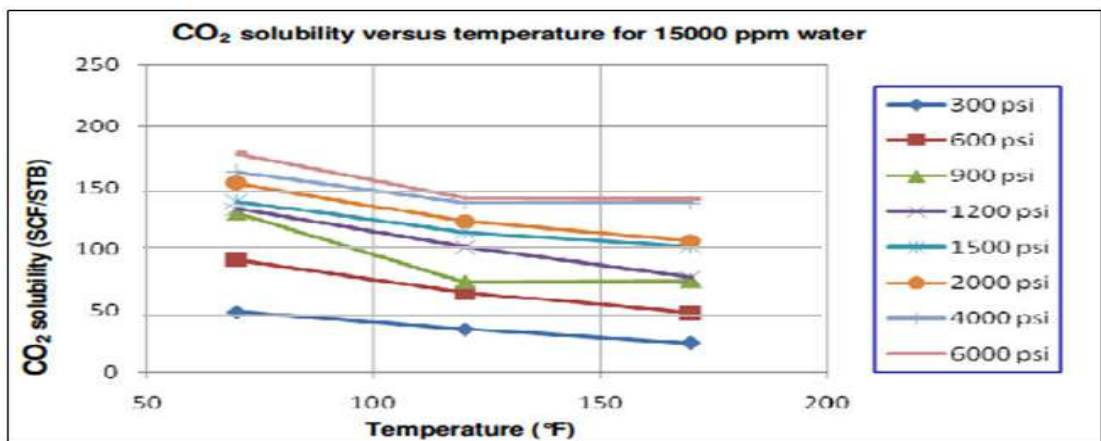


Fig. 67: Effect of the Temperature in the solubility (15000ppm NaCl water) [79]

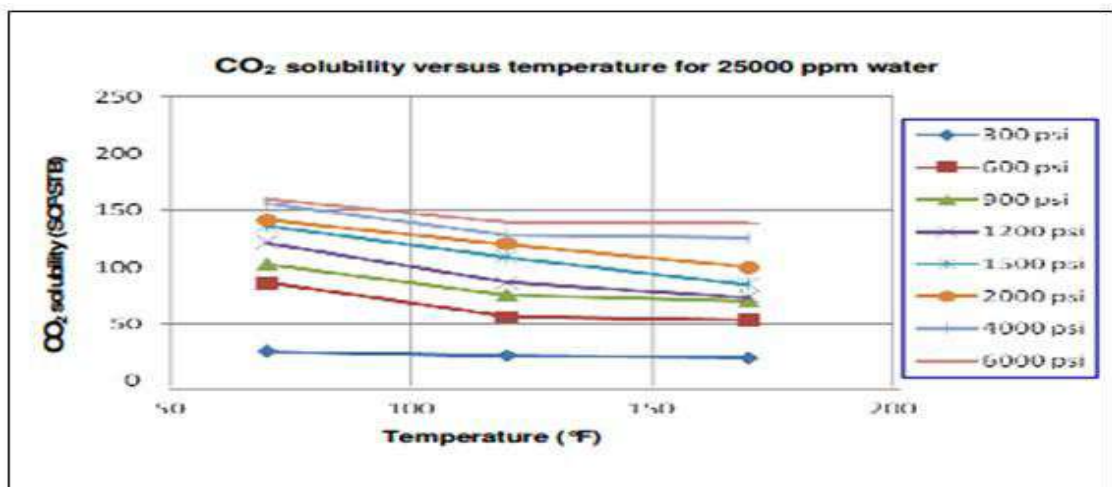


Fig. 68: Effect of the Temperature in the solubility (25000 ppm NaCl water) [79]

Running couple of simulation cases on the reservoir model by changing the reservoir temperature and fixing the salinity of the reservoir brine (250000 ppm) and reservoir pressure, the solubility of the CO₂ is changing

Based on the experimental results obtained, it is found that, as the temperature decreases the solubility increases for all prepared solutions at a given pressure, that is, the same results of distilled water, and for any brine salinities.

- Case 1: the reservoir temperature is 170 °F

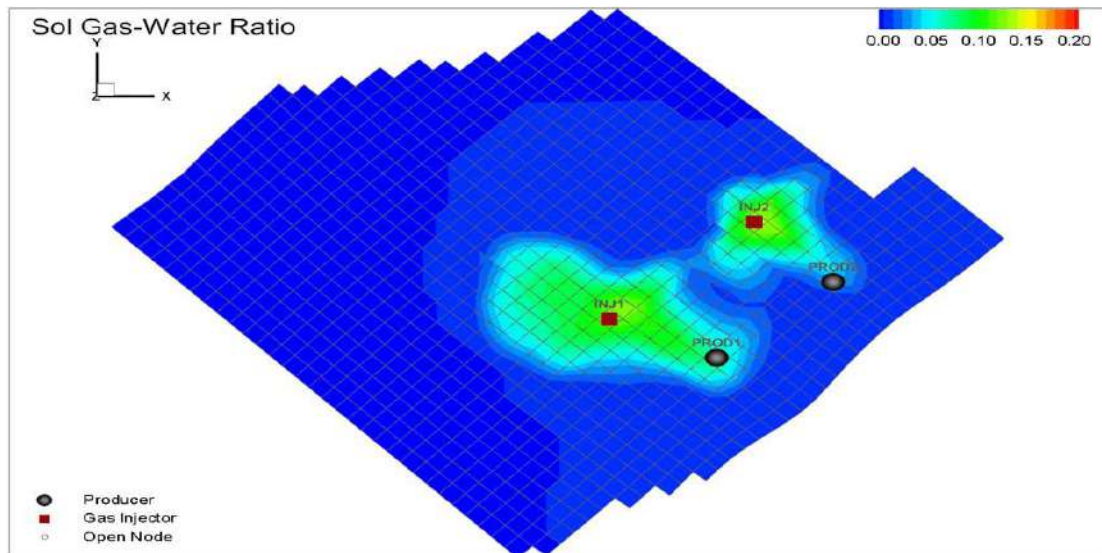


Fig. 69: Solubility of the CO₂ in fluid in place (Tr. = 170 °F)

- Case 2: the reservoir temperature is 120 °F

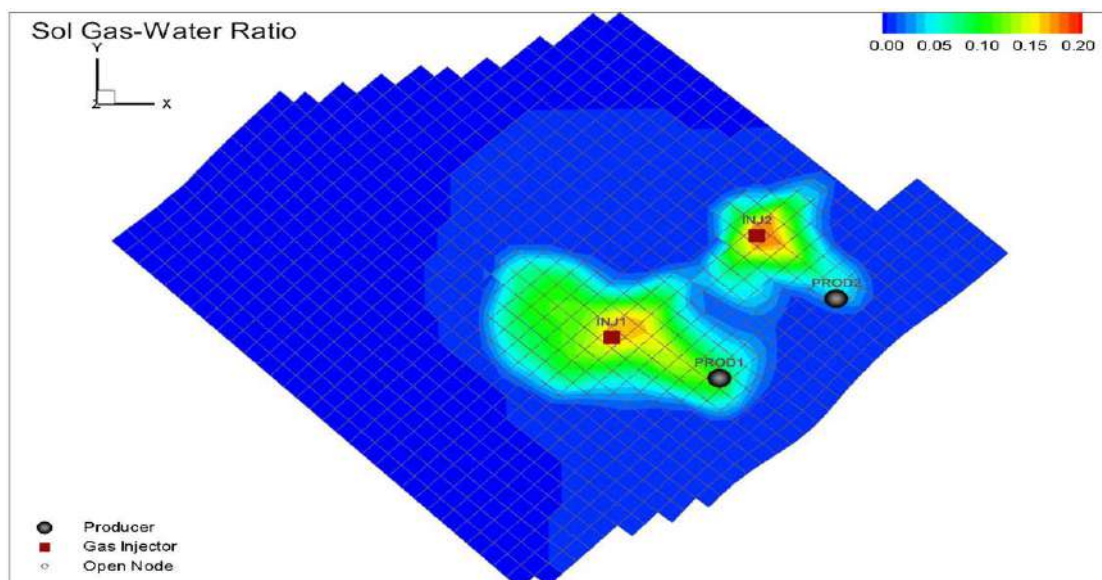


Fig. 70: Solubility of the CO₂ in fluid in place (Tr. = 120 °F)

- Case 3: the reservoir temperature is 70 °F

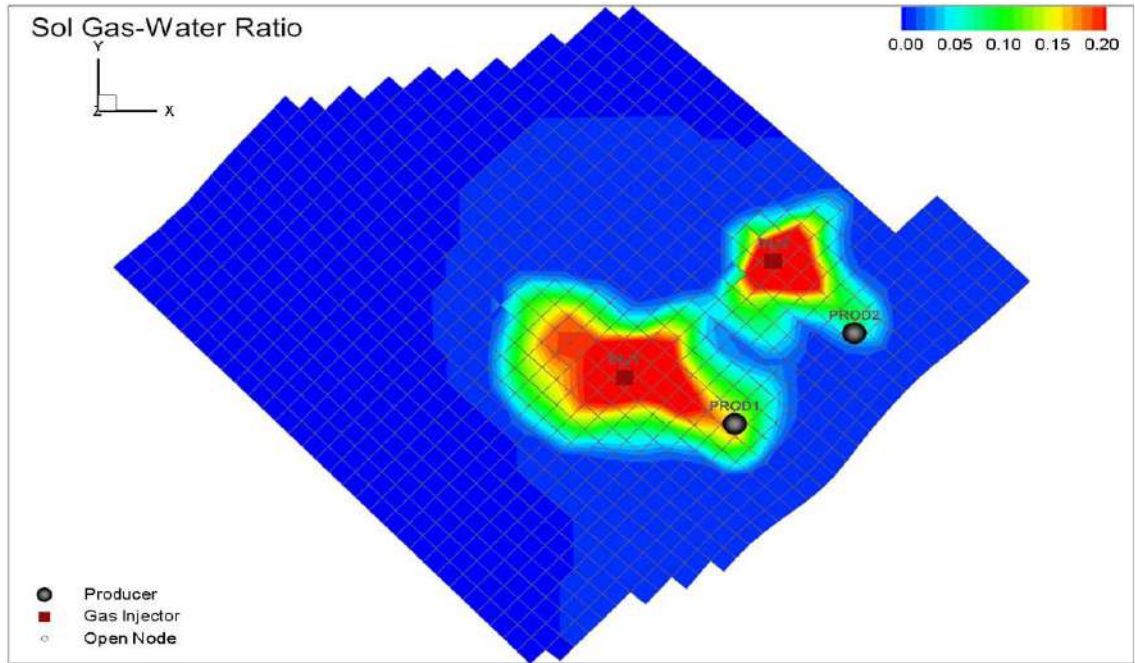


Fig. 71: Solubility of the CO₂ in fluid in place (Tr. = 70 °F)

The Solubility of the CO₂ in the fluid in place (brine) is highly affected by the reservoir temperature, according to the results obtained above the reservoir storage capacity is high in the coldest reservoir (less reservoir temperature).

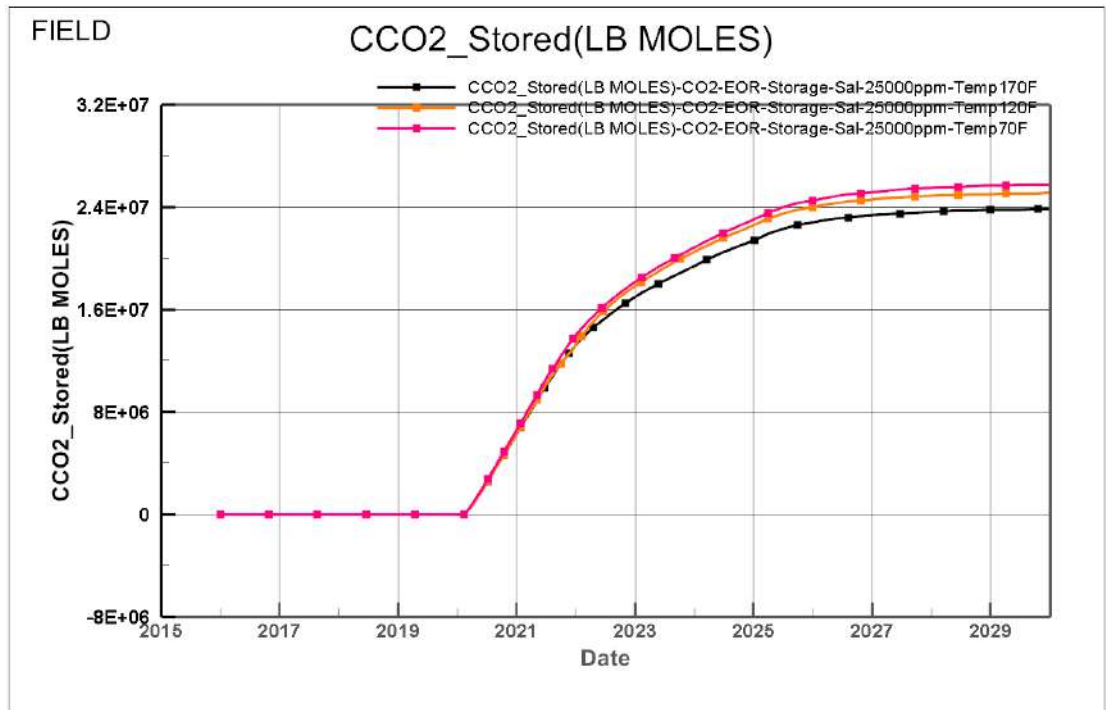


Fig. 72: Impact of the reservoir temperature in the Solubility of the CO₂

4.1.3. Effect of the Salinity in the CO₂ solubility

The salinity of the water in place in which the CO₂ is injected has high impact in the solubility of the CO₂, the experimental results shown above (Fig. 66, 67, 68 and Fig. 73, 74 , 75) indicate that for different salinities of 15 000 ppm and 25 000 ppm NaCl brines water, and distilled water the solubility increases with the decrease of the salinity, which mean the maximum storage capacity of the CO₂ is in the fresh water, this characteristic is very important for the reservoirs swept previously by water flooding, in the end of this mechanism the hydrocarbon reservoir will be fully of fresh water that was injected after its treatment in the surface for the purpose of increasing the injectivity by good treatment of the injected water.

A conclusion can be drawn that the increase of pressure increases the CO₂ solubility for different brine salinities and different reservoir temperatures. It is also clear that for temperature equal to or more than 120°F, the temperature effect diminishes and starts to have no effect, especially under pressures equal to or greater than 4000 psia. The reported data has real importance on validation simulation models describing the process of CO₂ storage in fresh and brine aquifers. It is also concluded that the increase of temperature and/or salinity increases the CO₂ solubility.

- Case 1: the reservoir brine salinity is 250000 ppm

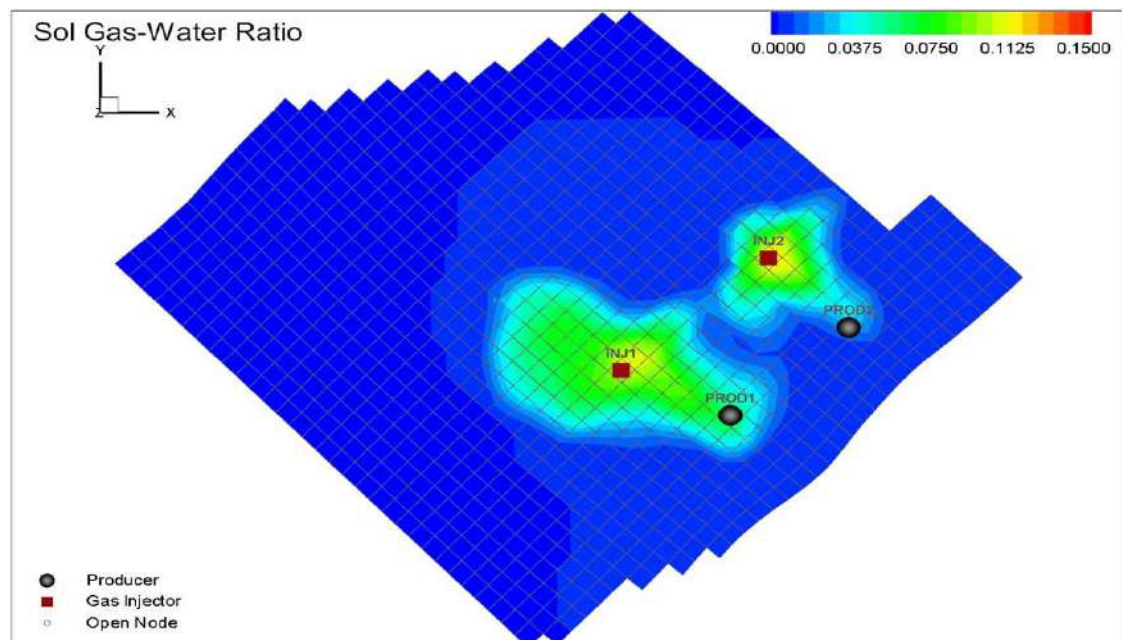


Fig. 73: Solubility of the CO₂ in fluid in place (Sal. = 250000 ppm)

- Case 2: the reservoir brine salinity is 250000 ppm

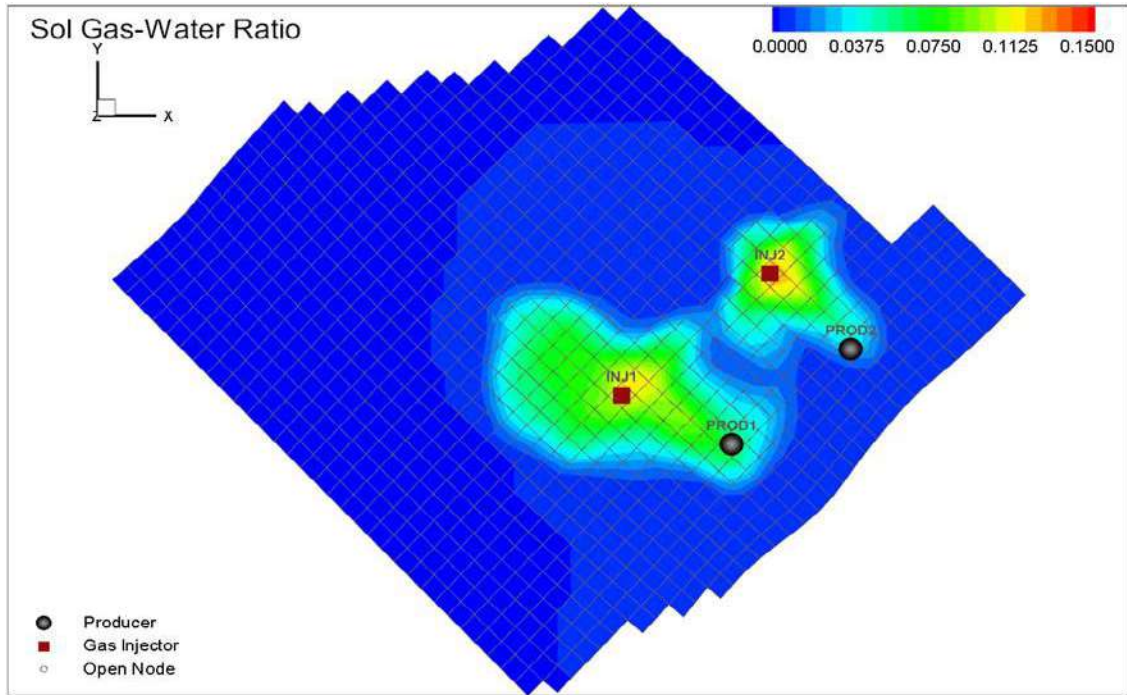


Fig. 74: Solubility of the CO₂ in fluid in place (Sal. = 15000 ppm)

- Case 3: the reservoir brine considered as Distilled water

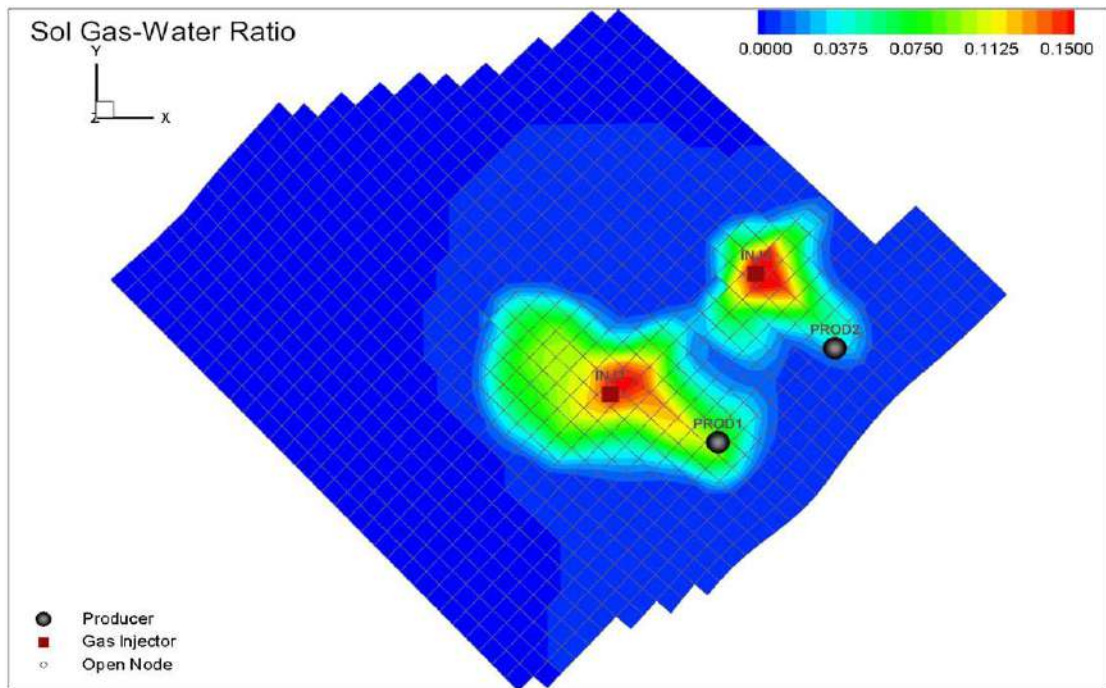


Fig. 75: Solubility of the CO₂ in fluid in place (Sal. = 15000 ppm)

The salinity of the brine in place should be well investigated for the success of the CCS project, the below plot shows the relationship between the salinity and the storage capacity of the reservoir, high storage capacity requests low brine salinity.

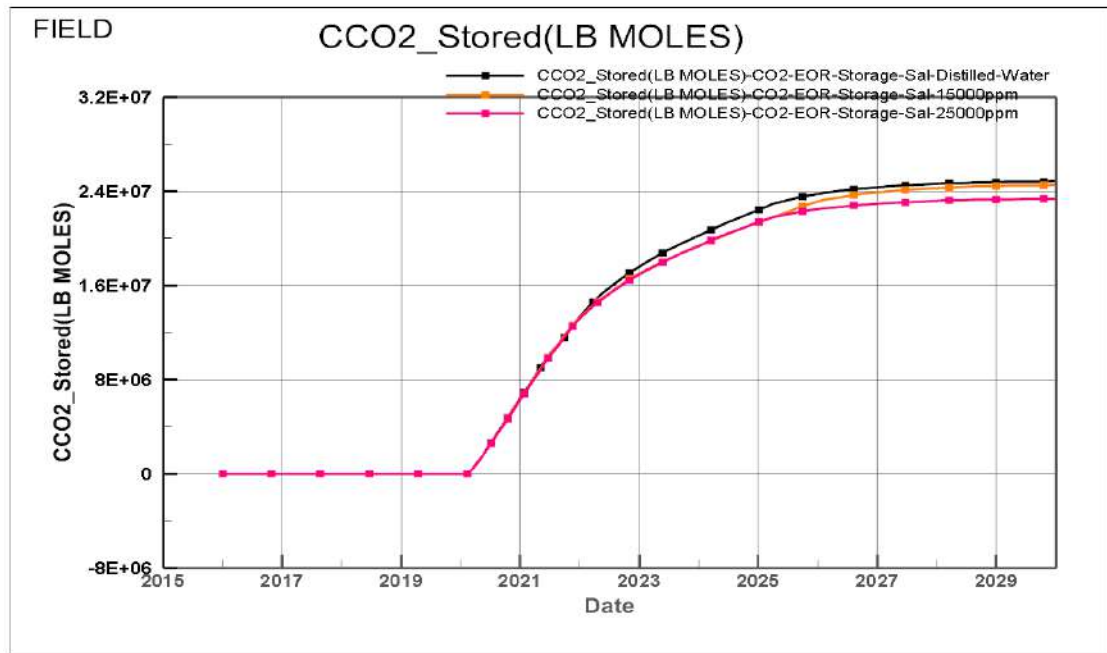


Fig. 76: Impact of the brine Salinity in the reservoir storage capacity

Conclusion

The main aim of this section is to validate the reservoir model and the simulation software that will be used in the CO₂ storage modeling in hydrocarbon reservoir. The solubility of the CO₂ in the brine in place is a key parameter as it involves in the trapping mechanism and the storage capacity.

Many authors proved that the solubility of the CO₂ in brine is much higher than that of hydrocarbon components. The CO₂ solubility depends essentially on pressure, temperature, total salinity and brine composition. In general, CO₂ solubility increases with increasing pressure and decreases with increasing temperature. An increase in the salinity of the formation brine decreases the CO₂ solubility significantly.

From the previous study, the geological model that will be used to perform various simulations of CO₂ flow and transport based on realistic injection scenarios is well modeled and the simulation software tool (Nexus) showed high capabilities to handle the major physical phenomenon that can be happen over CO₂ injection in hydrocarbon reservoir such as the solubility of the CO₂ in the fluid in place.

5. Storage of the CO₂ in hydrocarbon reservoirs

CO₂ injection into tertiary oil reservoirs has been widely accepted as an effective technique for enhanced oil recovery (EOR), and has been used by the oil industry for over 50 years. Concerns over greenhouse gas emissions are leading to the investigation and realisation of its potential as a carbon storage method in recent years. With the right reservoir conditions, injection of CO₂ into oil reservoirs can result in incremental oil recovery and permanent storage of CO₂ in geological formation. The potential of CO₂ storage combining EOR is high; approximately 60% injected CO₂ can be retained in the reservoir at the CO₂ breakthrough if reinjection is not considered. It has been accepted that there is little major technical challenges for CO₂ EOR projects, but there are economic constrictions if high cost anthropogenic CO₂ (such as from power plant) is used for EOR and storage operations.

CO₂ injection into oil reservoirs, leading to enhanced oil recovery (CO₂ EOR), thus gaining a financial return to offset the CO₂ capture and storage cost, has been considered as a favourable option for near-term action [72]. CO₂ EOR has been extensively investigated and is commercially pursued. There have been over 80 CO₂ EOR projects in the world, all of them are in onshore operations. Most CO₂ used for EOR is coming from naturally occurring sources. More recently, a large demonstration project using anthropogenic CO₂ has been conducted, namely the Weyburn CO₂ EOR project in Canada. Given appropriate circumstances, captured CO₂ from sources produced by human activities can be competitive for EOR as is demonstrated by the current field project. CO₂ has been considered as an effective injectant for EOR due to its high miscibility with oil. Field projects showed that CO₂ injection into water flooded oil reservoirs could yield an extra of 4-12% OOIP oil production. Over 8% OOIP has been achieved in the Permian Basin of West Texas by CO₂ miscible floods [72].

The CO₂ storage capacity of a reservoir include the CO₂ remained in the reservoir at the end of EOR operation and any extra CO₂ that can be injected after the EOR project. The US experience indicated that approximately 40% of the originally injected CO₂ is being produced in the producer wells and can be reinjected. This suggests a “gross” CO₂-retention efficiency of approximately 60% at CO₂ breakthrough if separation and reinjection is not considered after the breakthrough.

5.1. CO₂ as Enhanced Oil Recovery Mechanism (EOR)

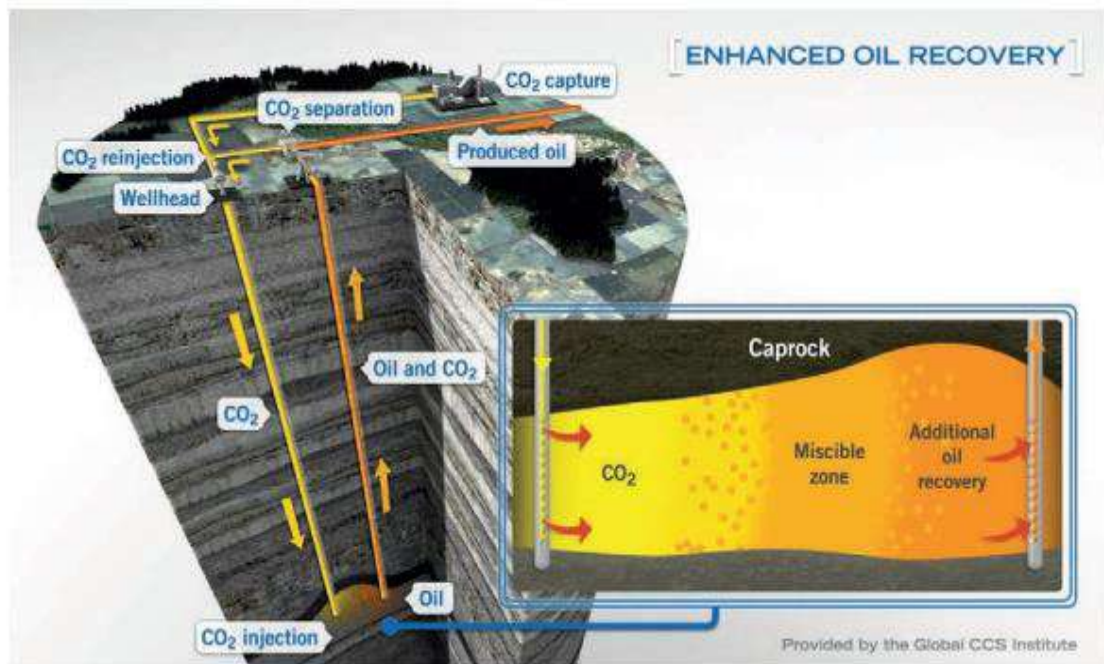
EOR methods are classified by the main mechanism of oil displacement. There are really just three basic mechanisms for recovering oil from rock other than by water alone. The methods are grouped according to those which rely on

- a) A reduction of oil viscosity,
- b) The extraction of the oil with a solvent, and
- c) The alteration of capillary and viscous forces between the oil, injected fluid, and the rock surface.

CO₂-EOR is one of many technologies that can be used to enhance oil recovery. Today, the main concentration of CO₂-EOR projects is in North America, mostly in the Permian Basin of the United States. So far CO₂-EOR has been undertaken with the primary aim of enhancing oil recovery. Climate change mitigation and long-term CO₂ storage goals are not principal drivers for EOR projects. Oil fields typically have various production phases. In the primary production phase, natural pressure drives oil to the production wells. In the secondary phase, pressure in the reservoir is increased by injecting fluids, pushing more oil to the production wells. In the tertiary phase, techniques are used not only to maintain pressure in the reservoir, but to also alter properties of the oil or reservoir, improving recovery of the existing oil. CO₂-EOR is a tertiary technique, based on injection of CO₂ and usually, but not always, water into the oil reservoir. CO₂ mixes with oil, improving its ability to flow towards production wells. Injected CO₂ is produced with the oil; this CO₂ is separated from the oil and re-injected for further oil recovery.

Injecting CO₂ into oil reservoirs to enhance oil recovery has been practiced on a commercial scale for nearly 50 years, with the first successful pilot tests conducted in the early 1960s in the state of Texas (Holm, 1987). Experience in the United States shows that CO₂-EOR can boost recovery by 5% to 15% of the original oil in place (IEA, 2013b).

Tertiary recovery is the third level of production enhancement, one option for which is CO₂-EOR (a schematic explanation of the CO₂-EOR process is shown in Figure below).



Source: Global CCS Institute (2015), website, www.globalccsinstitute.com/content/information-resources.

Fig. 77: Schematic of CO₂-EOR operation. [55]

CO₂, nitrogen and hydrocarbon gases (e.g. propane, butane) have been employed as injectants in tertiary recovery projects. In a miscible CO₂ displacement process relatively pure CO₂ (i.e. typically 95% by volume or greater) is injected into the reservoir and mixes with the oil. This has the effect of reducing the capillary forces that trap the oil in the reservoir rock and creates more favourable flow properties. Compared with injection of nitrogen and hydrocarbon gas, CO₂ achieves miscibility with oil at lower pressure and can therefore be applied in relatively shallow reservoirs.

Pressure balance is critical to CO₂-EOR, to achieve miscibility, the reservoir pressure must be maintained above the so-called minimum miscibility pressure (MMP) while the maximum reservoir pressure is limited by the reservoir fracture pressure. Pressure can be maintained in this window by balancing the injection and withdrawal of fluids from the reservoir. Should it be impossible to reach the MMP, for instance in shallow reservoirs, CO₂-EOR can still be applied, but operated as an immiscible flood in which the injected CO₂ physically pushes the oil towards the production wells (as described under secondary recovery). Operating the CO₂ flood above the MMP is preferable as the miscible process leads to more efficient oil recovery (although some miscible benefits may be achieved even where full miscibility is not achievable).

One impediment to CO₂ flooding arises from the fact that the viscosity of CO₂ under injection conditions is low compared to that of the oil; this creates a tendency for the CO₂ to channel or "finger" through to the production well

without mixing with the oil to a significant degree. As CO₂ also tends to be less dense than the reservoir, it rises towards the top (referred to as gravity override) and does not evenly contact the reservoir. These effects can be amplified or diminished by the geology of the reservoir (Green and Willhite, 1998). One approach to overcome this impediment and to achieve relatively even mixing of the CO₂ through the reservoir is known as the "water-alternating-gas" (WAG) process, which involves injecting alternating slugs of CO₂ and water produced from the reservoir. The presence of water hinders the movement of CO₂ through the rock, thereby enhancing mixing. WAG decreases the CO₂ demand per barrel of oil recovered, which is advantageous in a situation where CO₂ must be purchased and represents a cost factor.

When CO₂ reaches the production well, it is typically separated from the produced hydrocarbon so that it can be re-injected (i.e. recycled). In commercial projects, CO₂ typically "breaks through" at production wells relatively rapidly following the start of injection. This recycling is done for economic reasons, as the purchased CO₂ comes at a cost to the operator. Over the life cycle of the EOR project, the CO₂ injection and recovery cycles are repeated many times, with smaller amounts of new CO₂ added to the project in each cycle.

The role of CO₂-EOR in global oil production is currently limited: more than 140 projects globally produce around 300 000 barrels per day (bbl/d) of oil (Kuuskraa and Wallace, 2014) – i.e. only 0.35% of global daily oil consumption. Almost all operating CO₂-EOR projects are concentrated in the mid-west United States, not all that far from where the technology was first developed.

The viability of CO₂-EOR projects in the United States depends largely on three factors:

6. The existence of oil reservoirs in late stages of production with geological and petrophysical characteristics conducive to CO₂ flooding.
7. The availability of inexpensive CO₂ sources and an extensive, built-for-purpose CO₂ pipeline system to deliver this CO₂ to projects. Most CO₂ used in EOR projects today comes from naturally occurring volcanic accumulations.
8. The combination of a fiscal regime that supports EOR deployment to enhance energy security and a legal framework that facilitates development of EOR projects.

While the way in which these factors have emerged is very specific to the United States – in particular, the evolution of the CO₂ pipeline network and supply business – there is no reason that similarly supportive conditions for CO₂-EOR could not be created in other regions with suitable oil reservoirs.

5.1.1. Miscibility Mechanism using CO₂ gas

CO₂ utilization in an EOR system normally occurs at elevated temperature and pressure due to the characteristics of the individual oil reservoir in which CO₂ is injected. Oil reservoirs range in temperature and pressure with temperatures ranging from 100 degree Fahrenheit to 250 degree Fahrenheit and the pressures ranging from a few hundred psia to 5000 PSIA. Oil reservoirs generally exist at depths between 2000 feet to 15000 feet. With a pressure gradient of 100bars/km approximately, and a temperature gradient of approximately 25°C/km, it is expected that EOR will likely occur in the supercritical region of Carbon Dioxide.

Miscible oil recovery can be applied only at pressures higher than the minimum miscibility pressure (MMP), which can be estimated using a slim tube test [77] or available correlations. The minimum miscibility pressure (MMP) is defined as the pressure at which more than 80 percent of oil-in-place (OIP) is recovered at CO₂ breakthrough. Although more recently, an oil recovery of at least 90 percent at 1.2 HCPV (hydrocarbon pore volume) of CO₂ injected is often used as a rule-of thumb for estimating MMP [74]. Oil recovery increases rapidly with increasing pressure then flattens out when MMP is reached, as shown in figure below.

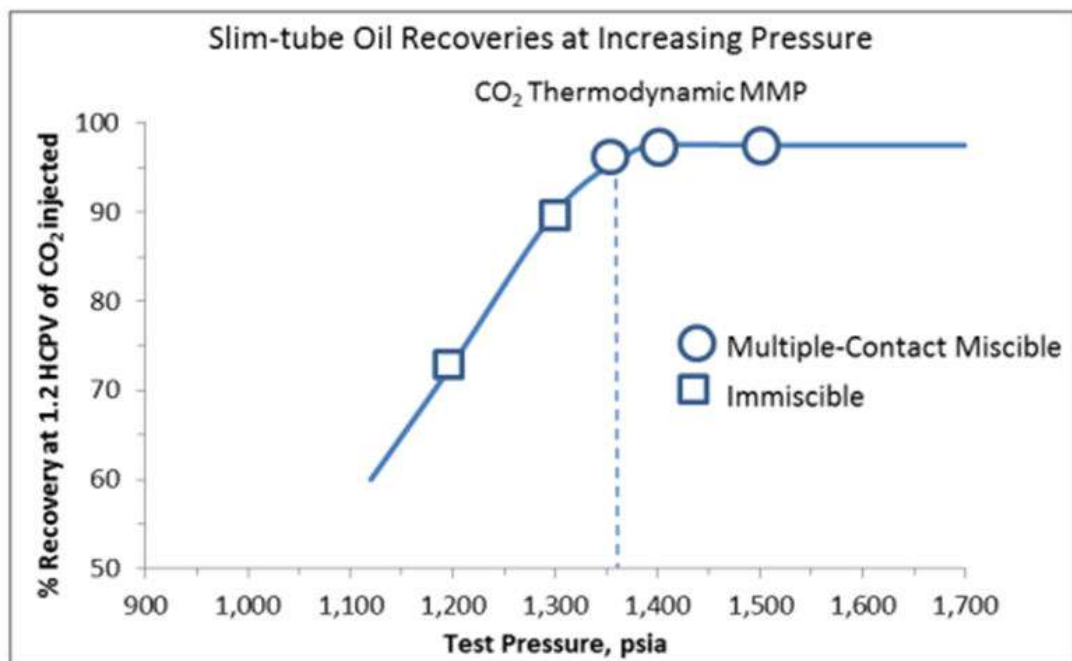


Fig. 78: Slim-tube oil recoveries at increasing pressures for fixed oil composition and temperatures [74].

Therefore, to achieve the highest oil recovery, the reservoir must be capable of withstanding pressure greater than the MMP. One of the main advantages of CO₂ compared to other types of oil enhancing gases such as produced gas, methane and nitrogen is the significantly lower MMP value. As a result, CO₂ can be used to enhance the miscible oil recovery process in a wide range of oil reservoirs. There are two basic types of miscibility mechanisms in the oil recovery process: first contact miscibility and multiple contact miscibility. First contact miscibility means that the solvent and oil become miscible when they first make contact, and the displacement of light oil using propane or LPG falls into this category. Multiple contact miscibility achieves miscibility through several different contacts, and most of the high pressure gas-enhanced oil recovery belongs to this category. CO₂ cannot achieve first contact miscibility in most oil reservoirs within a reasonable range of pressures and needs multiple contacts, in which components of the oil and CO₂ transfer back and forth until the formation of a homogeneous phase through the processes of vaporization/condensation.

5.1.2. What happens to the injected CO₂

Not all of the injected CO₂ is recovered at the production wells. To maintain pressure above the MMP, operators must carefully balance the volume of fluids produced and injected: as oil is being produced and removed from the system, roughly equal volumes of CO₂ and water must be injected (in WAG operations). A significant portion the CO₂ in the reservoir remains trapped due to capillary forces that act to immobilise its movement within pores and through dissolution in residual oil and water present in the reservoir.

With each recovery cycle, more of the injected CO₂ is progressively retained until a significant volume is securely trapped. The volume of CO₂ that can be stored in this way depends on properties of the reservoir and the oil it contains, and on operational factors of oil production, including the duration of the WAG and the water/oil ratio used, well spacing, and the relative position of injection and producing wells.

To maintain pressure and production, the CO₂ retained (stored) in the reservoir must be compensated through injection of additional CO₂ (or water). The “recovery efficiency” quantifies how many tonnes of CO₂ are injected to recover an additional barrel of oil, with low efficiencies indicating more CO₂ storage. The Weyburn-Midale EOR project in 2012 was producing about 18 000 incremental barrels per day (bbl/d) with an injection rate of 13 000 tCO₂/d. This injected CO₂ represents 6 500 t purchased and 6 500 tonnes recycled, or approximately 3 barrels per purchased tonne of CO₂ (IEA, 2014b).

At the end of the CO₂ flood, the volume of CO₂ that remains in the reservoir has been “incidentally stored” over the course of numerous CO₂ recovery and re-injection cycles. A portion of this CO₂ is trapped in the reservoir through capillary forces and would be very difficult to remove; however, much of the CO₂ exists either in the form of free phase CO₂ or is dissolved within the mobile oil and could be recovered. This leaves the operator with the choice to either produce the CO₂ so that it can be re-used elsewhere in the field or resold, or alternatively to take measures aimed at long-term CO₂ storage in the abandoned reservoir.

5.1.3. Current Projects Utilizing CCS for EOR

The first CO₂-EOR projects tested at a large scale occurred in the 1990’s in the Permian Basin of West Texas and southeast New Mexico. The first project was initiated in January 1972 in Scurry County, Texas and the second project was initiated in April 1972 in Crane and Upton Counties, Texas. These two CO₂ floods were encouraged by special tax treatments of oil income from experimental procedures and by a daily production allowable relief offered by the Texas Railroad Commission. Since then and over the following decades, a number of new projects have been implemented. Today, there are 111 floods underway in the United States; 64 of which are in the Permian Basin. A few examples of pilot projects and commercial CO₂-EOR projects either completed or in progress are listed below [75].

- Permian Basin (Texas, USA): It is the largest CO₂-EOR site by measure of oil production, Occidental Petroleum, Denbury Natural Resources, ExxonMobil, and ConocoPhillips among others have been utilizing CO₂-EOR technology in this region since 1972. Extensive pipeline infrastructure and plenty of nearby CO₂ sources have made it a prime location for expansion. Since 1986, Permian Basin projects have more than tripled and oil production has increased to approximately 1 million barrels of oil per day or approximately 5 percent of daily U.S. oil production.
- Poplar Dome Reservoir (Montana, USA): Magellan Petroleum Corporation obtained permits to drill five wells as part of a previously announced CO₂-EOR pilot program which began in October 2013. CO₂ is being supplied by Air Liquide Industrial U.S., LP for the two year long program.
- Ghawar Oil Field (Saudi Arabia): Saudi Aramco has been examining the use of CO₂-EOR in Ghawar Oil Field, the largest oil field in Saudi Arabia based on the production levels over the past 60 years. The Hawiyah gas plant is the planned CO₂ source which will require a 70 km onshore pipeline for transportation. Specific CO₂ monitoring objectives include

developing a clear assessment of the CO₂ potential for EOR and CCS as well as the testing of new technologies for CO₂ monitoring.

- Jilin Oil Field (China): PetroChina began its Jilin CO₂-EOR pilot project in 2009, making it China's first CO₂-EOR project. By the end of 8 May 2011, approximately 167,000 tons of CO₂ was successfully stored, and total oil production due to EOR reached 119,000 tons. Phase 2 is scheduled to begin in 2015, when the CO₂ sequestration and oil production is expected to quintuple.

5.1.4. Carbon Capture and Storage & Enhanced Oil Recovery (CCS & EOR)

CO₂ EOR has been used by the oil and gas industry for over 40 years, but only recently has its potential as a carbon sequestration method been realized and investigated.

CO₂ EOR is a promising method of sequestration for a number of reasons. First, the geologic structures that originally contained the oil and natural gas should also permanently contain the injected CO₂, provided the integrity of the structures is maintained. From seismic studies, the geologic structure and physical properties of many oil and gas fields are well understood. This, combined with the vast amount of industry experience with gas-injection EOR, provides a knowledge base from which to start researching the sequestration implications of CO₂ EOR. Another benefit of CO₂ EOR for sequestration purposes is the widespread distribution of depleted and operating oil and gas fields, making it likely that an oil field is near a CO₂ source. Finally, carbon sequestration from CO₂ EOR projects can create offsets resulting in trades in the emerging greenhouse gas market.

5.1.5. Weyburn-Midale: The front-runner in combining CO₂-EOR and CO₂ Storage

The Weyburn and Midale oil fields, located in southeast Saskatchewan, Canada, were brought into primary production in 1954. As is common, oil was initially produced from the reservoir without injection of other fluids; however, over time, production has been maintained in both fields through the use of water flooding coupled with the drilling of additional (infill) wells to reach parts of the reservoir that had not been previously accessed. In October 2000, Cenovus (formerly PanCanadian or EnCana) began injecting CO₂ into the Weyburn field in order to boost oil production. There are now over 100 injection wells. Apache followed suit in 2005, injecting CO₂ into the Midale field. The Weyburn and Midale fields combined are expected to produce at least 220 million barrels of incremental oil through miscible or near-miscible displacement with CO₂. EOR will extend the life of the fields by approximately two to three decades.

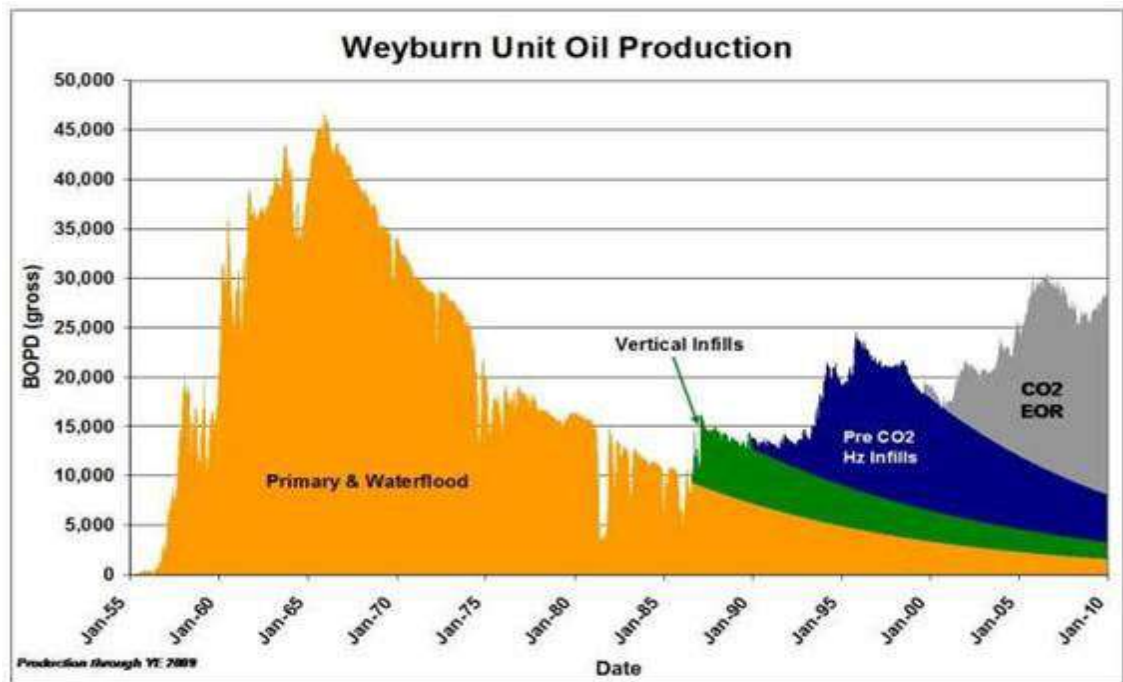


Fig. 79: Weyburn oil production processes [55].

What makes the Weyburn-Midale project unique among CO₂-based EOR operations is the comprehensive monitoring and verification pilot program undertaken between 2000 and 2012. Overall, it is anticipated that around 40 MtCO₂ will be permanently sequestered over the project's lifespan – 30 Mt at Weyburn and 10 Mt at Midale.

The key finding from this project relates to the successful coupling of EOR operations and CO₂ storage. Experience of the 12 years of operation clearly demonstrates that the two approaches can be complementary, that accurate CO₂ accounting is possible and that permanent storage of CO₂ can be achieved.

5.1.6. Examples of large-scale CO₂ capture projects linked with EOR

A number of new CO₂ capture projects in early operation or in construction are linked to conventional CO₂-EOR as practiced today. These projects will improve experience in large-scale capture of CO₂ from various sources, and EOR will provide necessary partial economic drivers and business models for the projects.

The Boundary Dam Unit 3, inaugurated by SaskPower in October 2014 (Saskatchewan, Canada), is the world's first large-scale power unit equipped with post-combustion CO₂ capture. This rebuild of an aging generator operates on continuous mode (producing 110 MW of power to the grid) and captures 95% of the CO₂ emissions (and 100% of the SO₂) of the lignite-fired power unit (reducing direct CO₂ emissions by 1 million tonnes per year (Mt/yr)). The

captured CO₂ is transported to nearby oil fields for EOR and a proportion is also stored in the associated Aquistore Project.

In the first half of 2016, the Kemper Project gasifier and capture unit, owned and operated by Mississippi Power (a subsidiary of Southern Company), is scheduled to come online in Mississippi, United States. This large-scale (582 MW) integrated gasification combined cycle (IGCC) plant will incorporate CCS technologies with the aim of significantly reducing the high emissions normally associated with transforming lignite coal into natural gas. The company intends to capture 65% of the plant's CO₂ emissions and hence deliver 3 MtCO₂ per year for EOR use in nearby fields.

Construction recently began on the NRG Petra Nova project in Texas (United States), a joint capture project by NRG Energy and JX Nippon Oil and Gas Exploration (with transport and storage held by Texas Coastal Ventures, a joint venture between Petra Nova Parish Holdings and Hilcorp Energy Company). This combined coal- (247 MW) and gas-fired (127 MW) plant is being retrofitted with post-combustion technology to capture 90% of emissions (1.4 Mt/yr), which would be fed into the West Ranch oil field (operational since 1938). Over the 20-year project span, the site may develop as many as 130 injection wells and 130 production wells.

Petrobras, BG Brazil and Petrogal Brasil are partners in the Lula oil field CO₂-EOR project located in the Santos Basin, some 300 kilometres off the coast of Rio de Janeiro, Brazil. The Lula project separates 0.7MtCO₂ per annum from natural gas production and injects the CO₂ for EOR in a pre-salt carbonate reservoir, some 5000- 7000 metres below the sea level. The Lula project, in operation since 2013, is a pioneer in ultra-deep water CO₂-EOR, operating currently the deepest CO₂ injection well in the world.

In Saudi Arabia, Saudi Aramco is implementing the Uthmaniyah CO₂-EOR project. In this project, CO₂ is captured from the existing Hawiyah natural gas processing plant and some 800 000 tCO₂/yr will be injected in the Uthmaniyah production unit (part of the super-giant Ghawar oil field) for EOR. The project will pilot new technologies in order to monitor and verify the behaviour of CO₂ underground.

Operation of existing projects demonstrates that, to date, climate change mitigation and long-term CO₂ storage goals do not figure within the rationale for EOR projects in the United States (Dooley et al., 2010). This is not a surprise given the lack of a focus on climate mitigation during the development of the industry. Two main impediments appear to be standing in the way of using CO₂-EOR as a mitigation option:

- There are few incentives, commercial or otherwise, that would lead the operator of a CO₂-EOR project to focus on CO₂ storage. Hence, most projects do not undertake dedicated activities to demonstrate that CO₂ remains contained in the reservoir. Such monitoring activities are generally agreed to be a critical component of geologic CO₂ storage (e.g. see IPCC, 2006); thus, CO₂ injected in EOR projects cannot be considered “as not being emitted” in the framework of climate policy.
- The laws and regulations that apply to CO₂-EOR operations have evolved to address the issues associated with oil and gas operations, not CO₂ storage. In the United States, for example, property law places limits use of the subsurface that, while allowing for efficient oil recovery, present barriers to CO₂-storage (Marston, 2013). Without changes to the laws and regulations that apply to CO₂-EOR, it may not be possible to reconcile the practice of CO₂-storage with that of CO₂-EOR.

Despite increasing interest worldwide in the potential for CCS as a climate change mitigation technology and the potential role CO₂-EOR could play in its deployment, few, if any, of the more recently identified opportunities have been developed outside the United States. In analysis carried out in the early 2000s, the International Energy Agency Implementing Agreement on Greenhouse Gas Research and Development Programme (IEAGHG) identified 488 CO₂-EOR candidate projects as “early opportunities” for CCS (Lysen, 2002).

5.2. Modeling of the CCS-EOR System

Because of the large physical dimensions and long time period of CCS in industrial scale projects, it is not feasible to analyze them using experimentation for each oil field of interest. Therefore, in order to simulate the effects of CO₂ injection in a large reservoir over a long period of time, Computational Fluid Dynamic (CFD) simulations provide the only feasible alternative. In recent history, CFD has been successfully employed in a variety of engineering applications such as aerodynamics and reservoir simulations. In this study a commercial simulator was deployed, the software is capable of simulating comprehensive 3-dimensional, 3-phase, 4-component fluid flows in reservoirs. Simulation of CO₂ sequestration in aquifers can also be modeled.

5.2.1. Parameters affecting the Modeling of the CO₂-EOR system

The Enhanced Oil Recovery mechanism by injecting CO₂ has many advantage, in addition of increasing the ultimate oil recovery factor, it helps to reduce the greenhouse gases effect, during the EOR process or Post-EOR process.

The following sections describe briefly the methodology employed in the simulation study and optimization deployed in determining the EOR performance of injecting CO₂ in hydrocarbon reservoir in order to improve the oil recovery factor and storing the injected CO₂ in the reservoir for long term storage.

An understanding of the thermodynamic and chemical properties of CO₂ is imperative for the proper analysis and implementation of CO₂ assisted EOR methods.

5.2.2. Physical Considerations in Modeling of the EOR Systems

In EOR systems, there are three main components found in the reservoir: oil, methane gas, and brine water. Prior to primary recovery, the predominant reservoir fluid is oil. After primary and secondary recovery, which both reduce the amount of oil in the reservoir and increase the level of water, there are varying levels of water, oil, and gas depending on the reservoir properties and the extent to which primary and secondary oil recovery procedures were performed and successful. Within the reservoir, there are complex interactions between the injected CO₂ and oil as well as interactions between the reservoir fluids and surrounding rocks. Therefore, multi-component, multi-phase flow modeling and simulations are necessary for understanding these interactions. Reservoir dimensions in EOR projects can range from a few acres to a few thousand acres in area, and the depths can be thousands of feet. However, despite the potential vastness of these reservoirs, CO₂ interactions with the in situ oil, methane, water, and rock formation occur at a microscopic level. The life-cycle for EOR projects can generally extend as long as five decades, and the four CO₂ trapping mechanisms can continue for thousands of years. However, the interactions between the aforementioned variables occur on the scales of a few nano-meters and nanoseconds. It is not feasible to represent all the spatial and temporal scales in a tractable physical model; therefore, the use of a simplified physical model that can accurately analyze the behavior of multi-component multi-phase flow from micro- to macro-scale in both space and time is essential. The physical model requires of additional simplifying assumptions to allow for a numerical solution without intensive computations and costs while still providing meaningful results of acceptable accuracy. For the EOR simulations, the pertinent processes modeled include the migration of CO₂ through the reservoir and the resulting migration of oil, gas, and/or water out of the reservoir depending upon the injection rate and pressure of CO₂ as well as the fracture pressure of the formation.

5.2.3. Applying CO₂ injection as EOR process in SFSW field

The main goal of this study is to identify and quantify the potential of this reservoir to retain CO₂ during the EOR process, as stated previously that 60% of the injected CO₂ will be retained in the reservoir before the breakthrough.

CO₂-EOR has two major advantages:

- Additional hydrocarbon recovery that promotes energy independence.
- CO₂ storage to reduce atmospheric emissions of CO₂

As explained previously injection CO₂ for miscibility purposes is more efficient than injecting other gases such as produced gas, from this study two simulation cases were ran to check the performance of injection CO₂ and produced gas in SFSW

The model presented early in this section will be used in this study (Fig. 56, 57), the cases are:

- CO₂-Gas-EOR-Inj: in this case, we inject 100% of CO₂ (CO₂ is the injection stream),
- Produced-Gas-EOR: in this case, we inject the produced gas (Produced gas is the injection stream)

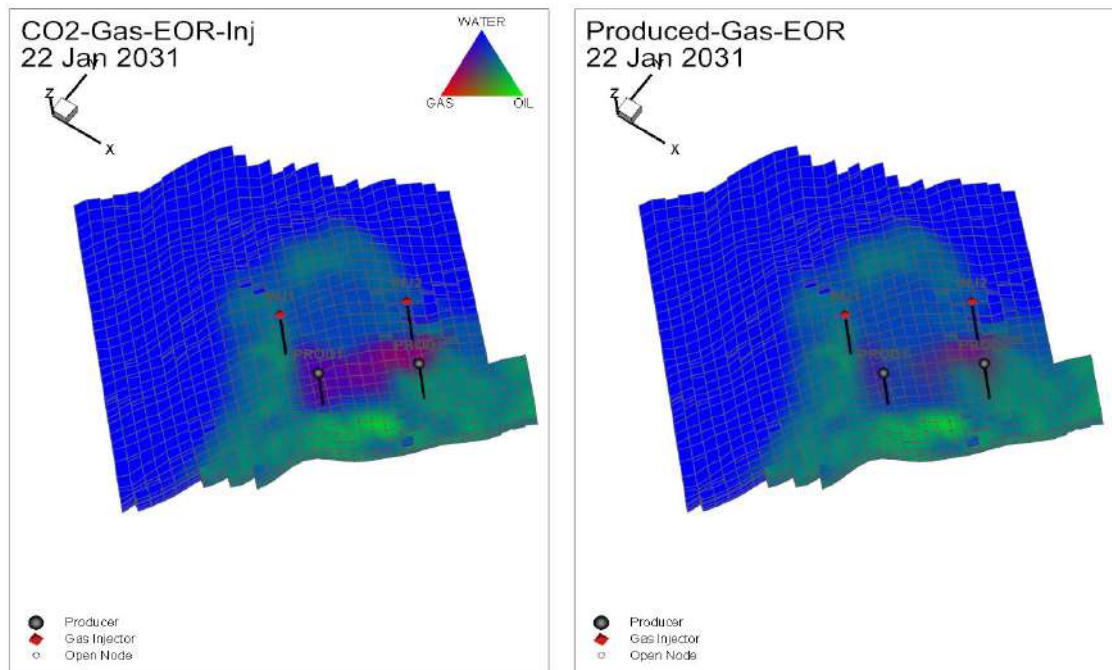


Fig. 80: Produced gas and CO₂ injection Performance.

The CO₂-EOR has proven to be an economically viable option for EOR, as can be seen by the number of currently active CO₂-EOR projects [74]. Therefore, it is expected that its scope will be further widened for its application to many more oil fields around the world.

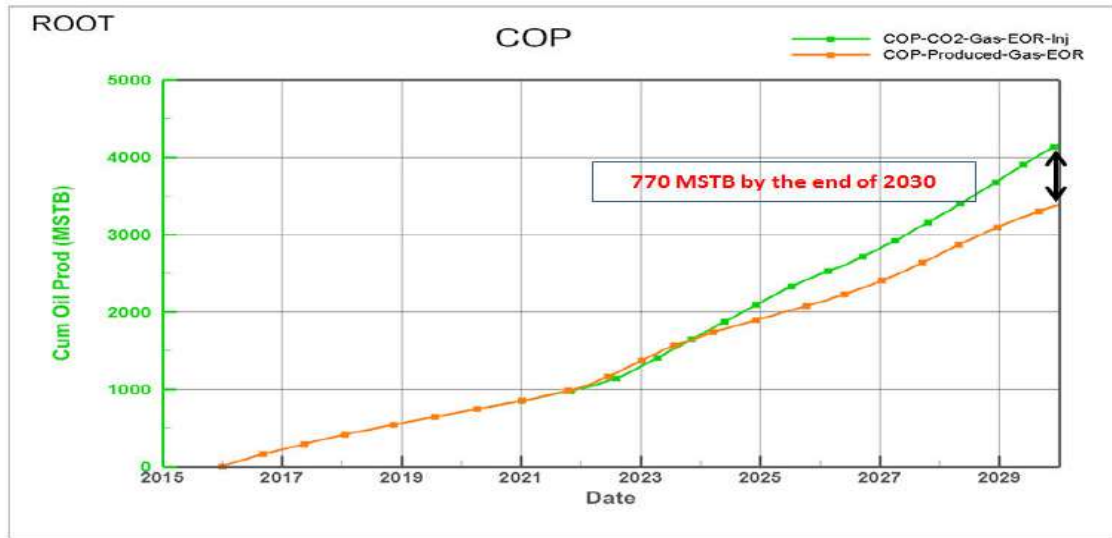
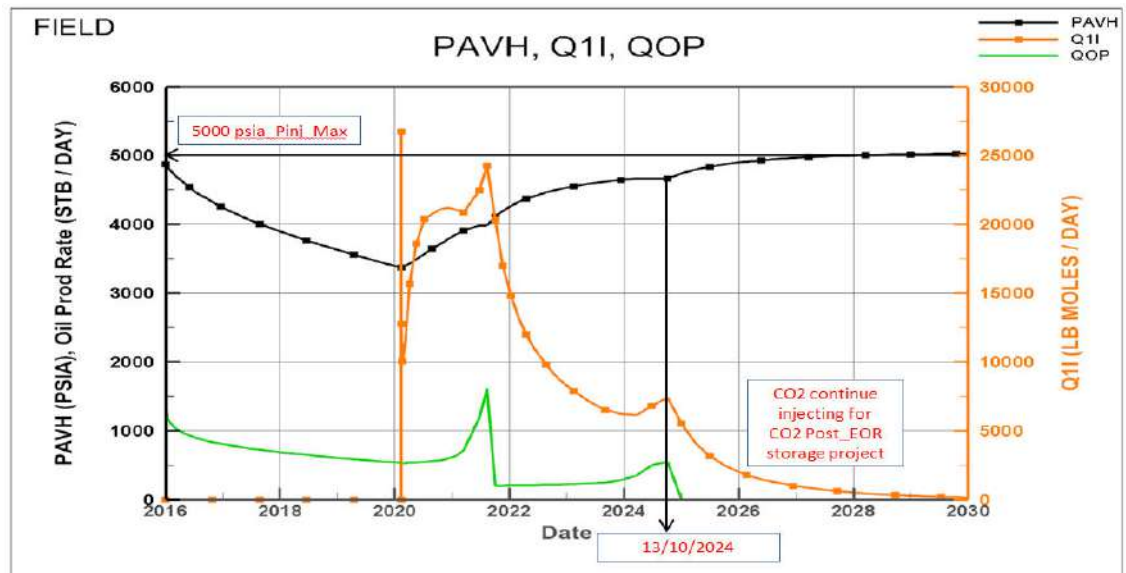


Fig. 81: The Performance of the CO₂ compared to produced gas



CO₂-EOR-Storage

13 Jan 2017

Fig. 82: Impact of the CO₂ injection as EOR process in the performance of the field

Most of the CO₂ used for EOR technique has come from naturally occurring reservoirs, but new technologies are being developed to extract CO₂ from industrial applications, most notably power plants. The primary driver for these new extraction technologies is not EOR, but carbon sequestration. Still, the resulting large supply of CO₂ could be vastly beneficial for EOR. Carbon dioxide (CO₂) enhanced oil recovery is carried out by injecting large quantities of CO₂ into the reservoir. The injected CO₂ extracts light-to-intermediate components of the crude oil provided the minimum miscibility pressure (MMP) is attained, and thus develops miscibility with the crude oil to displace

it from the reservoir. Immiscible displacements are less effective compared to miscible flooding. The injection pressure and solubility of CO₂ in water are largely affected the performance of the CO₂ storage during the EOR and even Post-EOR.

5.2.4. CO₂ EOR and Sequestration

Beyond its potential to augment oil production, CO₂ EOR is getting intensive scrutiny by industry, government, and environmental organizations for its potential for permanently storing CO₂. The thinking goes that CO₂ EOR can add value by maximizing oil recovery while at the same time offering a bridge to a reduced carbon emissions future. CO₂ EOR effectively reduces the cost of sequestering CO₂ by earning revenues for the CO₂ emitter from sales of CO₂ to oil producers. Although about 20 percent of CO₂ used in EOR comes from natural gas processing plants, the majority used for EOR comes from natural underground sources and does not represent a net reduction in CO₂ emissions. However, industrial carbon capture and storage (CCS) offers the potential to significantly alter this situation.

All of the injected CO₂ is retained within the subsurface formation after a project has ended or recycled to subsequent projects. After years of experience with CO₂ floods, oil and gas operators are confident that the CO₂ left in the ground when oil production ends and wells are shut in will stay permanently stored there, assuming the wells are properly plugged and abandoned.

One major oil industry operation that provides an example of such permanence is StatoilHydro's Sleipner CO₂ project in the North Sea off Norway. The company is developing a large gas field and must strip out CO₂ from the produced gas stream that is about 9 percent CO₂ by volume. Norway's imposition of a tax on emitted carbon of \$200 per metric ton—later reduced to \$140 per metric ton—led StatoilHydro to compress the captured CO₂ and inject it into a deep saltwater formation below the seabed. The project, initiated in 1996, required an \$80 million investment but has resulted in a tax savings of \$55 million per year. Regular monitoring of the subsurface shows that the formation is retaining the injected CO₂

In the current example, to quantify the potential of SFSW reservoir to retain CO₂ during the EOR process, a simulation case has been run supposing that the CO₂ will be injected for 5 years as EOR process (2020 to 2025), during this period the reservoir could retain more than 8.5 BSCF.

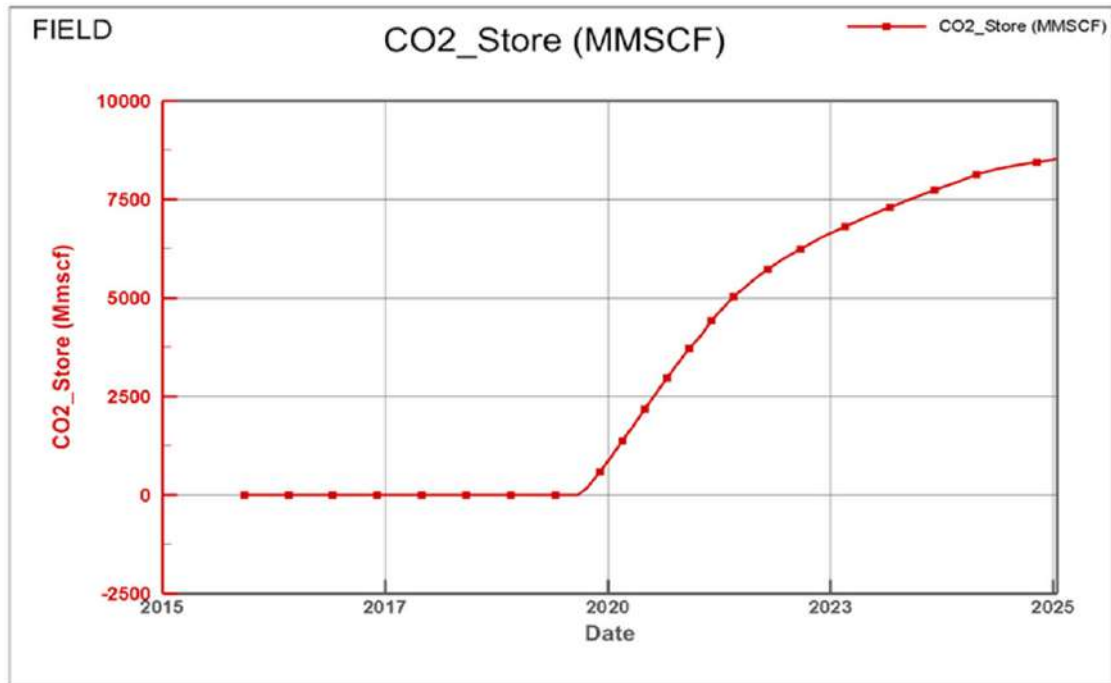


Fig. 83: Cumulative CO₂ stored during EOR process.

- **CO₂-EOR Sequestration Potential**

The previous example applied in SFSW field answered well the question saying “What is the potential for sequestration of CO₂ from EOR operations?”

In USA, the total volume of CO₂ consumed by CO₂ EOR process in March 2010 was about 11 trillion cubic feet (560 million metric tons). That pales in comparison with total U.S. CO₂ emissions from industrial sources alone of about 100 trillion cubic feet (5,090 million metric tons) per year. However, that does not mean that the potential demand for CO₂ for EOR will be insignificant, EOR could be an enabling catalyst for larger scale sequestration efforts. For example, a study by Montana Tech University found that CO₂ flooding of Montana’s Elm Coulee and Cedar Creek oil fields could result in the recovery of 666 million barrels of incremental oil and the storage of 2.1 trillion cubic feet (109 million metric tons) of CO₂.

All of the CO₂ required for the mechanism could be supplied by a nearby, coal-fired power plant, and would equate to 7 years of the plant’s CO₂ emissions. Furthermore, installation of a pipeline and CO₂ capture equipment for the project could provide the basic infrastructure for subsequent storage of CO₂ in other oil fields and in saline formations and unmineable coal seams elsewhere in the state.

6. CO₂ Risk Assessment and Monitoring

Introduction

The realization of a CCS project should be accompanied by a risk assessment study, as the injection and storage of CO₂ can be a cause of certain hazards related to CO₂ leakage at the surface, and contamination of drinking water, due to this reason, for every CCS project many means are implemented and strong monitoring systems are installed during and after CO₂ injection.

The purpose of the Risk Assessment is to identify the different risk scenarios and then to characterize or measure them (in probability and gravity in particular), in the most objective way possible.

In-salah project in Algeria is the first onshore CO₂ geological sequestration project in the world, Sonatrach and its foreign partners implemented a risk assessment and monitoring programs at high level in order to secure this project and avoid getting any risk which can be a danger to the environment instead of solving the problem of the greenhouse effect.

6.1. Learned lessons from In-Salah Project in Algeria

The In Salah project concerns a series of gas fields located in central South Algeria and containing ~1-10 % of CO₂. To export the natural gas, it is necessary for operators to reduce the CO₂ concentration to the sales gas export concentration threshold (0.3%). It was decided in the In Salah project to re-inject the captured CO₂ into the Krechba reservoir aquifer to study the CCS concept at an industrial scale avoiding in the same time the emission of ~17 million tonnes of CO₂ (Fig. 95). Gas is now produced with five wells and the CO₂ is injected in the northern part of the structure through three horizontal wells (Fig. 96). CO₂ is injected up to 1900 m depth in a 20-m thick Carboniferous sandstone of ~10 mD permeability and ~15 % porosity.

At reservoir conditions (90°C and 175 bar at 1800 m depth), CO₂ is supercritical. The first results relative to the initial plume development after an injection of 2.5 million tons of CO₂ (at end of 2008) suggest a NW migration (Ringrose et al., 2009). These results agree with satellite InSAR data interpretation (ground surface deformation - Vasco et al. 2008) and the CO₂ breakthrough at an old appraisal well (Kb-5) located 1.3 km from the Kb-502 injector. Tracer analysis confirms the Kb-502 origin of the CO₂. Surface deformation measurements (up to 20 mm near Kb-502) are coherent with both injection of CO₂ and gas production. They may reflect on first approximation the reservoir permeability distribution. The breakthrough at Kb-5 occurred between two well-head inspections (August 2006 and June 2007). At least, the

CO₂ migration trend is fully consistent with major faults and fracture network orientations.

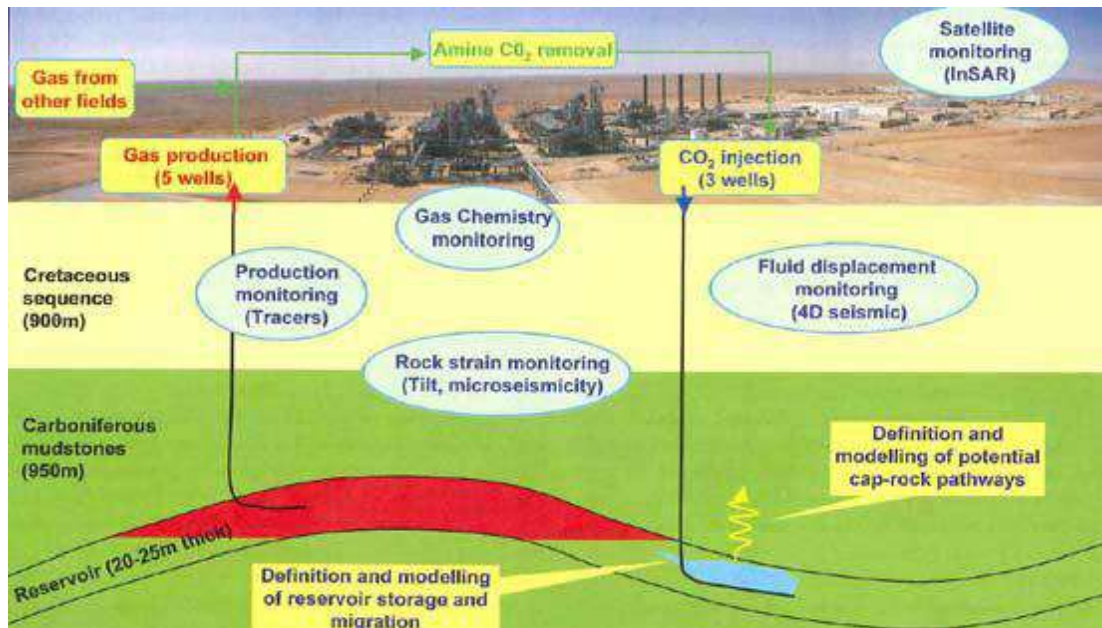


Fig. 84: Krechba field (Ringrose et al. 2009).

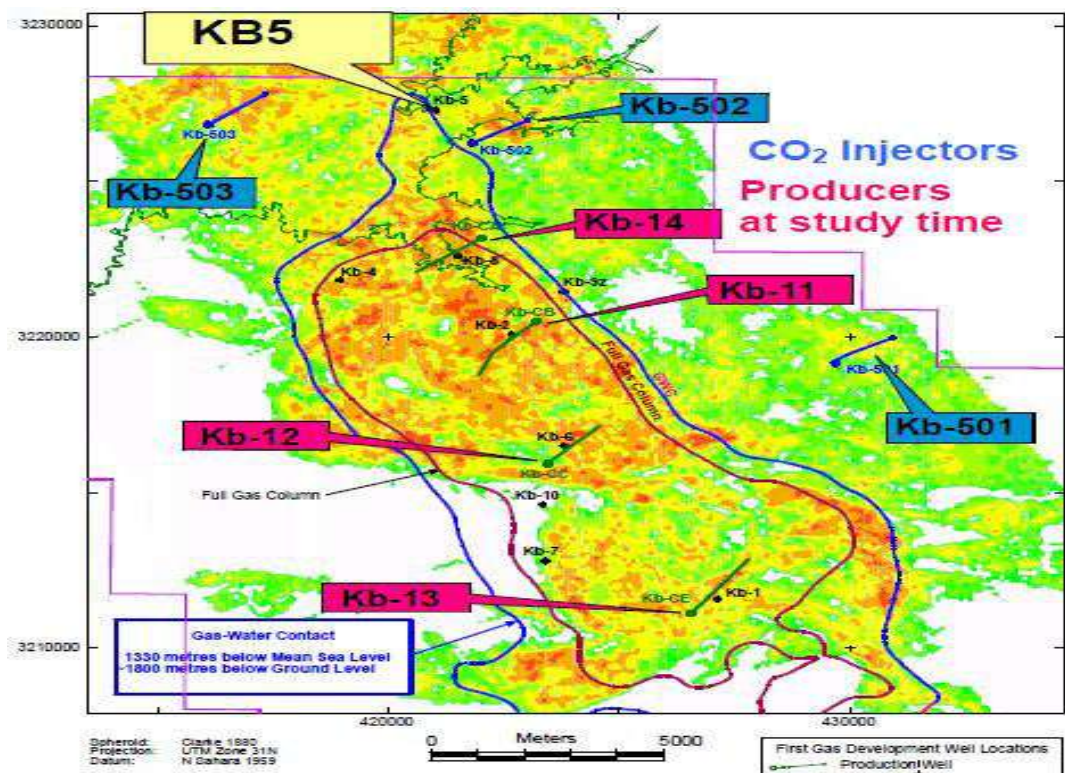


Fig. 85: Location of production and injection wells (at time of the study) [14]

As mentioned previously the properties reservoir description is the key task before starting any CCS projects, the permeability distribution and fracture network (preferential pathways) should be well defined to be able to predict the migration of the CO₂ plume across the reservoir, the breakthrough of the

CO₂ into KB-5 was expected, and the several monitoring technologies applied for this first experience project in Algeria were useful for any future similar projects.

The In Salah CO₂ Storage project has been a highly informative demonstration project and the data gathered has been extensively studied and reported in the scientific literature. However, some important general lessons learned can be drawn from this project, as follows:

- Monitoring should be part of the Field Development Plan (FDP) and routine field operations.
- The suite of monitoring technologies to be deployed at any CO₂ storage site mainly comprises standard oilfield techniques and practices, with surface monitoring methods derived from standard geotechnical and environmental monitoring practices.
- Satellite InSAR data has been especially valuable in understanding the geomechanical response to CO₂ injection, but needs to be integrated with high quality reservoir and overburden data and models.
- The storage monitoring programme needs to be designed to address site-specific leakage risks identified in the selection phase, but also needs to be adapted during the operational phase.
- Legacy wellbore integrity is a key leakage risk that has to be effectively managed.
- Acquisition, modelling and integration of a full suite of baseline data, including the overburden, are vital for evaluating long term storage integrity.
- CO₂ plume development is far from homogeneous and requires high resolution data for reservoir characterization and modelling
- Injection strategies, rates and pressures need to be linked to detailed geomechanical models of the reservoir and the overburden. Early acquisition of geomechanical data in the reservoir and overburden, including extended leak-off tests, is advisable.
- Regular Risk Assessments should be conducted to inform the on-going operational and monitoring strategies.

Probably the most valuable legacy of the In Salah project will be the pioneering deployment and interpretation of a unique set of MMV technologies. These technologies and the corresponding lessons learned are summarized in Table below, further work on these methods continues at the In Salah project and at the small but growing set of worldwide CO₂ storage projects.

Table 23: Summary of MMV technology applied and lessons learned. [85]

MMV Technology	As implemented at In Salah	Lessons learned for implementation elsewhere
3D seismic baseline survey	Acquired in 1997, Essential to the CO ₂ storage design and well placement plan.	Improved quality 3D seismic baseline survey with imaging of overburden in desirable.
4D seismic monitoring	First land time-lapse survey for CO ₂ monitoring acquired in 2009 (5years after injection start).	Time-lapse response with improved acquisition plan (but this is expensive).
Micro-seismic monitoring	Only one pilot well with a vertical array of geophones over one injector has been deployed.	Micro-seismic data has been very useful for monitoring geomechanical response to injection. Consider deploying a full array with relatively cheap shallow wells.
Satellite InSAR monitoring	Both C-Band and X-Band InSAR data acquired routinely during injection period (from 2007 and onwards)	Extremely valuable and cost effective monitoring data for onshore CO ₂ injection sites (e.g. Digital GPS) and careful processing of atmospheric and surface artefacts.
Tracers in CO ₂ injection wells	PerFlouroCabon gas soluble tracers (PMCH, PDMCH, n-PPCH) used in each injection well.	Valuable and cost effective method for checking the origin of CO ₂ observations at wells and in the storage complex.
Core analysis (storage unit)	Routine core plugs and SCAL data collected for reservoir interval.	Good petrophysical data is essential. Rock mechanical properties are especially critical.
Core analysis (caprock unit)	Some caprock samples were acquired close to the injection interval.	Core sampling throughout most of the caprock interval is desirable for long-term storage integrity assessment.
Well log data	Routine petrophysical logs throughout, Image logs and array sonic on selected wells, LWD in horizontal wells section.	An advanced array of well logging tools is highly valuable, resistivity image logs and array sonic especially useful for storage integrity issues.
Soil and surface gas sampling	Surface gas (open oath laser system), soil gas probes (flux and penetrative tubes), parasol and passive gas (charcoal) devices deployed in several campaigns. Natural low-level CO ₂ variation observed.	Need for more reference data on natural CO ₂ variation in different environment and associated seasonal fluctuations.
Groundwater monitoring wells	Five groundwater monitoring wells drilled to ~350m depth, pump tests and down-hole geochemical sampling, low CO ₂ concentrations observed (compatible with limited soil-zone productivity).	Establishing local and regional hydraulic gradients and natural variations in water chemistry is essential for establishing a useful baseline for groundwater hydrology.

7. Pilot CO₂ Geological Storage Project in Hydrocarbon Reservoir

Introduction

In the field of the geological storage of carbon dioxide (CO₂), a 'pilot' project is one that has a research objective, typically over a few years. Although CO₂ Geological Storage (CGS) is well advanced from a technological point of view, research based on real field sites is now strongly needed in order to maximize the efficiency of these technologies, to optimize the tools needed for monitoring and verification, and to be able to adapt to the specificity of local geological conditions. Pilot projects can thus benefit investment decisions for deployment of CO₂ Capture and Storage (CCS) in the foreseeable future.

7.1. CO₂ Flood/Injection Designs

Injection of CO₂ can be carried out in particularly, but not exclusively, in mature or depleted oil and gas fields. Mature oil fields are those where hydrocarbon production is in its final stages, while depleted fields are those where only residual oil (trapped in the pores of the reservoir rock) remains. This operation can increase production of hydrocarbons from these fields, resulting in economic benefits. Furthermore, these projects take advantage of the geological data acquired in their exploration and development.

In this section an optimum simulation case based on the previous analysis and results will be carry out to quantify the storage capacity and evaluating the risk of this project in term of eventual leakage through the caprock or the downhole of old wells in the vicinity of the CO₂ injection wells.

The reservoir model used in this study is always same reservoir model that have been presented previously, with some exceptions, by including the results of the previous works (precaution and recommendations), after screening the oil reservoirs for the CO₂-EOR candidates comes the task of developing a design for optimal recovery efficiency of the flooding process.

Depending on the reservoir geology, fluid and rock properties, and well-pattern configuration, the CO₂-EOR flood may use one of several recovery methods as described below [87].

The below are the SFSW CO₂ EOR-Storage designs

7.1.1. Continuous CO₂ injection

This process requires continuous injection of a predetermined volume of CO₂ with no other fluid. Sometimes a lighter gas, such as nitrogen, follows CO₂ injection to maximize gravity segregation. This approach is implemented after primary recovery and is generally suitable for gravity drainage of reservoirs with medium to light oil as well as reservoirs that are strongly water-wet or are sensitive to Waterflooding.

7.1.2. Wells configuration

Also, injection pattern improves sweep efficiency, and one of the widely used patterns is a normal five-spot (four injection wells at the corners and a production well at the centre) or an inverted five-spot (four production wells at the corners with an injection well at the centre), and in some cases, seven- or nine-spot patterns. The well pattern could even be a line drive, where the injection wells are located in a straight line parallel to the production wells, if the permeability distribution and other geologic features favour it. The selection of pattern is based on reservoir and fluid properties as well as on reservoir response to fluid injection, which is evaluated through analysis of reservoir performance manually but often using reservoir simulation as a tool as the case of the current study.

The different scenarios checked for better wells configuration were based on the oil recovery factor and the storage capacity and reservoir sealing properties, in our study 03 CO₂ injection wells were implemented, 2 injection wells in the oil leg (oil reservoir), and the third one is implemented in the water leg of the reservoir (adjacent aquifer) as shown below.

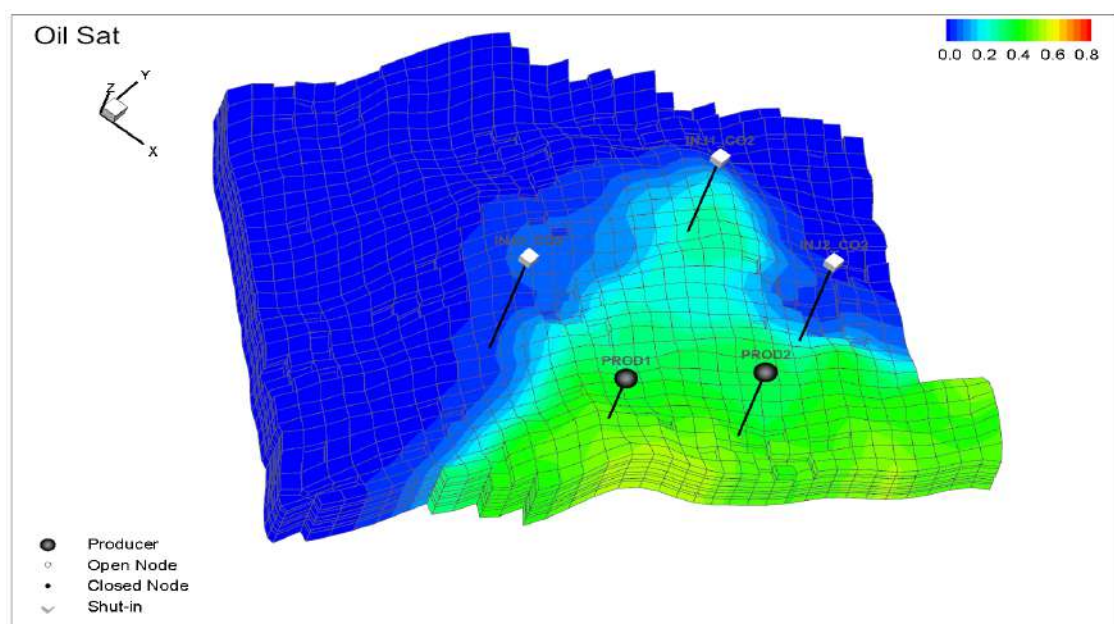


Fig. 86: 3-D geological model of the Pilot CO₂ storage project

7.1.3. Reservoir properties modeling

- Permeability

The permeability is a key parameter of the reservoir properties that can be used in the simulation work, implementing a good permeability model in the reservoir model can help to predict the flowing behaviour of the CO₂ across the reservoir (CO₂ plume migration), as showed in (chapter 6) the combined method between the hydraulic flow unit and the artificial intelligence method (ANFIS) provided a good permeability model with enough confident.

The permeability distribution of the reservoir used in our simulation case is mapped as below.

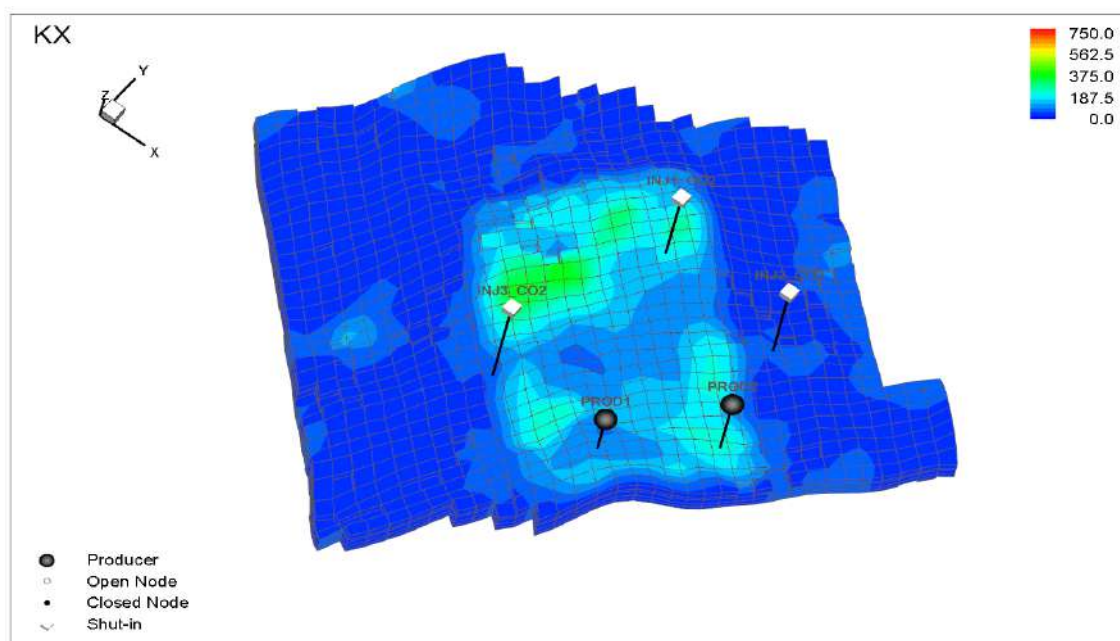


Fig. 87: Permeability Distribution across the reservoir

The permeability expressing the flow potential of the reservoir, from the above permeability map distribution, it is clear that the potential flow of the CO₂ will be through the high permeability paths (dark green zones).

- Flow Zone Indicator (FZI)

As explained previously, the flow zone indicator incorporates the static (geological) and the dynamic (flow) attributes of the reservoir, this feature to the FZI can be used in statistical techniques to classify the reservoir to flow units that can help to investigate the better horizons (layers) to be perforated in the reservoir as hydraulic flow unit technique.

The flow zone indicator is considered as perforation indicator, using IP (Interactive Petrophysics) as visualization tool to visualize the reservoir properties, in order to select the best layers to be perforated a several simulation scenarios have been ran with different perforation intervals, this process helped to select the best FZI interval based on the breakthrough time and gas injection rates.

The blow plots show the best layers perforated in our study case

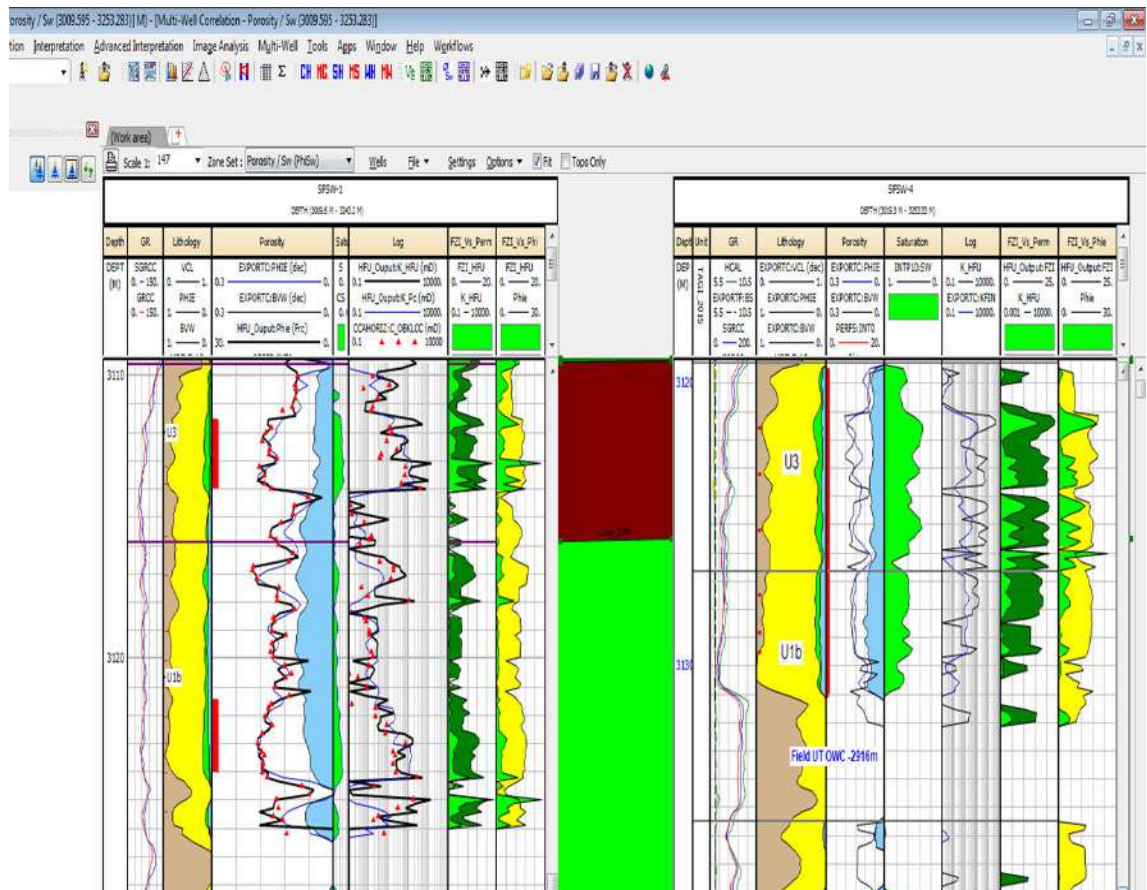


Fig. 88: Perforation layers based on FZI values

7.1.4. Surface Constraints

- Pressure limitation

The reservoir pressure is varying as function of the injection pressure, the successful of the CO₂ storage project is based on the mastering of the pressure across the reservoir, this value should be less than the minimum required value to overcome the capillary pressure, setting the initial reservoir pressure as maximum allowable pressure is not correct as the interfacial tension of the CO₂/brine is much lower than the IFT original hydrocarbon in place/brine.

The maximum injection pressure should determine and set in the begging of the CO₂ injection to avoid getting leaks through the weak point in the reservoir.

- **Surface Facilities handling capacity of produced gas**

The produced CO₂ is other constraint that should take into consideration since the beginning of the project, as this gas is very corrosive gas, high concentration of this gas in the surface pipelines and equipment may make serious problems, to avoid this issue a limitation of 35 Mmscfd has been fixed in the simulation model.

7.1.5. Simulation Running Time

Assumed that the field start producing in 01/01/2016, for four (04) years of natural depletion production through two (02) oil producer wells (PROD1 and PROD2), as these wells are close each other both have similar reservoir properties, the target intervals are shown in previous figure.

In 01/01/2020 after noticing the high performance decline of the reservoir an EOR project by using CO₂ as injection gas is implemented for enhancement of the oil recovery and mainly to evaluate the storage potential of the CO₂ during and after the EOR process.

For better evaluation of the reservoir potential of the CO₂ storage, 20 years of continuous CO₂ injection are divided into two periods

- CO₂-EOR process for 10 years (from 2020 until 2030).
- CO₂ Storage process for 10 years (from 2030 to 2040).

After this dynamic period, a static period by shut in every think (production and injection) should be investigated, for this purpose we kept the simulation running for 60 years in static status (from 2040 to 2100), in this period we will be able to investigate security of the project by ensuring that the dissolution of the CO₂ in the fluid in place is happening.

In overall the simulation running time is start from 2016 to 2100 divided in different periods as stated above each period has purpose to be checked.

7.2. Trapping mechanisms and constraints applied in Pilot Project

As stated early that the main aim of this pilot project is to evaluate the potential of SFSW reservoir in term of storage capacity and sealing capabilities. All the precautions and recommendations provided in the previous works are included in this pilot project.

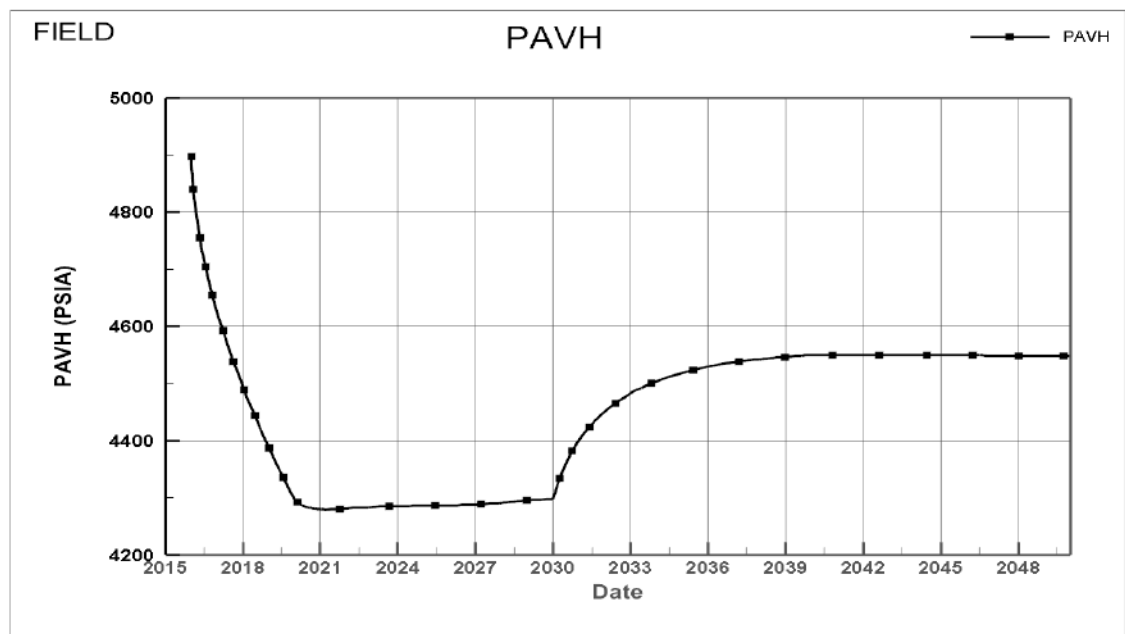
As the security of the project is highly important should well investigated before the beginning of the project by using the simulation (the aim of this project) and even during the project execution by implementing well monitoring and risk assessment programs (previous chapter).

The results of the project are investigated in the following order

7.2.1. The reservoir pressure constraint

The pressurization of the reservoir without respecting a limited defined before the beginning of the project is strictly unacceptable, that can potential escaping pathway of the CO₂ to return to the surface by following the more high flow potential pathways or old bad downhole completed wells, or even overcoming the capillary pressure of the caprock.

The reservoir pressure of our study case were below enough to the initial reservoir pressure, even the IFT of the new fluid in place/brine reduces the capillary pressure, we thought that the project is away from getting leak through the caprock.



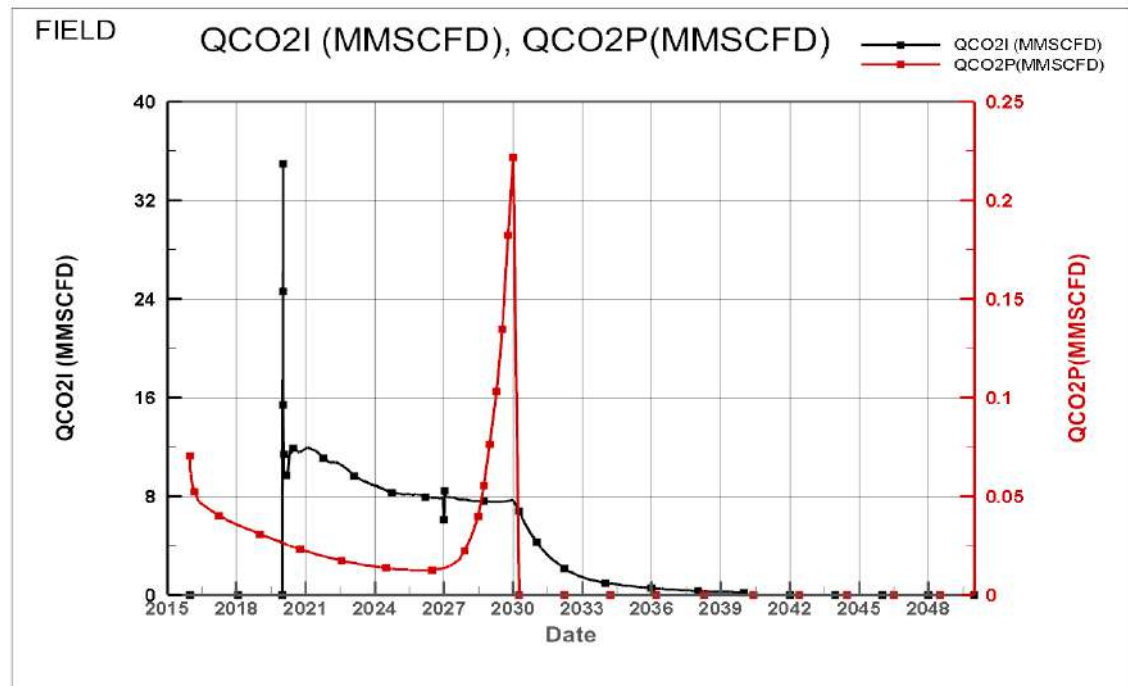
CO2-EOR-StoragePilot-Project-FZI-impact-Inj-Aquife

16 Jan 2017

Fig. 89: The Reservoir Pressure Response.

7.2.2. The produced gas (CO₂) constraint

The maximum allowable CO₂ produced is another important constraint need to be well investigated, and should well defined before starting CO₂ injection. As stated previously the maximum produced CO₂ (35 Mmscfd) is reached after 10 years of CO₂ injection combined with oil production, EOR process. Once this constraint is reached the oil producer wells will be shut in as shown below.



CO2-EOR-StoragePilot-Project-FZI-impact-Inj-Aquife

16 Jan 2017

Fig. 90: Total produced and injected CO₂ rates

7.2.3. The trapping mechanisms

As it is considered as the most important trapping mechanism and even it is included in the storage capacity evaluation, the solubility or the dissolution of the CO₂ into the fluid in place should investigated, and as showed previously that the simulation software used in the study (Nexus) could predict this important physical phenomenon, as stated, after 20 years of continuous injection of the CO₂, 60 years running time is carried out to check how the injected CO₂ is behaving during the injection and after the end of the project, the below figure provide the flowing mechanisms during the CO₂ injection period (dynamic phase) and after shut in injection wells (static phase).

As mentioned previously during the injection period the dissolution of the CO₂ into the fluid in place is highly affected by the pressure, it means the process of dissolving CO₂ into the brine is accelerated by the pressure. The differential pressure is the main driver of the CO₂ flow as well as the reservoir properties it means the flow goes through the high flow potential pathways (figures below).

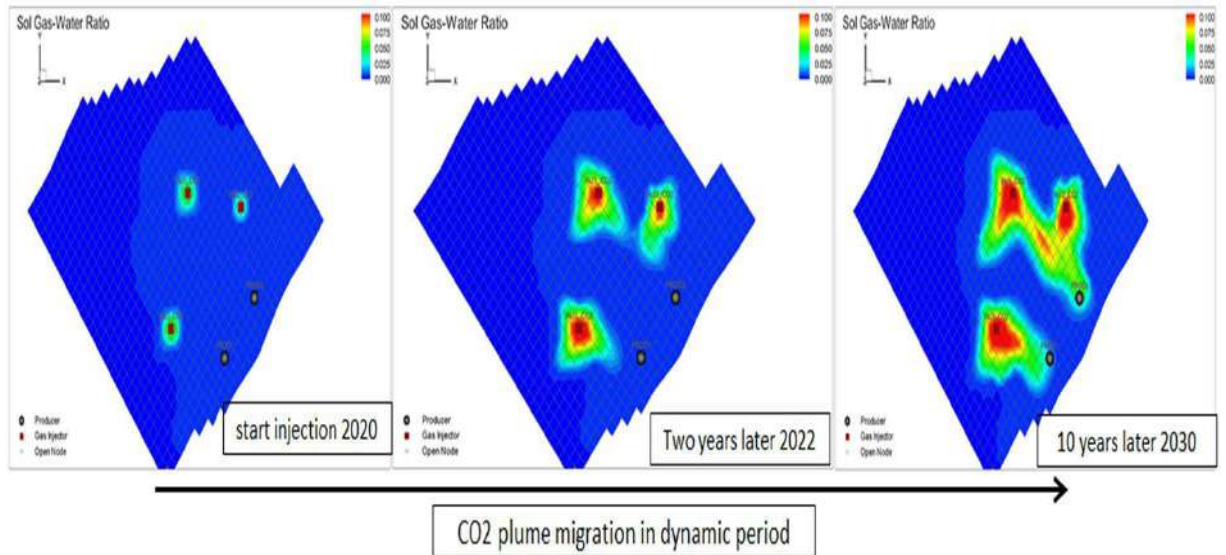


Fig. 91: CO₂ dissolved process in dynamic phases

After stopping CO₂ injection in 2040 the dissolution of the CO₂ into the fluid in place is very slow process, no external agents (pressure or temperature) impact to accelerate the process. The CO₂ flowing (transporting) from grid to grid is governed by the salinity of the fluid in place, it means, the CO₂ move from the high salinity grid to the neighbour low salinity grid (figure below).

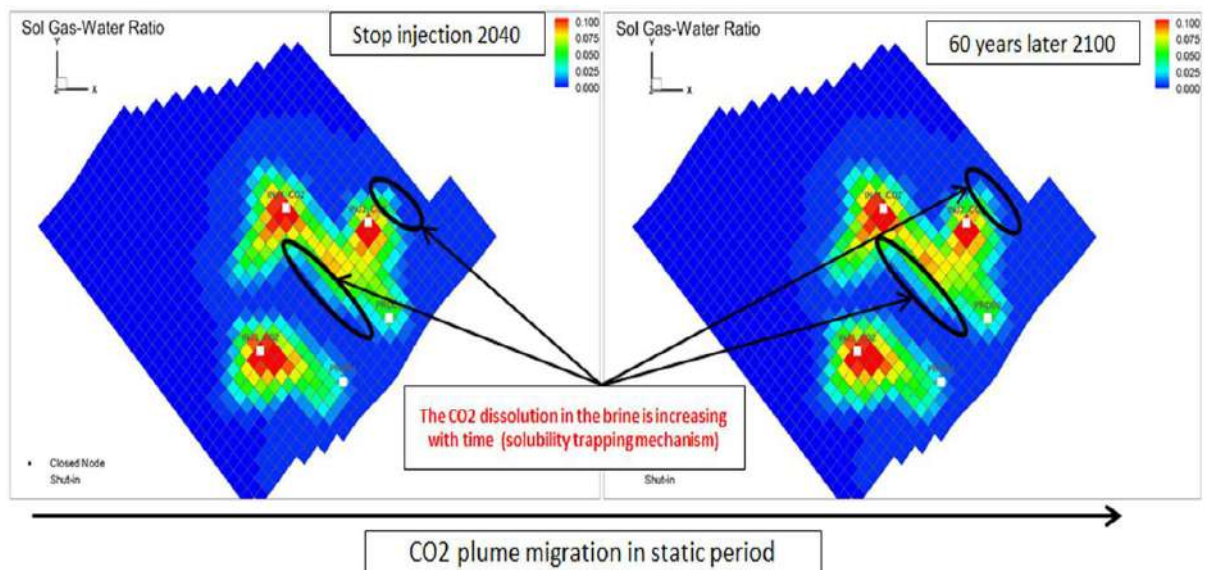


Fig. 92: CO₂ dissolved process in static phases

The saturation of free CO₂ across the reservoir is behaving inversely to the solubility behaviour, before shut in the injector wells the CO₂ saturation (free gas) is increasing with a time, otherwise, once the injection is stopped the free CO₂ start decreasing (CO₂ will be dissolved into the water rather than staying free in the reservoir) as show in the below figures.

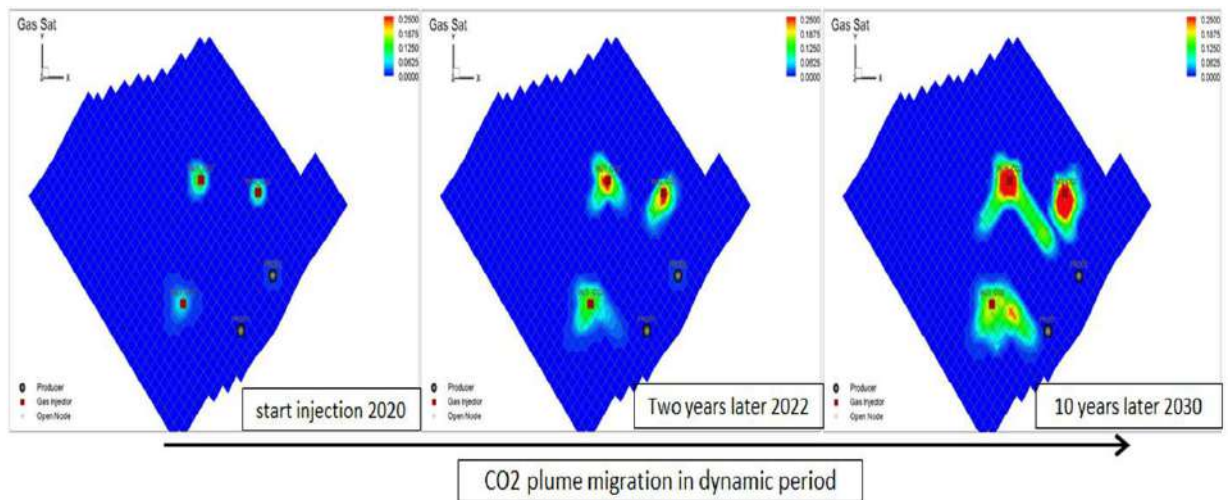


Fig. 93: CO₂ free gas saturation in dynamic phases

The reduction of free CO₂ saturation with time confirm the capability of handling the main physical phenomenon of the CO₂ geological storage by software used in this study, CO₂ flow in free status across the reservoir exhibits high leakage risk through the weak points of the reservoir.

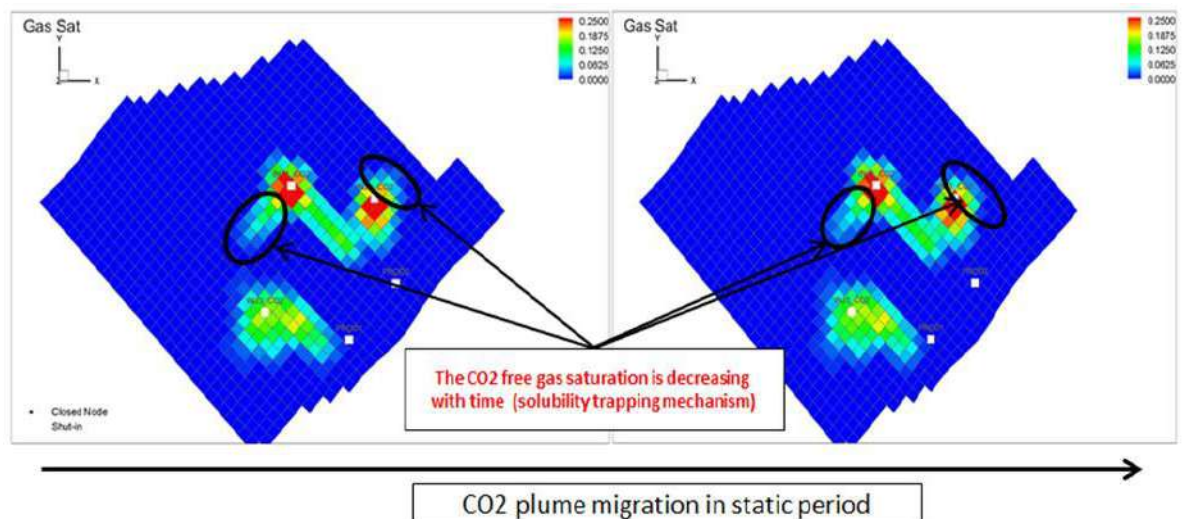


Fig. 94: CO₂ free gas saturation in static phases

As explained previously, the injected CO₂ is in supercritical status in reservoir pressure and temperature conditions, The flow behavior of supercritical CO₂ in an aquifer is similar to that of a fluid, Buoyancy drives the injected CO₂ to migrate upward until an impermeable cap rock traps it. Thus, the structural trapping mechanism needs a cap rock to prevent mobile CO₂ from leaking out of the storage reservoir. This mechanism is confirmed in this example as the pressure is below enough the initial reservoir pressure used to trap the original hydrocarbon in place (including the IFT impact in the capillary pressure).

The solubility trapping causes both mobile and immobile supercritical CO₂ to change into an aqueous phase via the dissolution process. Denser CO₂-

saturated water will be formed and it will tend to sink to the bottom of the formation. The convection effect will force the fresh water to replace the CO₂-saturated water. Consequently, more supercritical CO₂ dissolves into the water, this process is confirmed in the previous section.

Now, after confirming the security of this pilot project and the injected CO₂ will be trapped in the reservoir SFSW for long term without any leakage risk. The quantification of the storage capacity of SFSW field is the next parameter to be investigated.

7.3. Reservoir storage potential evaluation of SFSW field

7.3.1. Effect of the adjacent aquifer

The boundary conditions of an aquifer determine the extent to which fluids (including formation water and CO₂) and pressure can be transferred into adjacent geological formations, either laterally or vertically. Aquifer boundaries can be faults, lithological boundaries, formation pinch-outs, salt walls, or outcrop. In many cases compliance with regulations preventing CO₂ storage influencing areas outside artificial boundaries defined by non-geological criteria (international boundaries; license limits) may be necessary. A bounded aquifer is not necessarily a closed aquifer.

The boundary conditions of an aquifer have a significant impact on its capacity and pressure behaviour. Closed systems are subject to a general (average) pressure increase, as well as near-well pressure increase, that may approach imposed limits and thus limit capacity. Open systems are less susceptible to pressure increase, but injection wells do have a pressure footprint. Where multiple injection sites are used, these footprints may overlap to generate a more widespread pressure increase.

In order to quantify the impact of boundary conditions of an aquifer on the capacity and pressure behaviour, a two simulation cases have been ran as below, one with injector well in the aquifer and the other one without.

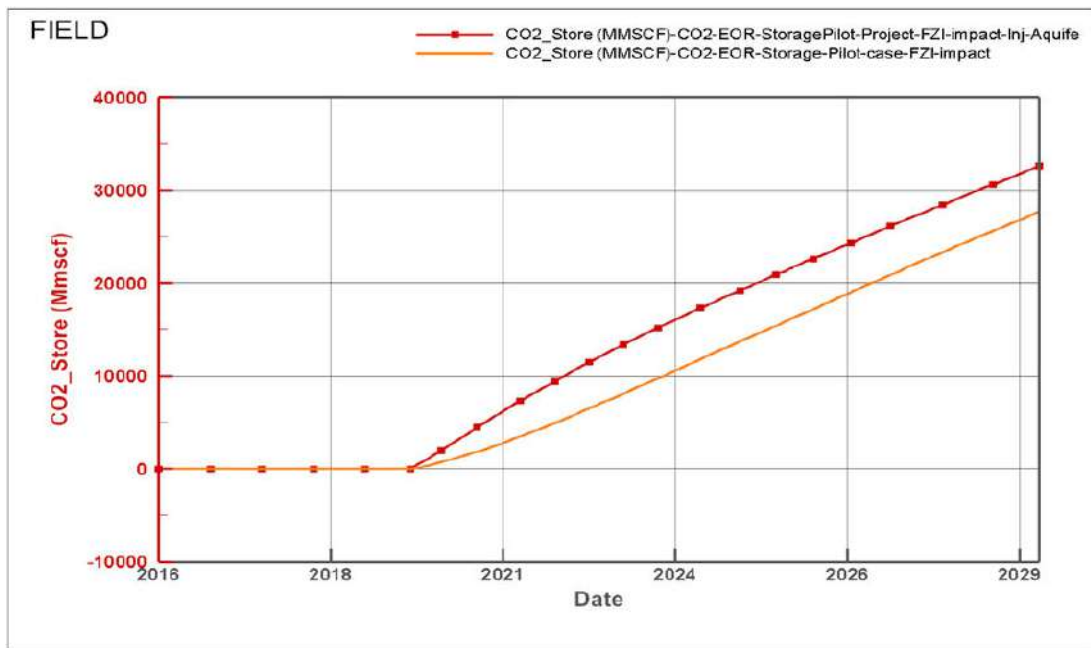


Fig. 95: Effect of the CO₂ injection in the aquifer (storage capacity)

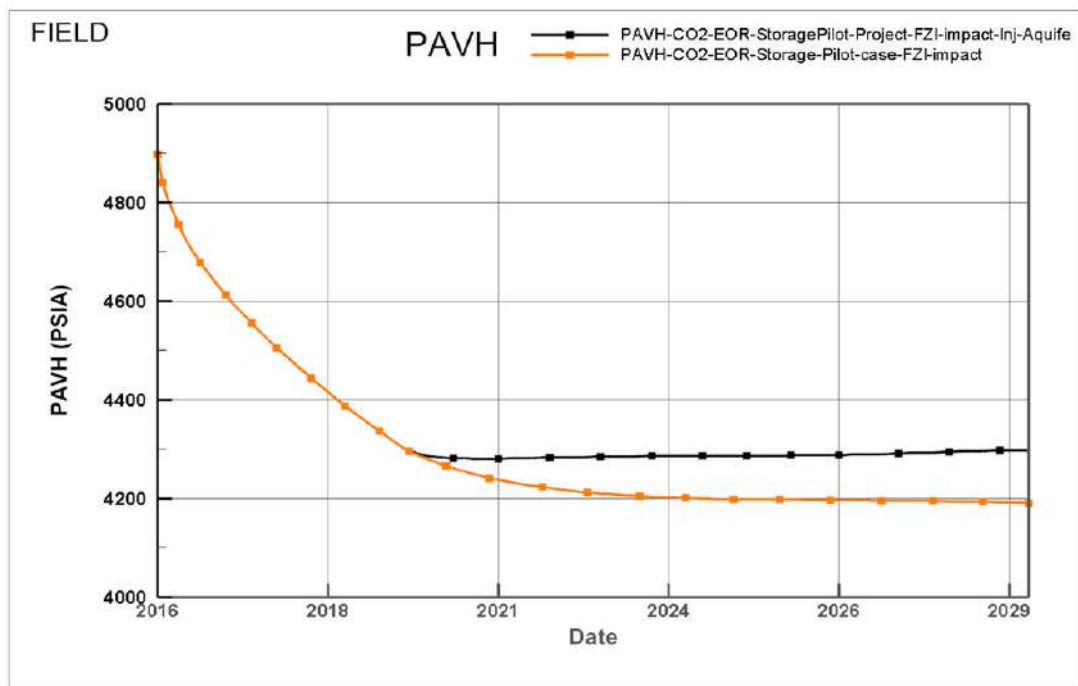


Fig. 96: Effect of the CO₂ injection in the aquifer (reservoir pressure)

Typically an open system is closed vertically (i.e. the caprock is very low permeability) but open laterally. For an open system, CO₂ injection may be into an aquifer so large that it is considered infinite, or an aquifer with an outcropping boundary. Static estimates assume that capacity is generated by displacing water out of the aquifer (or elsewhere in an “infinite” aquifer) and any increase in the pressure of the system is disregarded.

The dynamic simulation of CO₂ storage in a closed aquifer with a low permeability caprock shows that treating bounded aquifers as completely closed is a conservative assumption. The displacement of formation water through the overburden – through pore networks or fractures – can mitigate the pressure increase that results from CO₂ injection, to the point where the pressure profile more closely resembles an open system. Simplified solutions for capacity estimation in “semi-closed” aquifers [89], may be a useful tool in regional capacity estimates. The identification and characterization of regional aquifer boundaries – both laterally and vertically – is critical to the choice of estimation method and the setup of any simulations.

7.3.2. CO₂ Injection wells performance

As we have previously stated, the primary goal of CO₂ injection into the reservoir is sequestration in which it is also utilized as EOR scheme, in this section we compare the performance of wells to inject and sequestrate CO₂ in all injection wells, the performance of the CO₂ injection is more better in the well in which CO₂ is injected in the aquifer than injecting in the oil leg (oil reservoir) as shown below

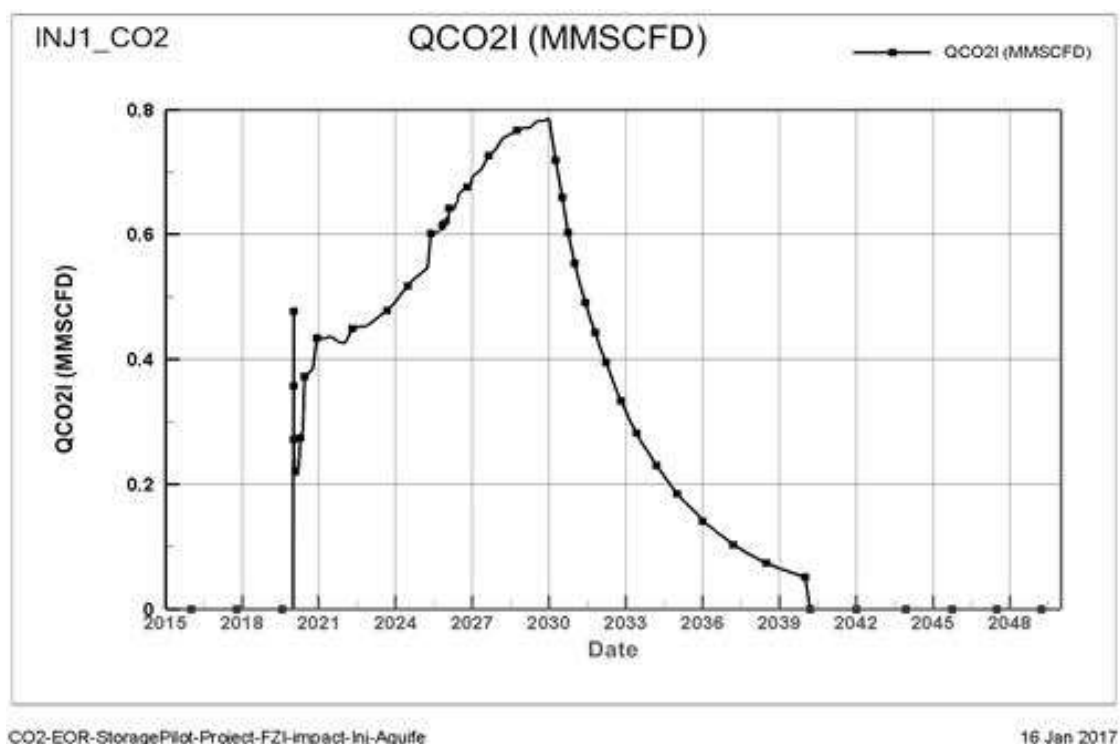
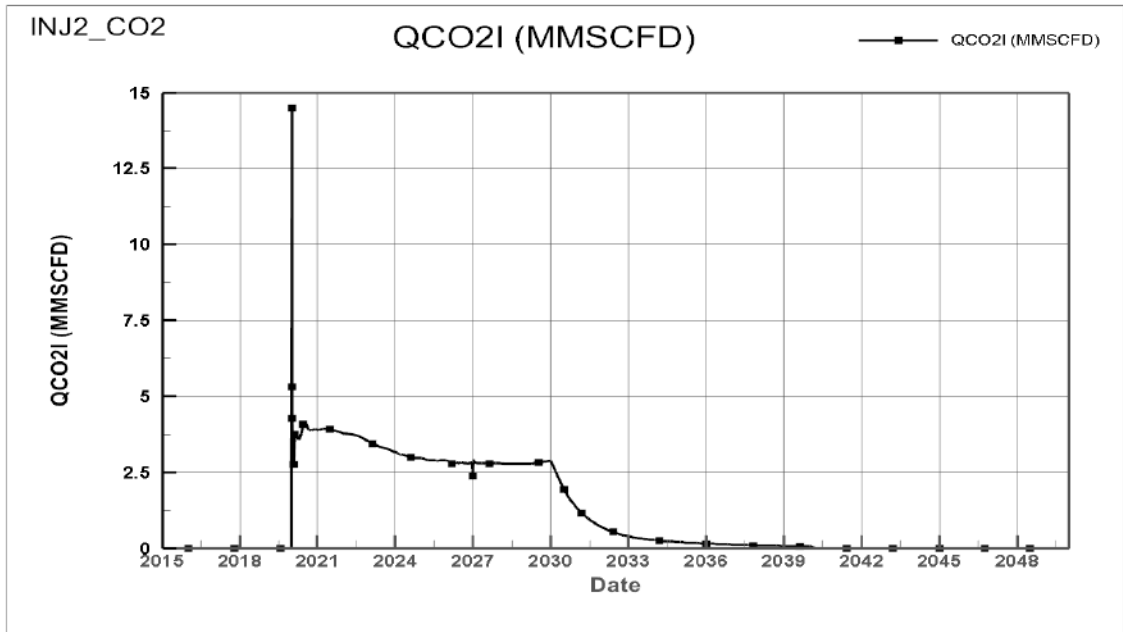


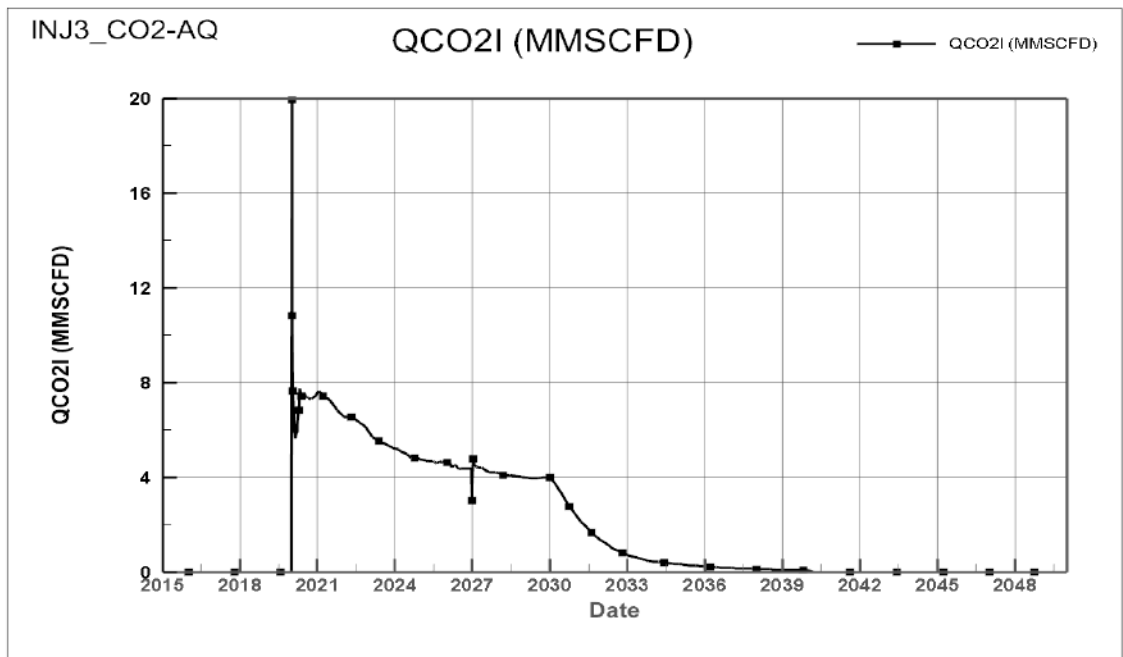
Fig. 97: CO₂ injection rate in the INJ1_CO₂ (in hydrocarbon reservoir)



CO2-EOR-StoragePilot-Project-FZI-impact-Inj-Aquife

16 Jan 2017

Fig. 98: CO₂ injection rate in the INJ2_CO₂ (in hydrocarbon reservoir)



CO2-EOR-StoragePilot-Project-FZI-impact-Inj-Aquife

16 Jan 2017

Fig. 99: CO₂ injection rate in the INJ3_CO₂-AQ (in adjacent aquifer)

7.3.3. Quantification of storage potential of SFSW

The main aim of this pilot project is to identify and quantify the amount of CO₂ stored during and post EOR process. Extending CO₂-EOR practice to qualify as CO₂ storage can be achieved with adjustments to the design and operations of a CO₂-EOR project. Besides CO₂ storage in depleted oil and gas reservoirs, enhanced oil recovery (EOR) through CO₂ flooding has captured attention because of the potential economic gain from incremental oil production. The opportunities offered by enhanced oil recovery (EOR) have therefore increased interest in CO₂ storage in the very recent years. As they are not designed for CO₂ storage (CO₂ EOR processes are typically designed to obtain maximum oil production while injecting minimum CO₂), CO₂-EOR projects demonstrate to some degree the associated storage of CO₂ as demonstrated in our current study.

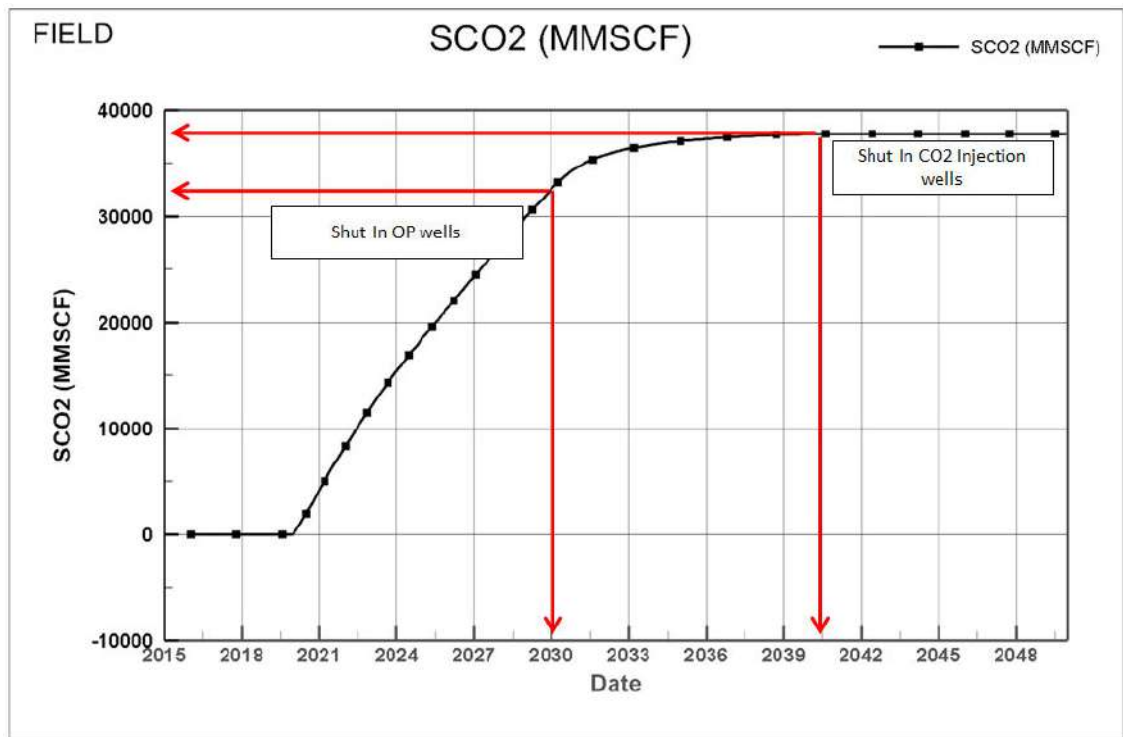
To evaluate the amount of the CO₂ stored in our case, we should calculate the volume of CO₂ retained during pre-storage process (EOR mechanism) and the volume of the CO₂ stored during the CO₂ storage process.

- CO₂ storage volume during the EOR mechanism

The EOR process were applied in our case for 10 years (2020 to 2030), the performance of the field were enhanced in term of oil production, the total CO₂ retained in the reservoir as it was the main goal of the project was very encouraging and the reservoir could store more than 32.5 BSF of CO₂ for 10 years, an average of 1.7 MegatCO₂/yr. as shown in the below plot.

- CO₂ storage volume Post-EOR mechanism, CO₂ storage process

After shut in the oil producer wells, the CO₂ injection life was extended and CO₂ storage process started with some adjustments to design and operations parameters. During 10 years of injection a total of 5 BSCF of CO₂ was stored, an average of 0.026 MgatCO₂/yr. as shown in the below plot.



CO₂-EOR-StoragePilot-Project-FZI-impact-Inj-Aquife

16 Jan 2017

Fig. 100: CO₂ Store in the pilot project

- Conclusion

The main objective of this pilot project is to evaluate the performance of geological CO₂ storage in hydrocarbon reservoir (SFSW field example), this pilot project includes investigation of all conditions and requirements for long term secure storage.

The CO₂ storage capacity of a reservoir include the CO₂ remained in the reservoir at the end of EOR operation and any extra CO₂ that can be injected after the EOR project is considered as the potential of the reservoir to store CO₂ during and post EOR process.

The US experience indicated that approximately 40% of the originally injected CO₂ is being produced in the producer wells and can be reinjected. This suggests a “gross” CO₂-retention efficiency of approximately 60% at CO₂ breakthrough if separation and reinjection is not considered after the breakthrough in our current project [28].

For our current case a total of CO₂ stored in SFSW field is more than 37.5 BSCF throughout of 20 years of continuous CO₂ injection, an average of 0.13 MegatCO₂/yr.

CO₂ injection into tertiary oil reservoirs has been widely accepted as an effective technique for enhanced oil recovery (EOR). Concerns over greenhouse gas emissions are leading to the investigation and realization of its potential as a carbon storage method in recent years. With the right reservoir conditions, injection of CO₂ into oil reservoirs can result in incremental oil recovery and permanent storage of CO₂ in geological formation.

The majority of previous and current CO₂ EOR projects uses low cost CO₂ sources and has good economic returns in terms of high gas utilization efficiencies (167-227 sm³ CO₂/STB oil). The potential of CO₂ storage combining EOR is high, approximately 60% injected CO₂ can be retained in the reservoir at the CO₂ breakthrough if reinjection is not considered. However, most of the CO₂-EOR projects operating today use naturally occurring CO₂ that is extracted from underground specifically for EOR purposes. Such practice is neither beneficial for the climate nor for the development of CCS.

There are over a hundred sites worldwide where CO₂ is injected underground as part of normal oilfield operations, either as part of an enhanced oil recovery (EOR) scheme or to prevent toxic acid gases being released to the atmosphere (CO₂ is injected mixed with hydrogen sulphide - H₂S). There are also several current and planned storage projects, specifically designed to reduce atmospheric emissions of CO₂. The challenge is how to design storage such that the CO₂ remains underground for thousands of years and how to handle the huge volumes necessary to make an impact on global CO₂ emissions – we will need to store several thousand times more CO₂ than is captured by current projects if CCS is to have a significant impact.

The importance of this pilot project is came from capability of SFSW to store 0.13 MegatCO₂/yr, which is more than 92 % of the total Algeria CO₂ emission estimated by EDGAR database created by European Commission and Netherlands Environmental Assessment Agency released in 2014.

Chapter 8

Conclusion & Perspectives

Conclusion

Carbon Capture & Storage technology is among the most promising solutions to fight against global warming, this technology is comingled with the oil and gas exploitation techniques and is built around the expertise of the oil and gas industry, in fact the CCS is the nature react of the oil and gas companies to the current climate challenges as it was one of the main causes of this problem.

Today, CO₂ storage process is quite well understood with over of one hundred sites in the worldwide where CO₂ is injected in the geological formations. Depleted or nearly depleted gas and/or oil reservoirs are considered as one of the most attractive storage locations for technical and economic reasons.

The main objective of this study is to identify and quantify the CO₂-EOR+ performance based on oil recovery factor and as well as the amount of stored CO₂ in mature oil reservoir located in the southeast of Algeria (Sif Fatima South West - SFSW)

As the CO₂ injection into tertiary oil reservoirs has been widely accepted as an effective technique for enhanced oil recovery (EOR), and in order to achieve a win-win solution for business and for climate change mitigation goals, offering commercial opportunities for oil producers while also ensuring permanent storage of large quantities of CO₂ underground. Transforming practices to support climate change carbon storage objectives in addition to oil extraction. The EOR mechanism was applied in SFSW field to justify the high cost of the CO₂ capture and transport to the storage location

Several works have been done before building a pilot project model using reservoir simulation tool to quantify CO₂ storage potential of SFSW, based all in the investigation of how can maximize the storage capacity of hydrocarbon reservoirs to store CO₂ for long term in safety manner.

The mains works that have been done in this thesis are summarized below

- 1) The effect of fractures presence in the reservoir on CO₂ storage efficiency, by comparing two identical reservoir models with including fractures features in one of them and check the performance of both models in term of capacity storage and security properties, from security perspective, the fractured reservoirs are not good storage location of the CO₂ because of security reasons.
- 2) Well description of the key petrophysical properties (permeability, porosity, FZI) of the reservoir by exploiting the large volume of existing

data brought from the exploitation phase, and using an artificial intelligence method (ANFIS) combined with the hydraulic flow unit concept.

- 3) Validation of simulation software used in this thesis (Nexus) and reservoir model (SFSW) using an experimental results provided by Adel M. Salem et al. (2013) by checking the ability of Nexus and the reservoir model to handle the main physical phenomenons happening in the CO₂ geological storage such as in the solubility of the CO₂ into the fluid in place (brine).

The main results and recommendations got from the above works were included in the pilot project in order to maximize the storage capacity and ensure the sealing capabilities of the reservoir.

The results of this study showed the capability of this reservoir (SFSW) to store 37.5 BSCF of CO₂ during 20 years of continuous injection, an average of 0.13 MegatCO₂/yr.

This amount have been stored over two process, firstly CO₂-EOR process, the reservoir could store 32.5 BSCF over 10 years of continuous injection, an average of 1.7 MegatCO₂/yr. the second process is CO₂ storage, the reservoir could store 5 BSCF over 10 years of continuous injection, an average of 0.026 MegatCO₂/yr.

The potential of CO₂ storage combining EOR is high, approximately 60% of the injected CO₂ can be retained in the reservoir at the CO₂ breakthrough if reinjection is not considered.

The challenge now is how to handle the huge volumes necessary to make an impact on global CO₂ emissions, as the most of the CO₂-EOR projects operating today use naturally occurring CO₂ that is extracted from underground specifically for EOR purposes. Such practice is neither beneficial for the climate nor for the development of CCS.

To show the importance of this project in the struggling against the dramatically increase of the greenhouse gases concentrations in the atmosphere, a comparison of the total CO₂ stored in SFSW to the total Algeria CO₂ emission provided by EDGAR database created by European Commission and Netherlands Environmental Assessment Agency released in 2014. 92.2 % of the total Algeria CO₂ emission has been sequestrated in SFSW field which was estimated to 0.134 MegatCO₂/yr.

Author Perspective

The results of the study show that there is significant potential in hydrocarbon reservoirs to store with enough security the greenhouse gas CO₂ which can help to contribute in the mitigation of the climate change.

The main objective of our study is to identify and quantify the potential of SFSW to store CO₂ for long term in hydrocarbon reservoir in safety manner.

From technical perspective, the geological storage of the CO₂ in hydrocarbon reservoirs is feasible solution that can help to curb the dramatically increase of the CO₂ concentration in the atmosphere.

The challenge today is to convince the governments of the countries to start thinking and believing that it's the right time to act against the climate change before being too late.

Many of the hydrocarbon reservoirs are in end-life and as they trapped the original oil and gas for long geological time they could store and trap also the CO₂ for long geological time. For instance, a small reservoir like the one used in this study was able to store the total CO₂ emission of Algeria.

References

References

- [1]. Bert Metz, Ogunlade Davidson, Heleen de Coninck, Manuela Loos and Leo Meyer. Carbon Dioxide Capture and Storage. Intergovernmental Panel on Climate Change (IPCC). Cambridge University Press, New York, USA, IPCC special report. 2005. 443p.
- [2]. International Energy Agency. Barriers to overcome in implementation of CO₂ capture and storage in disused oil and gas fields. Report number pH3/22. February 2000. 146p.
- [3]. F.M. Orr, Jr., A. Kovscek, K. Jessen, T. Tang, C. Seto, M. Hesse, T. Ide, W. Lin, and T. Chaturvedi. CO₂ sequestration in oil/gas reservoirs, saline aquifers and coal beds. Global Climate and Energy Project (GCEP), Energy Research at Stanford 2005-2006. 4p.
- [4]. Sally M. Benson. Carbon Dioxide Capture and Storage in Underground Geologic Formations. Lawrence Berkeley National Laboratory Berkeley, California 94720. Published in work shop proceeding "The 10-50 Solution: Technologies and Policies for a Low-Carbon Future.". USA. 19p.
- [5]. M. Bentham and G. Kirby. CO₂ Storage in Saline Aquifers. , Kingsley Dunham Centre, Nottingham, United Kingdom. 2005. 9p.
- [6]. Brent Lakeman, Bill Gunter, Bob Mitchell. A Technical Overview of CO₂ Capture & Geological Storage. Alberta Research Council Inc. Canada. May 2005. 45p.
- [7]. International Energy Agency (IEA). Near-Term Opportunities for Carbon dioxide Capture and Storage. Global Assessments WORKSHOP in support of the G8 Plan of Action. 2007. 25p.
- [8]. Heleen de Coninck and Sally M. Benson. Carbon Dioxide Capture and Storage: Issues and Prospects. Institute for Science, Innovation and Society, Faculty of Science, Radhoud University, 6500 GL Nijmegen, Netherlands, Annu. Rev. Environ. Resour. 2014. 39:243-70. Netherlands. 2014. 32p.
- [9]. Anusha Kothandaraman. Carbon Dioxide Capture by Chemical Absorption:A Solvent Comparison Study. Institute of Chemical Technology, University of Mumbai. India. 2005. 263p.
- [10]. Howard Herzog, Jerry Meldon, Alan Hatton. Advanced Post-Combustion CO₂ Capture. Clean Air Task Force, April 2009. 39p.
- [11]. Mohamed Kanniche, René Gros-Bonnivard, Philippe Jaud, Jose Valle-Marcos, Jean-Marc Amann, Chakib Bouallou. Pre-combustion, post-combustion and oxy-combustion in thermal power plant for CO₂ capture. EDF, Research and Development Division, Fluid Mechanics Energies and Environment Department. Published in Applied Thermal Engineering Journal. France. 2009. 10p.
- [12]. Redouane HADDADJI. The In-Salah CCS experience Sonatrach, Algeria. The First International Conference on the Clean Development Mechanism, Riyadh, Saudi Arabia. 19-21 September 2006.
- [13]. Cheng-Hsiu Yu, Chih-Hung Huang, Chung-Sung Tan. A Review of CO₂ Capture by Absorption and Adsorption. Department of Chemical Engineering, National TsingHua University, Hsinchu 30013, Taiwan, Aerosol and Air Quality Research. 2012. 25p.
- [14]. Yukun Hu. CO₂ capture from oxy-fuel combustion power plants. KTH Royal Institute of Technology School of Chemical Science and Engineering, Department of Chemical Engineering and Technology, Energy Processes. Stockholm, Sweden. 2011. 58p.
- [15]. Derouiche Belkacem, Haireche Youcef. L'efficacite du stockage du CO₂ a Krechba-In Salah: Par linvestigation sur la fuite du CO₂ au niveau du puits KB-5. Universite de M'hamed bougara Boumerdes, Faculte des hydrocarbures et de la chemie, departementd des gisements petroliers et miners, Boumerdes. Algeria. 2012. 200p.
- [16]. Dennis Y.C.Leung, GiorgioCaramanna, M.Mercedes Maroto-Valer. An overview of current status of carbon dioxide capture and storage technologies. Department of Mechanical Engineering, the University of Hong Kong, Hong Kong. Published in Renewable and Sustainable Energy Reviews. Hong Kong. China. 2014. 18p.
- [17]. International Energy Agency (IEA). Caprock systems for CO₂ geological storage, Report 2011/01, evaluating technology options to mitigate greenhouse gas emissions. May, 2011. 149p.
- [18]. Pierre BACHAUD. Stockage du CO₂ dans les aquifères profonds Etude en conditions réelles des propriétés de confinement des roches de couverture et de leur altération.

Institut National Polytechnique de Lorraine. Laboratoire de Réaction et de Génie des Procédés. France. 2010. 215p.

- [19]. Zhaowen Li, Mingzhe Dong, Shuliang Li, Sam Huang. CO₂ sequestration in depleted oil and gas reservoirs – caprock characterization and storage capacity. Petroleum Systems Engineering, University of Regina, 3737 Wascana Parkway, Regina, Saskatchewan, Canada S4S 0A2. 2005. 11p.
- [20]. YuLiu, Heming Wang, Zijian Shen, Yongchen Song. Estimation of CO₂ storage capacity in porous media by using X-ray. Key Laboratory of Ocean Energy Utilization and Energy Conservation of Ministry of Education Dalian University of Technology, Dalian, China. 2013. 8p.
- [21]. Changlin Liao, Xinwei Liao, Xiaoliang Zhao, Hongna Ding, Xiaopeng Liu, Yongge Liu, Jing Chen, Ning Lu. Comparison of different methods for determining key parameters affecting CO₂ storage capacity in oil reservoirs. Petroleum Engineering Department, China University of Petroleum, Beijing, People’s Republic of China. 2014. 10p.
- [22]. Scott M. Frailey. Methods for Estimating CO₂ Storage in Saline Reservoirs. Illinois State Geological Survey, 615 E. Peabody Drive, Champaign, IL 61820-6964, USA. 2009. 8p.
- [23]. Robert C. Burruss. CO₂ storage resources, reserves, and reserve growth: Toward a methodology for integrated assessment of the storage capacity of oil and gas reservoirs and saline formations. US Geological Survey, National Center MS956, Reston, VA 20192. USA. 2009. 5p.
- [24]. Stefan Bachu, Didier Bonijoly, John Bradshaw, Robert Burruss, Sam Holloway, Niels Peter Christensen, Odd Magne Mathiassen. CO₂ storage capacity estimation: Methodology and gaps. Alberta Energy and Utilities Board, Edmonton, Canada. 14p.
- [25]. John Bradshaw, Stefan Bachu, Didier Bonijoly, Robert Burruss, Sam Holloway, Niels Peter Christensen, Odd Magne Mathiassen. CO₂ storage capacity estimation: Issues and development of standards. Geoscience Australia, GPO Box 378, Canberra, ACT 2601, Australia. 2007. 7p.
- [26]. S. Thibeau and V. Mucha. Have We Overestimated Saline Aquifer CO₂ Storage Capacities?. TOTAL SA, 64018 Pau Cedex- France. Published in Oil & Gas Science and Technology - Rev. IFP Energies nouvelles, Vol. 66 (2011), No. 1. 2016. 12p.
- [27]. Wickstrom, Lawrence H., Venteris, Erik R., Slucher, Ernie R., Carter, Kristin M.; McDonald, James; Rupp, John A.; Greb, Stephen F.; Baum, Gerald R.; Harrison, William B.; and Hohn, Michael E. Geologic Storage Options and Capacities for Carbon Dioxide Sequestration in the Midwest Regional Carbon Sequestration Partnership(MRCSP). Published in fifth annual conference on carbon capture and sequestration - doe/netl. May 8 - 11, 2006. 23p.
- [28]. F. Gozalpour, S.R. Ren and B. Tohidi. CO₂ EOR and Storage in Oil Reservoirs. Institute of Petroleum Engineering, Heriot-Watt University, Edinburgh EH14 4AS - United Kingdom. Oil & Gas Science and Technology - Rev. IFP, Vol. 60 (2005), No. 3, pp. 537-546. 2005. 10p.
- [29]. P.N.K. De Silva, P.G. Ranjith. A study of methodologies for CO₂ storage capacity estimation of saline aquifers. Department of civil engineering, Monash University, VIC 3800. Published in Fuel Journal. Australia. 2012. 15p.
- [30]. Peter Probst. Numerical simulation of CO₂ Injection into Saline Aquifers: Estimation of Storage Capacity and Arrival Time using Multiple Realizations of Heterogeneous Permeability. Ph.D. These. University of Stuttgart - Institute of Hydraulic Engineering. Stuttgart, 5th August 2008. 78p.
- [31]. Kyung Won Chang, Susan E. Minkoff, Steven L. Bryant. Simplified Model for CO₂ Leakage and its Attenuation due to Geological Structures. Department of Petroleum and Geosystems Engineering, the University of Texas at Austin, Austin. USA. 2009. 8p.
- [32]. Stefan Iglauer. Dissolution Trapping of Carbon Dioxide in Reservoir Formation Brine-A Carbon Storage Mechanism. Curtin University, Department of Petroleum Engineering, ARRC Building. Australia. 2011. 31p.
- [33]. S.J.T.Hangx. Behaviour of the CO₂-H₂O system and preliminary mineralisation model and experiments. HPT Laboratory, Department of Earth Sciences Utrecht University. 2005. 43p.
- [34]. Frykman, Peter. D3.1 - Review of relevant trapping mechanisms based on site portfolio. CO₂ Site Closure Assessment Research (CO₂CARE). 7th framework program. 2012. 39p.

- [35]. Jinsheng Wang, Zhiyu Wang, David Ruan, Christopher Lan. A study of the effect of impurities on CO₂ storage capacity in geological formations. CanmetENERGY, Natural Resources Canada, 1 HaanelDr, Ottawa, ON, Canada K1A 1M1. Published in international journal of greenhouse gas control. 2015. 6p.
- [36]. Cesare Marchetti. On geoengineering and the CO₂ problem. International institute for applied systems analysis, Laxenburg, Austria. 1976. 10p.
- [37]. Anne-Catherine Dieudonné. Stockage géologique du CO₂ : l'étanchéité des puits. Faculté des Sciences Appliquées, Département ArGenCo, Université de Liège, Belgique. 2011. 104p.
- [38]. Carlos Chalbaud. Propriétés interfaciales du CO₂ : application aux écoulements en pression et en température. Chemical Sciences. Chemical Sciences. Arts et Métiers ParisTech, 2007. French. 2007. 230p.
- [39]. C.A. Aggelopoulos, M. Robin, O. Vizika. Interfacial tension between CO₂ and brine (NaCl + CaCl₂) at elevated pressures and temperatures: The additive effect of different salts. Published in Advances in Water Resources Journal IFP Energies nouvelles 1 & 4, Avenue de Bois-Préau 92852 Reuil-Malmaison Cedex, France. 2011. 7p.
- [40]. Junho Oh, Kue-Young Kim, Weon Shik Han, Taehee Kim, Jeong-Chan Kim, Eungyu Park. Experimental and numerical study on supercritical CO₂/brine transport in a fractured rock: Implications of mass transfer, capillary pressure and storage capacity. Korea Institute of Geoscience and Mineral Resources, Daejeon 305-350, Republic of Korea. 2013. 12p.
- [41]. Walt W. McNaba and Susan A. Carroll. Wellbore Integrity at the Krechba Carbon Storage Site, In Salah, Algeria: 2. Reactive Transport Modeling of Geochemical Interactions Near the Cement-Formation Interface. Lawrence Livermore National Laboratory, Livermore, CA, 94550, USA. 2011. 8p.
- [42]. DJEBBAS Faycal, ZEDDOURI Aziez, KHELIFA Cherif. Impact of the Fractures on the Capacity and Security CO₂ Geological Storage, Published in Advances in Environmental and Geological Science and Engineering, ISBN: 978-1-61804-314-6, University of Kasdi Merbah Ouargla, Algeria, 2015.
- [43]. DJEBBAS Faycal, ZEDDOURI Aziez, KHELIFA Cherif. Study of the fractures effect on the capacity and security geological storage of the CO₂ in hydrocarbon reservoirs, Published in INTERNATIONAL JOURNAL OF ENERGY and ENVIRONMENT, Volume 9, 2015, University of Kasdi Merbah Ouargla, Algeria, 2015.
- [44]. DJEBBAS Faycal, CABBI Abdelhalim Analyse de l'injection de gaz à Rhourd El-Baguel, Project of Engineer End Study, Department of Reservoir, University of M'hamed Bouguerra, Boumerdes-Algeria. 2005. 128p.
- [45]. K. Uleberg and J. Kleppe. Dual Porosity, Dual Permeability Formulation for Fractured Reservoir Simulation. Norwegian University of Science and Technology (NTNU), Trondheim RUTH Seminar, Stavanger. 1996. 12p.
- [46]. KHELIFA Cherif, ZEDDOURI Aziez, DJEBBAS Faycal. Study on the effect of the fracture on the capacity and security geological storage of the CO₂ in hydrocarbon reservoirs. University of Kasdi Merbah Ouargla. Published in International Journal of Energy and Environment, Volume 9, 2015. 16p.
- [47]. Craig Alexander Griffith. Physical Characteristics of Caprock Formations used for Geological Storage of CO₂ and the Impact of Uncertainty in Fracture Properties in CO₂ Transport through Fractured Caprocks. Dissertations. Paper 122. Carnegie Mellon University Pittsburgh. USA. 2012. 335p.
- [48]. L. Stephen Melzer. Carbon Dioxide Enhanced Oil Recovery (CO₂ EOR): Factors Involved in Adding Carbon Capture, Utilization and Storage (CCUS) to Enhanced Oil Recovery. Midland, TX. USA. 2012. 18p.
- [49]. Marc Andre Hesse. Mathematical Modeling and Multiscale Simulation Of CO₂ Storage in Saline Aquifers. A Dissertation Submitted To The Department Of Energy Resources Engineering And The Committee On Graduate Studies Of Stanford University. May 2008. 207p.
- [50]. Jude O. Amaefule, Mehmet Altunbay, Djebbar Tiab, and David G Kersey. Enhanced Reservoir Description: Using Core and Log Data to Identify Hydraulic (Flow) Units and Predict Permeability in Uncored Intervals/Wells. SPE 26436. U. of Oklahoma (1993). 16p.

- [51]. Tahar Aifa. Neural network applications to reservoirs: Physics-based models and data models. *Journal of Petroleum Science and Engineering*, Elsevier. 2014. insu-01084932. 123, pp.1-6.
- [52]. Ha Quang Man. Integrated reservoir characterization for fluid flow modeling of the Z gas deposit at the Carpathian Foredeep. Hanoi University of Mining and Geology. Published in 2nd International Geosciences Student Conference 9-12 July 2011, Krakow. Vietnam. 2011. 171p.
- [53]. S.E.D.M. Desouky. A New Method for Normalization of Capillary Pressure Curves. Published in *Oil & Gas Science and Technology – Rev. IFP*, Vol. 58 (2003), No. 5, pp. 551-556. King Saud University, College of Engineering, Petroleum Engineering Department, PO Box 800, Riyadh 11421 - Saudi Arabia. 2003. 6p.
- [54]. Jyh-Shing Roger Jang. ANFIS Adaptive-Network-Based Fuzzy Inference System. Department of Electrical Engineering and Computer Science, University of California. Berkley. USA. 1993. 21p.
- [55]. R. Juanes, E. J. Spiteri, F. M. Orr Jr., M. J. Blunt. Impact of relative permeability hysteresis on geological CO₂ storage. Published in *Water Resources Research Journal*. Department of Civil and Environment Engineering, Massachusetts Institute of Technology, USA. 2006. 13p.
- [56]. AliA bedini, Farshid Torabi. Pore size determination using normalized J-function for different hydraulic flow units. Faculty of Engineering and Applied Science, University of Regina, Regina, SK S4S 0A2, Canada. 2015. 6p.
- [57]. Soumi Chaki, Akhilesh K. Verma, Aurobinda Routray, Mamata Jenamani, William K. Mohanty, P. K. Chaudhuri, S.K. Das. Prediction of Porosity and Sand Fraction from Well Log Data using ANN and ANFIS: a comparative study. Department of Electrical Engineering, IIT Kharagpur. 2013. 7p
- [58]. Raouf Gholamia, Ali Moradzadehb, Shahoo Malekic, Saman Amiric, Javid Hanachid. Application of artificial intelligence methods in prediction of permeability in hydrocarbon reservoirs. Department of Chemical and Petroleum Engineering, Curtin University of Technology, Sarawak, Malaysia, and Department of Mining, College of Engineering, Tehran University, Tehran, Iran (2014). 14p.
- [59]. Tahar Aifa, Rafik Baouche, Kamel Badadari. Neuro-fuzzy system to predict permeability and porosity from well log data: A case of HassiR'Mel gas field, Algeria. Geosciences-Rennes, CNRS UMR6118, University of Rennes, France and Laboratory LIMOSE, Department of physic, Faculty of science, University of Boumerdes, Algeria . Published in *Journal of Petroleum Science and Engineering* 123 (2014). 13p.
- [60]. Syed Shujath Ali, M. Enamul Hossain, Md. Rafiul Hassan, and Abdulazeez Abdulraheem. Hydraulic Unit estimation from predicted permeability and porosity using artificial intelligence techniques. Paper published SPE 164747. King Fahd University of Petroleum & Minerals, Dhahran 31261, Saudi Arabia. 2013. 9p.
- [61]. Wafaa El-SHahat Afify, Alaa H. Ibrahim Hassan. Permeability and Porosity Prediction from Wireline logs Using Neuro-Fuzzy Technique. Faculty of Science, Benha University, Egypt. 2010. 10p.
- [62]. Tohid Nejad Ghaffar Borhani, Seyed Hossein Emadi. Application of Hydraulic Flow Units and Intelligence Systems for Permeability Prediction in a Carbonate Reservoir. Chemical engineering department, Faculty of chemical and natural resources engineering, University Technology Malaysia. Malaysia. 2011. 6p.
- [63]. M.taslimi, B. Bohloli, E. Kazemzadeh and M.R.Kamali. Determing Rock Mass Permeability in a Carbonate Reservoir, Southern Iran Using Hydraulic Flow Units and Intelligent Systems. School of Geology, College of Science, University of Tehran, Tehran, IRAN. 2008. 8p.
- [64]. Yasin Ellabad, Patrick Corbett and Richard Straub. Hydraulic Units Approach Conditioned By Well Testing For Better Permeability Modelling In A North Africa Oil Field. Department of Petroleum Engineering, Heriot-Watt University, Edinburgh, EH14 4AS. UK. 2001. 4p.

- [65]. Mohammad Izadi, Ali Ghalambor. A New Approach in Permeability and Hydraulic-Flow-Unit Determination. Colorado School of Mines and Oil Center Research International. SPE-151576-PA. USA. 2003. 8p.
- [66]. Adnan A.Abed. Hydraulic flow units and permeability prediction in a carbonate reservoir, Southern Iraq from well log data using non-parametric correlation. , Petroleum Eng. Dept/College of Eng./University of Kirkuk, IRAQ. 2014. 8p.
- [67]. Ata Allah Nadiri. Application of fuzzy Inference System to Estimating Rock Properties from Well Logs and Seismic Data for groundwater level prediction. OMICS Group eBooks, 731 Gull Ave, Foster City, CA 9440, USA. 2015.
- [68]. Odd Magne Mathiassen. CO₂ as Injection Gas for Enhanced Oil Recovery and Estimation of the Potential on the Norwegian Continental Shelf. NTNU - Norwegian University of Science and Technology Department of Petroleum Engineering and Applied Geophysics. Trondheim / Stavanger May 2003. 96p.
- [69]. Safi, Razi. Numerical Simulation and Optimization of Carbon Dioxide Utilization for Enhanced Oil Recovery from Depleted Reservoirs. Engineering and Applied Science Theses & Dissertations. Washington University in St Louis. 2015. 90p.
- [70]. Quanlin Zhou, and Jens T. Birkholzer. On scale and Magnitude of Pressure Buildup Induced by Large-Scale Geologic Storage of CO₂. Earth Science Division, Lawrence Berkeley National Laboratory, University of California, Berkeley, CA 94720. 16p.
- [71]. Niklas Gunnarsson, 3D modeling in Petrel of geological CO₂ storage site, Department of Earth Sciences, Uppsala University, Villavägen 16, SE-752 36 Uppsala ISSN 1401-5765, Sweden. 2011.
- [72]. Jean-Pierre Deflandre, Audrey Estublier, Axelle Baroni, Jean-Marc Daniel, Florence Adjémian. In Salah CO₂ injection modelling: a preliminary approach to predict short term reservoir behaviour. IFP Energies nouvelles, 1-4 avenue Bois Préau 92852 Reuil-Malmaison Cedex, France. 2010. 8p.
- [73]. Jean-Pierre Deflandre, Audrey Estublier, Axelle Baroni, Jean-Marc Daniel, Florence Adjémian. In Salah CO₂ injection modelling: a preliminary approach to predict short term reservoir behaviour. IFP Energies nouvelles, 1-4 avenue Bois Préau 92852 Reuil-Malmaison Cedex- France. 2010. 8p.
- [74]. Mahendra K. Verma. Fundamentals of Carbon Dioxide-Enhanced Oil Recovery (CO₂-EOR) – A Supporting Document of the Assessment Methodology for Hydrocarbon Recovery Using CO₂-EOR Associated with Carbon Sequestration. Open-File Report 2015-1071. U.S. Department of the Interior. U.S. Geological Survey, Reston, Virginia. USA. 2015. 24p.
- [75]. Pham V, Halland E. Perspective of CO₂ for Storage and Enhanced Oil Recovery (EOR) in Norwegian North Sea. Norwegian Petroleum Directorate, Stavanger, Norway. Published in 13th International Conference on Greenhouse Gas Control Technologies, GHGT-13, 14-18 November 2016, Lausanne, Switzerland. 2017. 5p.
- [76]. Kit Carruthers. Environmental Impacts of CO₂-EOR. The Offshore UK Context. The University of Edinburgh. June 2014. 99p
- [77]. International Energy Agency. Storing CO₂ through Enhanced Oil Recovery, Combining EOR with CO₂ storage (EOR+) for profit. IEA 9 rue de la Fédération 75739 Paris Cedex 15, France. 48p.
- [78]. Mandadige Samintha Anne Perera, Ranjith Pathegama Gamage, Tharaka Dilanka Rathnaweera, Ashani Savinda Ranathunga, Andrew Koay and Xavier Choi. A Review of CO₂-Enhanced Oil Recovery with a Simulated Sensitivity Analysis. Department of Civil Engineering, Deep Earth Energy Laboratory, Monash University, Building 60, Melbourne 3800, Victoria, Australia. 2016. 22p.
- [79]. Van Thi Hai Pham. CO₂ storage-Simulations for forecasting the behavior of injection CO₂ in geological formations. Department of Geosciences Faculty of Mathematics and Natural Sciences University of Oslo, Norway. 2012. 52p.
- [80]. Ran Qi. Simulation of Geological Carbon Dioxide Storage. Department of Earth Science and Engineering of Imperial College London, United Kingdom. 2008. 225p.
- [81]. DJEBBAS Faycal, ZEDDOURI Aziez. L'effet de la Tension Interfaciale IFT sur la pression capillaire, la perméabilité relative et la masse volumique au stockage géologique de CO₂ dans les Milieux poreux. University of Kasdi Merbah Ouargla. Published in Le séminaire Internationale sur l'Hydrogéologie et l'Environnement. 2013. 4p.

- [82]. Adel M. Salem and Shedid A. Shedid. Variation of petrophysical properties due to carbon dioxide (CO₂) storage in carbonate reservoirs. American University in Cairo (AUC) and Suez University, Egypt. 2013. 12p.
- [83]. C. Chalbaud, M. Robin, J.-M. Lombard, H. Bertin and P. Egermann. Brine/CO₂ Interfacial Properties and Effects on CO₂ Storage in Deep Saline Aquifers. Institut français du pétrole, IFP, 1-4 avenue de Bois-Préau, 92852 Rueil Malmaison Cedex - France. 2010. 15p.
- [84]. Zhaowen Li, Mingzhe Dong, Shuliang Li, Sam Huang. CO₂ sequestration in depleted oil and gas reservoirs – caprock characterization and storage capacity. Petroleum Systems Engineering, University of Regina, 3737 Wascana Parkway, Regina, Saskatchewan, Canada S4S 0A2, published in Energy Conversion and Management Journal 47 (2006) 1372–1382. 2005.11p.
- [85]. Ran Qi. Simulation of Geological Carbon Dioxide Storage. A dissertation submitted to the Department of Earth Science and Engineering of Imperial College. London. 2008. 225p.
- [86]. Irina Gaus, Pascal Audigane, Laurent Andre, Julie Lions, Nicolas Jacquemet, Pierre Durst, Isabelle Czenichowski-Lauriol and Mohamed Azaroual. Geochemical and solute transport modelling for CO₂ storage, what to expect from it?. BRGM-Geosciences for a sustainable Earth, Orleans. France. 2008. 56p.
- [87]. Abubakar Mohammed, Gabriel A. Ekoja, Akinola A. Adeniyi, Abdulkadir B. Hassan. Modelling Long Term CO₂ Storage in Saline Aquifers. School of Mechanical Engineering, University of Leeds, Leeds, United Kingdom. Published in International Journal of Applied Science and Technology. December 2012. 10p.
- [88]. P. S. Ringrosea, A. S. Mathieson, I. W. Wright, F. Selama, O. Hansen, R. Bissell, N. Saoula, & J. Midgley. The In Salah CO₂ storage project: lessons learned and knowledge transfer. Statoil ASA, Arkitekt Ebbells veg 10, Trondheim NO-7005, Norway and SONATRACH, Direction Generale, Djenane El Malik, Hydra 16035, Alger, Algeria. 2013. 11p.

Abstract

Climate change, also called global warming caused by the increasing concentration of greenhouse gases in the atmosphere mainly CO₂ has become a real risk that threatens the existence of humanity on the earth. Hydrocarbon reservoirs are considered as one of the most attractive storage locations for mitigating anthropogenic greenhouse gas emissions for technical and economic reasons. Following more than a century of intensive oil exploitation, many oil and gas reservoirs have approached or already exceeded their economic life and can be considered as good candidates for CO₂ storage locations. The main aim of the project is to investigate the potential of long term storage of CO₂ in hydrocarbon reservoirs using computational techniques (reservoir simulation), such as VIP/Nexus landmark software, and apply the study in an oil reservoir located in South East of Algeria SFSW (Sif Fatima South West). Several works have been carried out in the purpose of good evaluation of reservoir potential to investigate the constraints of the reservoir parameters and software limitations such as:

- Impact of fracture presence on CO₂ storage efficiency, in term of storage capacity and reservoir sealing capabilities.
- Description of the key reservoir petrophysical properties (permeability, porosity, FZI), using an artificial intelligence technique (ANFIS) to predict the FZI and Phi and implement them in the hydraulic flow unit technique to estimate a permeability model with enough accuracy.
- Validation of simulation software (VIP/Nexus) and reservoir model using experimental results.

After determining the reservoir model constraints for safety storage and software capability to handle major physical phenomenons such as trapping mechanisms, an optimum reservoir simulation case was used as pilot project to quantify the potential of SFSW to store CO₂ for long term, the project showed the reservoir capability to sequester roughly the total Algeria emission of CO₂.

ملخص

أصبح التغير المناخي، الذي يطلق عليه أيضا الاحتباس الحراري الناجم عن تزايد تركيز غازات الدفيئة في الغلاف الجوي، أساسا ثاني أكسيد الكربون، خطرا حقيقيا يهدد وجود البشرية على الأرض. وتعتبر الخزانات الهيدروكربونية واحدة من أكثر مواقع التخزين جاذبية للتخفيف من انبعاثات غازات الدفيئة البشرية المنشأ لأسباب تقنية واقتصادية. وبعد أكثر من قرن من الاستغلال المكثف للنفط، اقتربت العديد من خزانات النفط والغاز أو تجاوزت بالفعل حياتها الاقتصادية، ويمكن اعتبارها مرشحين جيدين كمواقع تخزين ثاني أكسيد الكربون. ويتمثل الهدف الرئيسي من المشروع في التحقيق في إمكانات تخزين ثاني أكسيد الكربون على المدى الطويل في خزانات الهيدروكربونات باستخدام التقنيات الحاسوبية (المحاكاة)، مثل البرمجيات البارزة (نيكسوس)، وتطبيق الدراسة في خزان للنفط يقع في جنوب شرق الجزائر (سيف فاطمة جنوب غرب). وقد تم تنفيذ العديد من الأعمال لغرض التقييم الجيد لقدرات الخزان للتحقيق في قيود الخزان وقيود البرمجيات مثل:

- تأثير وجود الكسر على كفاءة تخزين ثاني أكسيد الكربون، من حيث سعة التخزين وقدرات ختم المكامن.
 - وصف الخصائص البتر وفيزيائية للخزان الرئيسي (النفاذية، المسامية)، باستخدام تقنية النكاء الاصطناعي (أنفيس) وتنفيذها في تقنية وحدة التدفق الهيدروليكي لتقدير نموذج نفاذية مع دقة كافية.
 - التحقق من صحة برامج المحاكاة (نيكسوس) ونموذج الخزان باستخدام النتائج التجريبية.
- وبعد تحديد قيود نموذج الخزان لتخزين الأمان وقدرة البرمجيات على التعامل مع الظواهر الفيزيائية الرئيسية، استخدمت حالة المحاكاة المكمينة المثلى لمشروع تجريبي لتحديد إمكانات تخزين ثاني أكسيد الكربون على المدى الطويل، أظهر المشروع قدرة الخزان على عزل ما يقرب من مجموع انبعاثات الجزائر من ثاني أكسيد الكربون.

Abstract

Le changement climatique, également appelé réchauffement climatique causé par la concentration croissante de gaz à effet de serre dans l'atmosphère, principalement le CO₂, est devenu un risque réel qui menace l'existence de l'humanité sur la terre. Les réservoirs d'hydrocarbures sont considérés comme l'un des lieux de stockage les plus attrayants pour l'atténuation des émissions anthropiques de gaz à effet de serre pour des raisons techniques et économiques. Après plus d'un siècle d'exploitation intensive du pétrole, de nombreux réservoirs de pétrole et de gaz ont approché ou ont déjà dépassé leur durée de vie économique peuvent être considérés comme de bons candidats pour le stockage de CO₂. L'objectif principal du projet est d'étudier le potentiel de stockage à long terme du CO₂ dans les réservoirs d'hydrocarbures en utilisant des techniques de calcul (simulation de réservoir), comme le logiciel VIP/Nexus, et d'appliquer l'étude dans un réservoir pétrolier situé au sud-est de l'Algérie appelé SFSW (Sif Fatima Sud-Ouest). Plusieurs travaux ont été dans le but d'une bonne évaluation du potentiel du réservoir pour étudier les contraintes des paramètres du réservoir et les limites du logiciel tels que:

- Impact de la présence de fractures sur l'efficacité du stockage du CO₂, en terme de capacité de stockage et de capacités d'étanchéité du réservoir.
 - Description des propriétés pétrophysiques clé du réservoir (perméabilité, porosité, FZI), en modélisant une technique d'intelligence artificielle (ANFIS) en utilisant le code Matlab pour prédire le FZI et le Phi et les implémenter dans la technique du flux hydraulique pour estimer un modèle de perméabilité avec assez de précision.
 - Validation du logiciel de simulation (VIP/Nexus) et du modèle de réservoir en utilisant des résultats expérimentaux.
- Après avoir déterminé les contraintes du modèle de réservoir pour un stockage sécurisé et des capacités logicielles pour gérer des phénomènes physiques majeurs tels que les mécanismes de piégeage, un projet de simulation de réservoir optimal a été utilisé comme projet pilote pour quantifier le potentiel de stockage de CO₂ de SFSW. le projet a montré la capacité du réservoir à séquestrer à peu près l'émission totale de CO₂ en Algérie.